A SYSTEM DYNAMICS APPROACH TO STRATEGIC GROUNDWATER MANAGEMENT IN ÇUMRA REGION OF KONYA CLOSED BASIN

by

İzel Uygur

B.Sc. in Industrial Engineering, Boğaziçi University, 2020

Submitted to the Institute of Environmental Sciences

in partial fulfilment of the requirements for the degree of

Master of Science

in

Environmental Sciences

Boğaziçi University

2023

ACKNOWLEDGEMENTS

I am deeply grateful to Prof. Dr. Ali Kerem Saysel for supervising this research and for his unwavering support and guidance throughout my master's program. His expertise and patience have been invaluable to me and led to the success of this thesis. I would like to thank Prof. Saysel not only for his contributions to my academic development but also for all the non-work-related conversations we had, meals we shared, and trips we took. He has been a role model for me.

I am particularly thankful to Asst. Prof. İrem Daloğlu Çetinkaya, both as my academic advisor and co-advisor to my master thesis. Whenever I was struggling, she helped me take a step back and see the bigger picture, and she extended my vision a little more with every chat we had.

I would like to express my sincere appreciation to the examining committee members, Prof. Dr. Nadim Copty and Asst. Prof. Özge Karanfil for their treasured feedback and suggestions.

I very much appreciate the financial support of Innovative and Sustainable Groundwater Management in the Mediterranean (InTheMED) project (Boğaziçi University Project Number: 58000300) funded by PRIMA (Partnership for Research & Innovation in the Mediterranean Area). Special thanks goes to all the InTheMED community for their involvement in this research.

I would like to thank my lab mates Elif Bal, Mehmet Can Tunca, and Onur Cem Yoloğlu for all the fruitful discussions we had, and the moral support they provided me. Most importantly, I appreciate them for always answering my never-ending questions enduringly.

I am very lucky to have Mert Coşkun, who showered me with love and support for the last three years. He has been my escape from the hardships of life.

I am most grateful to my parents, Ferda and Özkan Uygur, who have always encouraged me to be whoever I am. They are my biggest treasure in life, and without their unconditional love and understanding, achieving a graduate degree would not have been possible for me.

ABSTRACT

A SYSTEM DYNAMICS APPROACH TO STRATEGIC GROUNDWATER MANAGEMENT IN ÇUMRA REGION OF KONYA CLOSED BASIN

Water is an essential input in agriculture; farmers all over the world depend on water availability to boost their production and profit. Lack of available surface water, especially in arid or semi-arid regions, render groundwater a vital resource for the continuity of agriculture. Konya Closed Basin is a semi-arid watershed located in Central Anatolia, Turkey. It has significant agricultural potential and is referred to as "the granary of the country" by Turkish people. In recent years, Konya Closed Basin has been brought to both local and national agenda, with its water scarcity and groundwater stress. In this research, we adopt a participatory system dynamics approach for exploring the drivers of unsustainable groundwater use and to build a shared understanding on future sustainable pathways in Çumra, an administrative district within Konya Closed Basin, Turkey. Following 3 field visits and 3 participatory model building workshops, we built a dynamic simulation model, and tested multiple environmental scenarios and policies that have been suggested by the stakeholders, such as inter-basin water transfer, crop rotation, crop repricing, well regulation, and groundwater extraction caps. The model simulates the 2004-2044 period on annual bases. The model structure and parameter values represent the field conditions in Çumra, and it is initialized based on the 2004 data. Based on the scenario and policy analyses performed in this research, the declining trend in the groundwater table in Çumra is not irreversible; when certain sets of policies are implemented, groundwater can be sustained while maintaining the desired agricultural production and farmer profits.

ÖZET

KONYA KAPALI HAVZASI'NIN ÇUMRA BÖLGESİNDE STRATEJİK YERALTI SUYU YÖNETİMİNE DİNAMİK BENZETİM YAKLAŞIMI

Su, tarımsal üretim için zaruri bir kaynaktır. Dünyanın her yerinde çiftçiler üretim seviyesini ve karlarını artırmak için suya ihtiyaç duymaktadır. Özellikle kurak ve yarı kurak bölgelerde yüzey suyuna erişim kısıtlı olduğundan, tarımsal üretimin devamlılığı için yeraltı suyu kaynakları kullanılmaktadır. Konya Kapalı havzası, Türkiye'nin İç Anadolu bölgesinde yer alan ve yüksek tarımsal üretim potansiyeli bulunan yarı kurak bir havzadır. Yakın geçmişten beri Konya Kapalı Havzası, su sıkıntısı ve yeraltı sularının çekilmesi ile gündeme gelmektedir. Bu çalışmada, Konya Kapalı Havzası'nın güneyinde yer alan Çumra ilçesinde yeraltı sularının sürdürülebilir bir şekilde kullanılamamasına neden olan faktörler araştırılmakta ve gelecekte yeraltı suyu kaynaklarının sürdürülebilirliğini sağlamak için ortak bir anlayış geliştirmek hedeflenmektedir. Bu amaçla, paydaş katılımlı dinamik sistem yaklaşımı ile organize edilen 3 saha gezisi ve 3 katılımlı modelleme atölyesini takiben bir dinamik benzetim modeli kurulmuştur. Bu model üzerinde, sahadaki paydaşların önerilerinden yola çıkılarak hazırlanan farklı çevresel senaryolar ve politikalar test edilmiştir. Bu senaryolar arasında havzalar arası su transferi, ekim nöbeti, tarımsal ürünlerin fiyatlarının değiştirilmesi, yeraltı suyu kuyusu açılması hakkında düzenlemeler ve yeraltı suyu çekim kotaları yer almaktadır. Model 2004-2044 yılları arasında, yıllık zaman birimiyle çalışmaktadır. Model yapısı ve parametreleri saha verilerini temsil edecek şekilde seçilmiş ve model ilk değerleri 2004 verilerine göre belirlenmiştir. Gerçekleştirilen analizler sonucu, bazı politikaların hem yeraltı sularındaki azalma trendini tersine çevirebileceği, hem de mevcut tarımsal üretim seviyesini ve çiftçi karlarını koruyabileceği gösterilmiştir.

TABLE OF CONTENTS

LIST OF FIGURES

LIST OF TABLES

LIST OF ABBREVIATIONS

CLD	Causal Loop Diagram
DSİ	State Hydraulic Works
GMB	Group Model Building
GW	Groundwater
KCB	Konya Closed Basin
MGM	Turkish State Meteorological Service
SD	System Dynamics

1. INTRODUCTION

Water is central to all human activities and at the base of human-nature relationships. It is essential and irreplaceable. With the world population growth, freshwater demand for drinking, domestic, agricultural, and industrial purposes increased considerably. Water security is currently a global concern. Agricultural practices, land use change, increasing population, rural-to-urban migration, industry, pollution, and climate change are some of the factors that result in the deterioration of water resources. Overuse and degradation of water resources lead to environmental externalities such as desertification, increased soil salinity, dust storms, and loss of biodiversity and agricultural productivity.

Driven by climate change, a decrease in precipitation, an increase in temperatures, and an increase in the frequency and severity of droughts further limit surface water availability in many regions. Therefore, especially in arid and semi-arid environments, freshwater supply is immensely dependent on groundwater, which constitutes nearly 99% of the world's freshwater supply (Re, 2015).

Agriculture is the largest user of groundwater globally, accounting for approximately 70% of total groundwater withdrawals, and even higher in semi-arid regions (Margat & Van der Gun, 2013; as cited in UNESCO, 2022). The value of groundwater for agriculture primarily lies in its availability and reliability, particularly in areas where the rainfall is limited, and surface water sources such as rivers and lakes are not available or are polluted (Scanlon et al, 2012). Unlike surface water sources, groundwater can be accessed year-round, even during periods of drought; it can be accessed through wells, allowing farmers to control the timing and amount of water applied to their crops. Irrigation scheduling is crucial for plant growth and yield, specifically for crops that require certain amounts of water at different stages of growth. Consequently, groundwater use can significantly increase agricultural productivity and crop yields. For example, Shah, Molden, Sakthivadivel, and Seckler (2000) found that irrigation with groundwater increased crop yields by an average of 39% compared to rain-fed agriculture in India. Furthermore, since groundwater is protected from many of the pollutants that might contaminate surface water sources, groundwater often has a higher quality than surface water, thus the additional value of groundwater for irrigation. Clean water helps maintain soil health and reduces expensive and harmful chemical use requirements.

Since the mid-20th century, groundwater withdrawal has boomed, particularly for agricultural irrigation (UNESCO, 2022). Farmers have been using groundwater with rather low costs and without being subject to the restriction of central governments, a process referred to as the “silent revolution” (Re, 2015; Schlager, 2007; Famiglietti, 2014). Over the last 50 years, groundwater utilization has peaked to supply agricultural demand (Villholth, Lopez-Gunn, Conti, Garrido, & van der Gun, 2018; Re, 2015). The development and widespread adoption of groundwater extraction and irrigation technologies resulted in significant increases in crop yields and allowed more agricultural production with less land. On the other hand, the silent revolution also led to the overexploitation of groundwater.

All around the world, both environmental and socio-economic indicators signal the unsustainable use of groundwater resources; the extraction rate has been exceeding the natural recharge rate in many parts of the world, resulting in declining water tables and the depletion of aquifers. The decrease in water tables not only restricts the accessibility of groundwater, but also causes loss of baseflow for many lakes and rivers, land subsidence, and saltwater intrusion in coastal aquifers (Giordano, 2009; Wada et al, 2010). Around 20% of the aquifers globally are being heavily overexploited; according to the study by Gleeson, Wada, Bierkens, and Van Beek (2012), 1,7 billion people live in regions where groundwater resources or groundwater-dependent ecosystems are under threat in the early 2010s. However, they also found that while the majority of the aquifers are utilized sustainably, some larger aquifers, particularly in North America and Asia, are being heavily exploited. In a more recent study, UNESCO (2022) reports that the global groundwater withdrawal rate has not changed significantly between 2010 and 2017; in fact, it seems to have stabilized in Europe, the USA, Canada, and Southeast Asia, either due to natural restrictions (absence or depletion of productive aquifers), water quality deficiencies, or decreased groundwater table which may have increased well construction and pumping costs up to a level that extraction is no more feasible. Yet still, climate change poses a serious threat to groundwater resources; rising temperatures, changing precipitation patterns, droughts, and other extreme weather events both impact the natural recharge rate of the aquifers and also are expected to increase dependency on groundwater (FAO, 2022).

The current situation of groundwater resources in Turkey reflects the global; it is a matter of significant concern due to urbanization, population growth, impacts of climate change, mismanagement, losses in distribution networks, and inefficient use. According to the State Hydraulic Works (Devlet Su İşleri, n.d.), the total amount of water supply potential of Turkey is 112 billion m^3 yearly, of which 94 billion is surface water and 18 billion is groundwater. DSİ also reports that 57 billion m^3 of water is utilized yearly, 44 billion for irrigation, and 13 billion for domestic and industrial purposes, which means that over 75% of the water is used for irrigation. Overall, approximately 77% of irrigation water is supplied from surface water and 23% is supplied from groundwater in Turkey. However, the surface water resources are not distributed evenly in the country, therefore, there exist significant differences in the relative shares of surface and groundwater in regional water supplies. Groundwater exploitation is a prominent issue in some agricultural basins in Turkey, such as Central Anatolia (Konya Closed Basin), Southeastern Anatolia (Gaziantep, Şanlıurfa, Mardin), and the coastal regions of the Aegean and Mediterranean (İzmir, Antalya, Mersin). The surface water availability may also change within an agricultural basin; dependency on groundwater may be higher in one district compared to another. Therefore, water management and allocation plans are expected to provide more desirable outcomes if designed on a regional scale.

2. PROBLEM DESCRIPTION AND RESEARCH OBJECTIVES

Groundwater is a typical common pool resource. Therefore, it is inherently vulnerable to overexploitation and degradation (i.e., the "*tragedy of the commons*" (Hardin, 1968, p.1)). As for all common pool resources, the hardship of preventing access is an incentive for free riding, which precludes the collective action necessary to sustain the resource in the long run (Dietz, Dolšsak, Ostrom, Stern, 2002; Schlager, 2007). Even if certain individuals or groups were successfully denied access to the resource, the coordination problems between the limited number of users are still likely to result in the overexploitation of groundwater (Dietz et al, 2002). Individuals have a high propensity to avoid precautions that require a certain amount of time and financial costs, because their altruistic behavior may easily be leveraged by free riders. As a result, users of the resource are likely to 'race to harvest' the resource. In other words, even if a certain group of users renounced their short-term benefits for the greater good, their efforts will be rendered useless unless most of the users cooperate. Those who try to do good will suffer the consequences of excess extraction even though they had no part in it. The prioritization of individual short-term benefits over long-term social benefits results in the tragedy of the commons (Hardin, 1968). To prevent the tragedy, ideally, groundwater management schemes must allow for communication between the stakeholders, an environment of trust, and decision mechanisms that provide coordinated action and prevent probable cooperation problems (Dietz et al, 2002).

One cannot identify a certain, prescriptive remedy that would provide more desirable outcomes in the management of commons. It is a "*panacea analytical trap*" (Basurto & Ostrom, 2009, p.36). Requirements of desirable management depend on the characteristics of the resource of interest (Dietz et al, 2002), and groundwater resources have a unique set of characteristics that set groundwater apart from other common pool resources. Therefore, identifying the hardships of groundwater management would be incomplete unless the idiosyncratic qualities of groundwater are considered.

2.1. Hardships of Sustainable Groundwater Management

First, both the temporal and spatial dynamics of groundwater should be addressed correctly. Like many other natural resources, groundwater cannot be approached independently from other Earth system components to which it is connected. Rural or urban land use, agriculture, industry, surface water, wetlands, and several other ecosystems are examples of groundwater-related systems

(Villholth et al, 2018). This high level of interconnectedness inevitably increases the complexity and uncertainty within such systems, through rich nonlinear feedback. Therefore, groundwater issues are not only about the resource itself but may have indirect and lagged impacts on other elements. For example, decisions on groundwater withdrawal may have unforeseen consequences on agricultural land systems, groundwater-surface water connection, or biodiversity (Re, 2015; Saito et al, 2021). Furthermore, lagged response to any human intervention in such interconnected systems makes it harder to comprehend system structure and estimate behavior (Saito et al, 2021).

Second, groundwater is an “invisible” resource (Saito et al, 2021, p.8). Even with the recent developments in science and technology, identifying the physical boundaries of aquifers and assessing groundwater depletion is not a simple task. Aquifer hydrogeology is quite heterogeneous. The invisibility of the resource makes it difficult to determine the recharge rate, discharge points, and flow of groundwater in between aquifers. Local users cannot know the aquifer capacities, boundaries, and the impact their extraction will have at the basin level, without help from experts such as engineers or hydrogeologists (Schlager, 2007). Therefore, local, and sustainable self-management of groundwater is unlikely.

Hydrological systems are dispersed in wide areas, and are compositely constructed; therefore, there usually is a mismatch between the administrative boundaries and the hydrological system boundaries (Theesfeld, 2010). This mismatch complicates groundwater management, and in some cases may result in conflicts between different administrative units or overlapping authority and responsibility. The wide dispersion of the resource also leads to considerable time lags between any human intervention to the resource and its impact on groundwater and other systems that they are connected to. Some interventions are likely to be irreversible and unpredictable (such as saltwater intrusion or sinkhole formation), but the over-extraction might not be noticed before the resource loses its renewability (Dietz et al, 2002; Theesfeld, 2010). The short-sightedness in that sense, should be a primal concern when dealing with groundwater-related issues.

The availability of continuous data is crucial for groundwater management. Today, unfortunately, many regions in the world lack sufficient empirical data, therefore aquifer characterization is inadequate. Decision-making is mostly based on estimations derived from outdated data (Schlager, 2007). Perhaps the most important role of central governments in groundwater management is to provide relevant and reliable data for those who have direct roles in management schemes. The required information covers not only the hydrological/hydrogeological data such as aquifer structure, storage capacity, groundwater levels, and water budgets but also the groundwater extraction and use data. Therefore, complete, and correct information about infrastructure (such as the number of wells, their depth, well capacities, etc.) is also necessary.

Identifying the relevant stakeholders and the social boundaries is as difficult as identifying the physical boundaries of groundwater (Theesfeld, 2010). The social boundaries are dynamic; therefore, the management schemes and the institutional structure should be adaptive to social, environmental, political, and economic changes. In addition, the number and variety of stakeholders in groundwater governance are usually high, leading to information asymmetries and inevitable conflicts of interest, further decreasing the probability of cooperation (Dietz et al, 2002). The information asymmetries could occur involuntarily, for example between central and local governing bodies, or voluntarily, when certain stakeholder groups knowingly misdirect others to gain an advantage over the resource (Theesfeld, 2010).

2.2. Groundwater Sustainability as a "Wicked" Problem

Groundwater can be considered a hub in a rich web of interconnections with both the physical and social worlds. These relationships are of a dynamic, non-linear feedback nature including a rather elusive human dimension; therefore, groundwater sustainability is a complex problem. The cause and effect might be distant in time and space; any intervention may trigger a potentially irreversible response far from the source both spatially and temporally, therefore it would be hard to deduce the cause of the response. Consequently, experimentation with different policies is off the table because it is likely to be too costly and too slow (Sterman, 2014). Additionally, improper characterization and inadequate observation of the resource render safe extraction limits and overall extraction unidentified, therefore science-based management is improbable.

In this research, we take this claim one step further to frame groundwater sustainability as a "wicked" problem: In most cases, the stakeholders describe the issue as over-extraction in the most general sense, yet, a well-defined and widely shared understanding of the problem and its drivers, and consensus on socially acceptable and achievable, high-leverage strategies to eliminate the problem is lacking. The reasons might be twofold:

(A) Misperceptions about the system: The non-linear feedback relationships within complex systems are challenging for the human mind to comprehend (Vennix & Forrester, 1999). The phrase "mental model" refers to how individuals perceive the mechanisms of systems that surround us, as opposed to how they operate. This suggests that people's perceptions of how a system functions may vary. Our mental models frequently underestimate the delays, accumulations, and circularity of complex systems (Hovmand et al, 2012). As a result, mental models frequently contain astonishing errors. More often than not, management failures are related to people's lack of understanding of the system they are dealing with. In other words, our ability to identify and implement high-leverage solutions is proportional to our ability to comprehend how the system works.

(B) Conflicting interests: Stakeholders assume different roles regarding groundwater sustainability. For example, while state actors whose responsibility is to ensure the sustainability of groundwater would likely be against over-extraction, farmers who support their families with irrigated agriculture would expectedly oppose any suggestions to limiting groundwater use.

In short, multiple stakeholders who have varying perceptions and agendas regarding the issue are involved in the decision-making process and their conflicting interests result in them incessantly blaming one another's perspectives for the groundwater depletion. Such settings give way to a clash between the three pillars of sustainability, in which the social pillar may overpower the environmental pillar (Murphy, 2012). This implies that disagreements on the definition of the problem and discussions on the "ideal" solution(s) are likely to result in little to no action, i.e., a wait-and-see approach, and collective pessimism among stakeholders.

Modeling and simulation might be useful in such situations in two steps (Barlas, 2002). First, the non-linear, dynamic feedback relationships that are both too complex for us to intuitively grasp and too difficult to be mathematically solved are translated into a formal model. Compared to our mental models, formal models are testable, explicit, and less biased; they compensate for the shortcomings of our mental models. Second, by way of computer simulations, the formal models are analyzed. Simulation provides an experimental platform to try out proposed solutions. In a matter of seconds, stakeholders can observe the long-term impacts furthering multiple decades without having to go through the process and compare the performances of multiple policies, saving time and money, and avoiding risks. Thusly, simulation may foster learning, converge stakeholder perspectives, and allow more informed decision-making in situations when the decision stakes are high, and the problem has a complex, dynamic nature (Gonzalez-Iwanciw, Dewulf, & Karlsson-Vinkhuyzen, 2019).

2.3. Research Objectives

In this research, we aspire to explore the drivers of unsustainable groundwater use and to build a shared understanding of sustainable pathways for the future in the Çumra district of Konya Closed Basin, Turkey. We adopt a participatory dynamic systems methodology to capture the rich web of causal feedback relationships between key system variables and thus recreate the structure underlying the observed behavior patterns, with the help of the stakeholders in the region. The model aims to represent groundwater hydrology, as well as farmer decisions on crop selection, and method and level of irrigation, and it allows users to experiment with various policy options such as crop rotation, surface water transfer, extraction limits, and repricing of crops. Our main objective is to create a user-friendly interface that is publicly available on the web, and on which both stakeholders (farmers, irrigation cooperatives, agricultural production unions, etc.) and policymakers can experiment to enhance their knowledge about the system, to improve their mental models, to collectively arrive at a common definition of the problem, and hopefully to agree on feasible solutions that will produce desirable outcomes in the long run.

3. CASE STUDY

Konya Closed Basin (KCB) is one of the 25 watersheds in Turkey. It is located in Central Anatolia and has a size of over 62.000 km^2 (Figure 3.1). The basin is surrounded by mountains; therefore, the streams within the basin cannot discharge to open waters, rendering KCB a “closed” basin. The climate is semi-arid; yearly precipitation is approximately 350 mm, which is less than half the average precipitation in Turkey (740 mm).

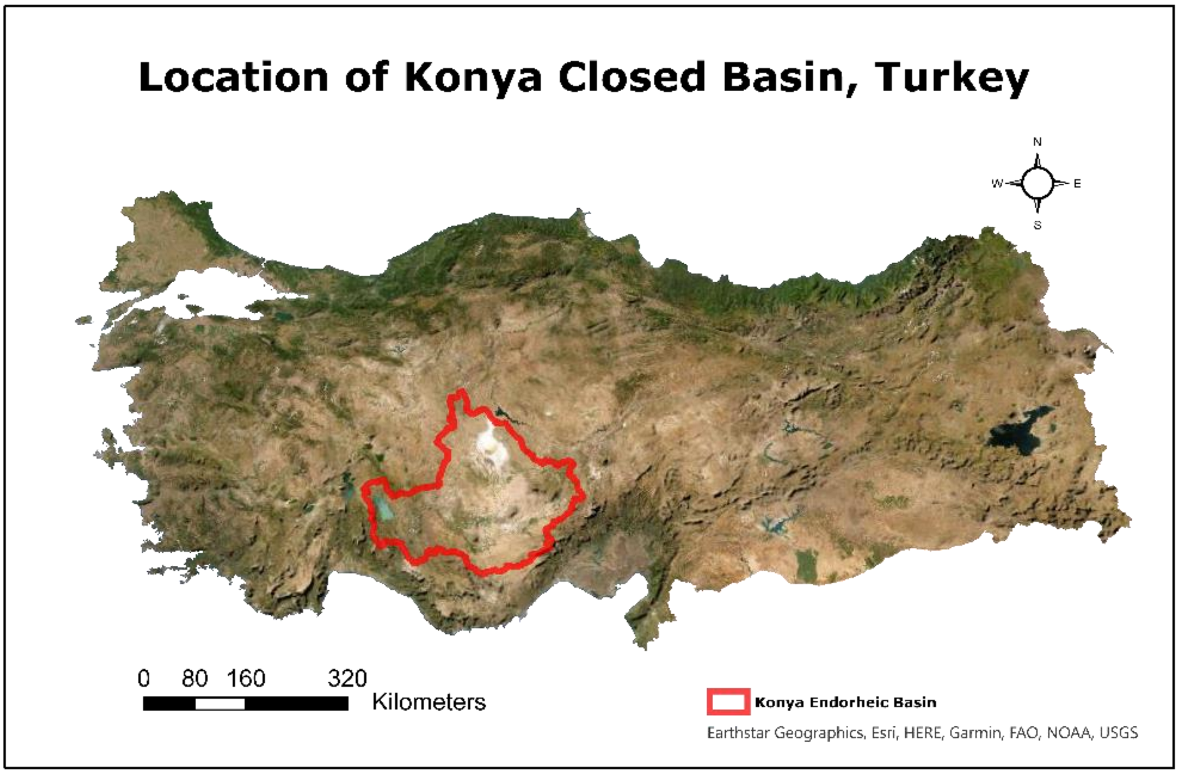

Acknowledgement: Map of Konya Closed Basin is obtained from 4th Regional Directorate of State Hydraulic Works thanks to research that is supported by the PRIMA programme under grant agreement No1923, project InTheMED. The PRIMA programme is supported by the European Union

Figure 3.1. Location of Konya Closed Basin.

The region is well known for its significant agricultural production potential; KCB has been referred to as “the granary of the country” by the Turkish people because of the reputation it has as the main grain – especially wheat – production hub in Turkey. Historically, agriculture has been the dominant sector for livelihood, and the majority of the industry has developed around agricultural production as well.

Farmers adopted irrigated farming in the 1960s and the main source of irrigation has been groundwater since then; the region went through the silent revolution along with the rest of the world. Before groundwater utilization, dry farming had been the dominant practice, because the basin holds 17% of all groundwater resources in Turkey and only 2% of the surface water resources (WWF, 2014).

3.1. Main Issues

Since the mid-20th century, governments – regardless of their political views – have followed policies that led to the increase in agricultural water demand. There are two main drivers of the said increase: the expansion of the total irrigated land, and the change in the crop pattern.

3.1.1. Expansion in Total Irrigated Land

The area of irrigated land has been increasing since irrigation practice was first adopted in the basin. According to the report by WWF (2014), one-third of the total farming land (890.000 ha) was irrigated in the early 2010s, and the rest (1.995.417 ha) was dry-farmed. In parallel with the past governments, the current government aims to increase the irrigated land up to 969.000.

3.1.2. Changes in the Crop Pattern

Summer crops (referred to as “green plants” by locals in KCB) such as corn, sugar beet, potatoes, etc. have a higher water requirement compared to grains that are grown in the winter season. Additionally, the uneven distribution of the precipitation allows grains to benefit from the winter precipitation, while the summer crops do not provide yield unless irrigated, during the dry summer period. Therefore, the transition in crop pattern from winter grains to summer greens is one of the main drivers of the increase in agricultural water demand.

The first summer plant to appear in the KCB was sugar beet. It first entered the crop pattern during the mid-20th century and has been recognized as one of the basin's primary crops by the 21st century. Over time, the food sector developed around the production of sugar beets; sugar refineries were set up, followed by fast-moving consumer goods (FMCG) companies in the food industry. For instance, Konya Şeker, one of the country's largest industrial conglomerates today and one of Turkey's oldest sugar refineries, began operations in 1954. Various stakeholders define the settling of sugar beet and related industry as an irreversible lock-in process, not only because of the economic development it brought to the region but also because of the sentimental loyalty the locals have for sugar beet production.

Then, in the early 2000s, the production of other summer plants such as corn, sunflower, potato, beans, and fruits started. Within a couple of years, corn became the most popular among those for three prominent reasons:

(A) Corn brings a satisfactory income to farmers. Although lately, some farmers argue that the profit of corn is more or less equal to that of wheat, because of the high input factor costs (especially water and fertilizer).

(B) Corn is a low-maintenance plant; growing corn does not require high farming skills or much labor. With drip irrigation technology, corn cultivation is very mechanical.

(C) Corn commerce is favorable for farmers because the industrial standards for marketing are easy to measure, and one of the largest agricultural stock exchanges is located in Konya. In addition, many farmers own livestock and some of them do not even need to market their corn as they use it for animal feed.

3.2. Changes Driven by the Increase in Water Demand and Current Status

Expansion in irrigated land and the transition in the crop pattern from winter crops to high water-demanding summer crops increased the overall agricultural water demand. Consequently, the decrease in the groundwater table started in the 1980s, and it has been decreasing ever since. However, the most severe drop in the water table has occurred in the last 10-15 years; when farmers first started irrigating their crops, they were able to get water from hand-dug wells. Nowadays, in some cases, they dig 400 meters and cannot find any water.

Currently, the most water-demanding sector is by far agriculture; the Ministry of Agriculture and Forestry estimated that up to 90% of water resources are used for irrigation purposes (T.C. Tarım ve Orman Bakanlığı Su Yönetimi Genel Müdürlüğü, 2018). Irrigation water demand is followed by drinking and domestic water demand, which is approximately 8% of the total water use.

3.2.1. Number of Wells

The increase in water demand was accompanied by a boom in groundwater wells. The more water farmers wanted to extract; the more wells were opened because the existing infrastructure fell short of demand. However, farmers complain that the bureaucratic process to get a groundwater well license is too long, therefore unlicensed (illegal) wells mushroomed around the basin over 3 decades. DSİ (State Hydraulic Works of Turkey) made an inventory study in which they identified 66.800 unlicensed wells. Today, the stakeholders estimate that there are more than 100.000 unlicensed wells in the basin.

3.2.2. Shifts in Irrigation Technology

The traditional method of irrigation in the basin was flooding the field. However, this method causes significant water loss. In an attempt to use irrigation water more efficiently, farmers first adopted sprinkler irrigation in the early 2000s, which is significantly more efficient than flooding. Then, drip irrigation started spreading in the early 2010s, and currently, it is very prevalent in the basin.

Since the 2000s, governments have provided financial incentives to farmers for switching to higher-efficiency irrigation methods. However, lack of training on how to use these results in the improper use of irrigation equipment; therefore, whether higher-efficiency technologies are helping save water is ambiguous.

3.3. Proposed Solutions

3.3.1. Land Consolidation and Adoption of Modern Irrigation Technologies

All stakeholders uniformly agree that land consolidation and transition to higher-efficiency irrigation methods are required to reduce the overall water demand in the basin. Through land consolidation, patchworked lands are aggregated, parcels are formed into appropriate shapes, machinery use, and irrigation investment costs are reduced, water distribution becomes more efficient, and arable land is increased (Ankara Valiliği İl Gıda Tarım ve Hayvancılık Müdürlüğü, 2015).

Farmers have abandoned open-channel irrigation since the early 2000s, because of the high seepage and evaporation loss in water delivery channels. Such traditional irrigation is now only observed in smaller areas where farmers irrigate with surface water or treated wastewater. Other than that, the prevalent practice is to use pressurized irrigation systems; sprinkler irrigation for winter crops (grains) and sugar beet, and drip irrigation for corn and other summer crops (sunflower, beans, etc.). This transition has been supported by the state since the 2000s with cheap loans.

While land consolidation and adoption of pressurized irrigation are almost completed in the basin, the current agenda of many farmers is sub-surface drip irrigation. Even though there are not yet any state incentives for that infrastructure and many farmers find investing in it unaffordable, sub-surface drip seems to be the next step in the advancement of irrigation technology in KCB.

3.3.2. Change in Agricultural Crop Pattern

The ratio of irrigated land over the total agricultural land has been increasing in recent decades. Many stakeholders find reducing the agricultural water demand by means of going back to traditional, less water-demanding winter crops necessary. To achieve that, managers of some large irrigation cooperatives that have higher institutional power enforce a mandatory crop rotation; farmers are expected to rotate between winter and summer crops every year, so they cannot grow high water-consuming summer crops multiple years in a row.

Additionally, in 2017, the Ministry of Agriculture and Forestry launched the Basin-Based Financial Incentives Project to encourage the production of several crops, including but not limited to wheat, barley, corn, sunflower, potato, and so on. The ministry provides financial support for seed and fuel, and deficiency payments for the undertaking. The agricultural products that should be promoted in each basin are chosen based on the climate, landscape, soil composition, water shortage, crop rotation, and suggestions from regional offices and non-governmental organizations. As of 2021, barley, wheat, corn, canola, beans, sunflower, potato, and chickpea are supported crops for Konya. However, due to water constraints in various Konya regions (such as Çumra, Karapınar, Kulu, Cihanbeyli, and Altnekin), drip irrigation is a requirement to receive financial assistance for corn.

3.3.3. Inter-Basin Water Transfer

To manage the water supply in the basin, many stakeholders argue that inter-basin water transfers are requisite. The most favored project is the Blue Tunnel (Figure 3.2), which will transfer annually 414 million m^3 of water from the Göksu River to the Çumra region, in the south of the basin. However, many oppose the project for various reasons: Despite being a financially burdening project, it would only fulfill 1/40 of the water demand in the basin (WWF, 2014). Moreover, there are some disputes on the ecological impact on both the supplying and receiving basins. The construction of the Blue Tunnel project started in 2009, but it is not yet completed. Around 100 million m^3 of the planned 414 million is being transferred, but that water is used for drinking and domestic purposes, not irrigation.

Currently, water from Beyşehir Lake is being transferred to the Çumra region in the basin through the Apa Dam. While surface water supply from Lake Beyşehir does not have a significant impact in reducing the stress on the groundwater resources of the whole basin, it compensates for a substantial proportion of groundwater demand in the Çumra region.

Figure 3.2. Map of the Blue Tunnel Project.

3.4. Çumra, Konya

Konya Closed Basin is one of the largest watersheds in Turkey; it occupies more than 5 million hectares (7% of the country), distributed over 7 cities (T.C. KOP Bölge Kalkınma İdaresi Başkanlığı, 2016). Both geographical attributes such as climate, water accessibility, availability, the existence of surface water bodies, topography, and social-economic attributes such as crop choice, irrigation infrastructure, and farmer demography vary within the basin. Therefore, focusing on a smaller unit of the basin was necessary for this study. During our first two field campaigns, we conferred with the stakeholders on which region to choose for this modeling activity. Most stakeholders suggested that we focus on the Çumra district, located in the southern part of the basin (Figure 3.3), mainly for two reasons: First, Çumra has a rich history of agricultural production. Since the 1960s, Çumra has had a pioneering role in agriculture in terms of its innovativeness and institutionalism. Some of the oldest irrigation cooperatives are located in Çumra; for example, the İçeriçumra Irrigation Cooperative was founded in 1954. Second, Çumra is considered “lucky” by all stakeholders because the region has access to surface water resources, which reduces the pressure on groundwater resources. This implies that stakeholders are more hopeful for Çumra than the other parts of the basin – especially the northern districts where the drop in the groundwater table is the most severe. After having visited different parts of the basin and having consulted the stakeholders, we chose to focus our efforts on Çumra, parallel to the stakeholders’ suggestions.

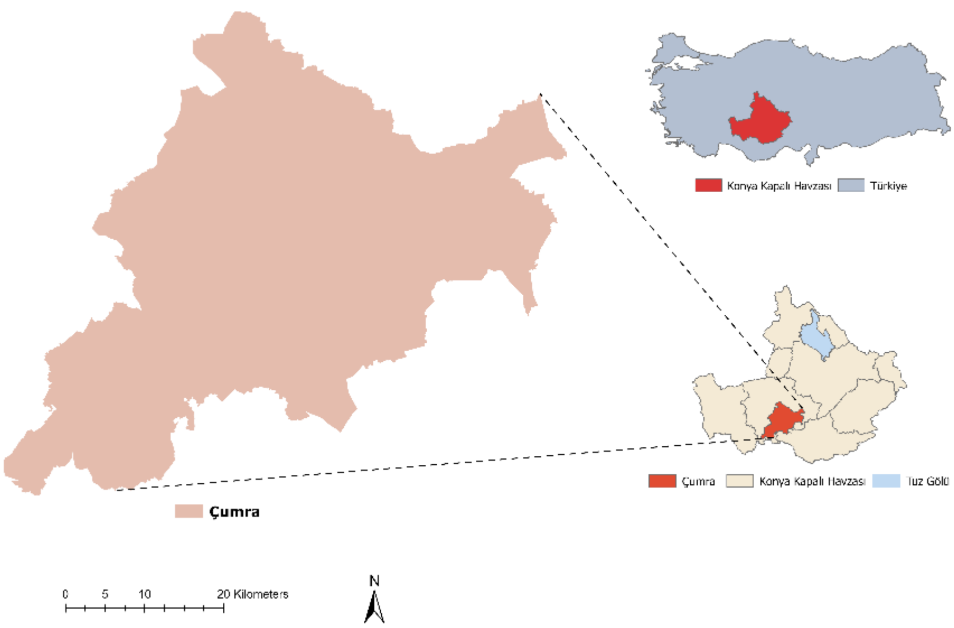

Figure 3.3. Location of Çumra district within the basin.

4. METHODOLOGY

Various modeling methods are commonly adopted in scientific research to investigate a problem and find feasible solutions (Barlas, 2002). “Model” is an umbrella term encompassing a wide range of modeling approaches that differ from one another in multiple dimensions: First, a model can be physical, such as scaled models of famous landmarks, or symbolic, such as diagrams or mathematical formulations. Another distinction is descriptive versus prescriptive models. Descriptive models aim to describe the emergence of the problem by examining the relationship between system variables. Prescriptive models are usually optimization models that operate to reach a certain goal, defined as an objective function. Models can also be classified as static or dynamic; while the former focuses on static relationships between variables, the latter produces insights into how variables change over time. Dynamic models further branch into two categories: discrete and continuous models. Within the broad range of modeling approaches, System Dynamics (SD) can be categorized as symbolic, descriptive, and dynamic. SD models can either be time discrete, continuous, or hybrid, based on the purpose of the research.

4.1. System Dynamics

The SD approach aims to identify the root causes of problematic dynamic behaviors or trends in complex systems, determine the structural basis for such behavior, and identify and test the leverage points within the system to stop or reverse the undesirable trend (Stave, 2010). To that end, SD adopts a “systemic thinking” philosophy and an endogenous feedback perspective, for “*Dynamic management problems in real life are typically feedback problems…*” (Barlas, 2002, p.1133). An endogenous perspective implies that the internal structure of the system generates the observed behavior; therefore, in SD, the main purpose is to capture the feedback structure by correctly identifying the causal relationships between the system variables and between human interventions and the system’s reaction, and not mere correlations; so that the model produces the observed behavior patterns, for the right reasons.

Causal loop diagrams describe the causal relationships and internal feedback mechanisms in a system. The arrows between the variables show the direction of the relationship; they are pointed from the cause variable to the affected variable, and the polarity of the arrow indicates the type of the causal relationship: The plus sign indicates a positive relationship, which means that the direction of the change in the affected variable is the same as the cause variable. In other words, other things being equal, if the cause variable increases, so does the affected variable, and vice versa. On the other hand, a minus sign indicates a negative relationship, which means that the direction of change in the cause and affected variables are expected to be opposite; other things being equal, if the cause variable increases, the affected variable decreases, and vice versa.

More often than not, the mutual causal relationships between multiple system variables form circular feedback connections or loops. The causal feedback loops also have polarities; they can be positive (reinforcing) or negative (balancing) loops. In reinforcing loops, the change in one direction is furthered and the change is compounded by the loop. In contrast, balancing loops damp the change in any direction. Examples of reinforcing and balancing loops are shown in the causal loop diagram in Figure 4.1. B1 balancing loop shows that other things being equal, if the groundwater table increases, so do the average well yield and extraction. However, increased extraction decreases the groundwater table, thus, the initial change in the groundwater table is countered by the balancing loop. On the other hand, the R1 reinforcing loop shows that other things being equal, an increase in the groundwater table increases the average well yield, therefore decreases the required number of active wells and the number of active wells. Due to fewer active wells, the annual groundwater extraction capacity decreases, and so does the extraction. When the extraction decreases, the groundwater table becomes higher than it would otherwise be, thusly the initial change in the groundwater table is amplified by the positive loop.

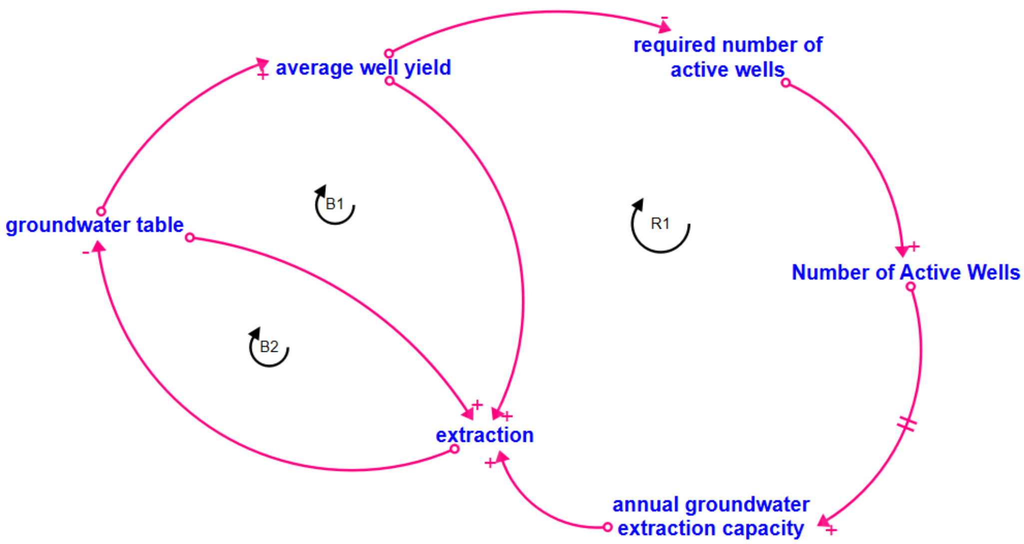

Figure 4.1. Exemplary causal loop diagram (CLD).

While CLDs provide valuable insight into the feedback relationships operating within the system, in quantitative SD research, the relationships between system variables are mathematically described, and appropriate stock-flow structures are developed to identify and incorporate significant feedback loops (Andersen, Vennix, Richardson, & Rouwette, 2007). Stock variables are accumulations, they may build up or dissipate over time. They provide the required information about the state of the system and are key indicators upon which the decisions are based (Sterman, 2000). Flow variables are the rate of change in stock variables; based on their nature, they can either be inflows, always increasing the stock, outflows, always decreasing the stock, or biflows, which may either increase or decrease the stock. By convention, stock variables are represented with rectangles and flow variables are depicted as pipes with arrowheads indicating the type of flow.

Figure 4.2. Illustration of a simple stock-flow structure.

For example, the basic stock-flow example illustrated in Figure 4.2 shows that the number of groundwater wells increases with well digging and decreases with well closing. Therefore, the net change in the number of operating groundwater wells is governed by the following equation (Sterman, 2000):

$$\frac{d(Stock)}{dt} = Inflow(t) - Outflow(t) \tag{4.1}$$

The main steps of a system dynamics study are as follows (Barlas, 2002):

- Problem Identification

Problem identification and articulation are crucial for an SD study. The problem of interest should be of a dynamic and feedback nature; externally driven problems are not appropriate for SD methodology. In this first step, all the available data is plotted to examine the dynamic behavior patterns and determine the reference behavior of key variables of interest.

- Dynamic Hypothesis and Model Conceptualization

In the second step, a dynamic hypothesis, a conceptual model that may explain the observed dynamic behavior, is developed. The major tasks are determining the drivers of the dynamic behavior, listing the relevant variables, examining the causal feedback relationships between those, creating causal loop diagrams, and identifying the main stock and flow variables.

- Formal Model Construction

In this step, the model structure (the stock-flow diagram) is constructed, mathematical formulations for all variables are written, and the stock initial values and parameter values are estimated. Lastly, model consistency is tested for internal consistency and also against the dynamic hypothesis for verification.

- Model Validation

Validation is required to build credibility in the model. An SD model should be validated both structurally and behaviorally: Structural validation tests assess whether the model structure can represent the relationships between the variables in the real system correctly, and behavioral validation tests check how well the pattern match is between the simulated behavior of system variables and the real-life data.

- Analysis

For model analysis, sensitivity tests are performed; the model is tested with different parameter values and stock initials to explore the responsiveness of the outputs to selected variables. These tests provide a deeper understanding of the important dynamics in the model.

- Design Improvement

Once the model is validated and analyzed, new policies and scenarios can be designed and tested on the model. The purpose of this step is to identify high-leverage, favorable policies that can help alleviate the problem identified in the first step.

- Implementation

The final step of an SD study is to implement the most feasible and favorable policies in real life. Eventually, the success of the study is best measured by the level of improvement in the behavior of key system variables after the suggested policy is implemented.

4.2. Group Model Building

Involving stakeholders is preferable in practical sustainability research. Scholars of system dynamics developed an approach named Group Model Building (GMB) in the 1980s to incorporate stakeholders in the research process. GMB, in its broadest sense, is a collection of methods for creating dynamic simulation models to aid decision-making by involving those who stand to gain or lose from the decision's outcome (Andersen et al, 2007). GMB aims to discover the potential leverage that stakeholder participation brings to the table, by including them in the model-building process from the beginning phase with problem identification to the end with policy analysis (Hovmand, 2014). Researchers find the opportunity to elicit stakeholders' beliefs, knowledge, ideas, and mental models through a facilitated GMB process, and help build a collective understanding of the linkages between system components so that the strategies proposed to manage the system will advance (Richardson & Andersen, 2010; Sterling et al, 2019). Also, the GMB process may foster a sense of ownership of the model among stakeholders, particularly non-experts within the group; they are likely to feel empowered as they see their opinions and knowledge being fed to the model. As a result, a higher level of compliance with the shared decisions may be achieved following the model experimentation phase and once the stakeholders are familiar with the potential outcomes of selected courses of action (Pahl-Wostl, 2008). Moreover, GMB attempts to bridge the gap between local and scientific communities by combining different knowledge systems; the process is fed by a formal analysis and empirical data as well as subjective knowledge and stakeholder perceptions of the dynamics of the system.

By definition, GMB is a specific method of participatory modeling, developed to build system dynamics models for decision-making by including stakeholders in the process, by way of carefully designed scripts and heuristics. GMB has four main components: namely, the participants, the team, the scripts, and the boundary objects.

4.3. Study Design

Table 4.1 outlines the main steps of the study. After having selected the study site as Konya Closed Basin, we conducted a rigorous literature review to familiarize ourselves with the region, before the first field campaign. We reviewed 50+ documents including scientific publications, national legislation on water, national and regional water management plans, publications by relevant environmental and agricultural NGOs, annual activity reports by public institutions, and grey documents. This desktop study provided us with a general overview of the groundwater-related issues in the Konya Closed Basin, relevant stakeholders, and management practices; yet still, there were some information gaps that we could only eliminate in the field. Therefore, we performed a stakeholder mapping exercise to pre-identify key stakeholders (Murray-Webster & Simon, 2006) and organized two field trips in March 2021, and July 2021. During these two first field trips, we met 31 and 33 people respectively, from state institutions, irrigation cooperatives and unions, local farms, and agricultural NGOs. We made semi-structured interviews (Whiting, 2008) and eliminated the information gaps regarding the following: information flow and communication in the social network, locale-specific groundwater resource state and agricultural practices, data availability and accessibility, rule enforcement, level of participation in groundwater management, and perspectives of various stakeholders on contentious groundwater-related topics. In doing so, we also created a network of stakeholders for the upcoming stages of the study, introduced the researchers, and built trust in the research.

We held the first participatory modeling workshop on September 30, 2021, in Konya city center with 26 stakeholders from 14 different institutions. We had two main goals for this workshop: to build consensus around the framing of the ‘wicked’ issue of unsustainable groundwater use in the region and to provide a preliminary evaluation of the solution alternatives favored by the stakeholders. Before the workshop, we made use of *Scriptapedia* (n.d.) and designed suitable divergent and convergent activities for the day.

Towards the second workshop, we iterated on a conceptual model to identify the model boundaries concerning the problem and collected data to verify the qualitative reference behavior patterns that resulted from the first workshop.

We held the second participatory modeling workshop on February 17, 2022, in Konya city center with 20 stakeholders from 10 different institutions who already joined the first workshop. The purpose was to build conceptual maps and seed models that would explain the emergence of identified problems and to qualitatively analyze the potential response of the system to the solutions proposed in the earlier phases of this study. The second workshop yielded a seed model that we developed into a formal model in the following year.

After having finished building the formal model after the second workshop, we revisited 10 prominent stakeholders from 5 different institutions, who had attended the first two workshops, to validate the formal model on January 16-18, 2023. In these visits, we presented them with a model interface on which we simulated model-based scenarios and made policy analyses.

Table 4.1. Summary of the study activities.

Activity	Dates	Purpose
Desktop Search	November 2020 – March 2021	Familiarization with the study area, legislation, and groundwater management practices
1st Field Campaign	March 23-26, 2021	Familiarization with the stakeholders, snowballing, stakeholder mapping
2nd Field Campaign	July 4-9, 2021	Further snowballing, workshop organization
1st Workshop	September 30, 2021	Trust building, dynamic problem identification
2nd Workshop	February 17, 2022	Conceptual model development
Modeling	October 2021 – March 2023	Model development, validation, analysis
3rd Field Campaign	January 16-18, 2023	Model testing and validation
3rd Workshop	March 21, 2023	Model-based policy analysis

After having evaluated the feedback we received from the stakeholders in the final field campaign, we put the interface in its final form and organized the third and final workshop on March 21, 2023. 28 people joined the workshop, 15 of whom had been following the research since the first field campaign in March 2021. In the final workshop, participants had the opportunity to explore the model interface and simulate the impact of various policy proposals on key system variables.

5. MODEL DESCRIPTION

In this section, the dynamic simulation model is presented in detail. An overview of the model is provided, followed by a detailed explanation of each model sector, including the key variables, structure, and equations. Causal loop diagrams and stock-flow diagrams are presented where relevant.

5.1. Model Overview

The purpose of the model is to aid its users in formulating policies for favorable groundwater resource management schemes. To that end, the model simulates the change in the hydraulic head in the Çumra district, mainly driven by the extraction for agricultural irrigation, as well as agricultural and economic outputs, under certain environmental and socio-economic conditions and policy settings. Figure 5.1 shows the conceptual map of the model.

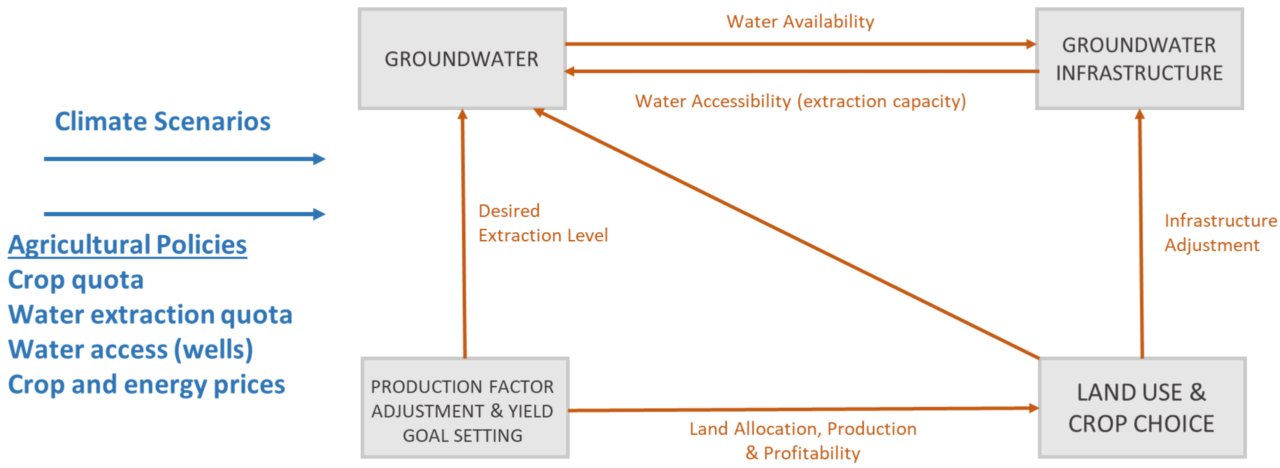

Figure 5.1. Conceptual map.

The model was developed on *Stella Architect.* The time unit of the model is years, the simulation horizon is 40 years from 2004 to 2044, and the computational time step is 0,03125 (1/32). The selected integration method of the model is Euler's.

5.1.1. Model Assumptions

Due to a lack of complete and reliable information regarding the sub-surface aquifer geometry, the model assumes that the aquifer beneath Çumra is uniform and cubic, as does the spatially disaggregated, MODFLOW based hydrogeological model (Yoloğlu et al, 2023) further used as a reference for model validation in this research.

The decisional agent in the model is the average farmer, i.e., the differences between farmers (land size, land ownership, active family labor force, and other social differences such as age, educational background, etc.) are overlooked. Our experience in the field showed us that such differences do not impact the decision-making process of the individuals (regarding the major decisions endogenized in the model) at a level that would yield significant divergence in the behavior of the key output variables.

The total arable land is assumed to be constant in the model. However, a portion of the total arable land might be bare in any year because of the fallowing practice in rainfed (non-irrigated) agriculture. In addition, while there are plenty of crop varieties grown in Çumra, crops are grouped under 3 categories for convenience, based on agricultural regulations and crop characteristics such as the water requirements and the season the crops are planted in. The first group of crops is green plants. These are summer crops with high water demands, such as corn, sunflower, trefoil, potato, and beans, and they require irrigation to provide yield. The second crop is sugar beet. Even though it shows similar crop characteristics to other green plants, it is represented in a separate group by itself. That is because sugar beet is cultivated once every four years in the region, as farmers say it drains the nutrients in the soil if cultivated in consecutive years. The third crop group consists of winter cereals, such as wheat, barley, rye, etc., that require less irrigation both because they have a lower water demand compared to green plants and also, they are grown in the rainy winter season. Farmers may either irrigate winter cereals or not; if they do, they receive higher yields in return for the additional irrigation cost and do not need to fallow their land in the following year. If they do not irrigate, they usually receive lower yields and need to fallow their land so that the soil can reaccumulate its water content. Provided that, the model assumes 5 different crop-land use options, as follows: green plants, sugar beet, irrigated cereal, rainfed cereal, and fallow.

5.1.2. Main Feedback View

Figure 5.2 presents the overview of the reinforcing (growth) and balancing (limit) feedback loops. One of the most important decisions included in the model is how much to irrigate each crop. Farmers obtain higher yields when irrigating a crop more, increasing their revenue and profit. However, as they extract more groundwater from the aquifer, the groundwater table declines, and the energy cost of pumping increases, therefore the profit decreases. The second major decision in the model is land allocation; the total land available for agriculture is assumed to be constant throughout the simulation period, and farmers decide how much land to spare for each crop-land use option in the model, based on the relative attractiveness of crops. In the most general sense, farmers' primary goal is to maximize their profits; therefore, the attractiveness of each crop type depends on their profitability. Ultimately, the *desired groundwater extraction* depends on how much the farmer decides to irrigate per crop, and how much land is allocated to each crop. These relationships are presented in the R1 and B1 loops in Figure 5.2. While the former fosters extraction, the latter puts a financial feasibility limit on extraction. On the other hand, increasing costs is not the only limitation to ever-increasing extraction. First, there is a natural limit: if the water in the aquifer is finished, further extraction is not possible as is presented in the B2 loop. Furthermore, the maximum possible extraction is also capped by the capacity of the pumping infrastructure at hand, such as the groundwater wells and the average pump power. One cannot extract infinitely from a well in a given period; the *annual extraction capacity* is determined by the number of active wells and average well yield. Other things being equal, when the groundwater head declines due to extraction, the average well yield decreases, as depicted in B3 loop. Therefore, whenever the existing infrastructure fails to satisfy the demand, more wells are dug, and the pump power is increased to fulfill the demand (R2 and R3 loops).

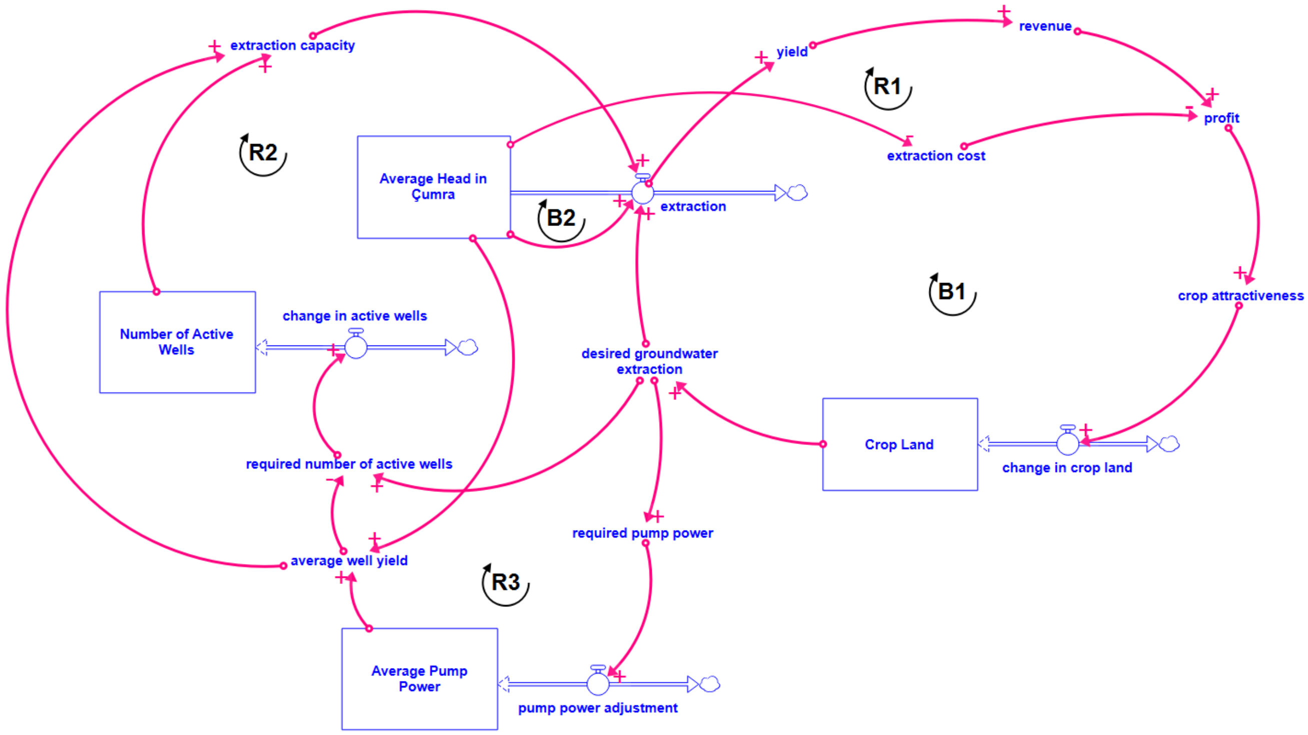

Figure 5.2. Feedback overview of the model.

5.2. Sector Descriptions

5.2.1. Water Resources and Groundwater Infrastructure Sector

The water resources and groundwater infrastructure sector consists of 4 stock and 8 flow variables. This sector has 3 reinforcing and 3 balancing feedback loops; Figure 5.3 shows the causal loop diagram.

The first balancing loop (B1) in this sector explains the relationship between extraction and groundwater extraction capacity. As extraction increases, the hydraulic head, i.e., the groundwater table decreases, leading to lower well yields (defined as the amount of water that one can pump from a well in a year). Therefore, the annual groundwater extraction capacity decreases and limits the extraction.

The second balancing loop (B2) shows the natural limits of extraction. Extraction lowers the hydraulic head in Çumra, and if the groundwater in the aquifer is depleted, there can no longer be any extraction.

The relationship between the hydraulic head in Çumra and the lateral flow is represented in the third balancing loop (B3). As the hydraulic head in Çumra increases, the amount of water flowing into Çumra underground decreases, and vice versa.

The first reinforcing loop (R1) shows the relationship between extraction and well-digging decision. When the extraction increases, the head in Çumra, thus the groundwater table decreases, resulting in lower well yields, as explained above. Therefore, more wells are required to be able to supply the desired groundwater extraction. Well-digging accelerates; thus, the number of active wells increases and compensates for the capacity reduction arising from lowered well yields.

Another way to compensate for the decreasing well yields due to increased extraction is to use higher power pumps. The second reinforcing loop (R2) shows that as the groundwater table decreases, the required power to pump the same amount of water in the same amount of time increases. Accordingly, the average pump power is adjusted; the well yields and the annual groundwater extraction capacity increase again, allowing for higher extraction.

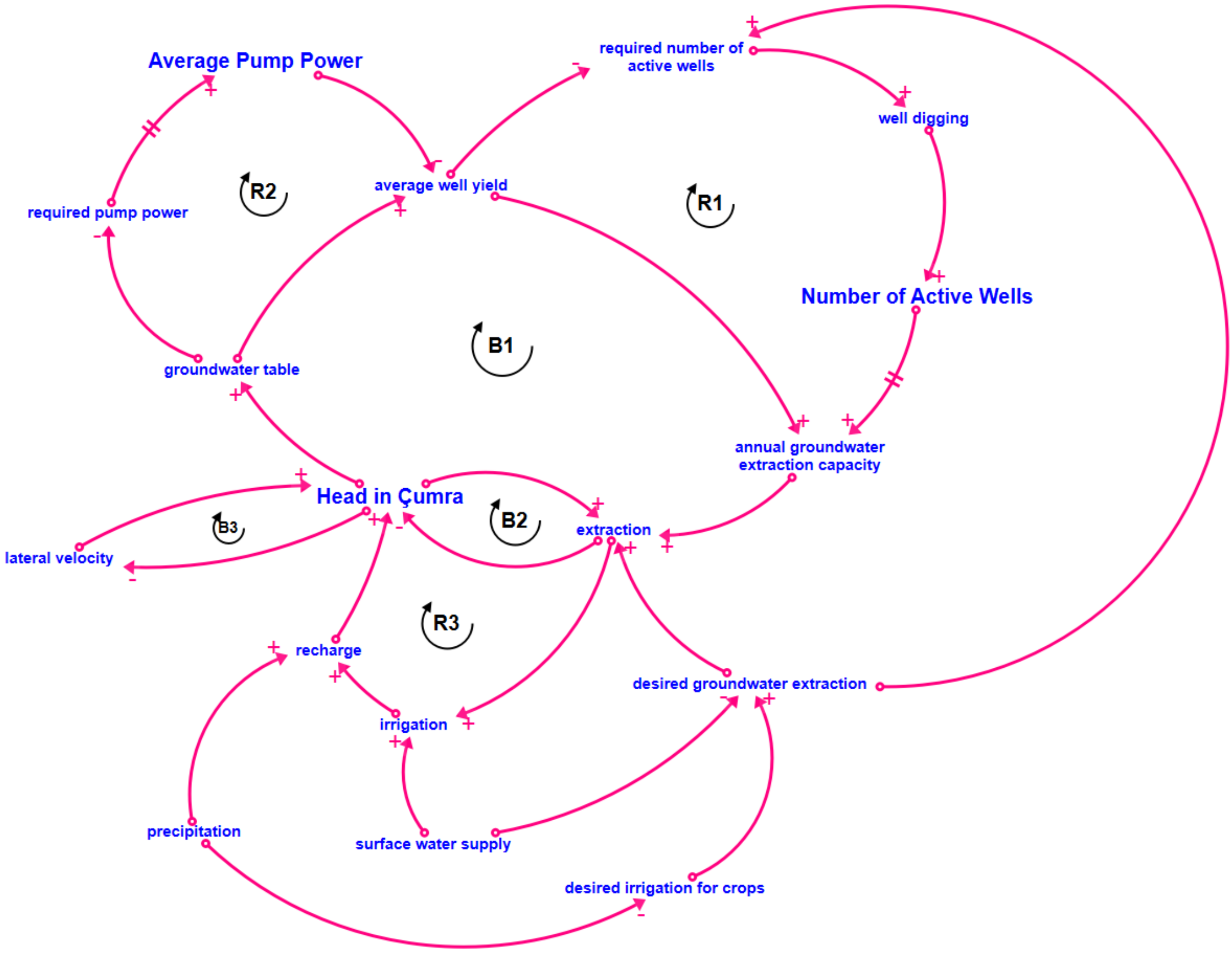

Figure 5.3. Causal loop diagram of water resources and groundwater infrastructure sector.

The third reinforcing loop (R3) explains the relationship between irrigation and recharge. An increase in extraction means a higher level of irrigation. Therefore, more water used for irrigation is recharged back into the aquifer.

Figure 5.4 shows the simplified stock-flow structure of the water resources and groundwater infrastructure sector. While in the model water resources and groundwater infrastructure is developed under the same sector, we find it more convenient to discuss the model formulations separately for the two sub-sectors, for clarity and simplicity.

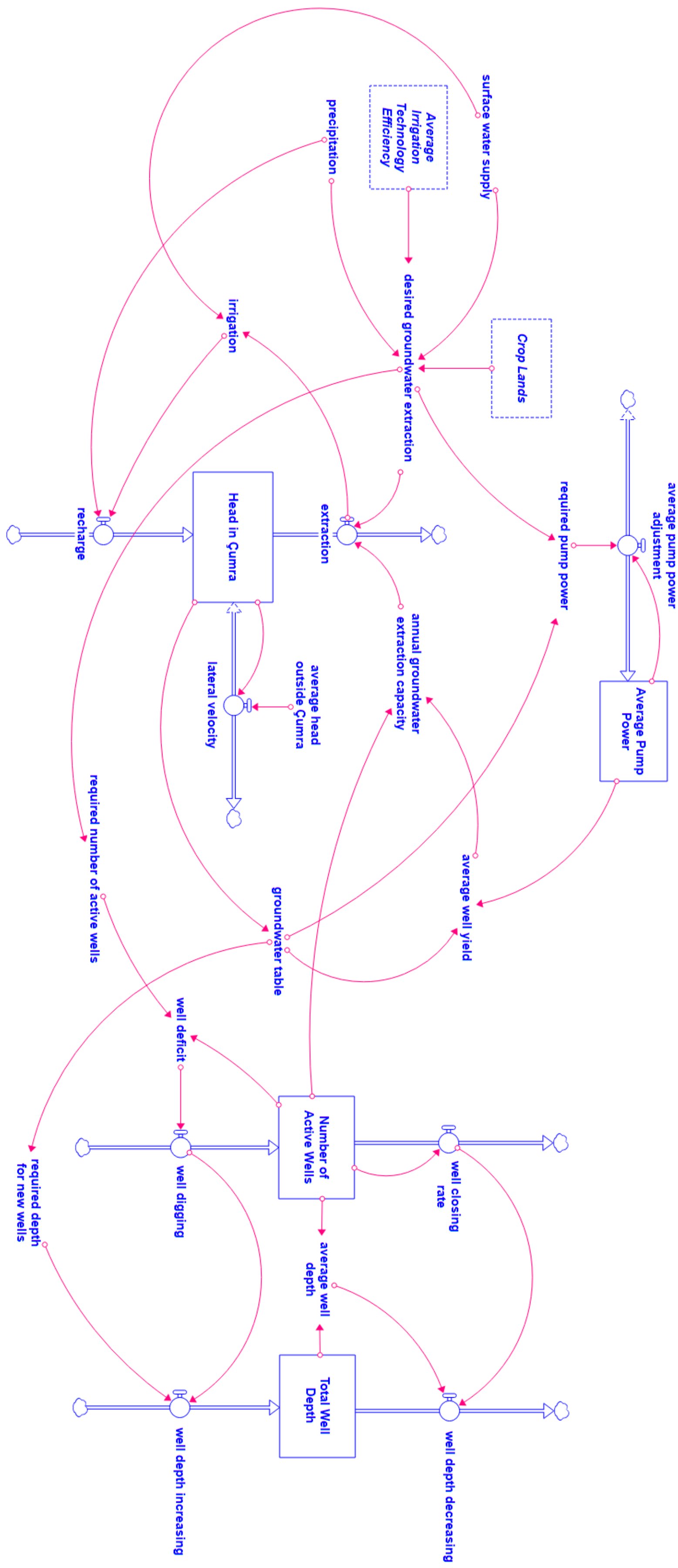

Figure 5.4. Simplified stock-flow structure of water resources and groundwater infrastructure sector.

5.2.1.1. Water resources sub-sector. Table 5.1 lists the water resources sub-sector's main stock and flow variables.

Table 5.1. Stock and flow variables of water resources sub-sector.

Stock Variables	Units
Head in Çumra	m
Flow Variables	**Units**
Extraction	m/year
Recharge	m/year
Lateral Velocity	m/year

Head in Çumra

Head in Çumra represents the average hydraulic head in Çumra, which is the altitude of the groundwater table above the sea level; therefore, its unit is meters (m). It accumulates with lateral inflow (m/year) and recharge (m/year) flows and depletes with extraction (m/year) and lateral outflow (m/year). The equation for the Head in Çumra is down below:

$$\frac{d(Head\ in\ Çumra)}{dt} = recharge + lateral\ velocity - extraction \tag{5.1}$$

While Head in Çumra is selected to be the main stock variable in this sector, most of the calculations in the model are based on the depth of the groundwater table from the soil surface. The reason why the hydraulic head is chosen as the stock instead of the groundwater table itself is that we mainly use the head variable for the validation of this sector (please see section 6). Therefore, calculating the depth of the groundwater table based on the hydraulic head is necessary. As can be inferred from the below equation, we assume the ground level (soil surface) to be 0, so the groundwater table (m) is always negative (or 0 at its theoretical maximum).

$$groundwater\ table = -(ground\ elevation - Head\ in\ Çumra) \tag{5.2}$$

Extraction

Extraction is the main outflow that drives the decline in the groundwater table. Two factors determine the level of extraction: groundwater demand, and groundwater supply capacity that caps the maximum possible extraction. Therefore, extraction is formulated as follows:

$$extraction = \frac{\boldsymbol{MIN}(annual\ groundwater\ extraction\ capacity\ ; desired\ groundwater\ extraction)}{aquifer\ surface\ area\ \times porosity} \quad (5.3)$$

The MIN built-in is used to ensure that if the groundwater demand exceeds the supply capacity, extraction does not exceed the capacity. Additionally, both annual groundwater extraction capacity and desired groundwater extraction are calculated in m^3/year, therefore we divide the output of the MIN function by the aquifer surface area to obtain extraction as m/year. We also divide it by the porosity to calculate the absolute height of water withdrawn from underground.

Annual groundwater extraction capacity is determined by the number of active wells and average well yield, which is defined as the volume of water that can be obtained from a single well within one irrigation season, given the average pump power. Its unit is m^3/well/year, and it is calculated as in Equation 5.4. In the equation, the unit energy requirement represents the amount of energy required to lift 1 m^3 of water 1 meter (kW*H/ m^3/m). The effect of the groundwater table on well capacity is inputted in the model as a table function and ensures that as the groundwater table approaches the aquifer bed depth, the average well yield decreases (Figure 5.5). In other words, if the aquifer is close to depletion or depleted, the average well yield will approach 0.

$$annual\ groundwater\ extraction\ capacity = average\ well\ yield\ \times Number\ of\ Active\ Wells \quad (5.4)$$

where,

$$average\ well\ yield = effect\ of\ gw\ table\ on\ well\ capacity \times \frac{Average\ Pump\ Power\ \times pump\ efficiency\ \times irrigation\ period}{-(unit\ energy\ requirement\ \times groundwater\ table)} \tag{5.5}$$

On the other hand, desired groundwater extraction is calculated as the difference between the total desired irrigation and surface water supply (Equation 5.6). Total desired irrigation is the sum of the desired water application (m^3/year) for all crops.

$$desired\ groundwater\ extraction = \boldsymbol{MAX}(0\ ; total\ desired\ irrigation\ - surface\ water\ supply) \tag{5.6}$$

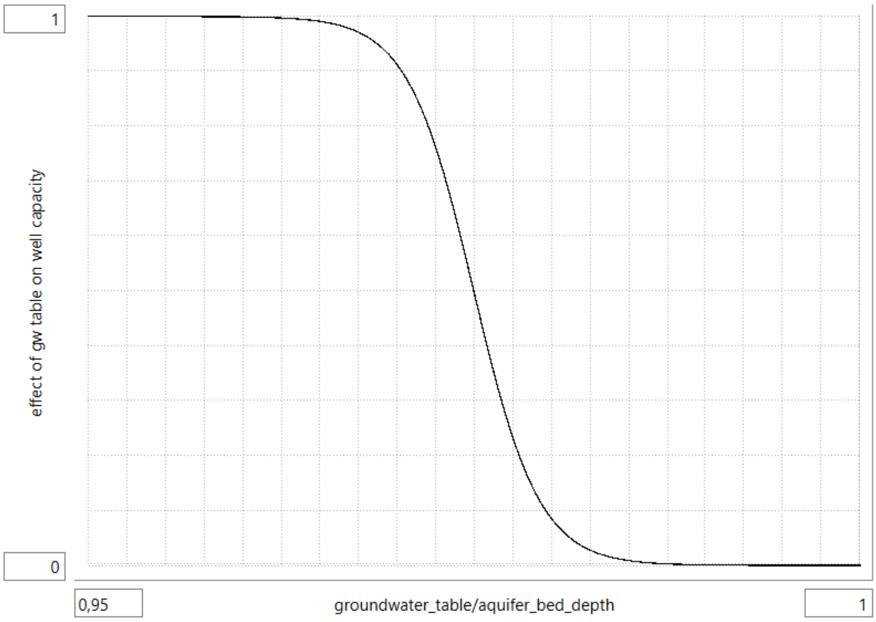

Figure 5.5. Table function: effect of groundwater table on well capacity.

The level of desired effective irrigation (m/year) is determined in the production factor adjustment and yield goal-setting sector, then the desired water application (m^3/year) is calculated in volume, according to crop-land size and the average irrigation technology efficiency (Equation 5.7). It should be noted here that the variables in the below equation (except for the Average Irrigation Technology Efficiency) are arrayed and have four dimensions, representing the four crop-land use options, namely: irrigated cereal, greens, sugar beet, and rainfed cereal. The array name is

Crops, and the same array is employed in other model sectors as well, as is explained later in this section.

$$desired\ water\ application = \frac{desired\ effective\ irrigation}{Average\ Irrigation\ Technology\ Efficiency} \times agricultural\ land \tag{5.7}$$

<u>*Recharge*</u>

Recharge is the penetration of water through the soil and into the aquifer. Even though the model is not a spatially distributed one, the recharge is calculated as the sum of recharge from unirrigated land, which refers to bare (fallow and non-agricultural) and rainfed cereal lands, and recharge from irrigated land, which refers to irrigated cereal, sugar beet, and green plants lands, over porosity, due to the fact that the recharge fraction varies based on the crop-land use type.

$$recharge = \frac{recharge\ from\ unirrigated\ land + recharge\ from\ irrigated\ land}{porosity} \tag{5.8}$$

The calculation of recharge from unirrigated land is simpler, given that there is no irrigation and only a fraction of the precipitation is recharged back into the aquifer. The equation is analogous for all unirrigated land use types.

$$recharge\ from\ bare\ land = precipitation \times recharge\ fraction\ for\ bare\ land \times bare\ land\ share \tag{5.9}$$

Calculating the recharge from irrigated land is more complicated; both irrigation and precipitation should be considered. However, the low time resolution of the model complicates the calculation because while precipitation is distributed throughout the year, plants are only irrigated during the growing season. The following equation is formulated to calculate the recharge from irrigated lands:

$$recharge\ in\ irrigated\ crop\ lands = precipitation\ return + growth\ season\ infiltration\ return \tag{5.10}$$

where,

$$precipitation\ return = precipitation\ \times precipitation\ return\ fraction\ \times land\ share\ of\ crop \tag{5.11}$$

and

$$growth\ season\ infiltration\ return = crop\ infiltration\ \times growth\ season\ recharge\ fraction \times land\ share\ of\ crop \tag{5.12}$$

Crop infiltration (m/year) refers to the water an irrigated plant receives during the growth season from both irrigation and precipitation, and it is calculated as the sum of effective precipitation (m/year), that is the amount of precipitation uptaken and used by the plant, and irrigation (m/year).

All the fractions are parameterized through a set of validation runs taken from the MODFLOW-UZFG model built to calculate the water budget of KCB (Yoloğlu et al, 2023). These tests are explained in detail in Section 6.

Lateral Velocity

Groundwater flow is driven by the potential energy; it moves from high elevation to low elevation. The following equation published in 1856 by Henry Darcy – today known as Darcy's Law – is used to calculate the flow of groundwater in a porous medium:

$$q = \frac{Q}{A} = -K \times \frac{dh}{dl} \tag{5.13}$$

where q is the specific discharge (Length/Time), K is the hydraulic conductivity (Length/Time), and dh/dl is the hydraulic gradient (unitless).

In the model, Darcy's equation is adapted as follows:

$$Lateral\ Velocity = \frac{k \times B \times W \times gradient}{aquifer\ surface\ area \times porosity}$$

(5.14)

Below, the equation parameters are explained briefly:

- Hydraulic conductivity (K) (m/year): K is calculated as transmissivity (k) over aquifer thickness (B) (Equation 5.15). Transmissivity value for the study area is available in the Green Reports published by the State Hydraulic Works, who carried out pump tests in the 1970s. The hydrogeological model uses these test results to calculate the hydraulic conductivity in the region.

$$k = K\ \times B$$

(5.15)

- Aquifer Thickness (B) (m): B is calculated as the difference between the Head in Çumra and the aquifer bottom (Equation 5.16).

$$B = Average\ Head\ Inside\ Çumra - aquifer\ bottom$$

(5.16)

- Width (W) (m): W represents the width of the vertical area through which the water flows.

- Gradient (unitless): The gradient is calculated as the head difference between two points over the distance between them (Equation 5.17).

$$gradient = \frac{dH}{dl}$$

(5.17)

- Porosity (unitless): Since groundwater is represented with one stock that corresponds to the saturated zone, the porosity is assumed to be uniform over the entire aquifer.

Further explanation regarding the above formulation (validation and parameter estimations) is provided in section 6.

5.2.1.2. Groundwater infrastructure sub-sector. The main stock and flow variables of the groundwater infrastructure sub-sector are listed in Table 5.2.

Table 5.2. Stock and flow variables of groundwater infrastructure sub-sector.

Stock Variables	**Units**
Number of Active Wells	Wells
Average Pump Power	kW/Wells
Flow Variables	**Units**
Well Digging	Wells/Year
Well Closing Rate	Wells/Year
Average Pump Power Adjustment	kW/Wells/Year

Number of Active Wells

The number of active wells represents the operational wells being utilized for groundwater extraction. This stock variable increases with well digging and decreases with well closing.

$$\frac{d(Number\ of\ Active\ Wells)}{dt} = well\ digging - well\ closing \tag{5.18}$$

Well-digging rate is driven by the well deficit (wells), which represents how many more wells are required to be able to supply the groundwater demand, given the average well yield. However, in the case of aquifer depletion, opening new wells would not be a rational choice. Therefore, we use a table function to include the effect of average well yield on well digging (unitless), which implies that as the average well yield approaches zero, so does the well digging rate (Figure 5.6). The effect variable is derived from the normalization of the observed average well yield, against a reference average well yield parameter, which is defined as an acceptable average well yield value.

$$well\ digging = \frac{well\ deficit}{well\ digging\ time} \times effect\ of\ average\ well\ yield\ on\ well\ digging \tag{5.19}$$

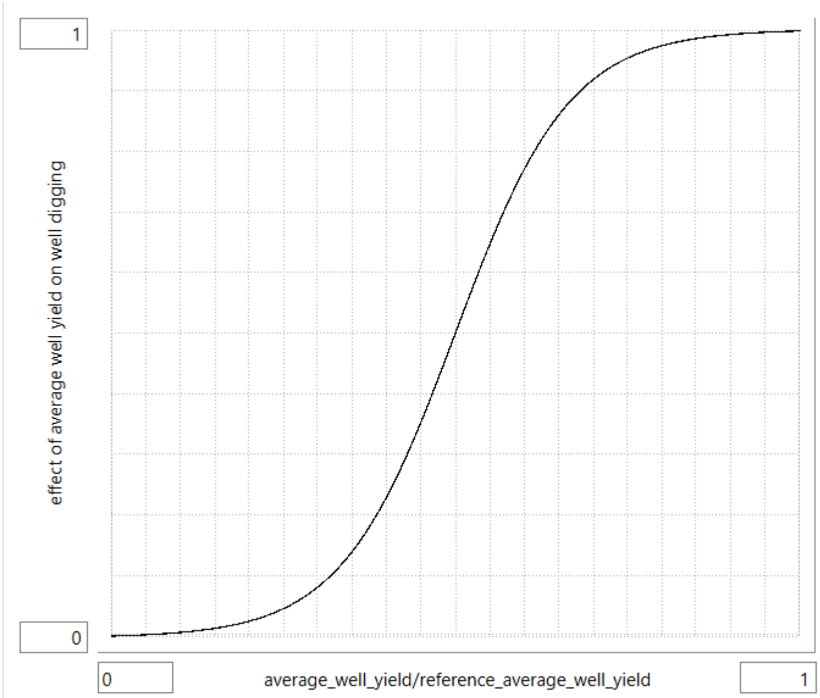

Figure 5.6. Table function: effect of average well yield on well digging.

Well closing rate is calculated as follows:

$$well\ closing = Number\ of\ Active\ Wells\ \times well\ closing\ fraction \tag{5.20}$$

Where the well-closing fraction (unitless) is calculated as the multiplication of the reference well-closing fraction (unitless) and the effect of depth discrepancy on the well-closing fraction (unitless). The reference well-closing fraction represents the average lifetime of a well and the effect variable implies that as the groundwater table approaches the average well depth, well closing accelerates. Figure 5.7 shows the inserted table function.

$$\begin{aligned} well\ closing\ fraction \\ &= reference\ well\ closing\ fraction \\ &\times effect\ of\ depth\ discrepancy\ on\ well\ closing \end{aligned} \tag{5.21}$$

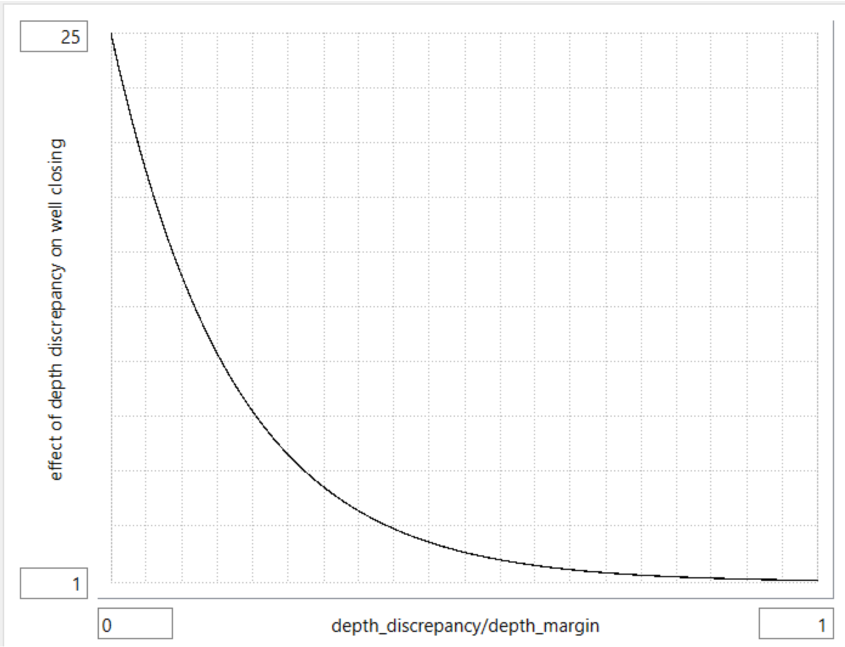

Figure 5.7. Table function: effect of depth discrepancy on well closing.

Average Pump Power

Average pump power (kW/wells) is included as a stock variable and adjusted according to the need through the average pump power adjustment (kW/wells/year) biflow. The stock is capped by a technological upper limit, the maximum obtainable pump power (kW/wells).

$$\frac{d(Average\ Pump\ Power)}{dt} = average\ pump\ power\ adjustment \tag{5.22}$$

Unless the required pump power (kW/well) surpasses the cap, the average pump power is adjusted to the required level as follows:

$$average\ pump\ power\ adjustment = \frac{\boldsymbol{MIN}(maximum\ obtainable\ pump\ power\ ;\ required\ pump\ power) - Average\ Pump\ Power}{pump\ adjustment\ time} \tag{5.23}$$

5.2.2. Crop-Land Use

This sector is composed of 5 stock and 14 flow variables (Table 5.3). Figure 5.8 shows the CLD and Figure 5.9 shows the simplified stock-flow structure of the crop-land use sector.

In the R4 reinforcing loop (Figure 5.8), the relationship between crop land and profit. Other things being equal, if the crop-land increases, the water cost per unit area decreases. Given that the revenue would be unaffected, the profit and thus the attractiveness of the crop and the desired share of crop land would increase, amplifying the initial change that triggered the loop.

Table 5.3. Stock and flow variables of crop-land use sector.

Stock Variables	Units
Land for Sugar Beet	m^2
Land for Green Plants	m^2
Land for Irrigated Cereal	m^2
Land for Rainfed Cereal	m^2
Fallow Land	m^2
Flow Variables	**Units**
Rainfed Cereal to Sugar Beet Transition	m^2/years
Rainfed Cereal to Green Plants Transition	m^2/Years
Rainfed Cereal to Irrigated Cereal Transition	m^2/Years
Irrigated Cereal to Sugar Beet Transition	m^2/Years
Irrigated Cereal to Green Plants Transition	m^2/Years
Irrigated Cereal to Rainfed Cereal Transition	m^2/Years
Sugar Beet to Green Plants Transition	m^2/Years
Sugar Beet to Rainfed Cereal Transition	m^2/Years
Sugar Beet to Irrigated Cereal Transition	m^2/Years
Green Plants to Sugar Beet Transition	m^2/Years
Green Plants to Irrigated Cereal Transition	m^2/Years
Green Plants to Rainfed Cereal Transition	m^2/Years
Fallowing	m^2/Years
Abandoning Fallowing	m^2/Years

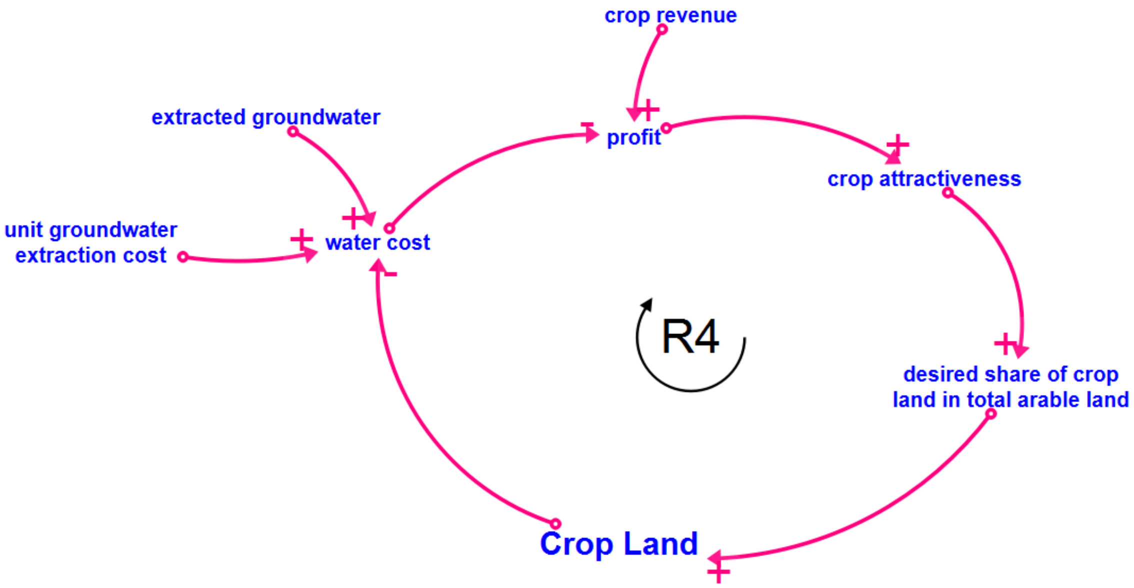

Figure 5.8. Causal loop diagram of crop-land use sector.

All crop types represented in the model are annual crops; farmers can switch from one crop to another every year, based on the desired share of each crop (unitless). For the irrigated crop types, the change in crop land is the difference between the sum of transition from other crop lands and the sum of transition to other crop lands. However, rainfed cereal lands are fallowed regularly, therefore the fallowing and abandoning fallowing flow variables are also included in the equation. The generic equation for all crop-land use stocks is summarized as follows:

$$\frac{d(Land\ for\ Crop\ A)}{dt} = \sum Crop\ X\ to\ Crop\ A\ transition - \sum Crop\ A\ to\ Crop\ X\ transition \tag{5.24}$$

The flows that conduct the transition between cultivated lands are formulated similarly, as follows:

$$Crop\ A\ to\ Crop\ B\ Transition = \frac{Land\ for\ Crop\ A\ \times desired\ share\ of\ Crop\ B}{Crop\ B\ rotation\ time} \tag{5.25}$$

where the rotation time (year) represents the allowed frequency of growing Crop B. If there are not any specific regulations for that crop, it is 1 year.

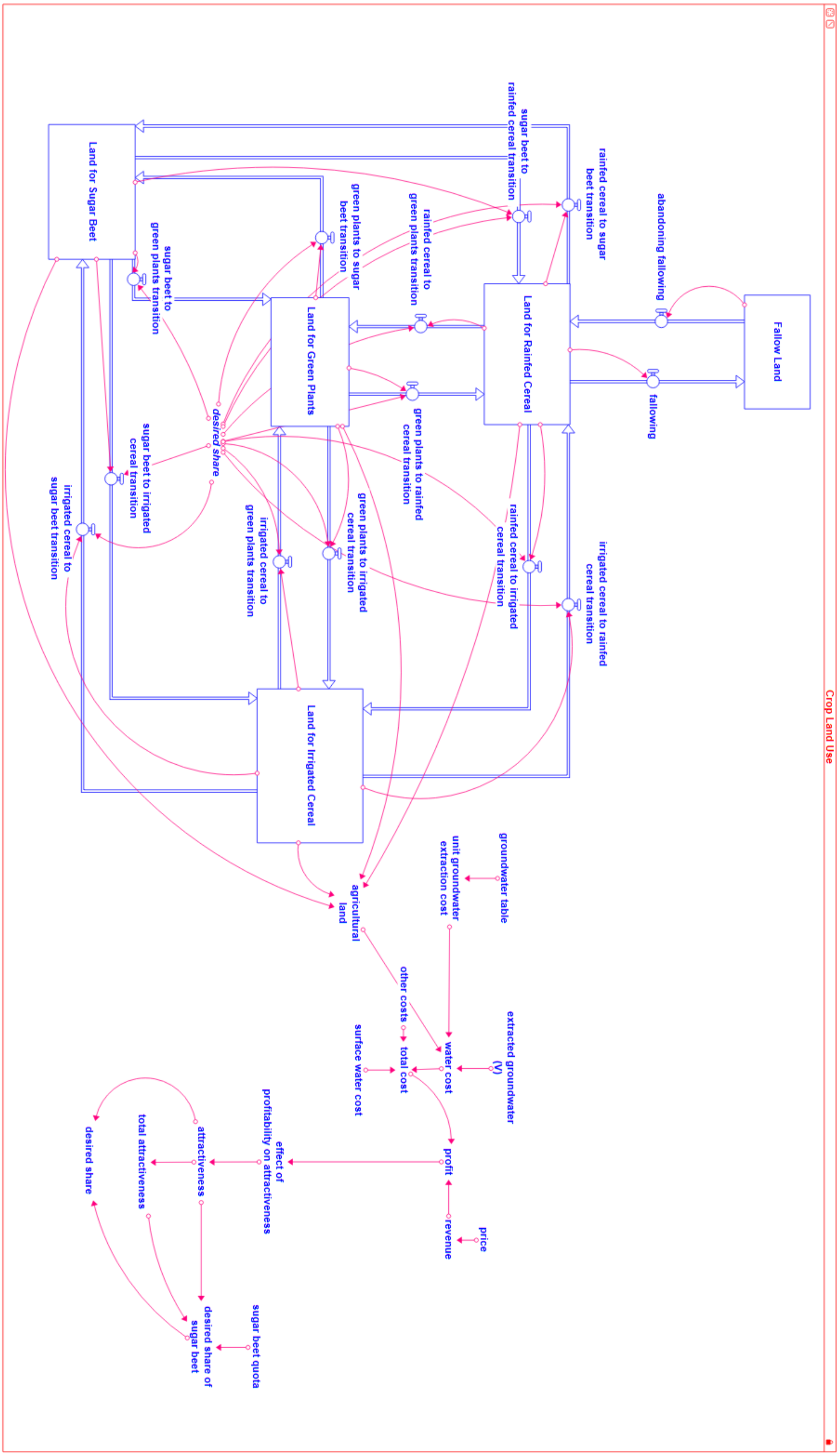

Figure 5.9. Simplified stock-flow structure of the crop-land use sector.

Crop Attractiveness and Desired Land Share of Crops

Allocation of the total land to different crop-land use options is one of the most important decisions that is endogenized in the model and it is driven by the relative attractiveness of these options (Sterman, 2000). Due to the quota restriction on sugar beet, the share of sugar beet is capped, as equation 5.26 suggests:

$$desired\ share\ of\ sugar\ beet = MIN(sugar\ beet\ quota\ ;\ \frac{attractiveness[Sugar\_Beet]}{total\ attractiveness}) \tag{5.26}$$

Given that the sum of the desired share for all land use options should always be equal to 1, the desired shares of other crops are calculated based on the desired share of sugar beet. The desired share formulations for green plants, irrigated cereals, and rainfed cereals are analogous to one another, as in equation 5.27.

$$desired\ share[Crop\ A] = (1 - desired\ share\ of\ sugar\ beet) \times \frac{attractiveness[Crop\ A]}{sum\ of\ attractiveness\ of\ crops\ other\ than\ sugar\ beet} \tag{5.27}$$

On the other hand, attractiveness is not a physical property governed by the laws of nature, i.e., there does not exist a predefined way to calculate the attractiveness of any service or product. Thus, calculating crop attractiveness is another challenge. A multitude of factors may have an impact on the attractiveness of crops; our interviews with the farmers revealed the following: profitability, labor and machinery requirement, vulnerability to disease, or other factors that negatively influence yield. However, the model only takes the profit into account, because regardless of the other factors, farmers mainly consider profitability in their decisions, as they expressed in the interviews. The equation for attractiveness is formulated as a logit model (Sterman, 2000), as suggested by Equation 5.28.

$$attractiveness = EXP(sensitivity\ of\ attractiveness\ to\ profitability \times \frac{profit}{reference\ profit}) \tag{5.28}$$

where the reference profit equals the highest among all crop profits.

The profit (TRY/m^2/year) is calculated as the difference between revenue (TRY/m^2/year) and total cost (TRY/m^2/year). While revenue is crop price (TRY/kg) times crop yield (kg/m^2/year), the total cost is the sum of groundwater (extraction/energy) cost (TRY/m^2/year), other costs (TRY/m^2/year) including seed, fertilizer, pesticide, and labor costs, and - if applicable - surface water cost (TRY/m^2/year).

It should be noted here that the *Crops* array is used for the following variables in this sector: desired share, attractiveness, sensitivity of attractiveness to profitability, profit, revenue, price, total cost, groundwater cost, other costs, and surface water cost.

5.2.3. Production Factor Adjustment and Yield Goal Setting

The production factor adjustment and yield goal-setting sector consists of 2 stock variables and 2 biflows. The causal loop diagram is shown in Figure 5.10; the 4-dimensional *Crops* array is used for all the variables represented in this figure. Therefore, all the loops depicted in Figure 5.10 operate separately for all crop-land use types.

Figure 5.11 shows the simplified stock-flow diagram of the production factor adjustment and yield goal-setting sector.

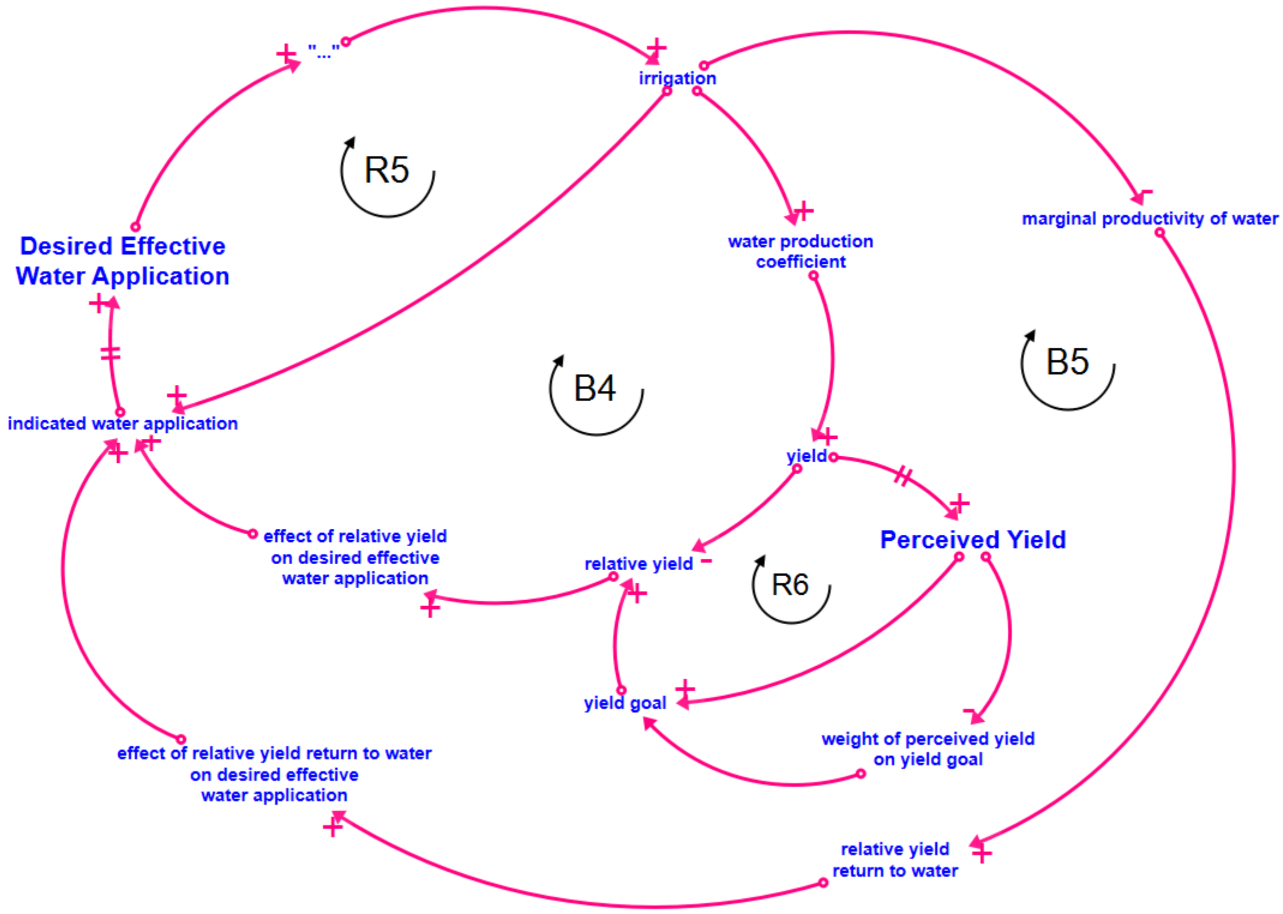

Figure 5.10. Causal loop diagram of production factor adjustment and yield goal-setting sector.

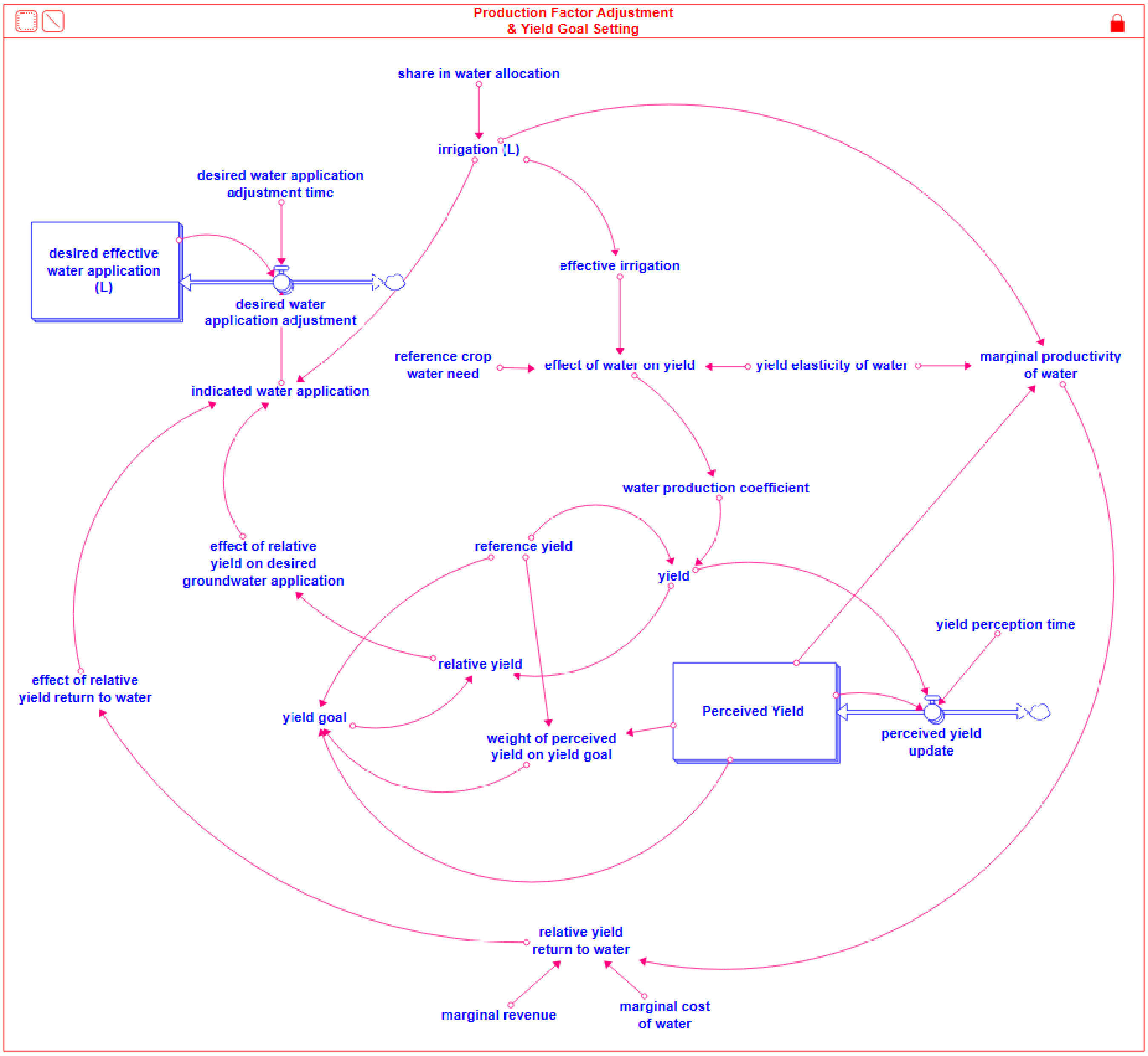

Figure 5.11. Simplified stock-flow structure of production factor adjustment and yield goal-setting sector.

5.2.3.1. Production factor adjustment sub-sector. The production factor adjustment sub-sector includes the R5, B4, and B5 loops (Figure 5.12), and the main stock and flow variables of this sub-sector are listed in Table 5.4.

Table 5.4. Stock-flow variables of the production factor adjustment sub-sector.

Stock Variables	Units
Desired Effective Irrigation	m/year
Flow Variables	**Units**
Desired Effective Irrigation Adjustment	meters/year/year

The R5 reinforcing loop explains the relationship between desired effective water application and irrigation. As irrigation (m/year) increases, the desired effective water application that drives the extraction (in the water resources and groundwater infrastructure sector) also increases. More extraction means a higher level of irrigation, and the loop reinforces the initial direction of change.

In the B4 balancing loop, the relationship between desired effective water application and yield (kg/m^2/year) is depicted. If the former increases, so does the irrigation and the water-production coefficient (unitless), which is the impact of water use on yield. A higher water-production coefficient produces higher yields, and the relative yield (unitless), which represents how close the yield (obtained) is to the yield goal (kg/m^2/year), decreases. A lower relative yield implies that the yield goal is closer to being achieved, and the necessity to increase irrigation disappears. In other words, desired effective water application becomes less than it would otherwise be, and the loop damps the initial change.

The last balancing loop that operates in this sub-sector, B5, shows that irrigation provides diminishing returns; if we keep increasing irrigation proportionally, the yield response to each additional unit of water would be smaller. Therefore, as irrigation increases, the marginal productivity of water (kg/m^3) decreases. Low marginal productivity implies that investing more in irrigation water is not profitable for the farmer, therefore the desired effective water application becomes lower than it would otherwise be, and so does irrigation. As a result, the initial change is countered by the B5 loop.

The stock is adjusted yearly (Figure 5.13) since farmers evaluate the previous production performance in terms of yield and adapt their intended water use accordingly.

$$\frac{d(Desired\ Effective\ Water\ Application)}{dt} = desired\ water\ application\ adjustment \tag{5.29}$$

where the flow variable is governed by the following equation for irrigated crops, and is always zero for rainfed cereal:

$$desired\ water\ application\ adjustment = \frac{indicated\ water\ application - Desired\ Effective\ Water\ Application}{desired\ water\ application\ adjustment\ time} \tag{5.30}$$

Indicated water application (m/year) variable is the outcome of a decision-making process, it represents how much water farmers decide to use based on their most recent yield perception for each crop type.

$$indicated\ water\ application = irrigation \times Average\ Irrigation\ Technology\ Efficiency \times effect\ of\ relative\ yield\ return\ to\ water \times effect\ of\ relative\ yield \tag{5.31}$$

Irrigation (m/year), as mentioned above, is an arrayed parameter. Therefore, the total water supply, including the extracted groundwater and (if available) surface water needs to be allocated to irrigated crops. To that end, each irrigated crop's share in water allocation (unitless) is calculated based on the ratio of the irrigation demand of each crop over the sum of irrigation demands for all crops. Given that the total water supply has a volumetric unit (m^3/year), the volume of water allocated to each crop is divided by the land size of that crop, to obtain irrigation in length (m/year).

$$irrigation = \frac{total\ water\ supply \times share\ in\ water\ allocation}{crop\ land} \tag{5.32}$$

The effect of relative yield return to water and the effect of relative yield are inserted as table functions, as shown in Figures 5.12 and 5.13, respectively. The boundary values and shapes of both table functions are estimated in model calibration.

The relative yield return to water (unitless) is an indicator that compares the return from production (marginal revenue (TRY/kg)) to a benchmark, which in this case is the investment in production (marginal cost of water (TRY/m^3)), and it is proportional to the marginal productivity of water (Sterman, 1980). Marginal revenue represents the monetary return a farmer would receive in case an additional unit of yield is obtained, i.e., the crop price (TRY/kg). Similarly, the marginal cost represents the amount of money a farmer would need to spend to extract an additional unit of irrigation water, i.e., unit groundwater extraction cost (TRY/m^3).

$$relative\ yield\ return\ to\ water = \frac{marginal\ revenue \times marginal\ productivity\ of\ water}{marginal\ cost\ of\ water}$$

(5.33)

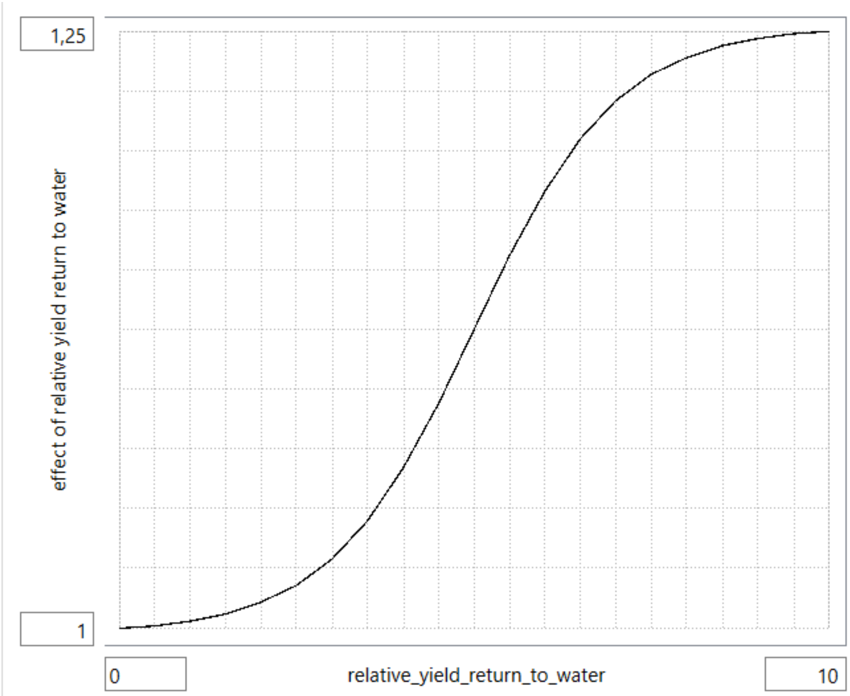

Figure 5.12. Table function: effect of relative yield return to water.

On the other hand, the marginal productivity of water (kg/m^3) is an indicator of the diminishing returns property of irrigation, as explained above. It is formulated as follows (Sterman, 1980):

$$marginal\ productivity\ of\ water = \frac{yield\ elasticity\ of\ water\ \times Perceived\ Yield}{irrigation\ \times\ Average\ Irrigation\ Technology\ Efficieny + effective\ precipitation}$$

(5.34)

It should be noted here that the marginal productivity of water is calculated with a perceived yield instead of yield because the information available to decision-makers, who are farmers, should be used when formulating decision parameters (Sterman, 2000).

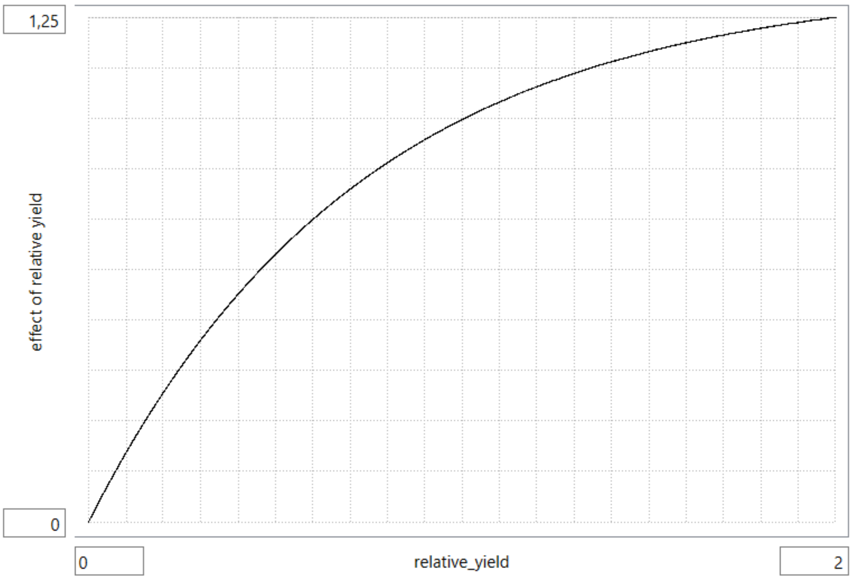

Figure 5.13. Table function: effect of relative yield.

The relative yield indicates how close the yield is to the set yield goal. It is inversely proportional to yield.

$$relative\ yield = \frac{yield\ goal}{yield}$$

(5.35)

Many factors impact crop yield, ranging from the level of nutrients in the soil to existing pests, weather conditions, etc. However, the model only takes water into account, assuming the other factors are adequate. In other words, all factors besides water are exogenous to the model.

$$yield = reference\ yield\ \times water\ production\ coefficient$$

(5.36)

Moreover, the relevant literature offers various methods to estimate crop yield, many of which derive yield through evapotranspiration estimations (FAO, 2012). In this model, we do not estimate evapotranspiration, but employ a Cobb-Douglas production function for two main reasons: First, the reason why we do not estimate evapotranspiration is that plant growth is a complex process itself, and we prefer to avoid overcomplicating the model with intricate feedbacks that are not directly related to the model purpose. The second reason relates to why we chose the Cobb-Douglas production function; Cobb-Douglas both offers a simplification to estimate the yield and also allows building intelligible feedback loops (such as B4 and B5 loops in Figure 5.10) that depict a boundedly rational decision-making process.

$$effect\ of\ water\ on\ yield = \left(\frac{effective\ precipitation + effective\ irrigation}{reference\ crop\ water\ need}\right)^{yield\ elasticity\ of\ water} \quad (5.37)$$

The downside of the Cobb-Douglas production function is that it is an exponential function; while it is suitable for industrial production where additional input of materials increases the level of output continuously (ignoring other constraints such as the labor or facility capacity, which do not apply to this comparison), plants have a biological capacity that caps the yield, regardless of how much water is applied. Therefore, Cobb-Douglas performs poorly in the upper extreme. To eliminate this disadvantage, we introduce a table function as shown in Figure 5.14. The upper boundary of the x-axis in this table function is estimated in model calibration.

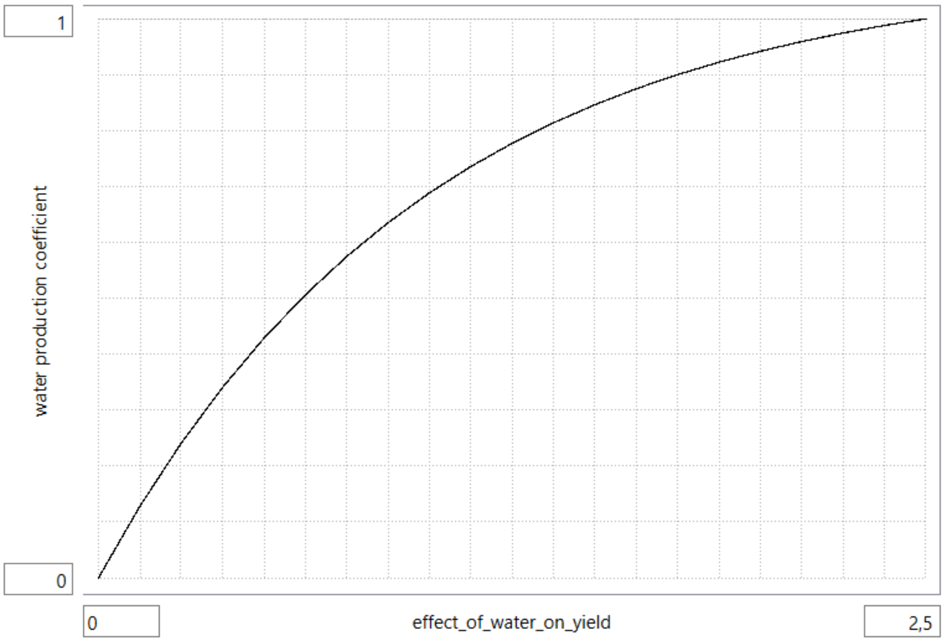

Figure 5.14. Table function: water production coefficient.

5.2.3.2. Yield goal-setting sub-sector. Table 5.5 shows the main stock and flow variables of the yield goal-setting sub-sector.

Table 5.5. Stock-flow variables of the yield goal-setting sub-sector.

Stock Variables	**Units**
Perceived Yield	$kg/m^2/year$
Flow Variables	**Units**
Yield Perception Update	$kg/m^2/year/year$

The yield goal-setting sub-sector is governed by the R6 loop (Figure 5.12). This loop explains the relationship between yield and yield goal. An increase in crop yield is reflected in the perceived yield with a delay, which drives the yield goal up. To achieve the new, higher yield goal, farmers prefer to increase the level of irrigation, further increasing the yield.

Perceived yield is adjusted to yield with a one-year delay.

$$\frac{d(Perceived\ Yield)}{dt} = yield\ perception\ update$$

(5.38)

where,

$$yield\ perception\ update = \frac{yield - Perceived\ Yield}{yield\ perception\ time}$$

(5.39)

Intuitively, one would assume that the yield goal would be equal to the reference yield ($kg/m^2/year$), as it represents the plant's biological potential. While the reference yield may be an explicit, or an ideal, goal, systems usually create an implicit goal, based on past performance (Barlas & Yaşarcan, 2006). Depending on the performance update, as perceived by the goal-setters, this implicit goal may improve or erode. Therefore, we compute the yield goal as a weighted average of the perceived yield and reference yield,

$$\begin{aligned} yield\ goal = {} & weight\ of\ perceived\ yield \times Perceived\ Yield \\ & + (1 - weight\ of\ perceived\ yield) \times reference\ yield \end{aligned}$$

(5.40)

where the weight of the perceived yield itself is also a variable, inserted as a table function (Figure 5.15).

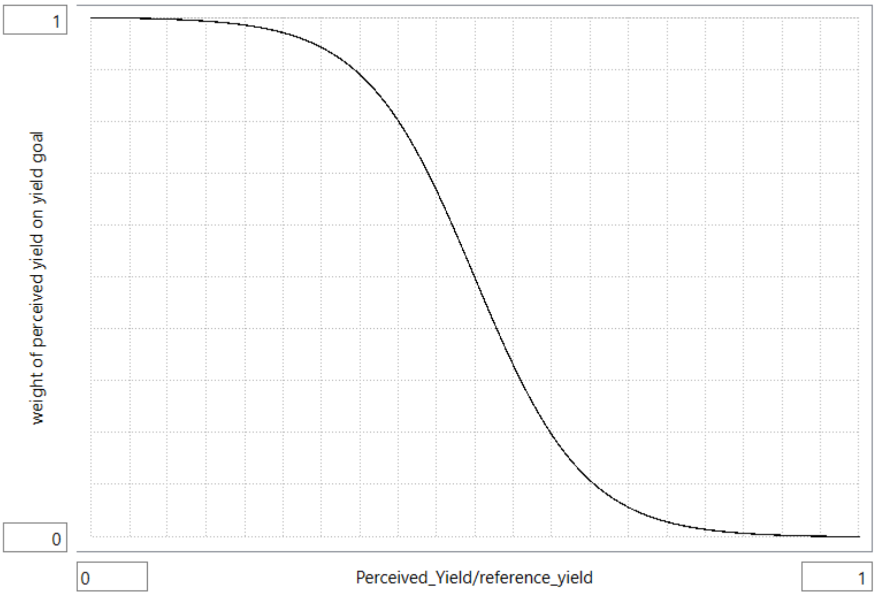

Figure 5.15. Table function: weight of perceived yield on yield goal.

The above table function implies that as the perceived yield falls short of the reference yield, the weight of the perceived yield on the yield goal increases. Therefore, the yield goal tends to lean against the perceived yield, i.e., it erodes. Oppositely, as the perceived yield approaches the reference yield, the weight of the perceived yield decreases, thus the yield goal draws near the reference yield; in other words, it improves.

5.2.4. Irrigation Technology Sector

The irrigation technology sector is the smallest in the model. It consists of only one stock and 2 flows (Table 5.6). The stock-flow structure of this sector is depicted in Figure 5.16.

Table 5.6. Stock-flow variables of the irrigation technology sector.

Stock Variables	Units
Average Irrigation Technology Efficiency	Unitless
Flow Variables	**Units**
Investment in Irrigation Technology	Per year
Equipment Depreciation	Per year

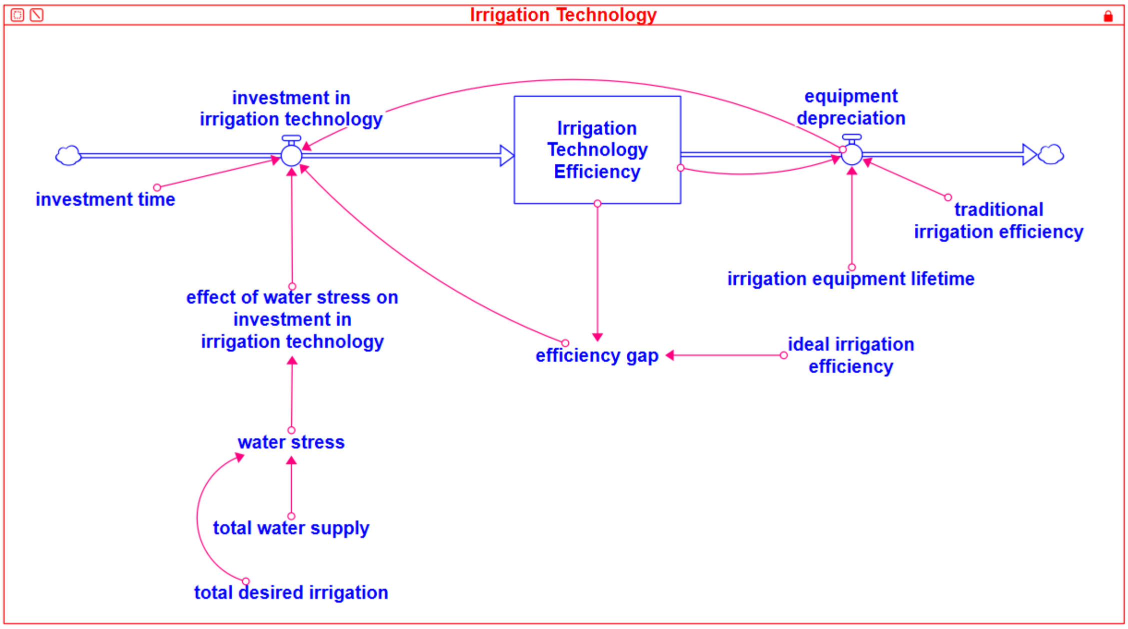

Figure 5.16. Stock-flow diagram of the irrigation technology sector.

The average irrigation technology efficiency increases with investment in new irrigation technology and decreases with equipment depreciation.

$$\frac{d(Average\ Irrigation\ Technology\ Efficiency)}{dt} = investment\ in\ irrigation\ technology - equipment\ depreciation \tag{5.41}$$

The rate of investment is mainly driven by the gap between the ideal irrigation efficiency, which represents the theoretical efficiency of the highest irrigation technology available, and the current average irrigation technology efficiency. Also, it compensates for the depreciation of the equipment at hand.

$$investment\ in\ irrigation\ technology = equipment\ depreciation + MAX\left(0\,;\frac{efficiency\ gap}{investment\ time}\right) \times effect\ of\ water\ stress\ on\ investment\ in\ irrigation\ technology \tag{5.42}$$

However, when there is water stress (unitless), i.e., when the total water supply (m^3/year) fails to fulfill the total desired irrigation (m^3/year), the investment rate increases so that the available water at hand is used more efficiently. The effect of water stress on investment in irrigation technology is inserted as a table function, presented in Figure 5.17.

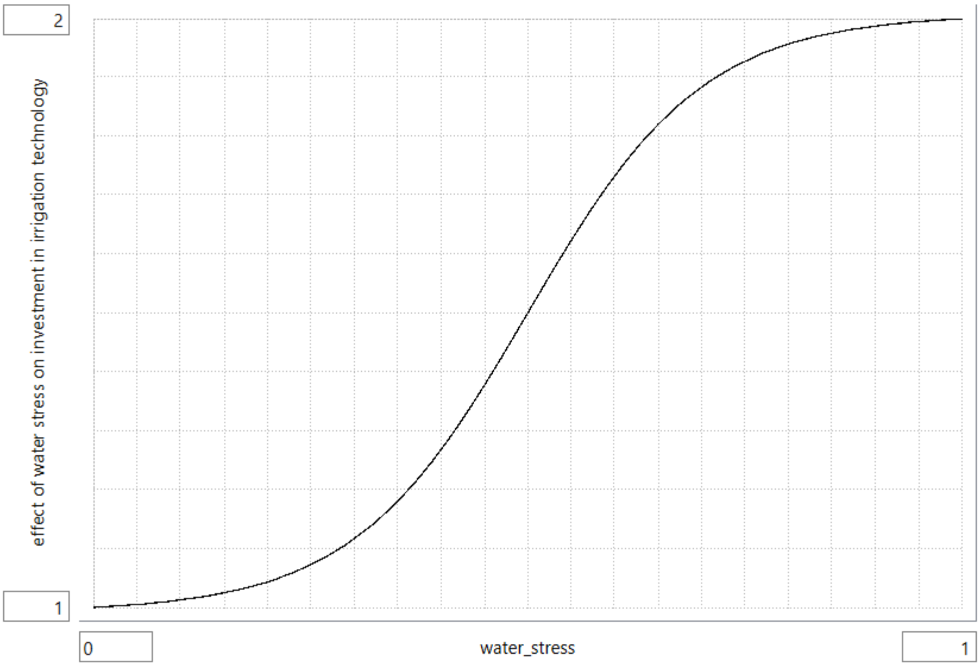

Figure 5.17. Table function: effect of water stress on investment in irrigation technology.

The irrigation equipment depreciates at a constant rate equal to the lifetime of the equipment. The lowest possible efficiency is the traditional irrigation efficiency; the traditional method of irrigation has been flooding in the KCB, and it does not require any high-technology equipment.

$$equipment\ depreciation = \frac{(Irrigation\ Technology\ Efficiency - \ traditional\ irrigation\ efficiency)}{irrigation\ equipment\ lifetime} \tag{5.43}$$

6. MODEL VALIDATION

Validation is an essential aspect of modeling studies. Model validity has a significant impact on the shared confidence in the model and its outputs, and the credibility of the policy recommendations generated by model simulation. Since SD models are described as causal-descriptive; they aim to capture the underlying structure of real-life systems, which create the problematic behavior of interest that the model is built to analyze (Barlas, 1996). Therefore, an SD model outputs should not only imitate the observed behavior pattern, but the model should recreate the problematic behavior pattern for the right reasons.

The model developing process comprises model validation; thus, instead of validating the model as a whole at the end of the model development phase, model validity is assured progressively throughout the modeling activity (Barlas, 1996). On the other hand, in SD, there are two main steps of a formal model validation process: namely, structural, and behavioral validation.

First comes the structure validity. Two groups of tests are applied to the model (Barlas, 1996; Sterman, 2000): Direct structure tests evaluate model validity by comparing it directly to the actual system, without requiring simulation. These tests are theoretical and empirical. Structure assessment, boundary adequacy, and dimensional consistency tests fall under this category. In contrast, structure-oriented behavior tests implicitly validate the model structure through simulation. Extreme condition and behavior sensitivity tests are examples of structure-oriented behavior tests. These tests may be performed both on the complete model and selected sub-models.

Once the model structure is confirmed to be fitting, behavioral validation tests can be run. Simply put, behavioral validation refers to assessing the extent to which the model represents the real system. Through behavior pattern tests, we can evaluate the representativeness of the behavior patterns generated by the model in comparison to the observed behavior patterns in reality (Barlas, 1996).

The SD model introduced in this thesis is validated in three steps: First, we partially validate the model against a process-based, UFZ-MODFLOW model that has been developed to calculate the water budget in Konya Closed Basin. Then the model is structurally validated; structure assessment, boundary adequacy, parameter assessment, and dimensional consistency tests are performed as direct structure tests. Additionally, extreme condition and behavior sensitivity tests are run as indirect structure tests, and the simulation results of these tests are covered in this section. Lastly, the model-generated behavior is validated.

6.1. Partial Validation Against the Hydrogeological Model

Data insufficiency has been one of the main obstacles to the science-based management of groundwater resources globally. For the Konya Closed Basin, reliable information regarding the recharge into the aquifer and the pumping rate is lacking. So far, the water budget calculation for the basin has been static and based on estimates, arousing suspicion about the accuracy of the said calculation. Therefore, within the scope of the Innovative and Sustainable Groundwater Management in the Mediterranean (InTheMED) project, a dynamic, process-based hydrogeological model was developed with UZF-MODFLOW by the project team, in parallel to the system dynamics model presented in this thesis. The hydrogeological model aims to estimate the pumping and the recharge and analyze the water budget for the Konya Closed Basin. The two models are compared in Table 6.1.

Table 6.1. Comparison of the hydrogeological and SD models.

	Hydrogeological Model	SD Model
Purpose	Water budget analysis	Socio-economic policy analysis
Model Characteristics	Dynamic, process based	Dynamic, process based
Software	UZF – Modflow	Stella Architect
Spatial Scale	Konya Closed Basin	Çumra District
Spatial Resolution	10 km x 10 km grid based	Non-spatial
Time Horizon	40 years	40 years
Temporal Resolution	Months	Years

In the partial validation of the water component of the system dynamics model (a box model), we make use of the hydrogeological model, postulating it as the best representation of reality. To that end, we acknowledge the three main structural differences between the two models:

- For simplicity, the system dynamics model incorporates groundwater component with a single stock, representing the saturated zone. It has three main flows: namely, extraction, lateral velocity, and recharge (Section 5.2.1.). Therefore, it ignores the impact of various soil layers on groundwater dynamics such as evaporation from the root zone and varying hydraulic conductivity between different soil layers. In contrast, the hydrogeological model is a physical model that represents changing soil conditions in different vertical layers.

- The system dynamics model is non-spatial and lumped, but the hydrogeological model is spatially distributed; it operates on 10 km x 10 km grids.

- While the time unit of the system dynamics model is yearly, the hydrogeological model operates on a monthly basis and thus has a higher temporal resolution.

To eliminate the potential deviations that the structural difference in the two models may cause, we designed an initial experimental setup (Table 6.2). The experiments are summarized in Table 6.3 and each set of experiments is explained in detail below.

Table 6.2. Initial experimental setup for the partial validation of the water resources sub-sector.

LATERAL VELOCITY	
Initial Average Head in Çumra	**Average Head Outside Çumra**
Reference Head	Higher Head
	Lower Head
EFFECTIVE PRECIPITATION & PRECIPITATION RETURN	
Crop - Land Use (x4)	**Precipitation (x5)**
Wheat	1,50 x Reference Precipitation
Corn	1,25 x Reference Precipitation
Sugar Beet	Reference Precipitation
Bare Land	0,75 x Reference Precipitation
	0,50 x Reference Precipitation
IRRIGATION RETURN	
Crop - Land Use (x3)	**Irrigation Efficiency (x5)**
Wheat	0,3
Corn	0,4
Sugar Beet	0,5
	0,7
	1

Table 6.3. Summary of partial validation experiments.

Test	Information Received from Modflow	Variable / Parameter Estimated in the SD Model
Lateral Flow	Hydraulic Conductivity, Width, Gradient, Aquifer Surface Area, Porosity	Aquifer Bottom
Effective Precipitation	Annual Precipitation, Evapotranspiration	Effective Precipitation Fraction
Precipitation Return	Annual Precipitation, Recharge	Precipitation Return Fraction
Irrigation Return	Annual Extraction, Recharge	Irrigation Return Fraction

6.1.1. Lateral Velocity

The lateral flow is calculated with Darcy's Law, as explained in Section 5.2.1.1. Table 6.2 explains the estimation procedures for the equation parameters of the lateral velocity formulation (Eq 5.14). In these tests, the aquifer bottom is the calibration parameter because it is the most uncertain parameter of all the parameters used in the lateral velocity formulation. Additionally, we assume that there is no extraction, no precipitation, ipso facto no recharge, and that the average head outside Çumra (head in the grids surrounding Çumra grids) is constant throughout the simulation period in each run. Under these assumptions, we take two runs from the hydrogeological model, where the average head outside is higher than the initial head inside Çumra in one, and lower in the other (Table 6.4.).

Table 6.4. Parameter estimation for the lateral velocity formulation.

Parameter	Unit	Parameter Estimation
Hydraulic Conductivity (K)	Meters/Year	Transmissivity and aquifer thickness values for the study area are available in the Green Reports published by the State Hydraulic Works, who carried out pump tests in the 1970s. The hydrogeological model uses these test results to calculate the hydraulic conductivity in the region and that value is inputted in the system dynamics model.
Width (W)	Meters	It is calculated as the sum of the length of the outer edges of the grids representing the Çumra district in the hydrogeological model.
Gradient (dH/dl)	Dimensionless	The head inside and outside Çumra are aggregated and averaged in the system dynamics model, even though they have a heterogeneous distribution over the grids in the hydrogeological model. Therefore, the system dynamics calculates the gradient as the difference between outside and inside averaged heads over the distance between the centers of two grids in the hydrogeological model: a boundary within Çumra, and an adjoining cell outside Çumra.
Aquifer Surface Area	Square Meters	Instead of the area of the Çumra administrative unit, it is calculated as the sum of the grid areas representing Çumra in the hydrogeological model. As would be expected, the administrative boundaries of the district do not completely align with the grid edges. However, the difference between the actual area of the district and the total area of the 22 grids representing Çumra in the hydrogeological model is neglected in the SD model.
Porosity	Dimensionless	It is taken as the saturated zone porosity in the hydrogeological model.
Aquifer Bottom	Meters	It is an unknown parameter; it is estimated for every cell in the hydrogeological model. It has the highest uncertainty among the equation parameters; thus, we estimate the aquifer bottom in our lumped box model. The average aquifer bottom in the hydrogeological model input is 899 meters. The adjusted value of the aquifer bottom in the system dynamics model is 920 meters.

The outputs from the two models are compared for each run, as shown in Figure 6.1.

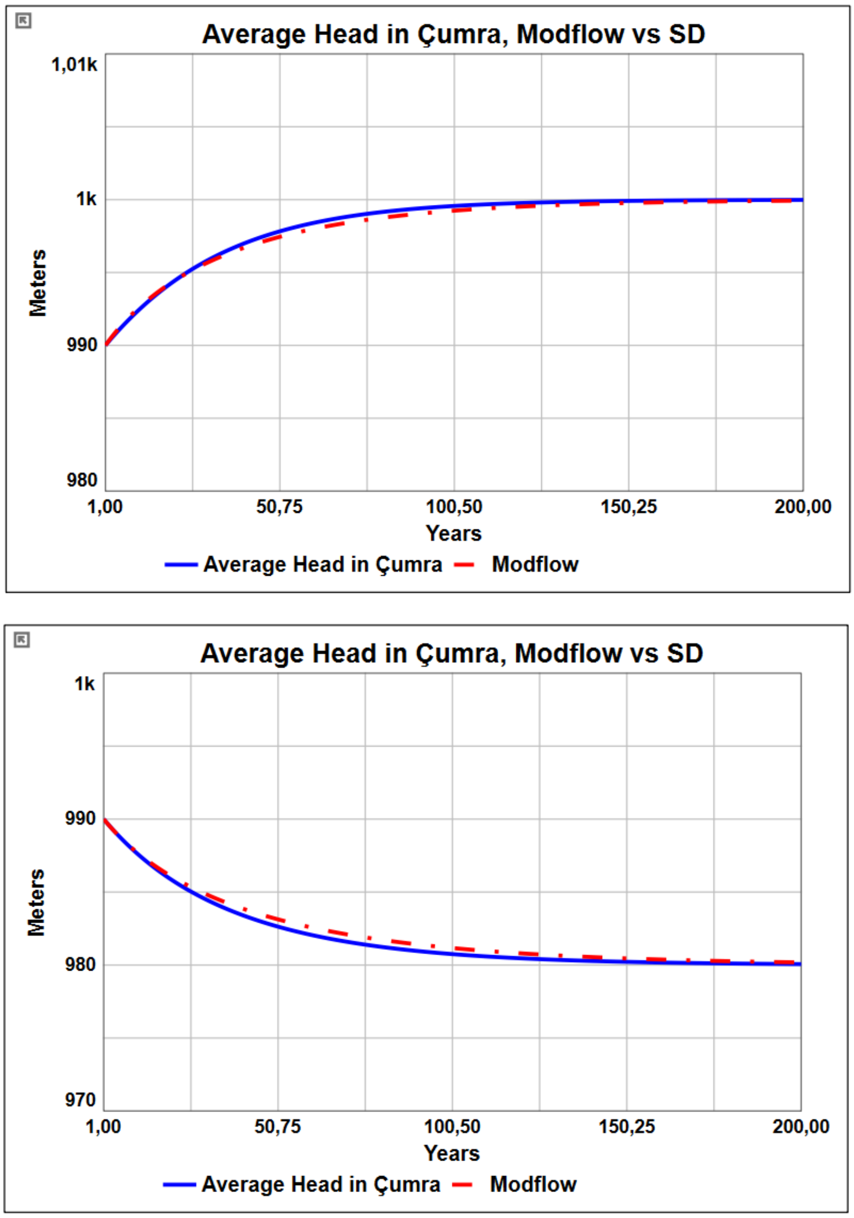

Figure 6.1. Outputs of the lateral flow validation runs.

6.1.2. Effective Precipitation

Effective precipitation refers to the fraction of precipitation received and utilized by the crop. We calculate it for each crop separately, as follows:

$$Effective\ Precipitation = Precipitation \times Effective\ Precipitation\ Fraction \tag{6.3}$$

That is due to the lower time resolution in the system dynamics model; the yearly time unit is unable to capture the impact of seasonality on plant water needs and in the precipitation regime. Therefore, we calibrate the effective precipitation fraction variable for crops, based on the outputs of the test runs from the monthly hydrogeological model.

To that end, we make the following assumptions: there is no water exchange between Çumra and outside (no lateral flow), no extraction (no irrigation), the whole Çumra area is covered with the same crop type (wheat, corn, or sugar beet) and that the yearly precipitation is constant over the simulation period (20 years). Under these assumptions, we take 15 runs from MODFLOW; we test 5 precipitation levels for each of the three crops. Then, we determine the fraction of effective precipitation per run (calculated as the cumulative evapotranspiration over 20 years divided by the cumulative precipitation over 20 years) and obtain 5 different fractions for all levels of precipitation (mm). We fit curves to the 5-point data for each crop type, to find good-enough equations that can represent the relationship between precipitation and effective precipitation fraction, as a function of precipitation.

Figures 6.2 to 6.4 shows the precipitation vs effective precipitation fraction graphs for all crops, and Table 6.5 shows the selected equations and the R^2 values.

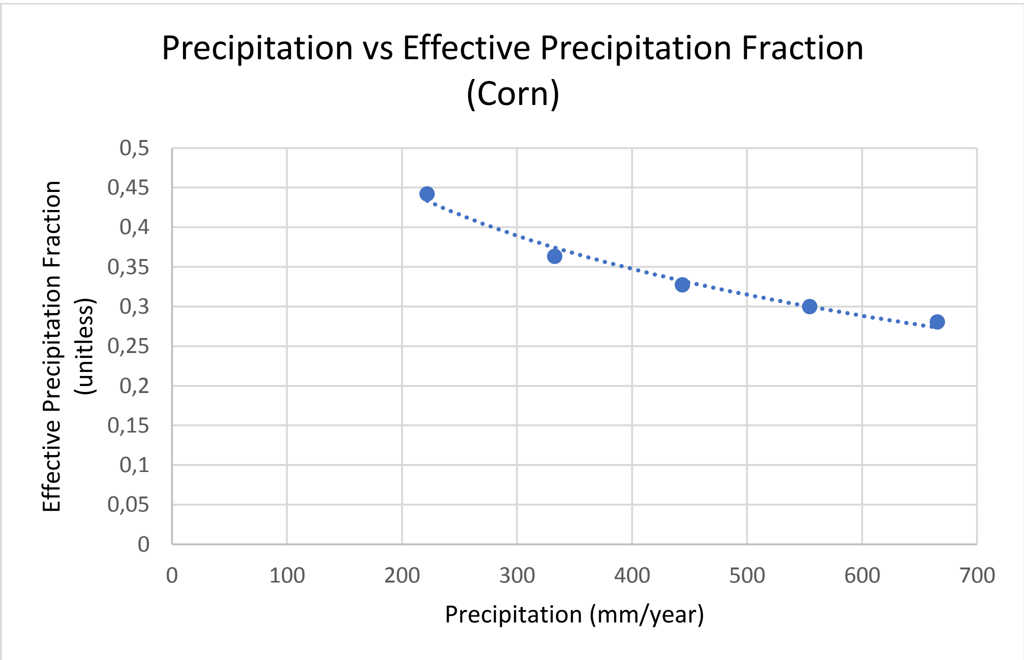

Figure 6.2. Precipitation vs effective precipitation fraction graph of corn.

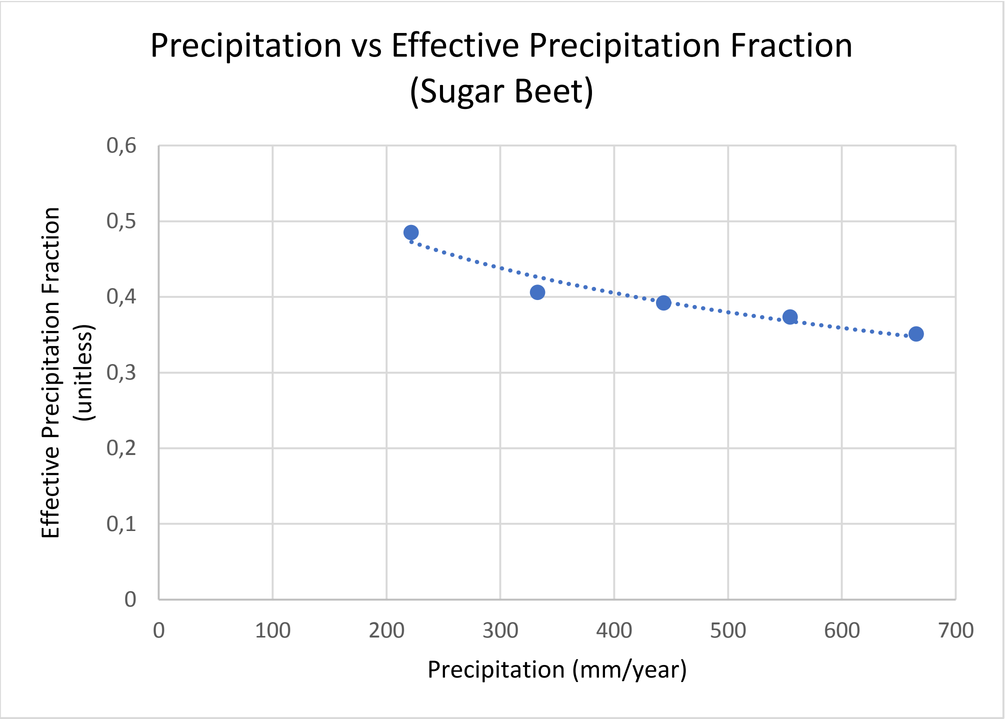

Figure 6.3. Precipitation vs effective precipitation fraction graph of sugar beet.

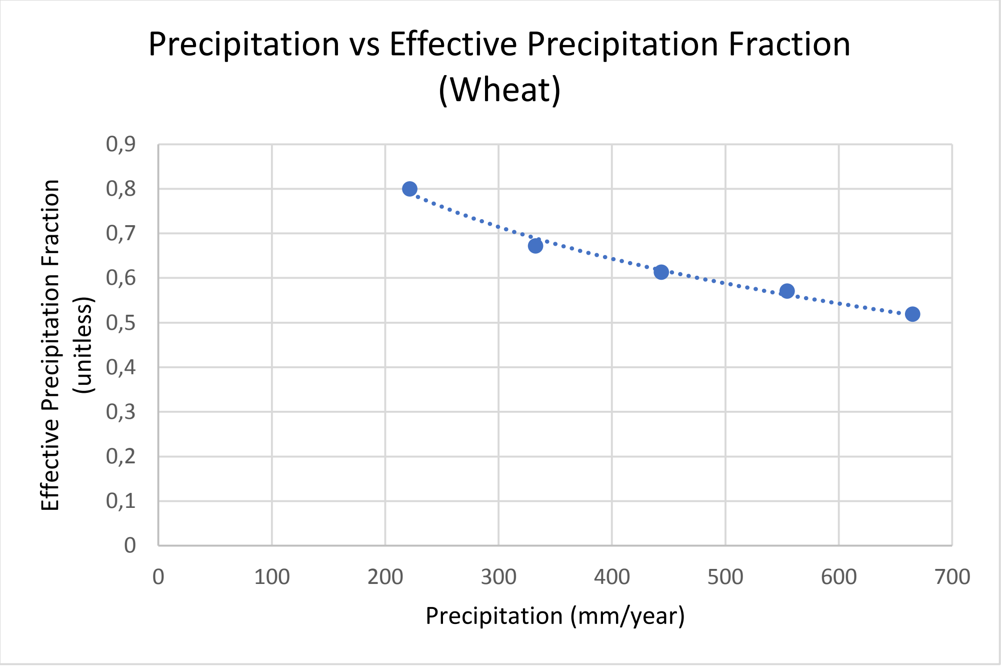

Figure 6.4. Precipitation vs effective precipitation fraction graph of wheat.

Table 6.5. Fitted functions for effective precipitation fraction and their R2 values.

CROP	EQUATION	R^2
Corn	$y = -0{,}146 \times \ln(x) + 1{,}2201$	0,9832
Sugar Beet	$y = -0{,}122 \times \ln(x) + 1{,}1426$	0,942
Wheat	$y = -0{,}248 \times \ln(x) + 2{,}1278$	0,9895

The inadequacy of these equations is that they would fail in case of extremely low precipitation; the calculated fraction may surpass 1, which would imply that more than 100% of the precipitation would be uptaken by the crop. To avert that, we formulate the effective precipitation fraction as follows:

$$effective\ precipitation\ fraction = \boldsymbol{MIN}(1\ ; calculated\ effective\ precipitation\ fraction) \quad (6.4)$$

6.1.3. Precipitation Return

Precipitation return refers to the amount of precipitation water recharged into the aquifer, and it is formulated as follows:

$$precipitation\ return = precipitation\ \times precipitation\ return\ fraction \quad (6.5)$$

We make use of the same set of tests as we do to estimate effective precipitation and we calibrate the precipitation return fraction for crop lands and bare land. Following the same steps, we determine the fractional return from precipitation by dividing the cumulative recharge over 20 years by the cumulative precipitation over 20 years, as provided by the hydrogeological model and then we plot the data for each precipitation level and land type. Figures 6.5 to 6.8 show the precipitation versus precipitation return fraction graphs for each crop land and also for bare land.

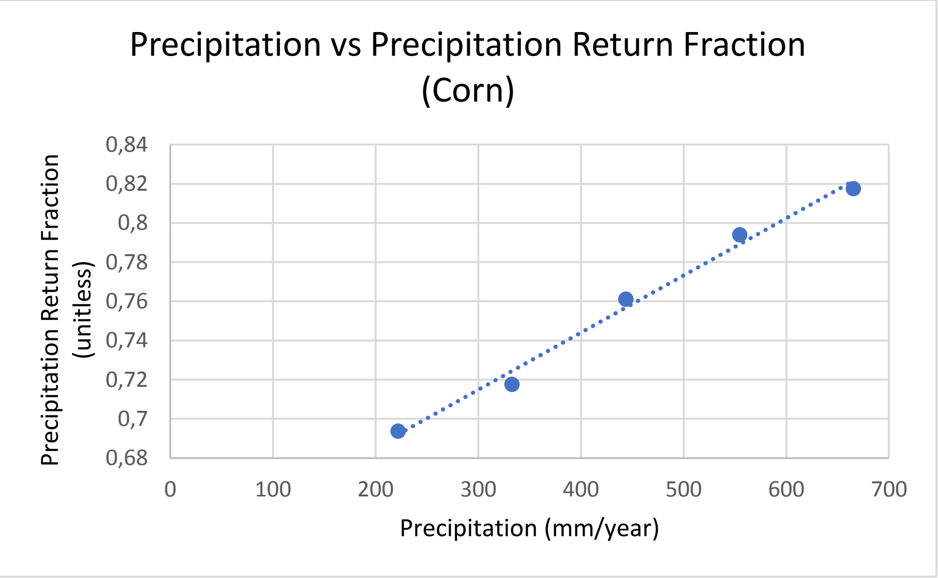

Figure 6.5. Precipitation vs precipitation return fraction graph of corn.

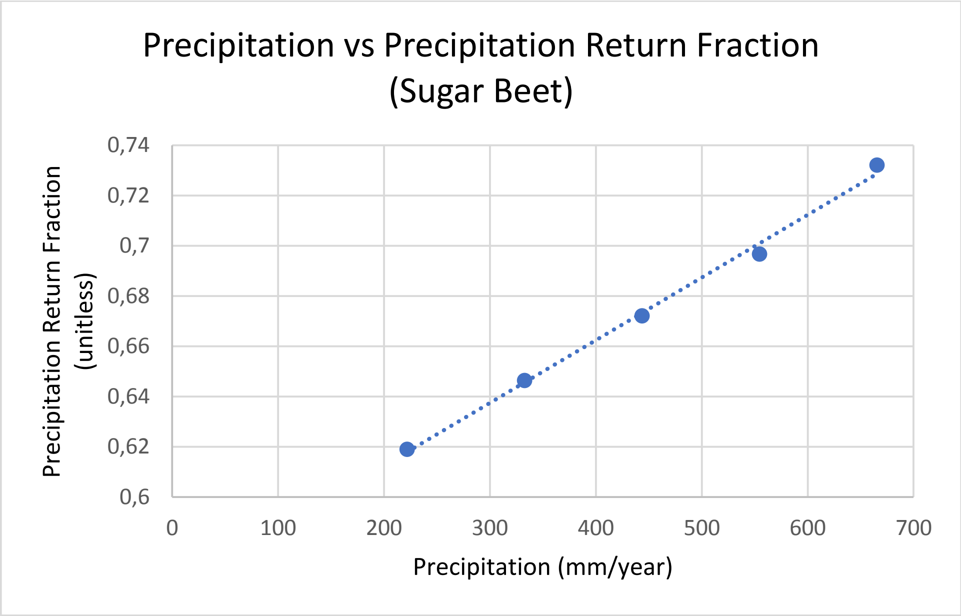

Figure 6.6. Precipitation vs precipitation return fraction graph of sugar beet.

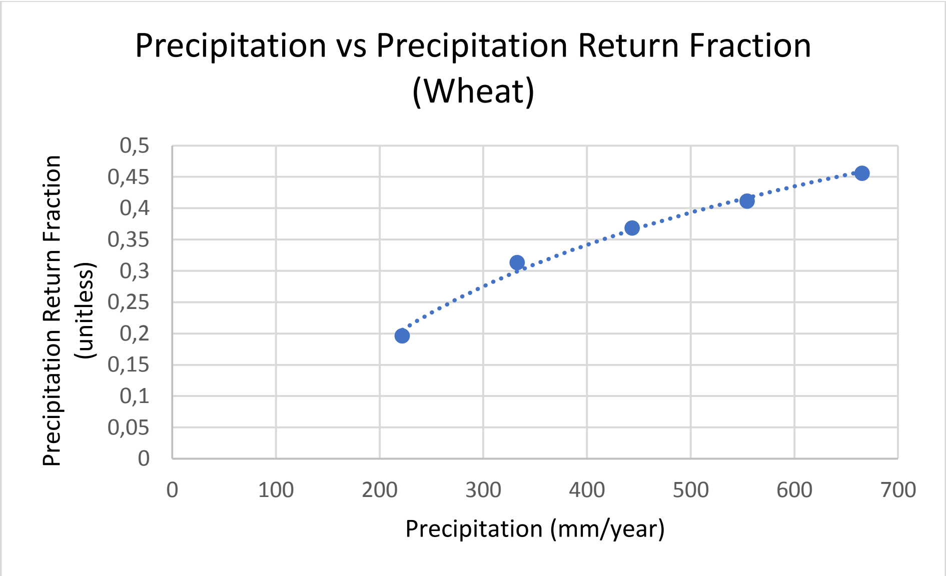

Figure 6.7. Precipitation vs precipitation return fraction graph of wheat.

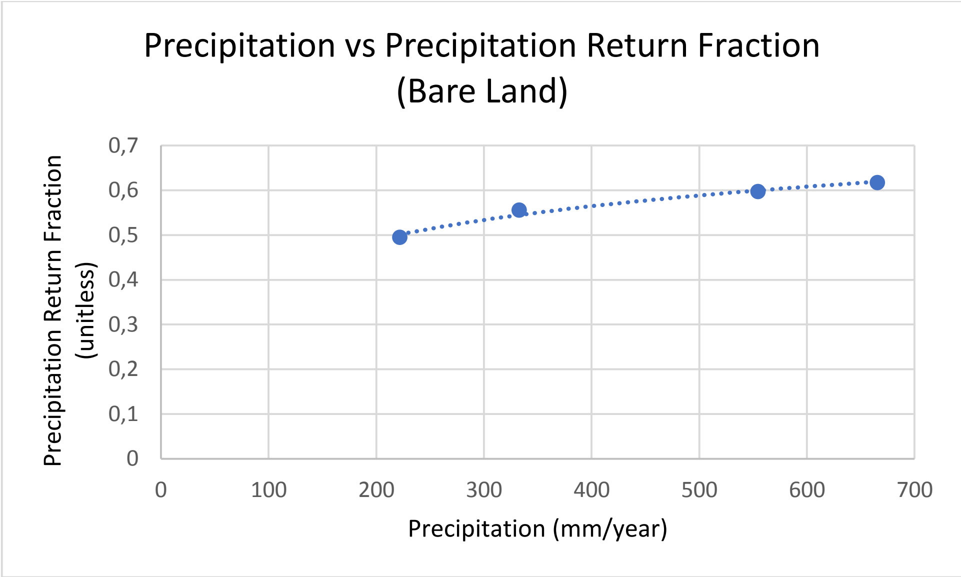

Figure 6.8. Precipitation vs precipitation return fraction graph of bare land.

Then, we fit appropriate curves for each; Table 6.6 shows the equations as well as the R^2 values.

Table 6.6. Fitted functions for precipitation return fraction and their R2 values.

CROP	**EQUATION**	**R^2**
Corn	$y = 0{,}0003 \times x + 0{,}6272$	0,9896
Sugar Beet	$y = 0{,}0002 \times x + 0{,}5626$	0,9956
Wheat	$y = 0{,}2305 \times \ln(x) - 1{,}0394$	0,9917
Bare Land	$y = 0{,}1074 \times \ln(x) - 0{,}0792$	0,9808

Precipitation return fraction cannot be higher than one, however, the equations in Table 6.4 would allow it to be, for certain precipitation values. Therefore, similar to the effective precipitation fraction, we formulate the precipitation return fraction as follows:

$$precipitation\ return\ fraction = \boldsymbol{MIN}(1\ ;\ calculated\ precipitation\ return\ fraction) \quad (6.6)$$

Figures 6.9 to 6.12 show the outputs of test runs for effective precipitation and precipitation return. The blue lines in the graphs represent the average head in Çumra as simulated by the SD model and the dotted red lines show the average head data that is produced by MODFLOW.

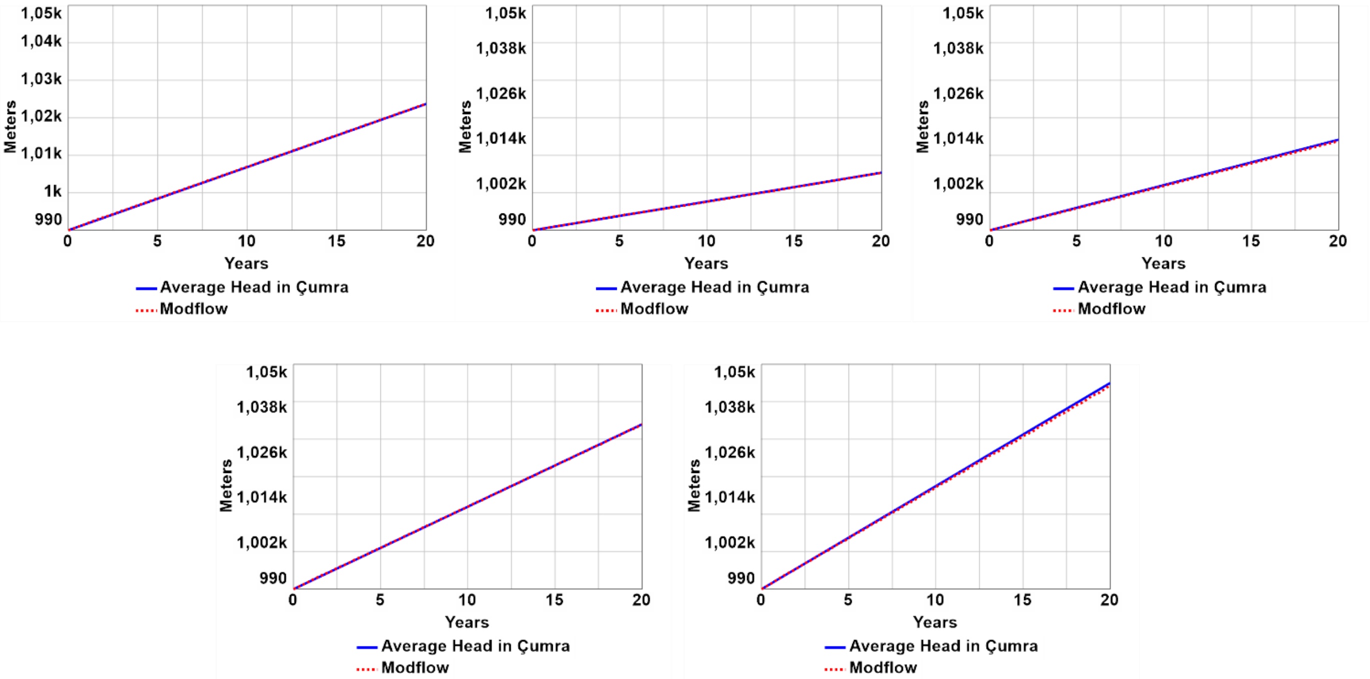

Figure 6.9. Corn effective precipitation and precipitation return runs.

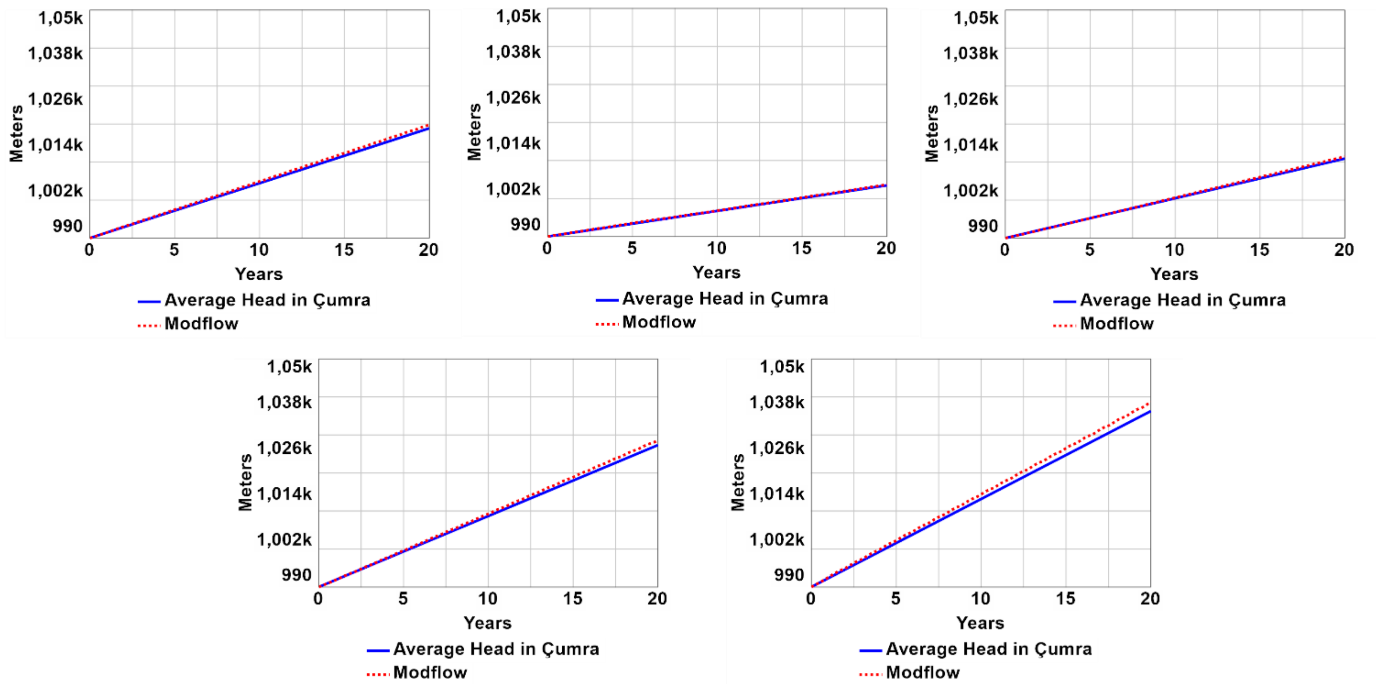

Figure 6.10. Sugar beet effective precipitation and precipitation return runs.

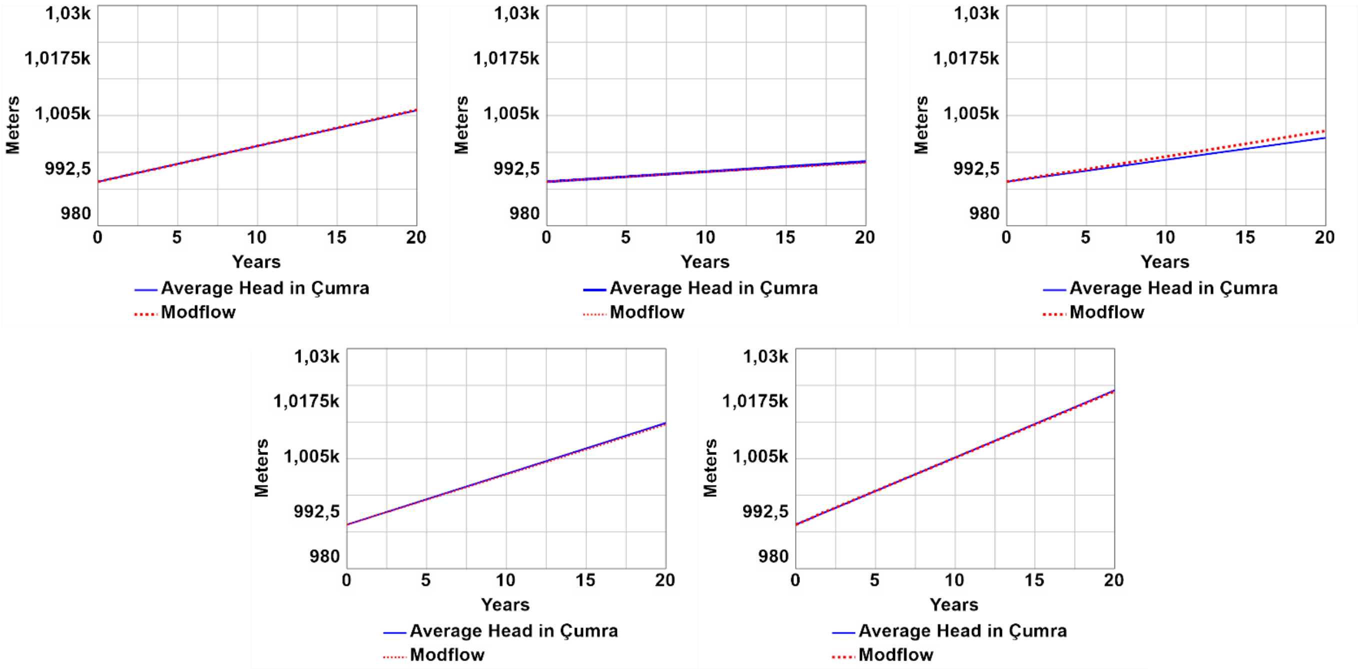

Figure 6.11. Wheat effective precipitation and precipitation return runs.

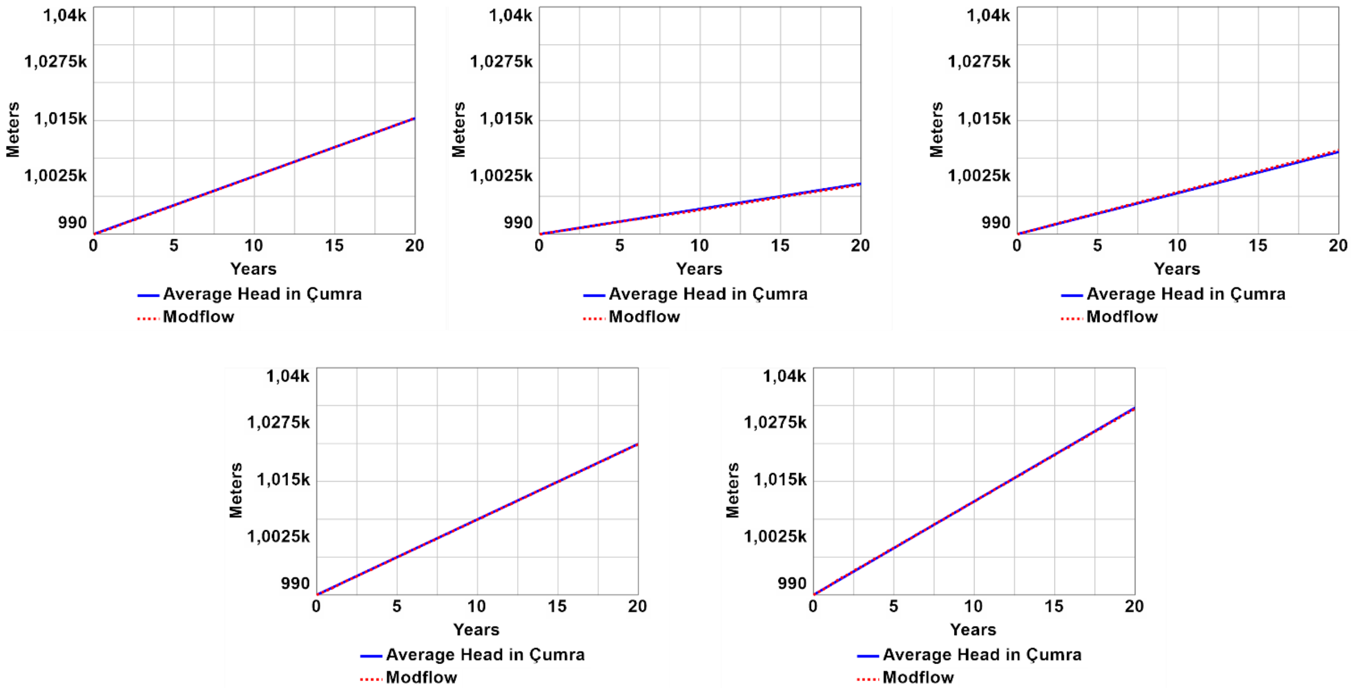

Figure 6.12. Bare land precipitation return runs.

6.1.4. Irrigation Return

The main purpose of these tests is to estimate the recharge from the total amount of water that the crop receives during its growth period which we name as "growth season infiltration" (m/year). In reality, plants receive water from both precipitation and irrigation during the growth period. However, while precipitation is distributed over the whole year, irrigation is scheduled only when the plant is on the soil. Therefore, while the monthly hydrogeological model treats precipitation and irrigation as the same and combines them under the infiltration variable, the SD model separates the two.

For the sake of these tests, we formulate the irrigation return as:

$$irrigation\ return = extraction\ \times irrigation\ return\ fraction \tag{6.7}$$

In these test runs, we calibrate for the irrigation return fraction to estimate the irrigation return. To that end, we take 15 runs from MODFLOW; we test 5 different irrigation efficiency levels for all 3 crop types. We do not test for bare land because non-agricultural land is not irrigated. Additionally, we assume that the whole area is covered with the same crop, irrigation efficiency is constant for the whole duration of the simulation (20 years), and also that there is no precipitation or lateral flow.

The irrigation return fractions are computed as the cumulative recharge over 20 years divided by the cumulative irrigation over 20 years. We plot the irrigation versus irrigation return fraction graphs, based on the hydrogeological model outputs (Figures 6.13 to 6.15), and fit appropriate curves to derive the equations for irrigation return fraction, which are presented in Table 6.7.

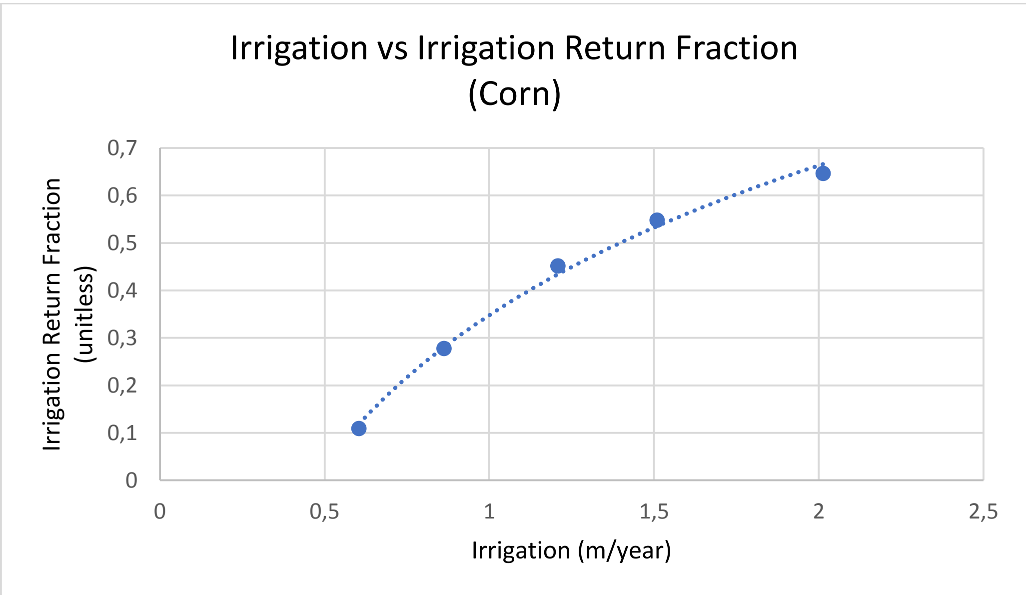

Figure 6.13. Irrigation vs irrigation return fraction graph of corn.

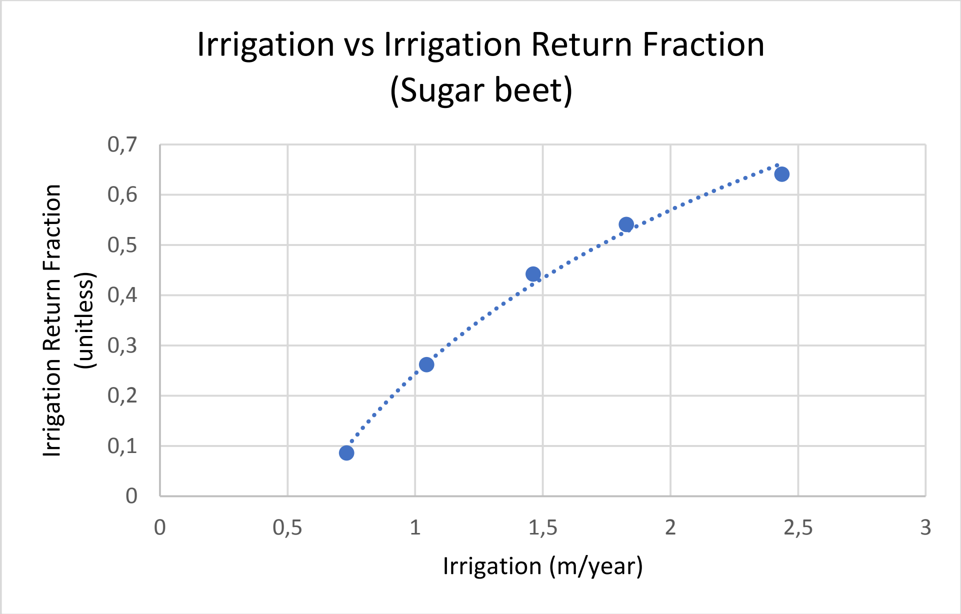

Figure 6.14. Irrigation vs irrigation return fraction graph of sugar beet.

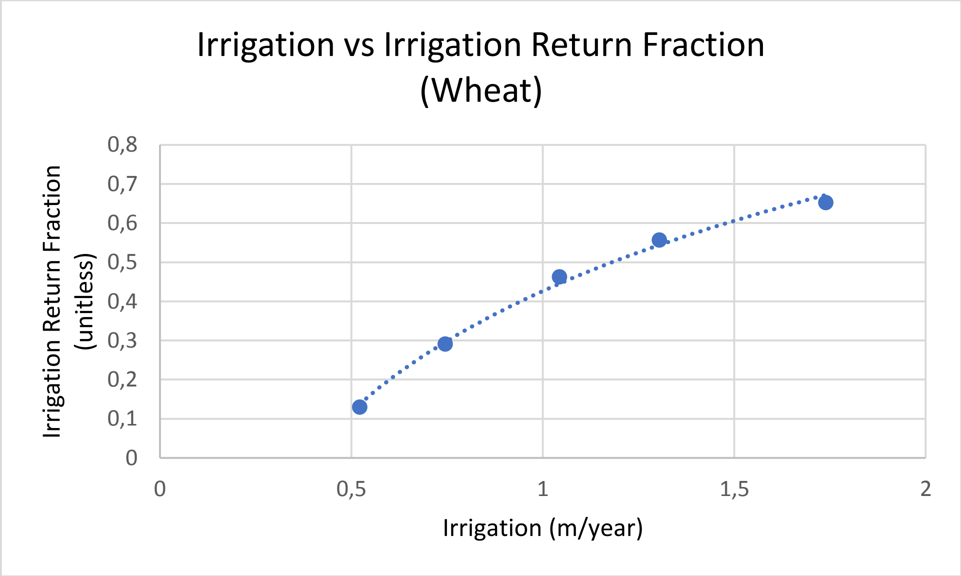

Figure 6.15. Irrigation vs irrigation return fraction graph of wheat.

Table 6.7. Fitted functions for irrigation return fraction and their R2 values.

CROP	**EQUATION**	**R^2**
Corn	$y = 0,455 \times \ln(x) + 0,3478$	0,9947
Sugar Beet	$y = 0,47 \times \ln(x) + 0,2437$	0,9941
Wheat	$y = 0,4431 \times \ln(x) + 0,4263$	0,9947

On the other hand, the logarithmic functions in Table 6.4 imply that the irrigation return fraction could be higher than 1, which shows that these curves fail under extreme conditions. To prevent that, we formulate the irrigation return fraction as follows:

$$irrigation\ return\ fraction = \boldsymbol{MIN}(1\ ;calculated\ irrigation\ return\ fraction) \quad (6.8)$$

The comparative outputs of the 15 test runs are presented in Figures 6.16 to 6.18. The blue lines represent the average head in Çumra obtained from the SD simulation, and the dotted red lines show the head outputs that MODFLOW generated.

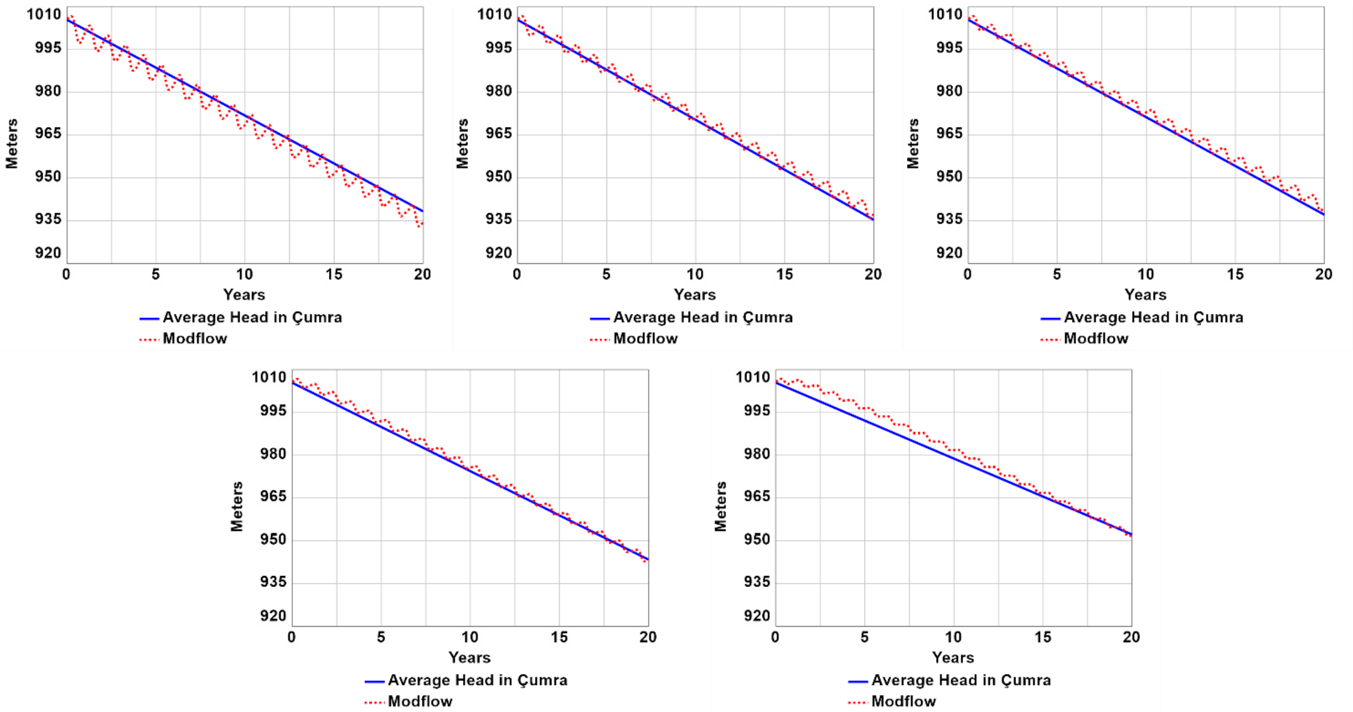

Figure 6.16. Corn irrigation return runs.

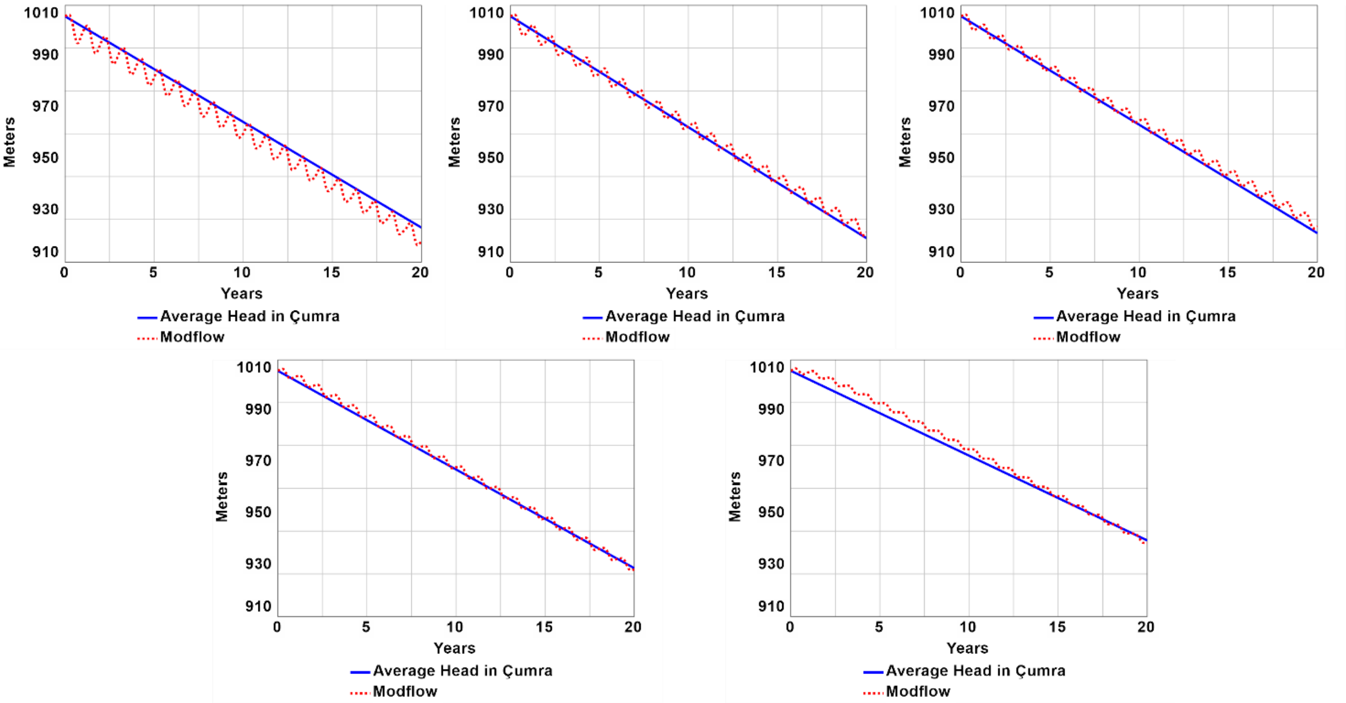

Figure 6.17. Sugar beet irrigation return runs.

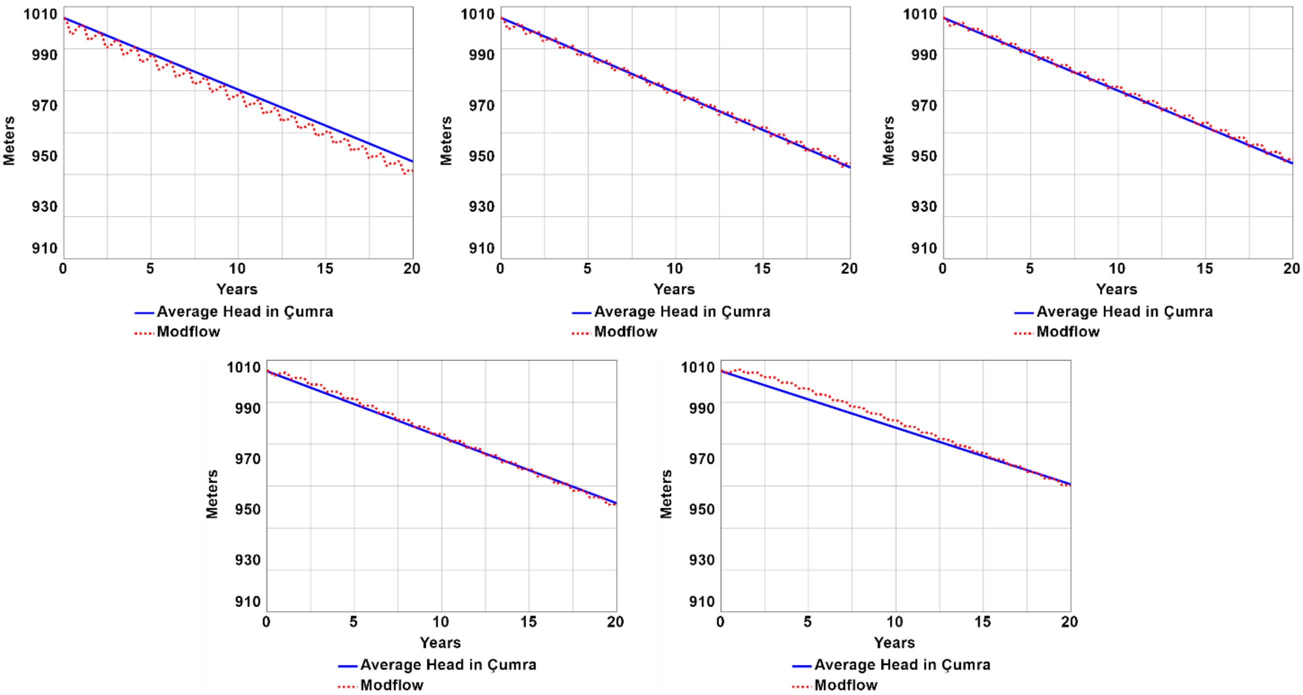

Figure 6.18. Wheat irrigation return runs.

Since we assume zero precipitation in these tests, growth season infiltration equals irrigation in the test runs. However, in the full model, the growth season infiltration is calculated as the sum of effective precipitation and irrigation. Therefore, we insert the derived irrigation fraction equations in the full model as the growth season infiltration return fraction.

6.1.4.1. Evaporation loss correction. Another difficulty for both the hydrogeological and SD models has been to identify the values of reference evapotranspiration and crop evapotranspiration under standard conditions (FAO, 1998). Reference evapotranspiration (ET_0) refers to the evaporative power of the atmosphere when there is sufficient water. Therefore, the actual evapotranspiration from the bare soil can be conceptualized as the minimum of available water and the potential evaporation. ET_0 depends only on climatic conditions and is independent of soil characteristics and crop types. Crop evapotranspiration under standard conditions (ET_c) refers to the evapotranspiration level when the plant achieves full production, i.e., when it has access to sufficient nutrients, is disease-free, and soil-water conditions are optimal. However, calculating the ET_0 and ET_c is not straightforward; multiple methods require a considerable amount of data.

In the two models, we incorporate the ET_0 and ET_c values provided by TAGEM (2017) since it is the only data source we have. However, the document mainly targets the farmers, and the purpose is to inform them about the irrigation requirements and scheduling for different crops in different regions in Turkey. Therefore, the document does not take into consideration non-standard conditions in the calculations. Treating the ET_c values provided in TAGEM (2017) as potential maximums results in recharge overestimation in the hydrogeological model (and thus in the SD model) because if the potential ET_c were to be equal to crop ET_c under standard conditions, irrigation efficiency would have minimal to zero impact on the water budget, which is not the case, as inefficient irrigation causes additional evaporative losses. To eliminate this issue, the hydrogeological model incorporates ET_0 in the evapotranspiration calculation, and we introduce an evaporation loss correction variable in the SD model.

As a result, the growth season infiltration return is calculated as follows:

$$\begin{aligned} &\mathit{growth\ season\ infiltration\ return} \\ &\quad = \mathit{growth\ season\ \ infiltration} \times \mathit{infiltration\ return\ fraction} \\ &\quad \times \mathit{evaporation\ loss\ correction} \end{aligned} \tag{6.9}$$

6.1.5. Additional Runs

After having estimated the required fractions through the initial experimental setting, we test how well the binary combinations of the three test structures operate; we take three more runs from MODFLOW, as follows:

The first run tests the precipitation – lateral flow combination, without irrigation. In the setting, half of the total land is bare, and the remaining half is distributed equally between corn, sugar beet, and wheat. There is no irrigation. The precipitation is at its reference test level, and the average head outside is constant. The outputs are shown in Figure 6.19. The blue line shows the simulated head in Çumra in the SD model and the red line shows the hydrogeological model output.

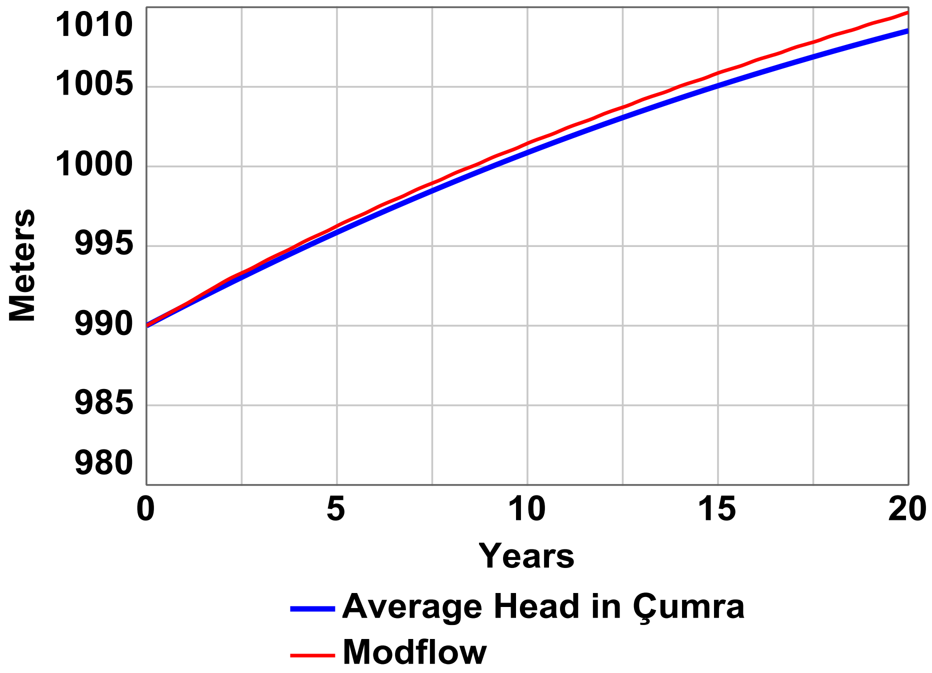

Figure 6.19. Precipitation-lateral flow run.

The second run incorporates precipitation and irrigation, without lateral flow. The total land is divided equally between corn and wheat, precipitation is at its reference test level and the irrigation efficiency is constant over the simulation period. The comparative outputs are presented in Figure 6.20.

The third and last run tests the combination of lateral flow and irrigation; precipitation is assumed to be zero. The whole land is distributed equally among corn, sugar beet, and wheat. The irrigation efficiency and the average head outside are constant. The outputs are compared in Figure 6.21.

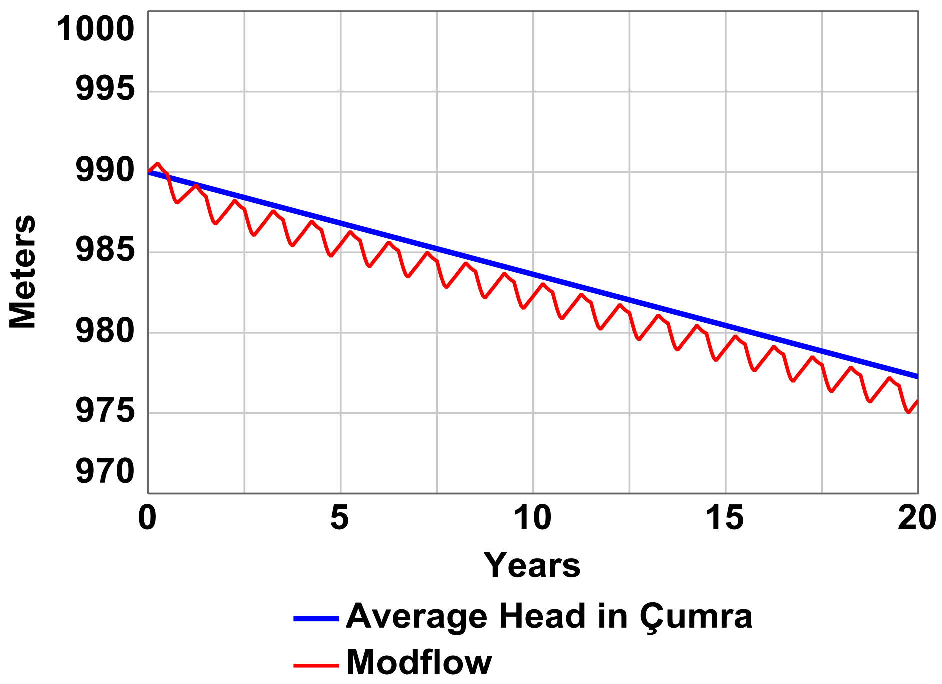

Figure 6.20. Precipitation-irrigation run.

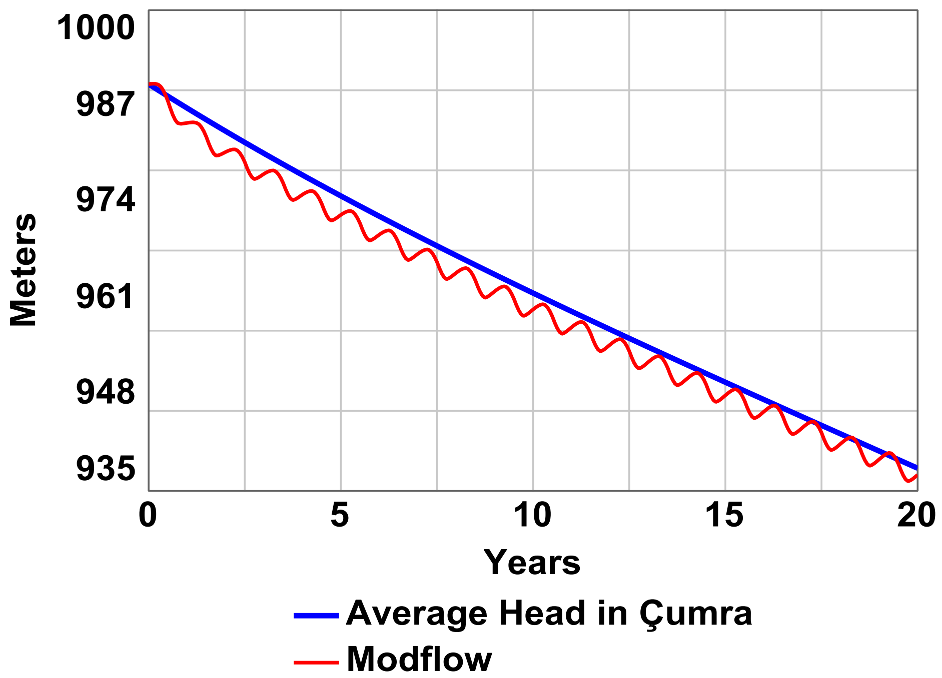

Figure 6.21. Irrigation-lateral flow run.

Lastly, we test the lateral flow, precipitation, and irrigation all together in one run. The land cover is half bare, and the other half is divided equally between the three crop types. The average head outside, precipitation, and irrigation efficiency are assumed to be constant throughout the simulation period.

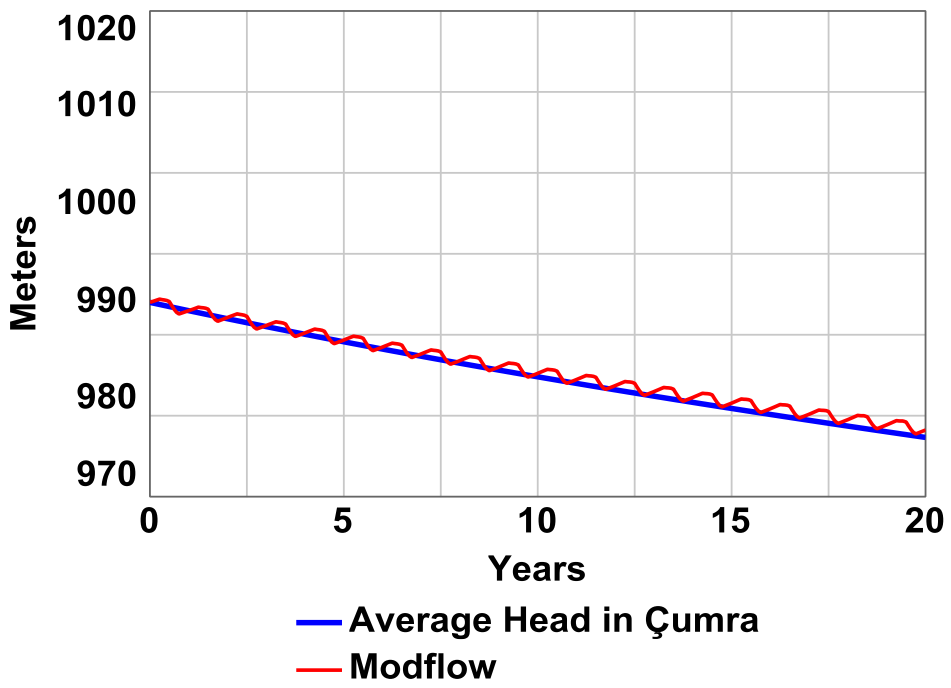

Figure 6.22. Precipitation-irrigation-lateral flow run.

6.2. Structural Validation

6.2.1. Direct Structure Tests

6.2.1.1. Structure assessment and boundary adequacy. In determining the model boundary and constructing the model structure, we benefitted from local groundwater users' and experts' participation in the group model-building workshops. In the first workshop, we were able to establish the issues and relevant system components. In other words, the first workshop revealed a framework for model boundaries, as well as some causal loop and conceptual model diagrams.

A seed model that served as the foundation for the model presented in this thesis was created in the second group model-building workshop. As a result, the fundamental framework of the model relies on stakeholder expertise; it was produced using data from semi-structured interviews and extensive qualitative SD work.

Lastly, once the model was fully developed and prior to the final GMB workshop, we organized another field trip to meet with the prominent stakeholders one on one to further discuss model validity.

6.2.1.2. Parameter assessment and dimensional consistency. To check for unit errors, every mathematical equation in the model is examined individually. Below is an example.

$$average\ well\ capacity = \frac{Average\ Pump\ Power\ \times pump\ efficiency\ \times irrigation\ period}{-1\ \times groundwater\ table\ \times unit\ energy\ requirement} \tag{6.10}$$

The average well capacity describes how much water a single well can produce in one irrigation season; therefore, its unit is the volume per well per year. It follows that the right-hand side of the equation must yield the same unit. The average pump power is measured in kW/well, and pump efficiency is unitless. The irrigation period is the number of hours that farmers irrigate their crops annually. The groundwater table is measured in depth, therefore is measured in length (meters). The unit energy requirement indicates the energy required to lift one cubic meter of water, one meter, and it is measured in kWh per cubic meter per meter (kWh/m^4). The units hold when all parameter units are inputted accordingly in the equation.

We did partial model calibration for parameter assessment by incorporating the data we obtained from multiple state institutions and the hydrogeological model, as well as the anecdotal data we obtained during the field campaigns.

6.2.2. Indirect Structure Tests

6.2.2.1. Extreme condition tests. We performed extreme condition tests on each model sector, and the results are provided below.

Extremely high and low groundwater demand

In the first experiment, we set the desired groundwater extraction variable, which represents the groundwater demand, to zero. As expected, the extraction is zero throughout the simulation, as shown in Figure 6.23. Thus, there is no need for pumping infrastructure. Average pump power and wells depreciate over time, and they are not replaced. As a result, annual groundwater extraction capacity approaches zero.

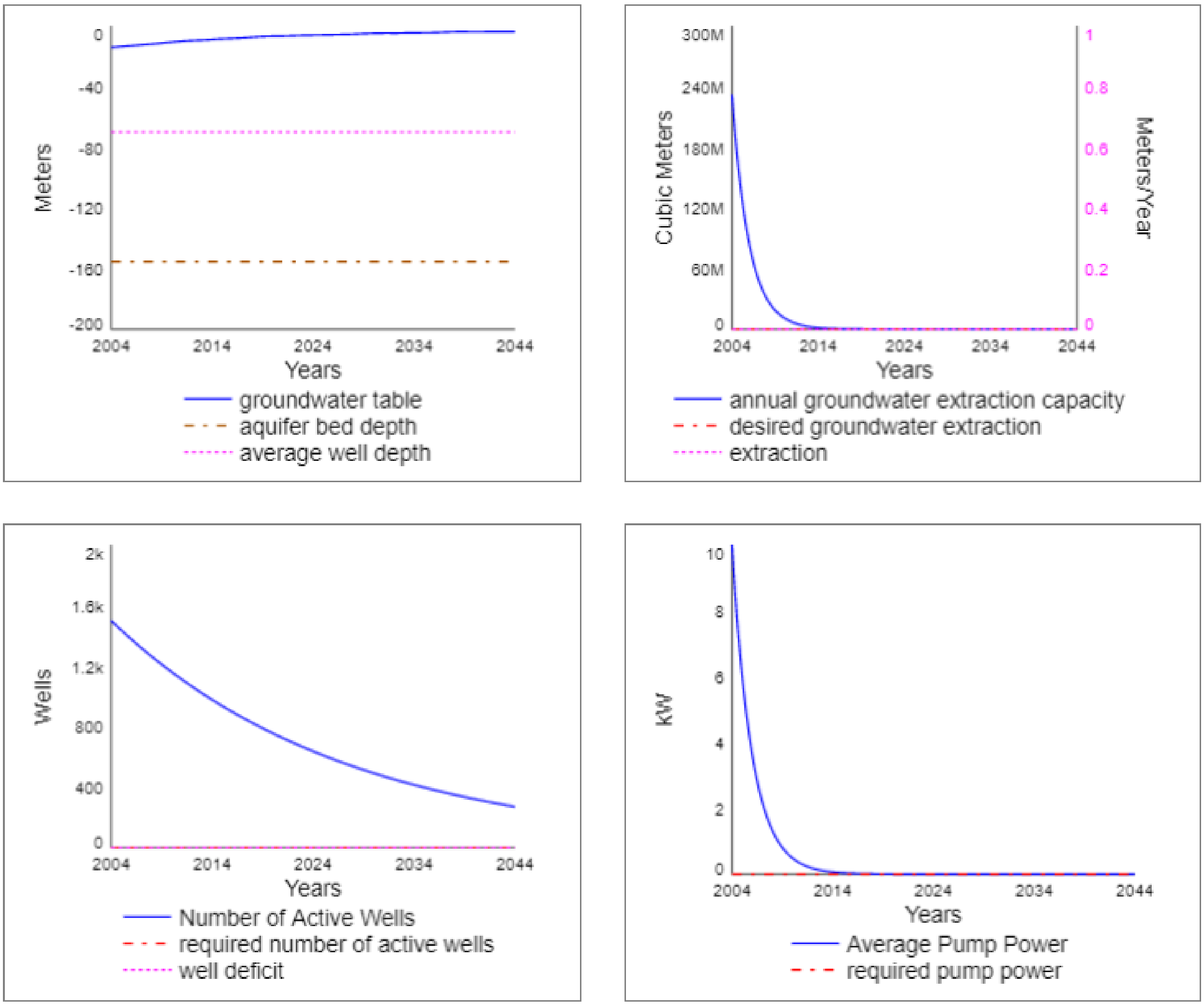

Figure 6.23. Simulation results for zero groundwater demand extreme case.

Then, we set the desired groundwater extraction to 3 billion cubic meters, which corresponds to more than twice the average desired extraction in the reference model behavior. At this extreme, it is anticipated that the groundwater table declines steeply, and pumping infrastructure is developed rapidly because the initially existing infrastructure is insufficient to fulfill the demand. Figure 6.24 shows the simulation results under this extreme test. As expected, we observe a sharp decline in the groundwater table. Additionally, infrastructure (groundwater wells and pump power) is built up fast in the first couple of years, resulting in a massive extraction capacity increase, through which groundwater supply approaches groundwater demand.

In the first half of the simulation horizon, the number of active wells keeps increasing and then starts decreasing. In contrast, following the rapid initial increase in the pump power, the rate of increase declines, and then the average pump power increasingly increases again, until it approaches its maximum value. The difference in the behavior patterns of the two extraction infrastructure types is due to the change in the average well yield (Figure 6.25), which is dependent on the pump power and groundwater table. First, the initial increase in the average pump power drives the average well yield up; however, as the increase in the average pump power slows down and the groundwater table lowers, the average well yield starts decreasing. Thus, more wells are opened to keep the groundwater supply close to the demand. In the meantime, the groundwater table lowers even more, so the need to further increase the pump power arises. The increasing trend in the average pump power fastens, and the average well yield goes up. As a result, since the water supplied from a single well increases, the same amount of water can be extracted from fewer wells, therefore the active number of wells decreases.

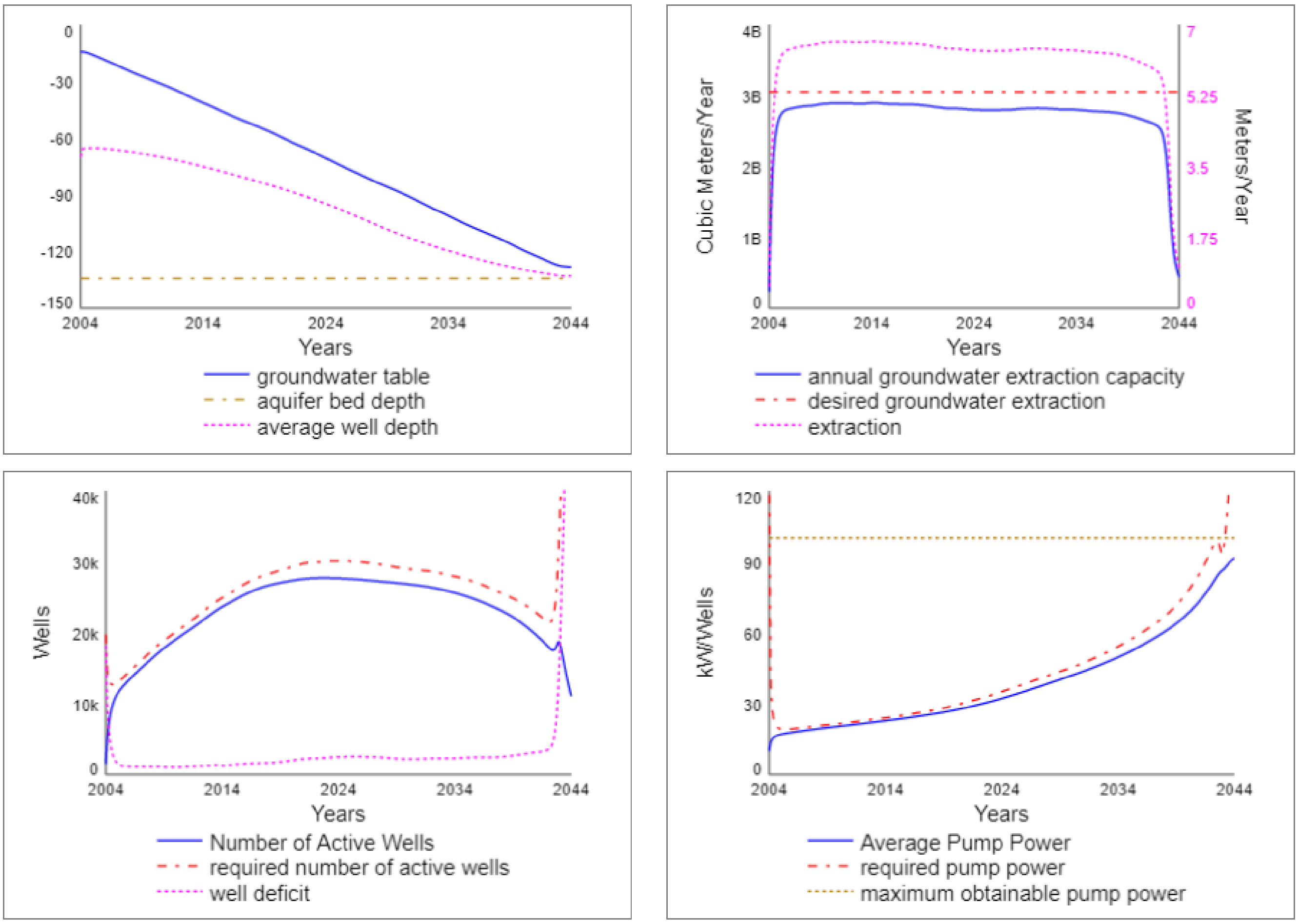

Figure 6.24. Simulation results for extremely high groundwater demand case.

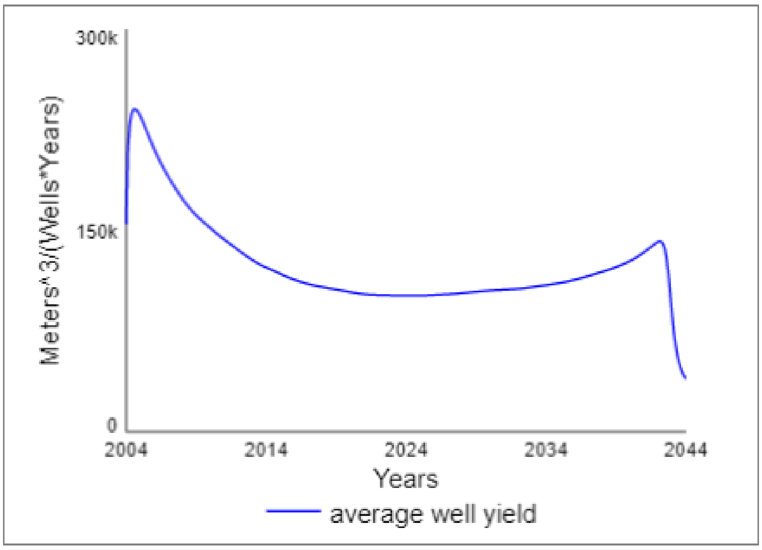

Figure 6.25. Average well yield under extremely high groundwater demand.

Near the end of the simulation, we see that the groundwater is almost depleted; the groundwater table approaches the aquifer bed depth. Therefore, the average well yield declines steeply. At this point, farmers possibly would not have realized that the groundwater is depleted, due to groundwater being an invisible resource and the aquifer bed depth being an unknown. So, they may open new wells initially, to fulfill the groundwater demand. However, soon, groundwater depletion is comprehended, and thus the number of wells declines sharply. The well opening behavior is presented in Figure 6.26.

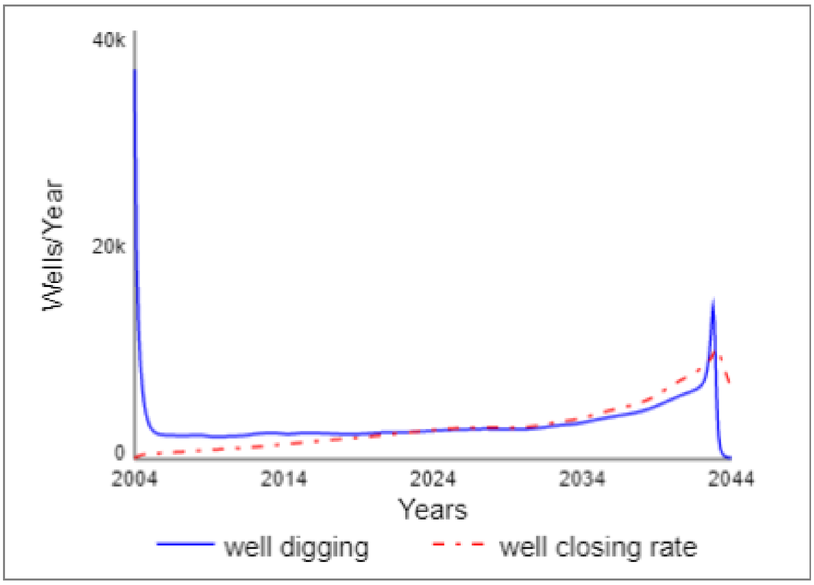

Figure 6.26. Well-digging and closing rates under extremely high desired groundwater extraction.

Extremely high and low well-digging time

First, we set the well digging time to 3 years. Considering that 3 years is a very long time to open a new well, we anticipate a very slow increase in the number of wells, and we expect to see a higher rate of increase in the pump power, to compensate for the slow rate of well digging. The simulated result of this extreme case is shown in Figure 6.27.

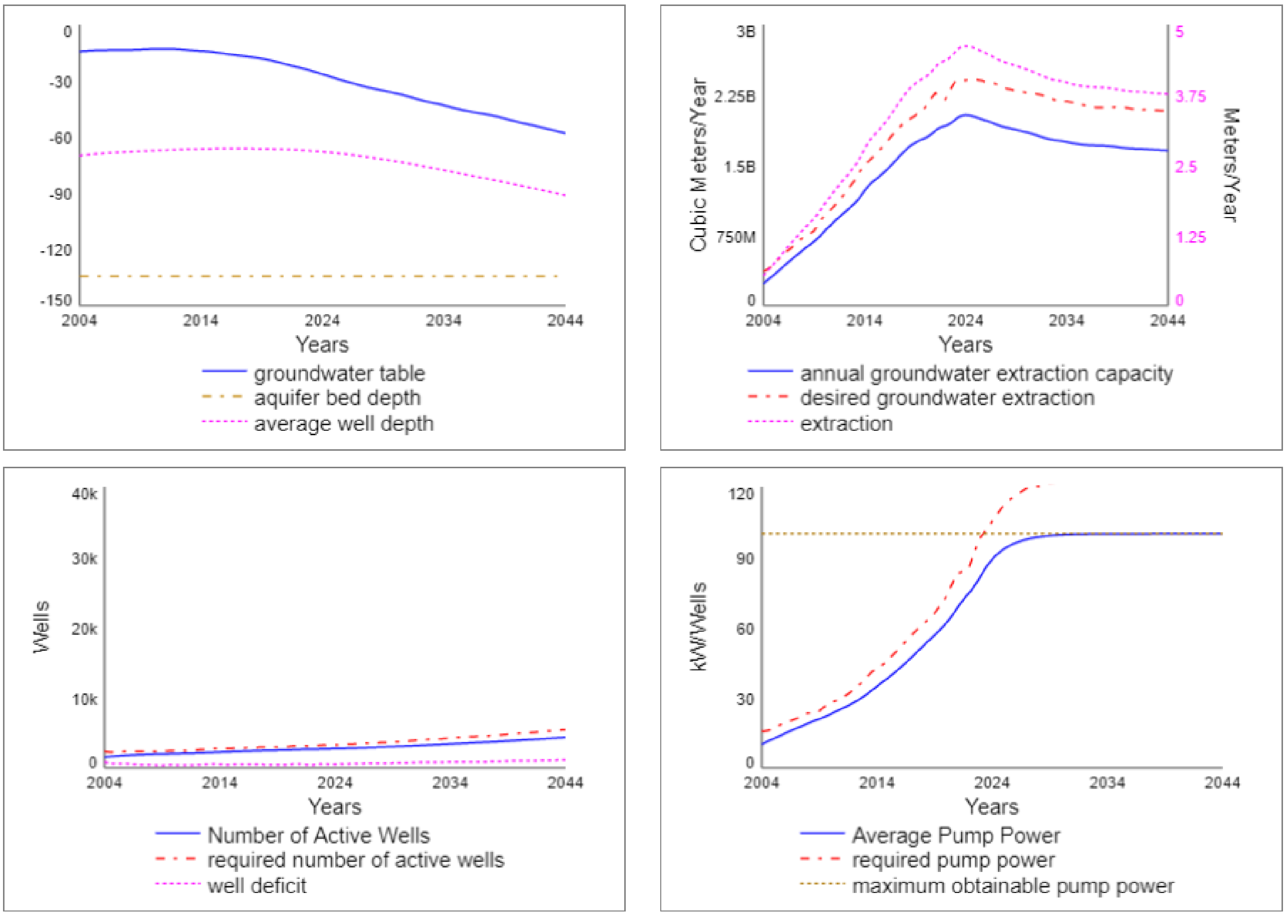

Figure 6.27. Simulation results for extremely high well digging time case.

Average pump power is capped by technological upper limit. Therefore, an increase in the average pump power cannot fully compensate for the gap between groundwater demand and supply that is caused by the long well-digging time. As a result, the decline in the groundwater table is lower than it would otherwise be.

Next, we set a very low well digging time, which implies that as soon as a need to open one more well emerges, a new well can be opened under ideal conditions. In that scenario, we expect to see a very low well deficit, which is the gap between the existing and the required number of active wells. Additionally, given that a well can be opened almost momentarily, we anticipate that the system tends towards increasing the groundwater supply mostly by higher well digging rates, instead of adjusting the average pump power. The simulated result of this extreme case is presented in Figure 6.28, and the outputs match our expectations.

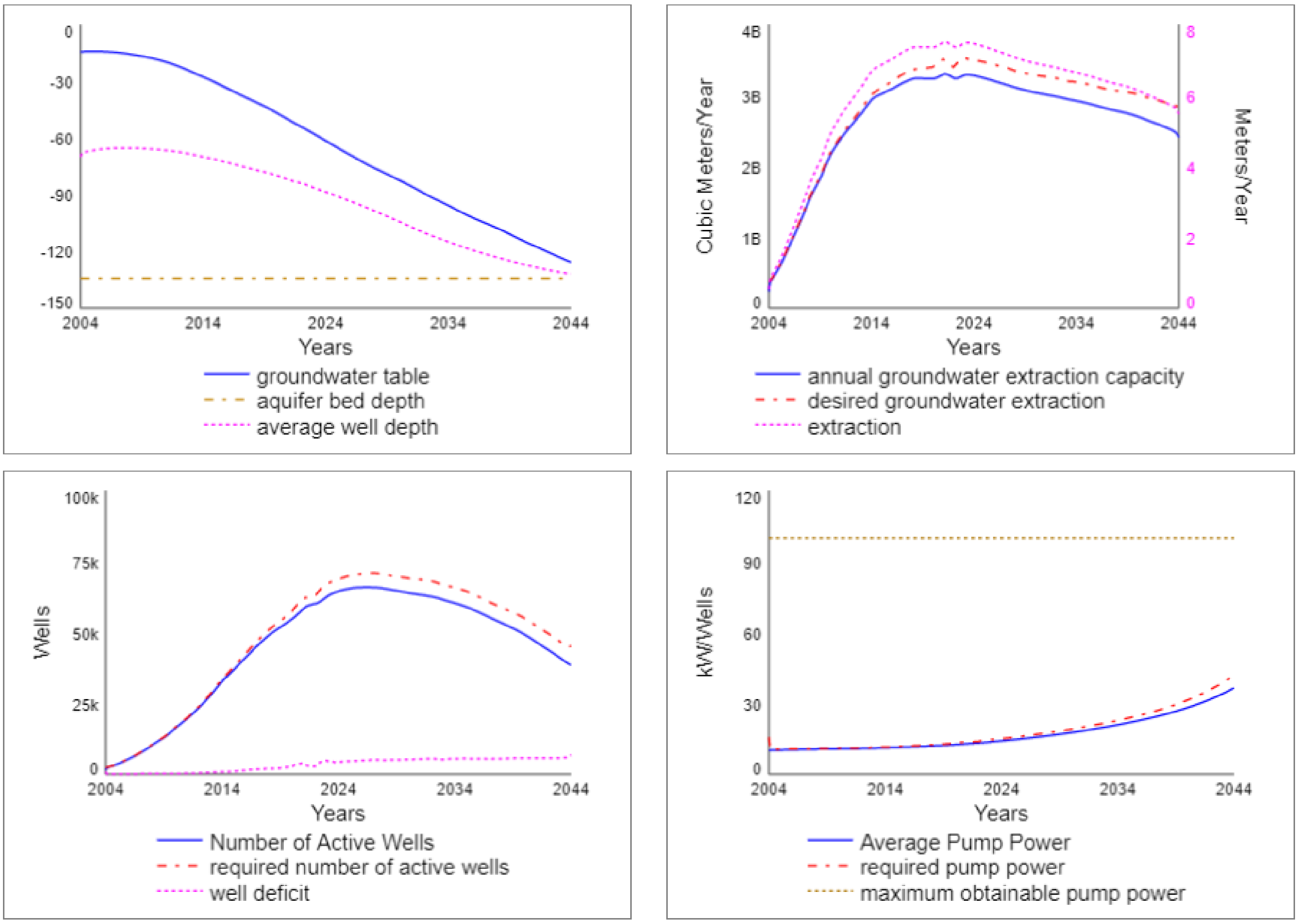

Figure 6.28. Simulation results for extremely low well digging time case.

Extremely high and low crop prices

In this set of experiments, we change the price of green plants to present the simulations under extremely high and low crop prices. First, we increase the green plants' price up to 5 TRY/kg without changing the prices of other crops. We anticipate that the price increase in green plants will make them more profitable, and thus more attractive. Therefore, we expect to see a considerable increase in the land for green plants. Figure 6.29 presents the simulated outputs of this extreme case.

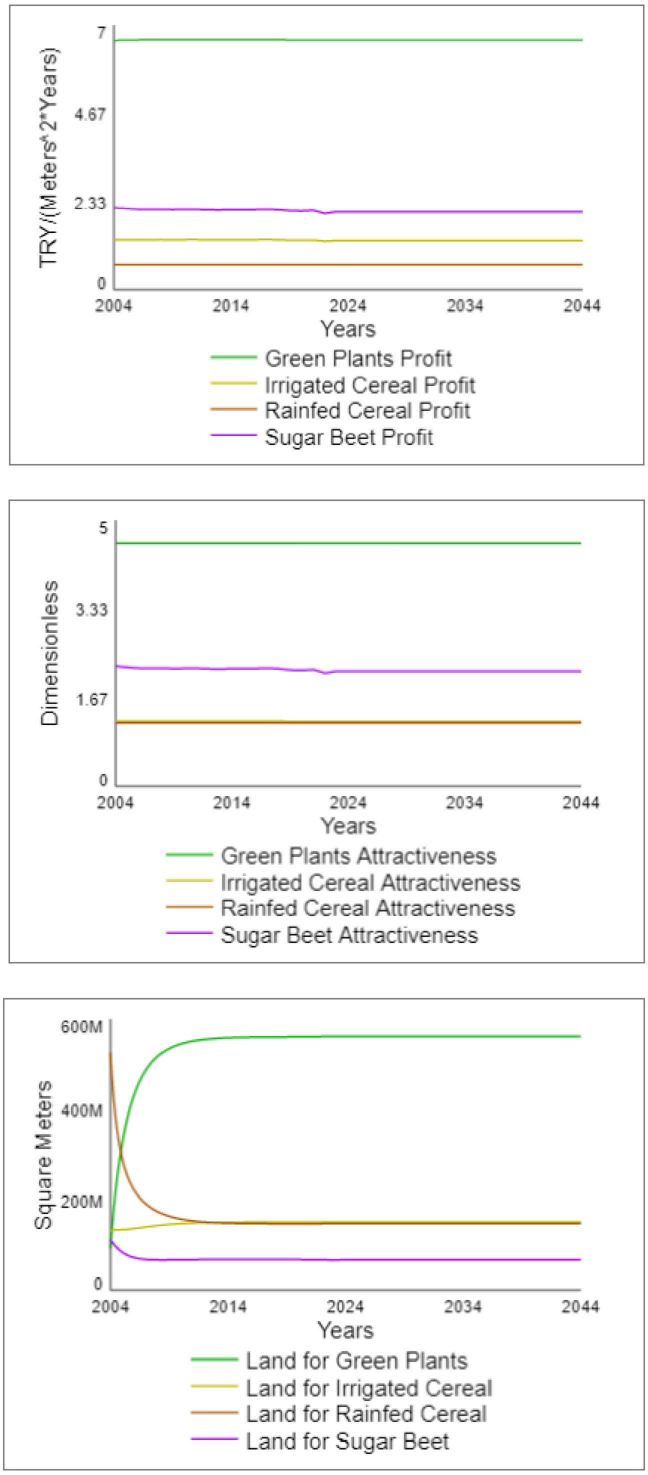

Figure 6.29. Simulation results for extremely high green plants price.

After that, we lowered the price of green plants to 0,55 TRY/kg, without changing the prices of other crops. We expect that the low price will render green plants the least attractive crop for farmers, therefore, its share in the total arable land will be smaller compared to the other crops. The simulated results of this case are presented in Figure 6.30. Overall, the model outputs meet the expectations. However, a rather interesting result is that even though sugar beet appears to be the most attractive crop, its land share is low compared to cereals. The factors limiting the sugar beet land are twofold: There is a quota on sugar beet land, and a 4-years rotation time, which implies that sugar beet can be cultivated once every four years.

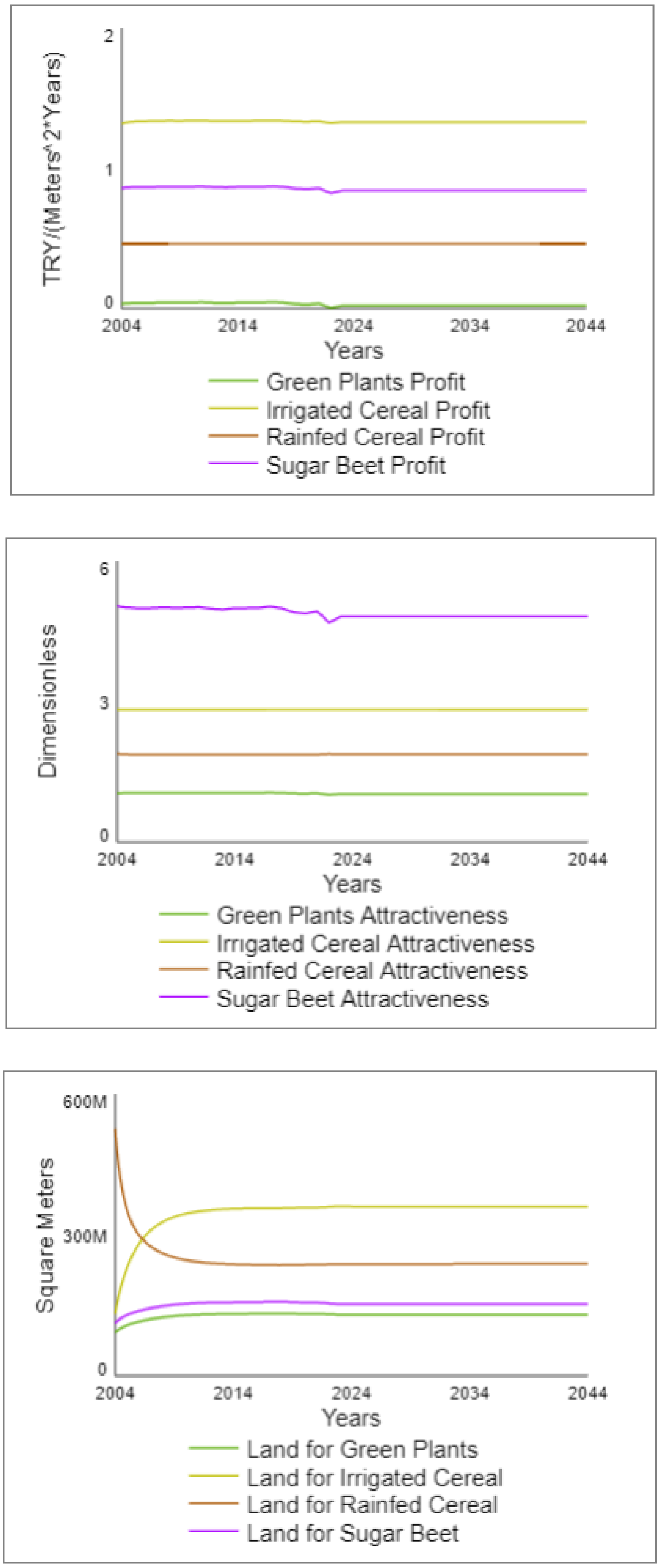

Figure 6.30. Simulation results from extremely low green plants price.

6.2.2.2. Behavior sensitivity tests. We carry out two different behavior sensitivity tests on the model to assess the sensitivity of the model to different parameters. First, we test the sensitivity of the logit model in the crop land use sector by comparing three levels of crop sensitivity of attractiveness to profit. Second, we test the sensitivity of the Cobb-Douglas production function to yield elasticity of water. We use three different values of yield elasticity of water to investigate the model behavior.

Behavior sensitivity of crop land allocation to crop sensitivity to profit

In this test, we run three simulations on the crop-land use sector with different values of irrigated cereal sensitivity to profit. Given that the relative attractiveness drives the land cover change, we leave the other crops' sensitivity parameters unchanged and test with a single sensitivity parameter. There is no specific reason why we choose to test with irrigated cereal; the tests may be repeated for each of the crops. In all three test runs, the initialization of land stocks is the same as that of the base run, i.e., land cover data of the year 2004. For the sake of simplicity, we use constant crop prices and production costs for each crop. In these tests, we keep the four-year rotation practice in sugar beet, and the sugar beet quota enforcement in the model. The values set for the test runs are presented in Table 6.8.

We expect that the attractiveness of irrigated cereal will increase as the sensitivity to profit increases because the attractiveness is formulated as an exponential function of the sensitivity parameter (and relative profit). As a result, under constant price and cost conditions, we anticipate that the attractiveness value of the irrigated cereal will be constant, but different in each run, and thus the land cover will reach varying steady-state conditions.

Table 6.8. Test runs for the irrigated cereal sensitivity to profit.

Runs	**Irrigated Cereal Sensitivity of Attractiveness to Profit**
I	1
II	0
III	2

Figure 6.31 shows the attractiveness of crops in the three test runs. As expected, the attractiveness of crops other than irrigated cereal are unchanged, while the attractiveness of irrigated cereal is the highest in Run III and lowest in Run II.

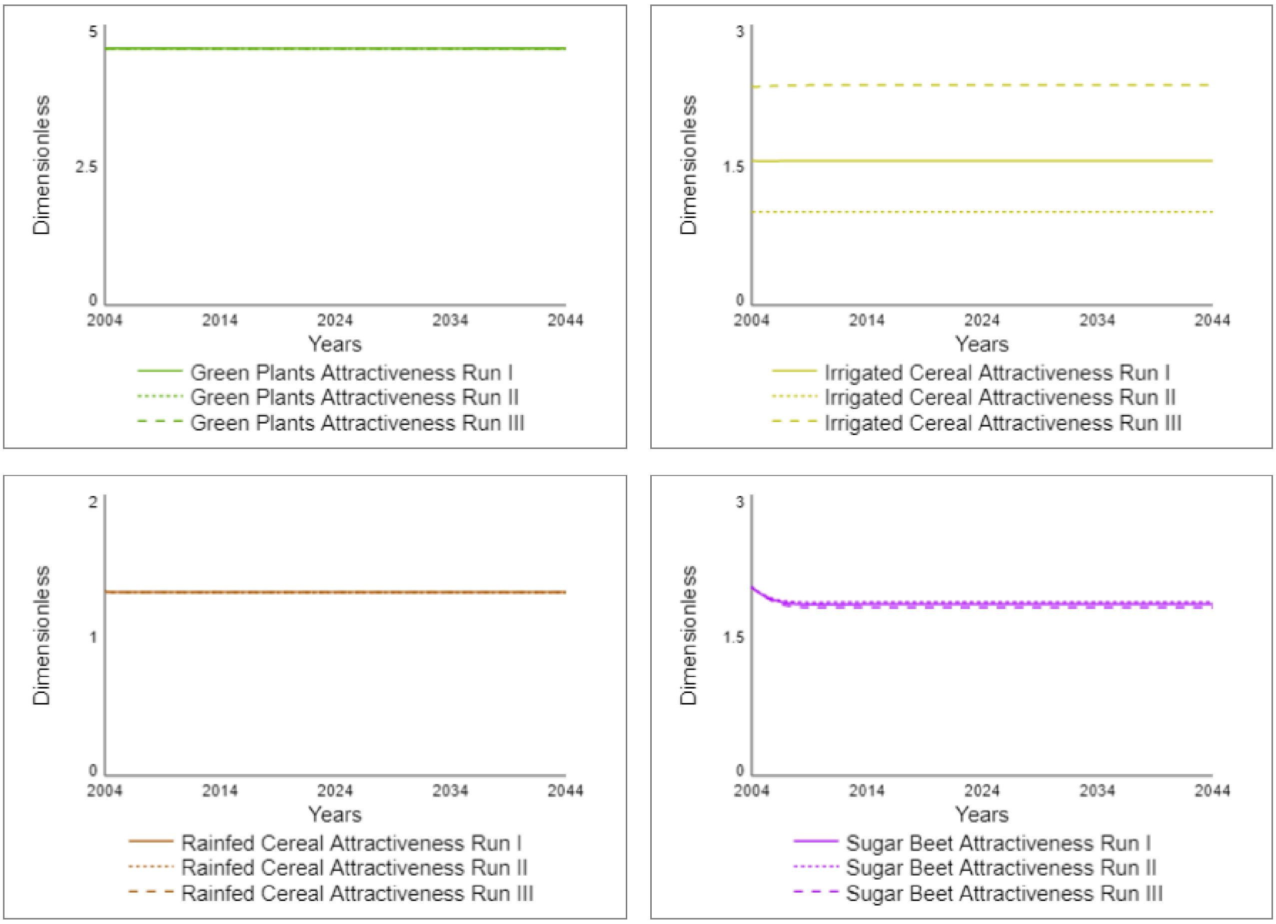

Figure 6.31. Sensitivity test 1: crop attractiveness.

Since the total agricultural land is constant in the model, the change in one crop land stock affects the others as well, even though their attractiveness is unchanged. Figure 6.32 presents the change in the crop land stocks.

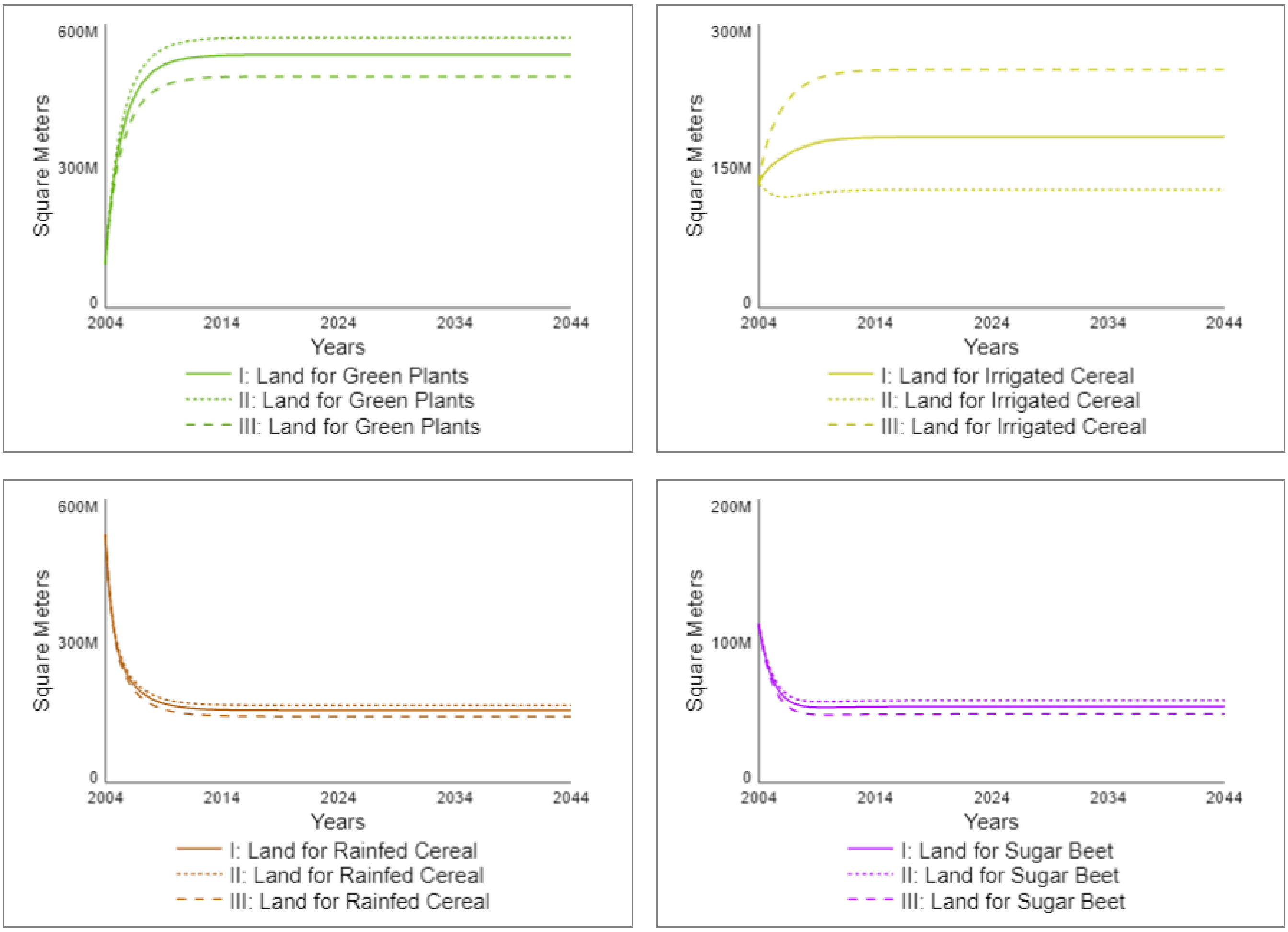

Figure 6.32. Sensitivity test 1: Crop land stocks.

Behavior sensitivity of irrigation and yield goal setting to yield water elasticity

In these tests, we aim to investigate the sensitivity of yield, as well as the desired irrigation, to the yield water elasticity of crops. For the sake of simplicity, we only run the water and groundwater infrastructure, and production factor adjustment, and yield goal-setting sectors. In other words, land cover, irrigation technology efficiency, and economic parameters are assumed to be constant in the tests. Additionally, we consider only one crop, green plants. To that end, we set the desired irrigation water and share in water allocation variables to zero for crops other than green plants. Therefore, the model extracts only for the green plants and we take three runs with different values of green plants yield elasticity to water. Table 6.9 shows the elasticity values used in the three test runs.

A lower elasticity value implies that the crop is rather inelastic to water. In other words, the yield is affected less by potential water stress, compared to a crop with a higher elasticity.

Therefore, we anticipate that the desired irrigation level will be higher in the test runs with higher elasticity values.

Table 6.9. Test runs for the green plants yield elasticity of water.

Runs	Green Plants Yield Elasticity of Water
I	0,3
II	0,5
III	0,7

Figure 6.33 presents the simulation results of the three test runs. The outputs reflect the expectations.

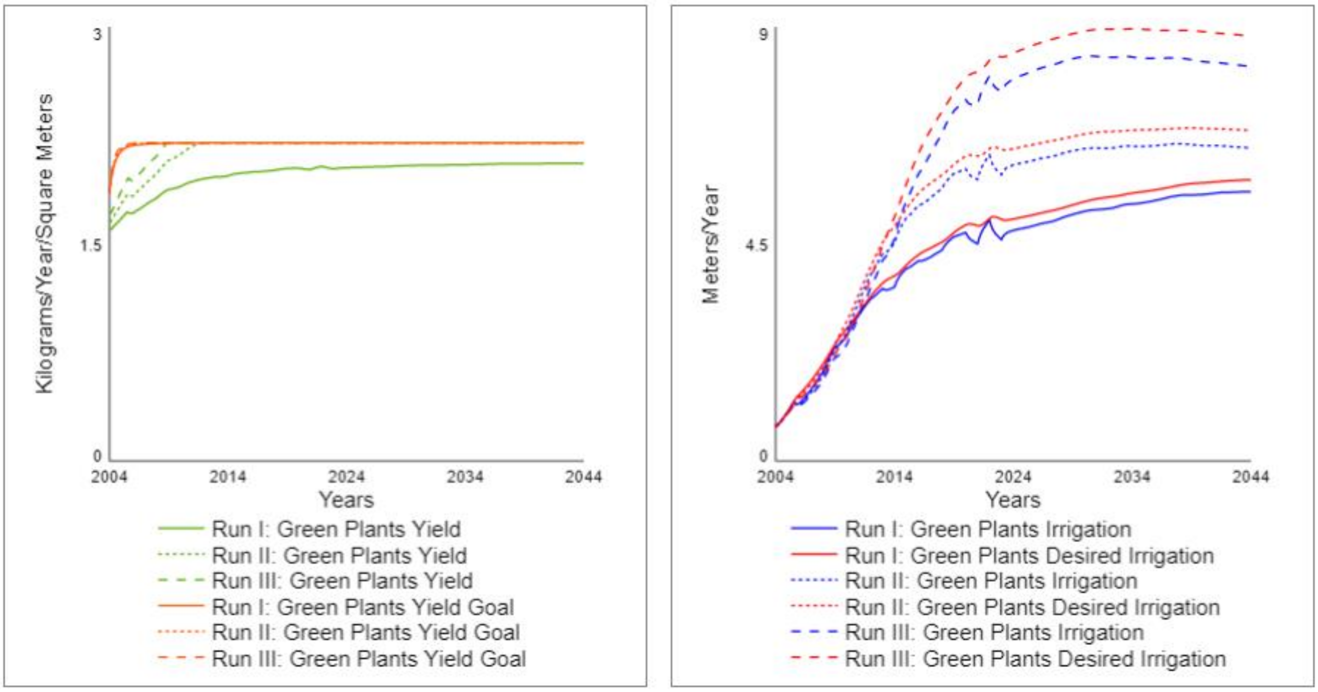

Figure 6.33. Sensitivity test 2: Green plants yield and irrigation.

Behavior sensitivity of number of active wells to reference average well yield

In this test, we investigate the sensitivity of the number of active wells to the reference average well yield. In the model, well digging decision is driven by both the requirement of new wells, and the comparison how much water an additional well can produce, compared to the reference average well yield. Therefore, we test with three different values of reference average well yield (Table 6.10) and compare the outputs.

Table 6.10. Test runs for the reference average well yield.

Runs	Reference Average Well Yield (m^3/year/well)
I	150.000
II	200.000
III	250.000

Figure 6.34 shows the test results. We observe that the number of active wells are highly sensitive to the reference average well yield. As expected, when the reference average is lower, the perception is that the amount of groundwater obtainable from an additional well is worth the effort of digging the new well. Therefore, the number of active wells increases from Run I to Run III. On the other hand, the peak-then-decline behavior pattern is common in all three runs. While the number of active wells peak first in Run III and last in Run I, there is not a significant difference. In terms of groundwater table, the model is less sensitive because the model adjusts the average pump power to keep the annual extraction capacity at a desired level.

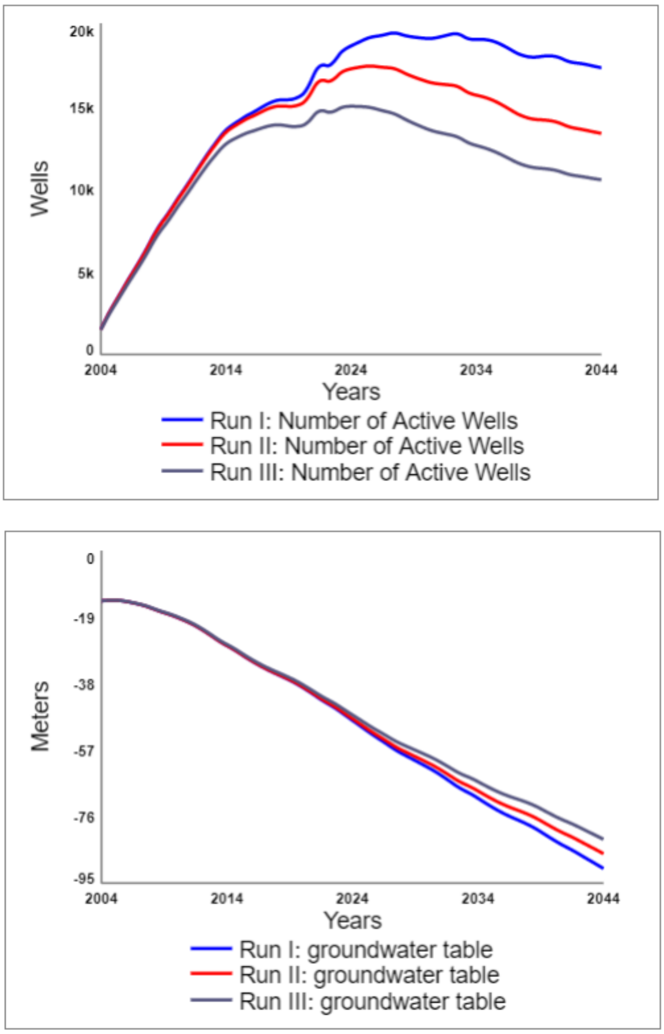

Figure 6.34. Sensitivity test 3: Number of active wells and groundwater table.

6.3. Behavioral Validation

After building enough confidence in the model structure, we test the validity of the behavior patterns simulated by the model. To that end, we collected several data sets from various state institutions. However, most data that we wanted to collect are either lacking, inapplicable, or unreliable. Therefore, we validate the behavior of some of the variables by the anecdotal data that we obtained during the semi-structured interviews in the field visits. To assess the behavior validity of the model, we simulate from 2004 to 2022.

The graph in Figure 6.35 shows the groundwater table data obtained from the State Hydraulic Works (DSI) and the simulated groundwater table. There are 8 observation wells in the Çumra district, and the plotted data is the average of the observations from these 8 wells between 2004 and 2021. Even though the dataset demonstrates a decreasing trend, the groundwater table rises between 2010 – 2013. We do not have an explanation regarding the cause(s) of this behavior; therefore, it is not reflected in the model behavior. Moreover, the observations in the wells do not comply with the statements of the farmers regarding their well depths; farmers claim the groundwater table is lower than the DSI data. However, we validate the model behavior with the DSI data both because the groundwater table farmers observe in their wells may vary based on the season, while observation wells are not used for pumping, and also because the measurement with professional equipment is more reliable.

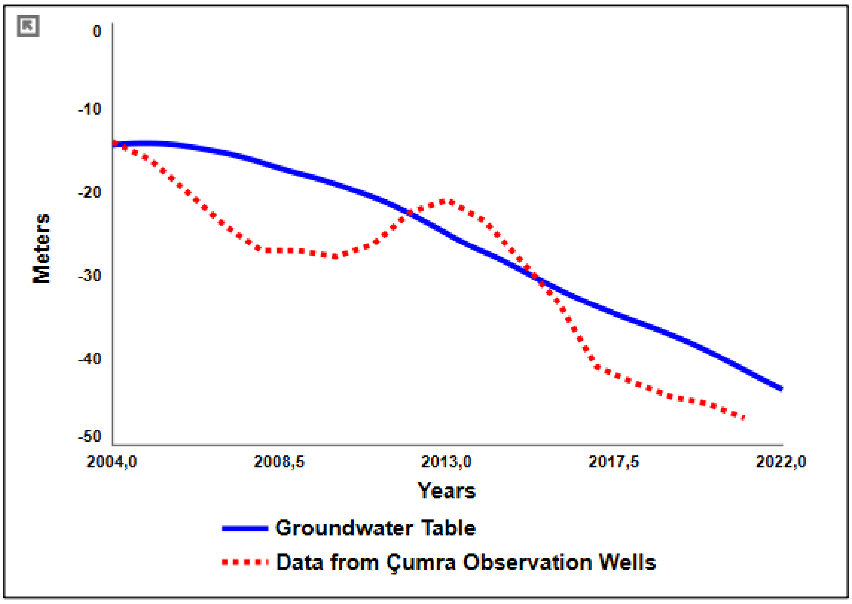

Figure 6.35. Groundwater table: data and simulation.

Figure 6.36 presents the crop land use data and the simulations. The data were downloaded from Turkish Statistical Institute’s (TÜİK) open-source database; it is yearly, and the scale is Çumra district itself, which matches the model’s spatial boundaries and the temporal resolution. So, we did not need to adjust the data to our needs. However, while we have data on sugar beet, green plants, and fallow land for the 2004-2022 period, the data we have on irrigated and rainfed cereal land covers only the 2012-2022 period. The cereal land data between 2004-2012 are not differentiated as irrigated and rainfed.

It should be mentioned that during our interviews with responsible officers from TÜİK and Çumra District Directorate of Agriculture, we discovered two reasons why the data is not completely reliable. The first one regards the data collection method; it is based on farmers' statements. Each year farmers declare the crops they are planning to cultivate and receive financial incentives accordingly. However, sometimes the farmers declare one crop and cultivate another. If the district directorate discerns such a situation, they correct the data; yet in many cases, the situation goes unnoticed. The second reason is related to the publication of the data; TÜİK manipulates them before publishing.

The two abnormalities observed in the data are the abrupt increase in irrigated cereal land around 2013 and the abrupt increase and decrease in fallow land data around 2006 and 2013, respectively. Since the model does not include any dynamics regarding the increase or decrease of the total agricultural land, we do not observe such behavior in the simulated results. Still, the published data shows the overall trend, and the model produces similar trends.

Simulated crop yields and crop yield data are shown in Figure 6.37. The crop yield data was obtained from TÜİK’s open-source database. However, the data strongly contradicts the farmer statements. We asked every farmer whom we interviewed, about the average yields for each crop presented in the model. Their answers were very close to one another, and much higher than the TÜİK data. We calibrated the model according to farmer declarations because we do not know how the yield data was collected, but we know that the data published by TÜİK understates the production. Additionally, TÜİK’s yield data is not separated as rainfed cereal yield and irrigated cereal yield, therefore, we needed to rely on farmer statements for cereal yield.

For green plants, farmers state that the yield used to be around 12 – 15 tons/hectare. Over the years, farmers started using more fertilizers and more water to increase yields, and currently, they obtain 18 – 20 tons/hectare. When cereal is not irrigated, the average yield ranges between 3 – 5 tons/hectare, based on the precipitation level. According to farmers, the average yield for irrigated cereal increased from 5 – 6 tons/ hectare to 8 tons/hectare over the years. Lastly, the current average yield in sugar beet is 100 tons/hectare, while it used to be 60 – 80 tons/hectare before. The model behavior is in line with the anecdotal data obtained in the field trips.

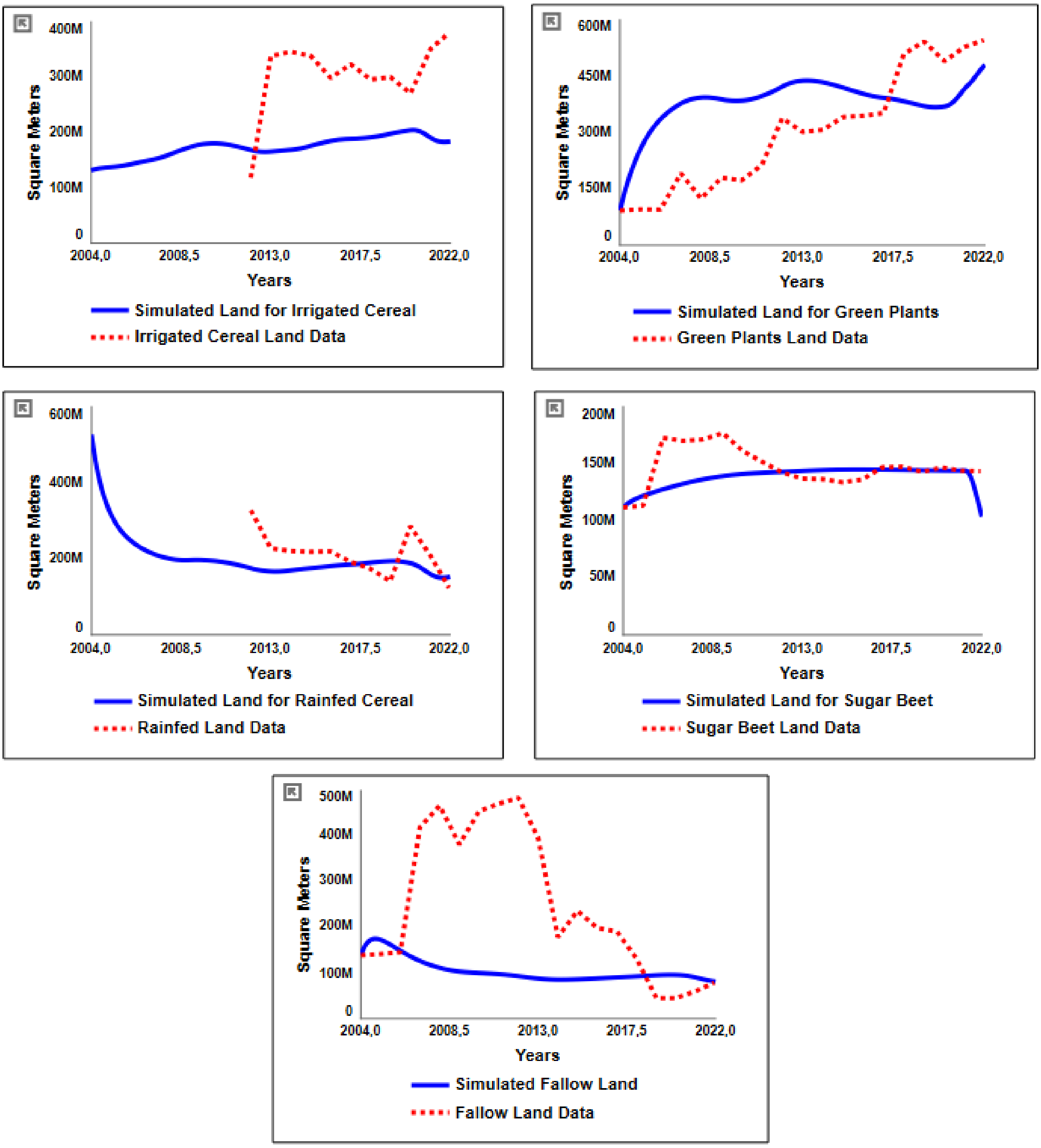

Figure 6.36. Crop-land cover: data vs simulation.

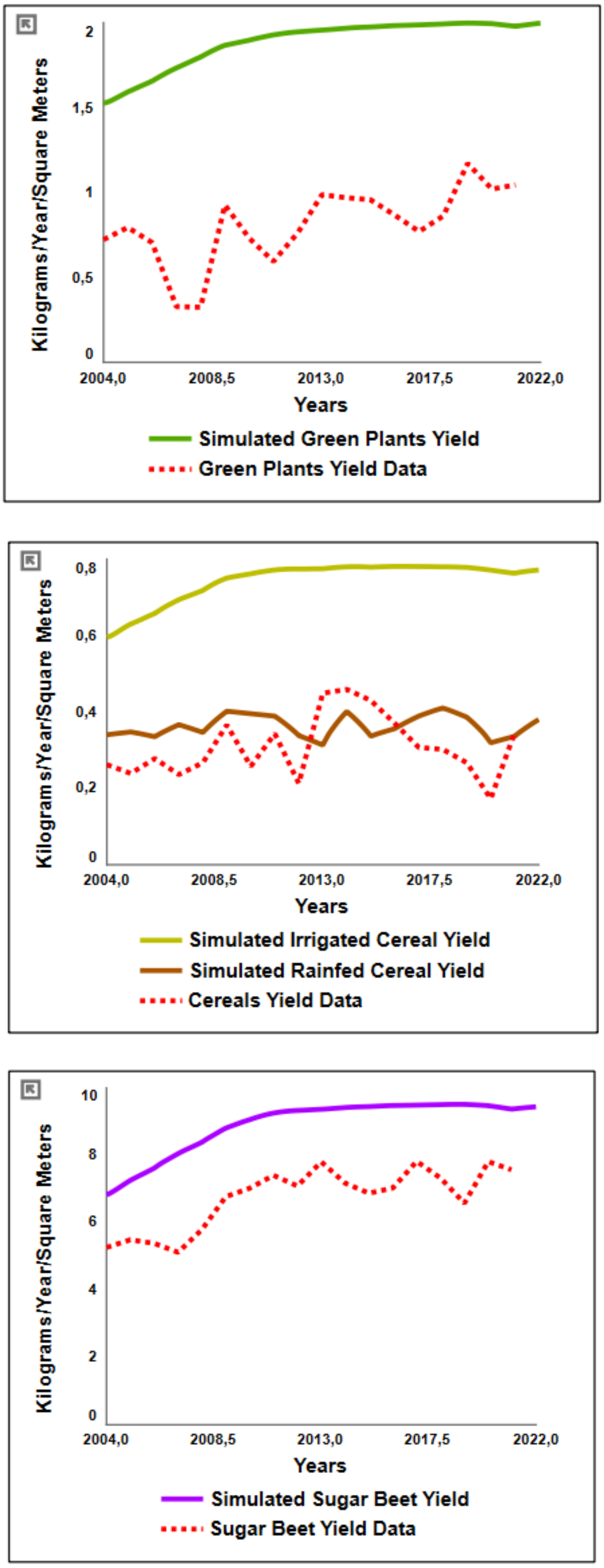

Figure 6.37. Crop yields: data vs simulation.

Unfortunately, even though the number of groundwater extraction wells is considered one of the most important issues in the basin by all stakeholder groups, there is not any data regarding the number of wells in the region; it is the elephant in the room. Stakeholders have varying estimates about the current number of wells in the basin; these estimates range from 100.000 to 180.000 illegal wells in the whole basin, and they are all on illegally drilled wells because DSİ stopped distributing new permits in the early 2010s. The only reference point we have is the inventory study carried out by DSİ in 2007, in which they identified 94.000 groundwater wells in Konya Closed Basin in total. Starting from this, we estimated a range regarding how many of those 94.000 wells could have been in Çumra in 2007. First, we calculated how many wells would be in Çumra if the wells were distributed equally in the basin. However, Çumra has always been a pioneering district in agricultural practices, and it is a rather water-rich region compared to other districts in the basin. Therefore, we presume that the well density (wells per area) would be higher in Çumra. As a result, we estimated a range of 3-8%, which corresponds to 2.820 to 7.520 wells in the Çumra district in 2007. The red dashes in Figure 6.38 show the upper and lower estimates, and the simulated number of groundwater wells is within the range in 2007.

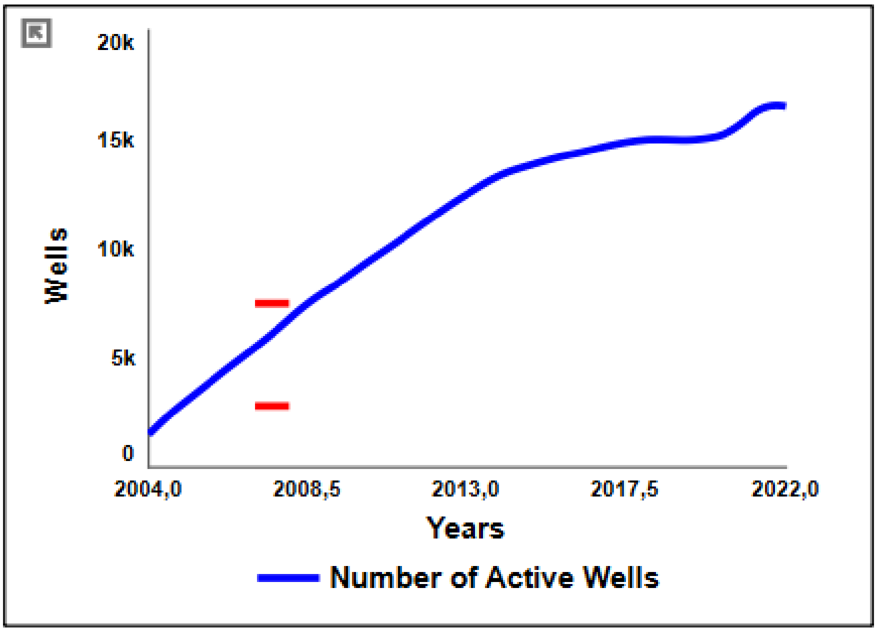

Figure 6.38. Number of active wells: estimate vs simulation.

Similar to the number of wells, there is no data on the power of the pumps used to extract groundwater in the region. From the anecdotal data we obtained during the field visits, we know that the average pump power has been increasing over the years due to the lowering groundwater table. We initialized the average pump power stock based on the anecdotes. We also asked the farmers about the power of the pumps they used and the depth they observe in their wells. Based on the answers, we figured that different pumps can be used to extract from similar depths. However, we needed an estimate for the average pump power, so we used the maximum and minimum pump power values we heard in the field for similar depths and adjusted the values to the 2022 groundwater table depth. As a result, we came up with 18,5 and 33,5 kW for lower and upper bounds respectively. The estimated bounds are shown as red dashes in Figure 6.39, and the blue line shows the simulated average pump power.

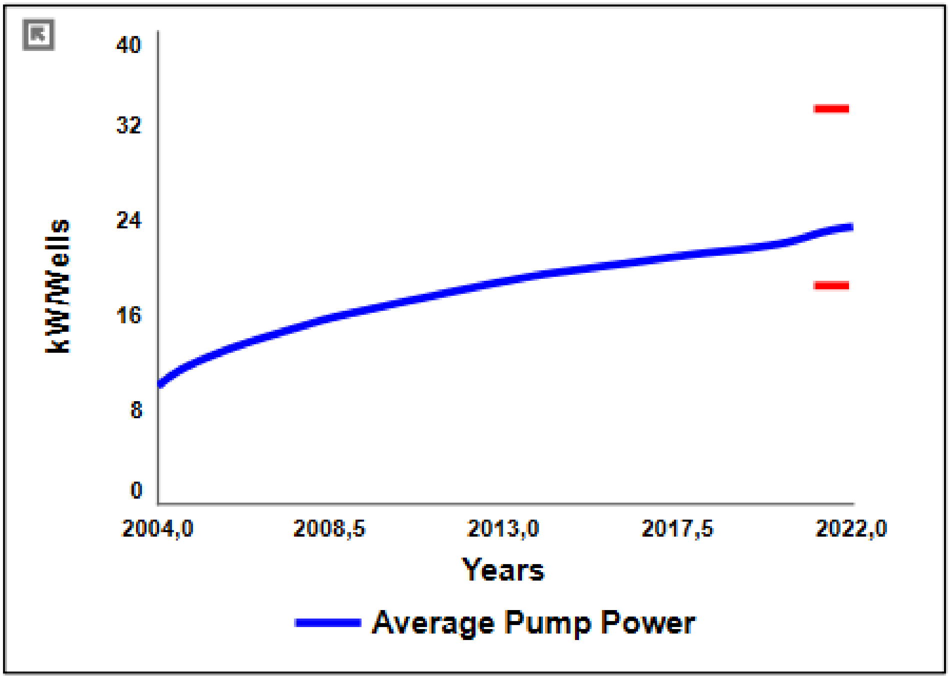

Figure 6.39. Average pump power: estimate vs simulation.

6.4. Reference Model Behavior

The reference model behavior is presented in this section. For the reference run, i.e., the base run, the same set of parameters and initial conditions are used as the behavior pattern test.

Figure 6.40 shows the groundwater table and average well depth. The aquifer bed depth (representing the aquifer bottom) and the zero line (representing the soil surface) are shown as references. We see that from 2022 onwards, the decreasing trend in the groundwater table continues, and in 2044; it reaches -86,6 meters accounting for a 72,2-meter drop in 40 years.

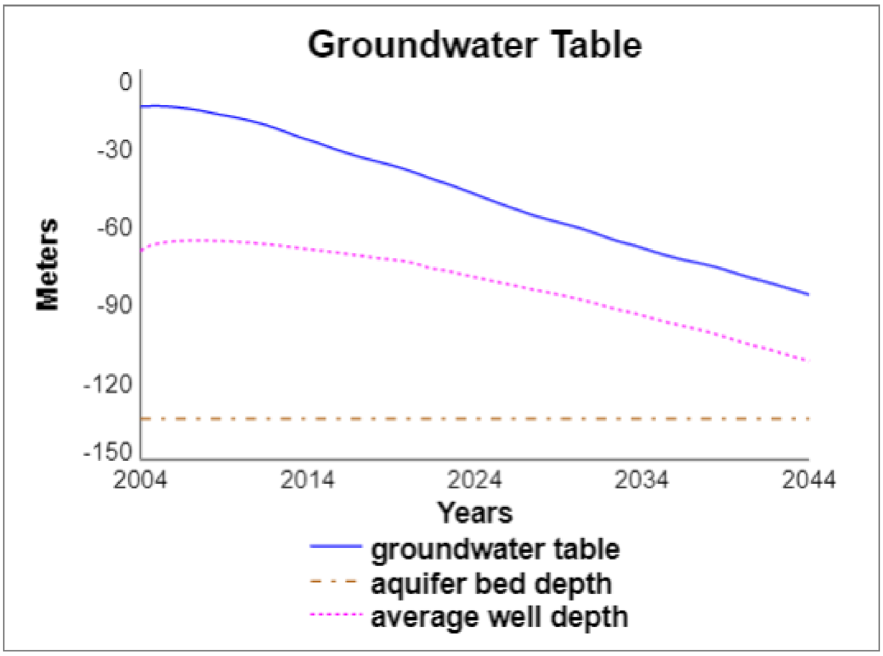

Figure 6.40. Reference model behavior of groundwater table and average well depth.

Figure 6.41 shows the crop-land changes from 2004 to 2044. We observe that from 2022 onwards, the land cover changes are minimal. That is because we keep the 2022 prices until the end of the simulation in the reference run, given that we do not know how the prices will change in the upcoming years. It should be noted here that to eliminate the impact of inflation, the price inputs in the model are adjusted to the 2020 level, based on the annual consumer price index (CPI) of Turkey.

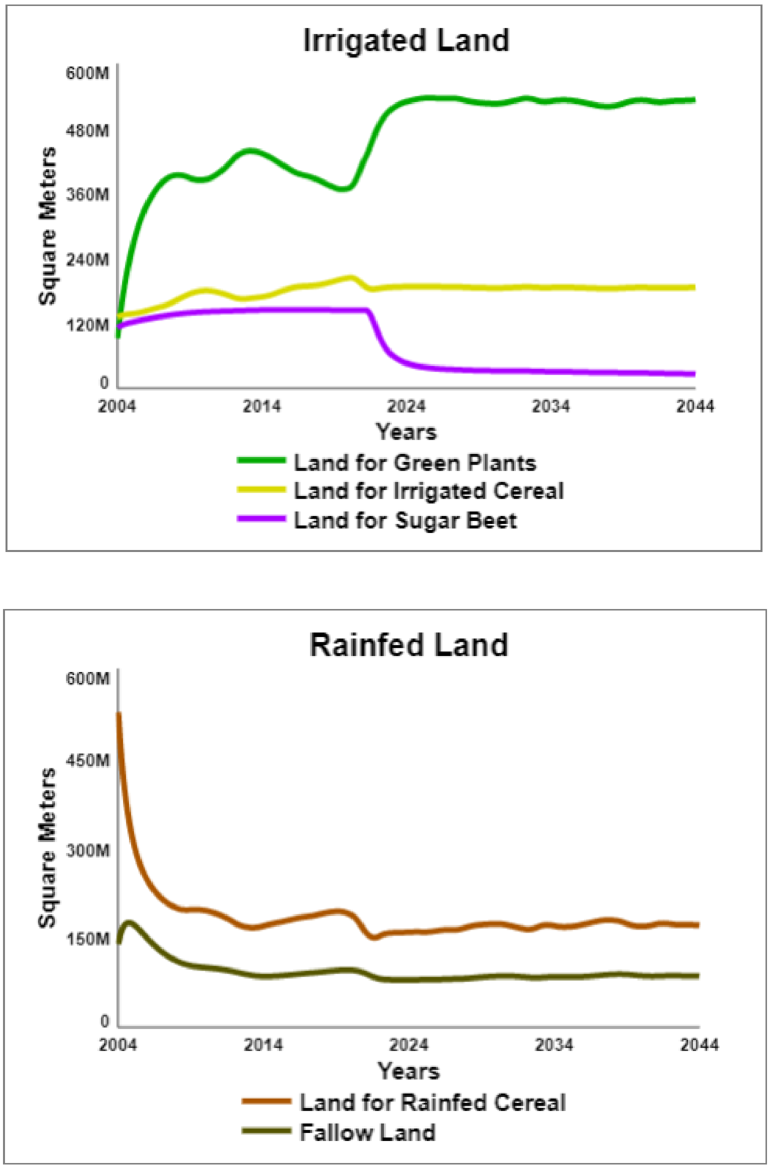

Figure 6.41. Reference model behavior of crop-land cover.

The reference behavior of the groundwater extraction infrastructure, i.e., groundwater wells and pump power are presented in Figure 6.42. The number of wells peak around 2025 and then start declining. This is a counterintuitive and surprising behavior; we expected to see a point where extraction might become economically infeasible due to the drop in the groundwater table, however, that is not the case in this run. The number of wells starts decreasing because the groundwater demand decreases, as we will explain below. On the other hand, the pump power continues to increase until the end of the simulation, because more power is required to extract water from deeper levels.

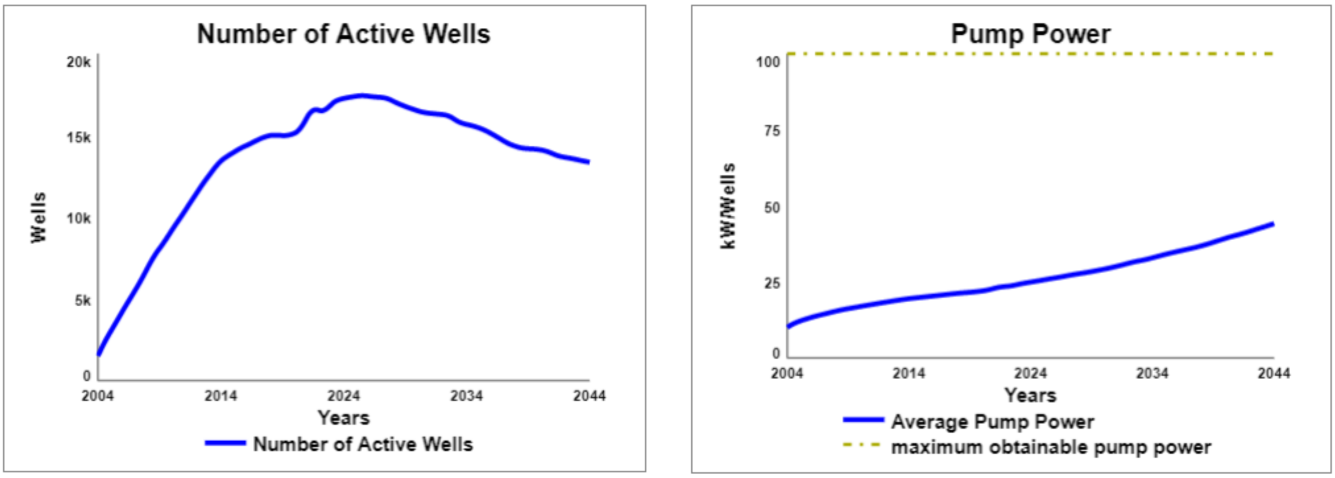

Figure 6.42. Reference model behavior of the number of active wells and average pump power.

Figure 6.43 displays the reference model behavior of desired irrigation and irrigation for different crops. We observe a similar behavior pattern for all crops: increase then decrease. Two factors drive the desired irrigation level. At the beginning of the simulation, the irrigation level is increased to acquire the yield goal. As the groundwater table is not deep and thus the irrigation cost is rather low, the desired irrigation rapidly increases. However, as the groundwater table lowers and the cost of irrigation increases, overirrigation becomes costly and the desired irrigation level is adjusted to achieve the highest possible profit. Additionally, the improvement in the average irrigation technology efficiency helps reduce groundwater demand.

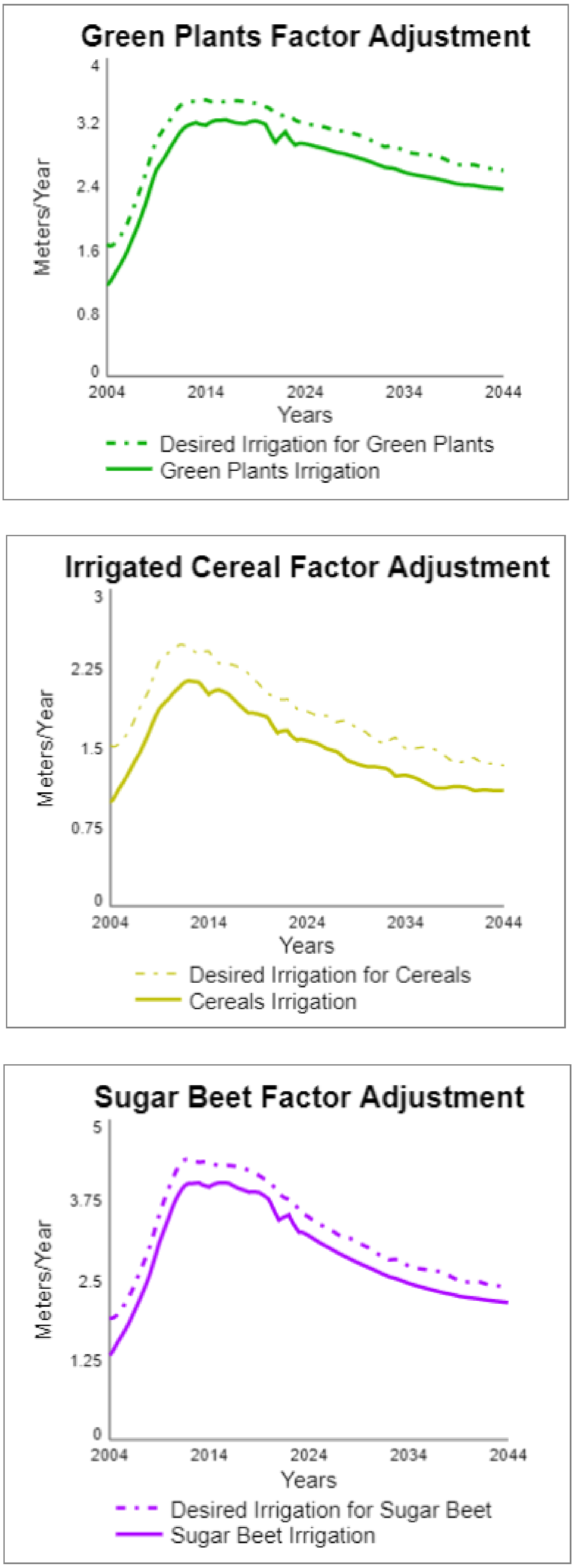

Figure 6.43. Reference model behavior of desired irrigation and irrigation for crops.

The crop yields are presented in Figure 6.44. Due to increased irrigation, we observe an increase in the yields of irrigated crops, namely, green plants, irrigated cereals, and sugar beet. The rainfed cereal yield fluctuates because it is dependent on precipitation. After the irrigation levels start decreasing, green plants' yield is the least impacted. Irrigated cereal and sugar beet yields decrease by around 7%.

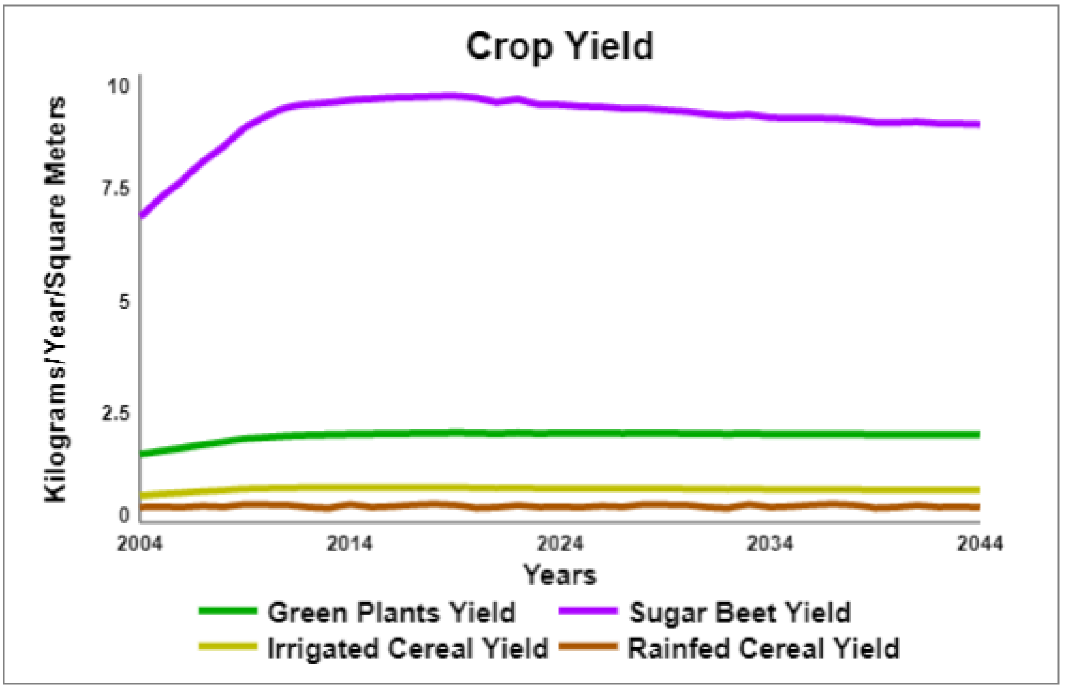

Figure 6.44. Reference model behavior of crop yields.

In Figure 6.45, we see that the average irrigation technology continues increasing throughout the simulation and approaches the technological cap, which is the efficiency of the most water-conserving irrigation technology available. Currently, that is drip irrigation, with an approximate 90% efficiency; however, during our field visits, farmers mentioned that they would like to upgrade to sub-surface drip irrigation, which is 95% efficient. Yet, they cannot afford to switch because the equipment is expensive and the state does not offer any financial incentives, as it does for drip and sprinkler irrigation equipment. However, we assume that in the upcoming years, farmers may start using subsurface drip irrigation technology, therefore, the technological efficiency cap in the model is inputted as 0,95.

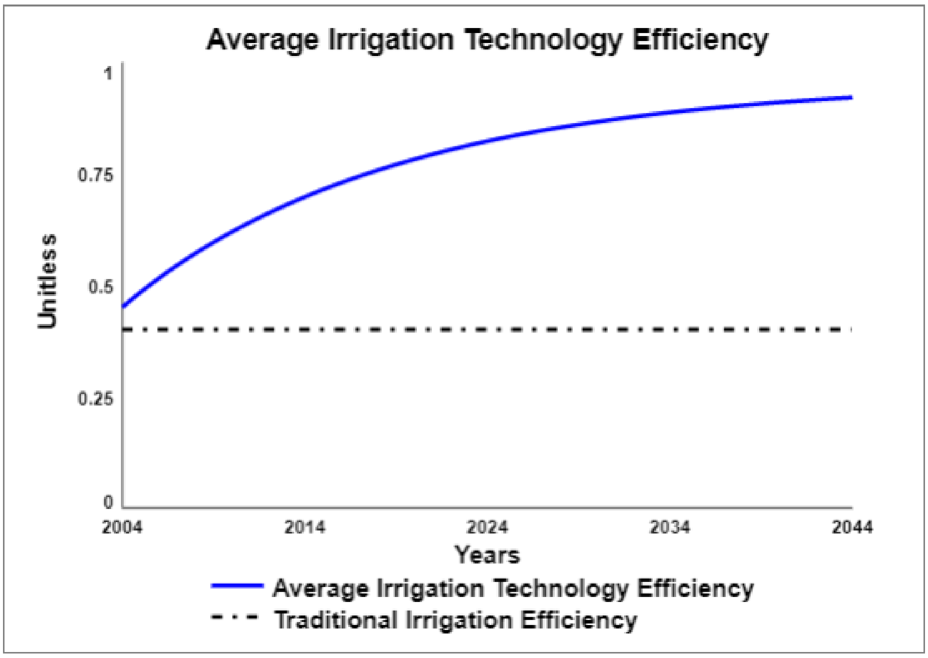

Figure 6.45. Reference model behavior of average irrigation technology efficiency.

We observe that the green plants bring the highest profit throughout the simulation (Figure 6.46). Additionally, after the price changes in 2022, the profit from sugar beet decreases, while the profit from green plants and cereals increases.

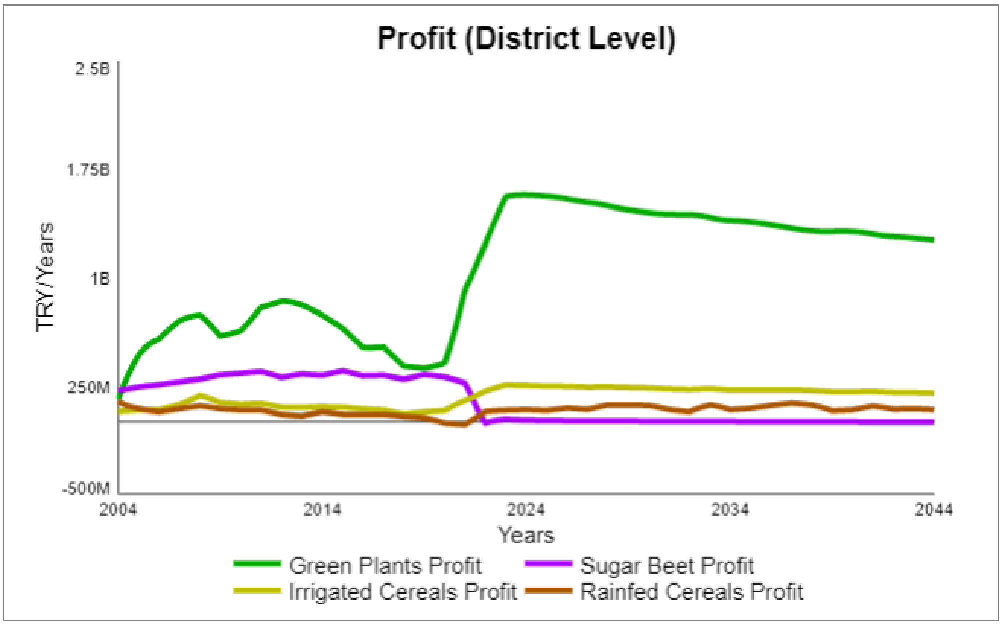

Figure 6.46. Reference model behavior of total profit.

7. SCENARIO ANALYSES

In this section, we present the environmental scenario analyses. We perform two different analyses under hypothetical scenarios, which are produced based on the output of the stakeholder interviews and group model-building workshops. The first scenario is about surface water transfer. The stakeholders want and expect the state to undertake large inter-basin surface water transfer projects to increase the water supply and reduce the demand for groundwater. The second scenario is about climate change; all stakeholder groups are aware of the changing climate and expect to be impacted more by it over the following years.

7.1. Surface Water Transfer

Surface water supply data for the 2004-2021 period is inserted into the model as a table function in the "past surface water supply" variable (hm^3/year) shown in Figure 7.1. The surface water has been supplied from the Apa Dam, which stores the water coming from Lake Beyşehir, Suğla Storage, and Bozkır-Çarşamba Channel (T.C. Çumra Kaymakamlığı, 2019). For the second half of the simulation period, the table function points are deliberately inputted as 0, for testing.

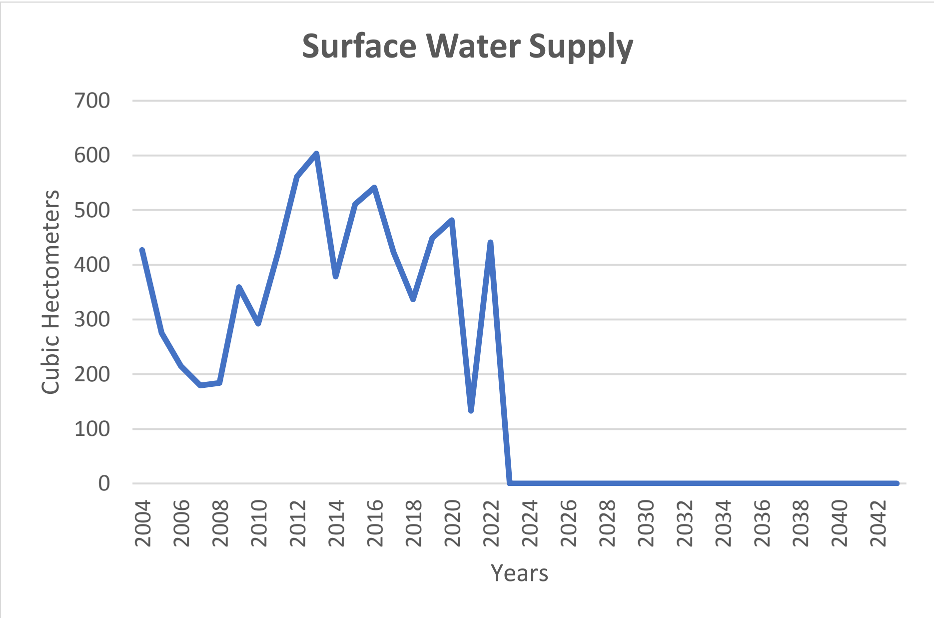

Figure 7.1. Surface water supply data (DSİ, 2023).

The Blue Tunnel project mentioned in Section 3.3.3. is expected to feed the Apa Dam, once it is operational after 2023. Currently, the surface water supply from the Blue Tunnel project is only used as drinking water, thus it is not included in the historical run. However, an additional 300 hm^3 of surface water will be transferred to Çumra through the Blue Tunnel to support agricultural irrigation. Therefore, it is included in the model as a scenario for the following years. The below formulation is used:

$$\begin{gathered} surface\ water\ supply = \ \boldsymbol{IF}\ (surface\ water = 1) \\ \boldsymbol{THEN}\ past\ surface\ water\ supply + \boldsymbol{RAMP}(0{,}2\ ; 2025; 2030) \\ \times\ goal\ for\ surface\ water\ supply \\ \boldsymbol{ELSE}\ past\ surface\ water\ supply \end{gathered} \tag{7.1}$$

IF-THEN-ELSE and RAMP builtins that are available in Stella Architect are used in this equation. It means that if there will be a surface water plan for the future, it will start supplying water in 2025 and it will reach its full potential over five years, in 2030. Otherwise, it will be 0.

To analyze the surface water impact on the system, we run three simulations with three different surface water transfer values. First, we run with an annual 300 hm^3 goal for surface water supply, which gives us an idea about the impact of the Blue Tunnel project. Then, we run with rather excessive surface water transfer goals, 700 and 1500 hm^3/year. The purpose of these scenarios is to see whether the inter-basin water transfer would yield the expected impact, because certain groups of stakeholders (some of the farmers and some irrigation cooperatives) are eagerly expecting the transfer because they believe it will resolve the water scarcity issue, and their hopes for the future depends on it.

Figure 7.2 shows the groundwater table for the base run and the three surface water transfer scenarios. From the graph, we see that the 300 hm3 of water that is planned to be transferred through the Blue Tunnel would have a minor impact on groundwater conservation. In this scenario, the final depth of the groundwater table is -84,3 m, accounting for a 2,3 meters difference compared to the base run. As expected, the groundwater table drops less as we increase the amount of surface water transfer. However, considering the financial and ecological burden of the inter-basin water transfers, which are not included in this model, the costs and benefits of such projects should be thoroughly analyzed before decision-making.

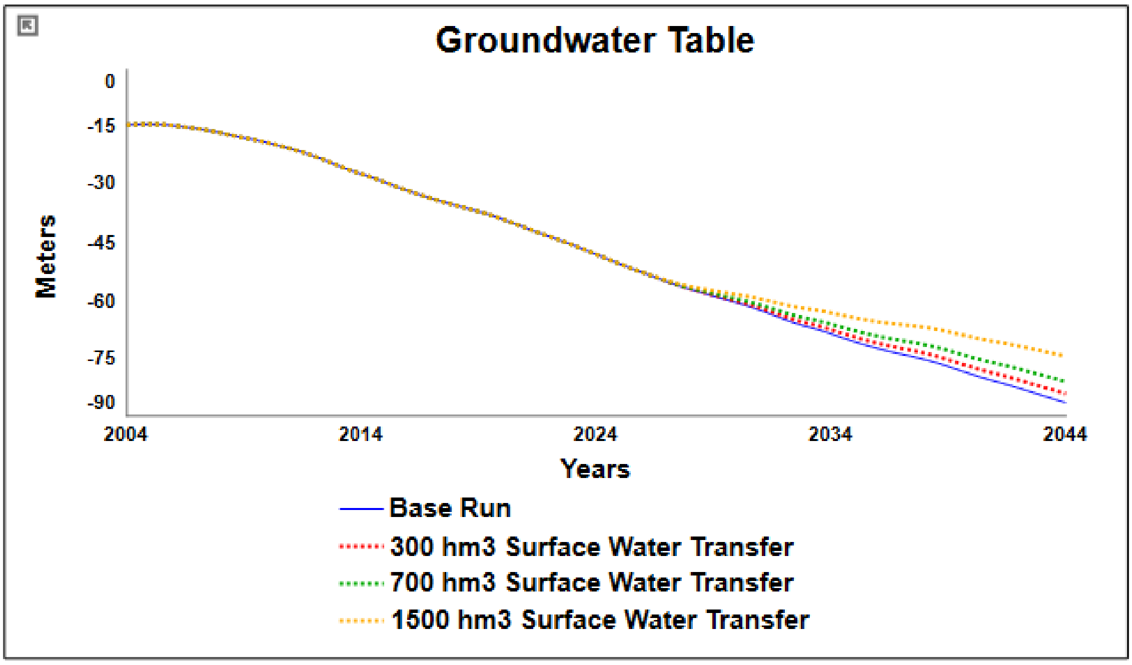

Figure 7.2. Scenario analysis 1: Groundwater table.

In Figure 7.3, we see the number of active wells and average pump power under the surface water transfer scenario and base run. A fraction of the groundwater demand is supplied by the transferred surface water, therefore the need to build groundwater pumping infrastructure decreases, resulting in fewer wells and lower pump power as the annual surface water transfer increases.

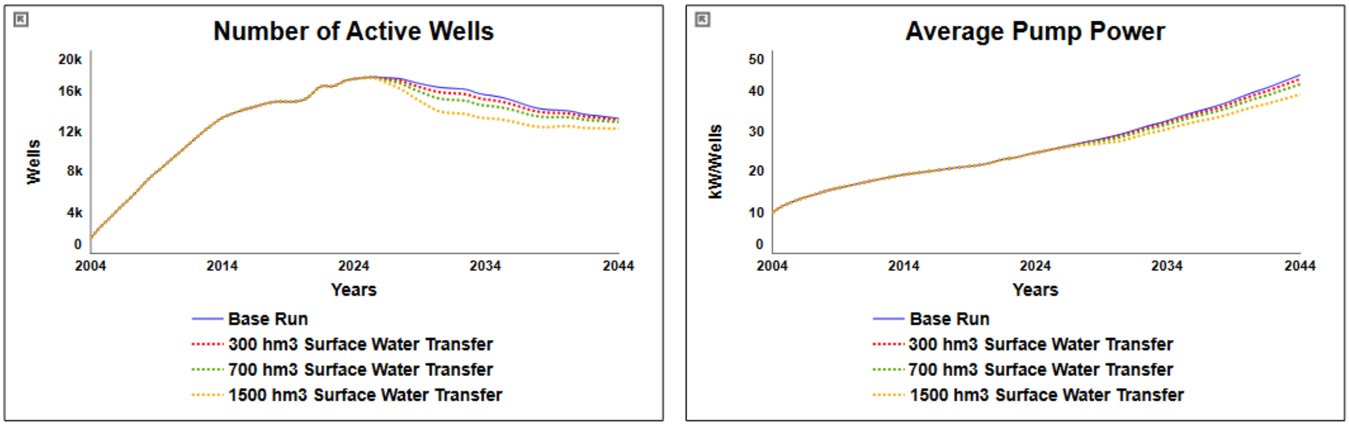

Figure 7.3. Scenario analysis 1: Number of active wells and average pump power.

Figures 7.4 and 7.5 show the crop land covers and crop yields, respectively. We observe a small increase in the land for sugar beet with higher levels of surface water transfer and a slight decrease in the rainfed cereal land. Similarly, the yields of the irrigated crops are slightly improved because the surface water is cheaper than groundwater extraction, and the farmers can afford to irrigate more in these scenarios.

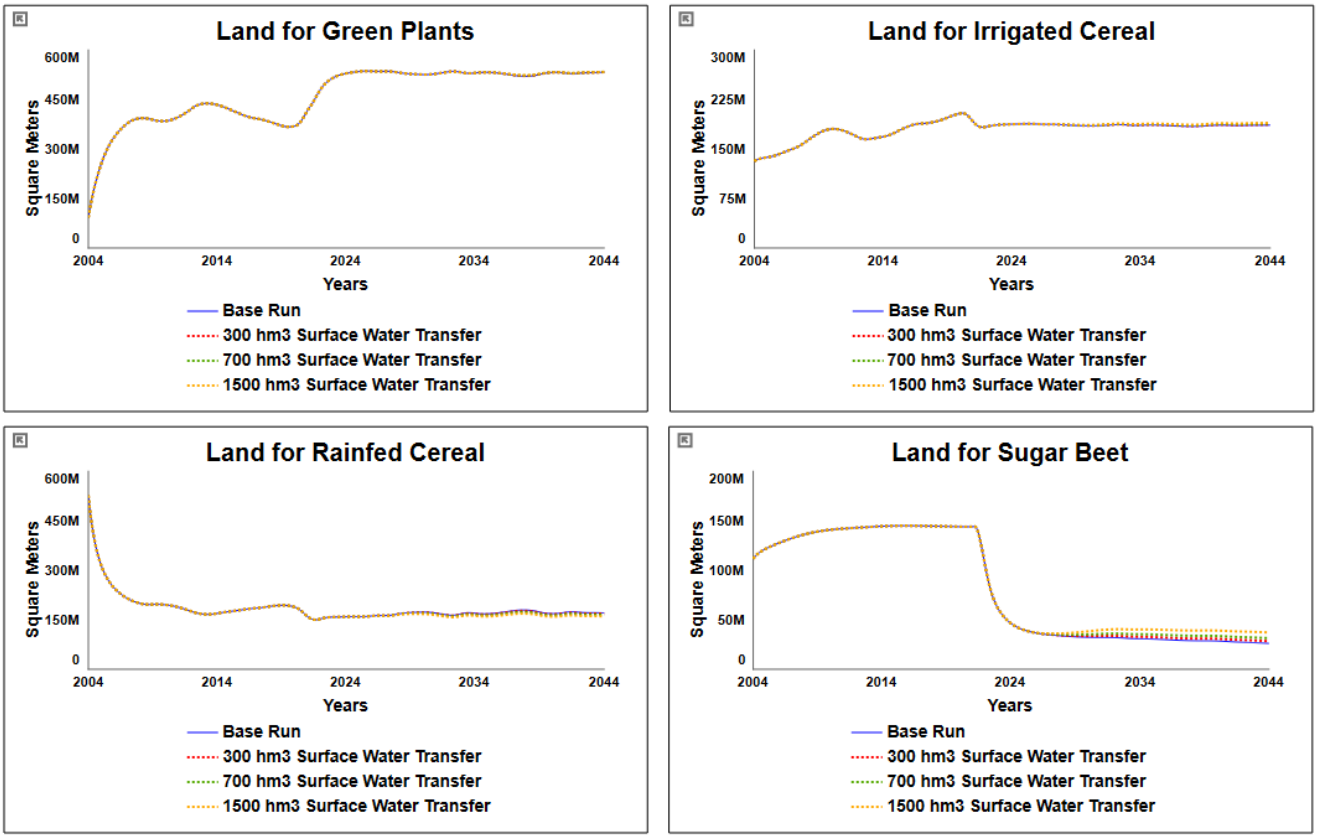

Figure 7.4. Scenario analysis 1: Crop land covers.

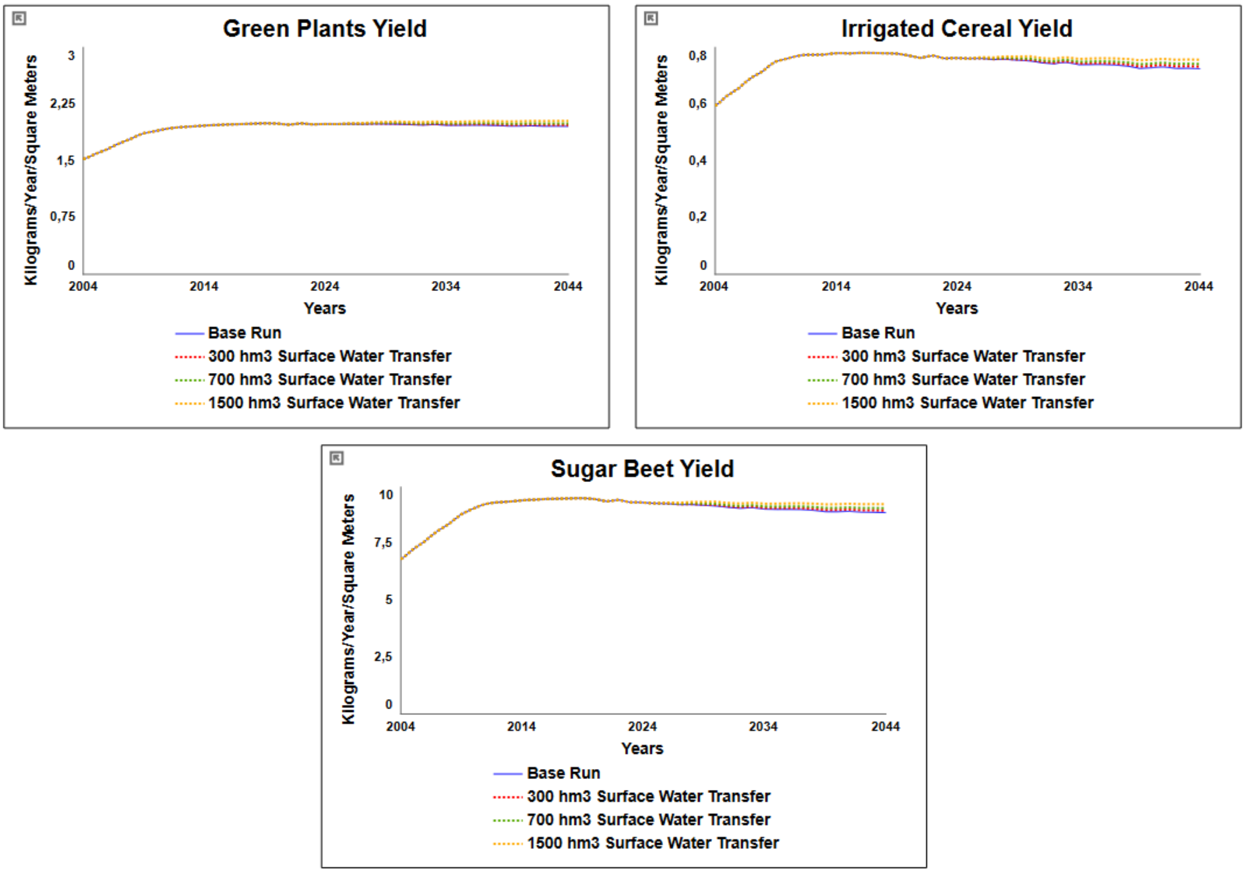

Figure 7.5. Scenario analysis 1: Irrigated crop yields.

As we see in Figure 7.6, the adoption of high-efficiency irrigation technologies is not impacted by the surface water transfer.

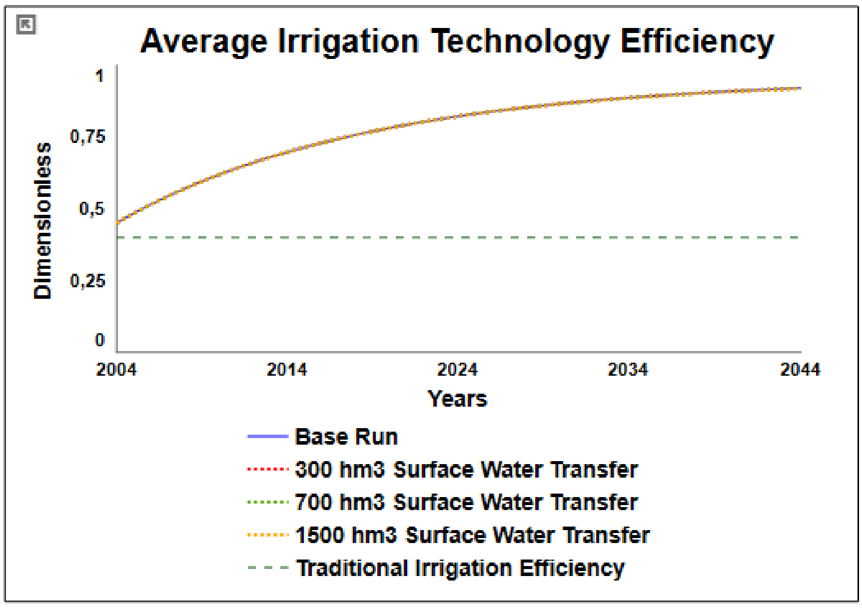

Figure 7.6. Scenario analysis 1: Average irrigation efficiency technology.

Figure 7.7 compares the total profit in the Çumra district under different surface water transfer scenarios. Since there is not a significant difference in crop lands and crop yields, the revenue does not change significantly. However, surface water is cheaper than groundwater, therefore, as the supply of surface water increases, the total irrigation cost decreases, expanding the total profit.

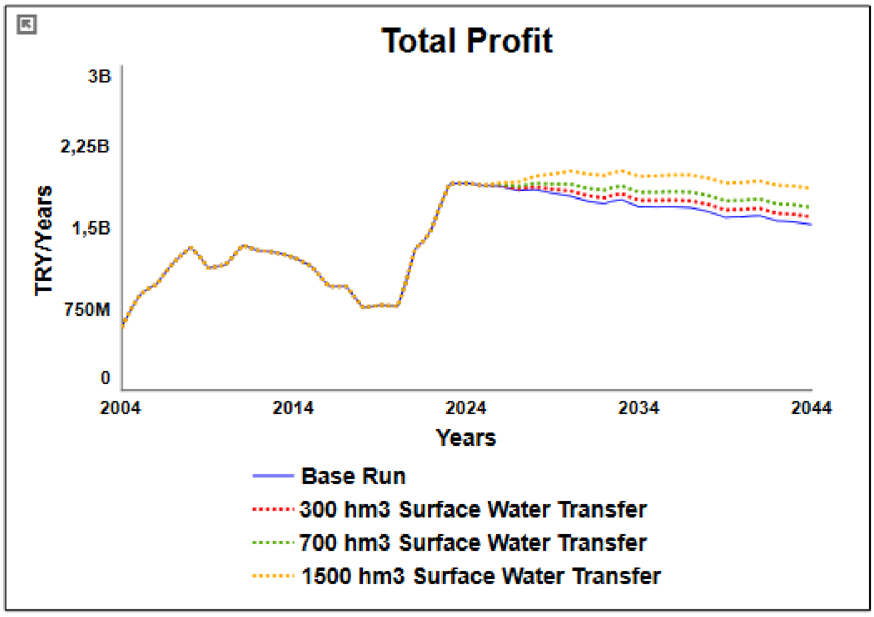

Figure 7.7. Scenario analysis 1: Total profit.

7.2. Climate Change

Precipitation (mm/year) data is inserted into the model as a table function (Figure 7.8). For the 2004-2022 period, the data by the Turkish State Meteorological Service (2021) is inputted.

According to the future climate projections by Todaro et al (2022), there will not be a significant change in the yearly average precipitation in KCB, over the model time horizon and beyond (until 2100). Therefore, the precipitation pattern observed between 2004-2022 is repeated until 2044 in the model.

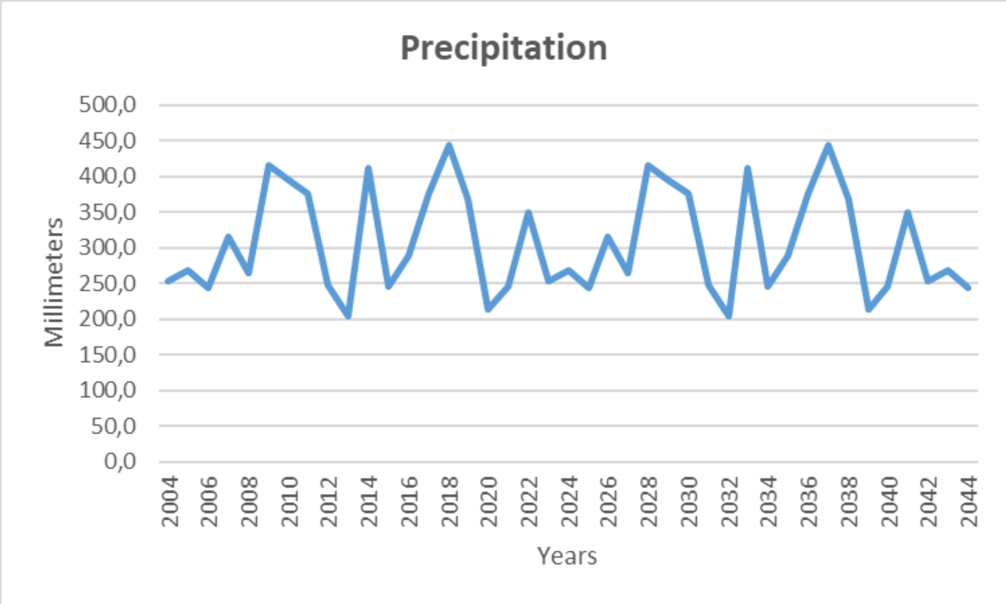

Figure 7.8. Precipitation data (MGM, 2021).

On the other hand, decision-making depends on the mental models of agents, and when some relevant information is unavailable to us, we form expectations regarding what is likely to happen (Sterman, 2000). In this case, farmers would need to know the precipitation to decide exactly how much they prefer to irrigate their crops. However, they cannot know how much precipitation their land will receive in the following year. So, to plan ahead, they need to rely on their expectations. There are multiple ways to formulate expectation formation, depending on the cues used for forecasting, ranging from simple exponential smoothing to econometric modeling (Sterman, 2000). In our model, farmers can only form expectations based on past data, i.e., previous years' precipitation. Therefore, we employ the TREND built-in function, which provides an estimate for the fractional growth rate (unitless) in the selected variable. Expected precipitation (m/year) is formulated as follows:

$$\begin{aligned} &\mathit{expected\ precipitation} \\ &= MAX(0\,;\ \mathit{precipitation}\ \times (1 + \mathit{trend\ in\ precipitation}) \\ &\times \mathit{time\ to\ perceive\ the\ trend\ in\ precipitation}) \end{aligned} \tag{7.2}$$

where,

$$\mathit{trend\ in\ precipitation} = \boldsymbol{TREND}(\mathit{precipitation}\,;\mathit{precipitation\ trend\ averaging\ time}\,;0) \tag{7.3}$$

While Todaro et al (2022) do not forecast a significant change in the precipitation pattern, their study shows that under different RCP scenarios, the annual mean temperature may rise approximately up to 3°C until the mid-2040s. An increase in the annual mean temperature would mean higher water demands for crops, as well as higher fractions of evaporation loss. Therefore, we produce a hypothetical climate change scenario, where the precipitation reduces by 20%, and the plant water requirements, and evaporation loss increases by 40% over the 2025-2035 period. We formulate these changes with the RAMP builtin in Stella Architect, as follows:

$$precipitation\ under\ climate\ change = precipitation - \boldsymbol{RAMP}(0{,}1\ ; 2025; 2035) \times 0{,}2 \tag{7.4}$$

We formulate the changes in crop water requirement and evaporation loss fraction with analogous equations.

Figure 7.9 compares the groundwater table outputs in the base run and under the climate change scenario. We observe that under climate change, the drop in the groundwater table is significantly higher than that of the base run. There is a 10,9 meters difference between the two scenarios.

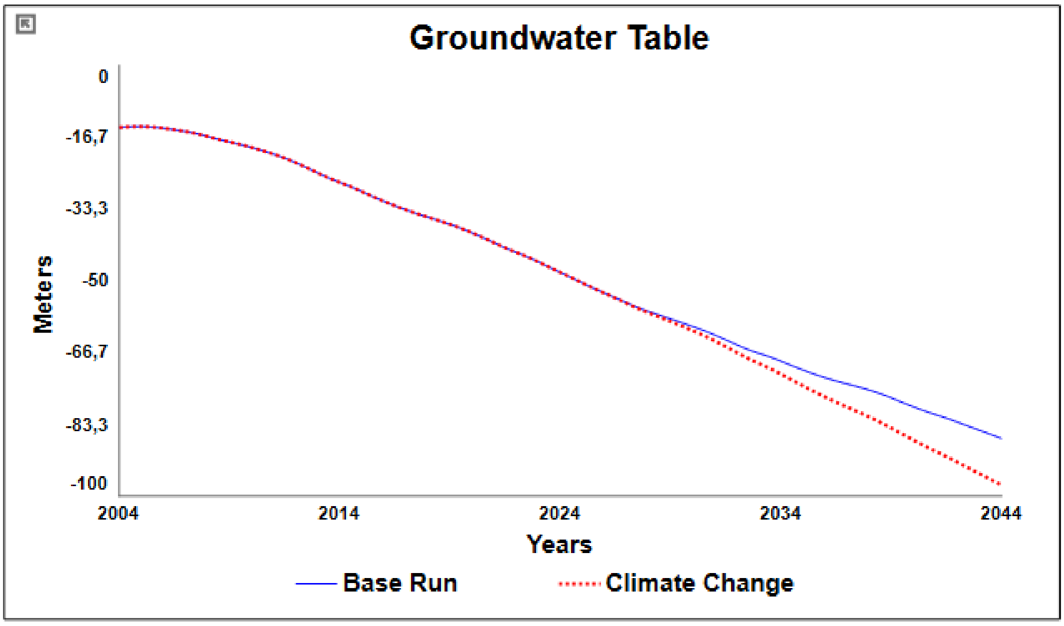

Figure 7.9. Scenario analysis 2: Groundwater table.

The pumping (groundwater extraction) and recharge in the base run and climate change scenario are presented in Figure 7.10. The extraction is higher under the climate change scenario both because the crops require more water, and the precipitation is reduced. On the other hand, the recharge is lower compared to the base run, because the evaporation loss is higher.

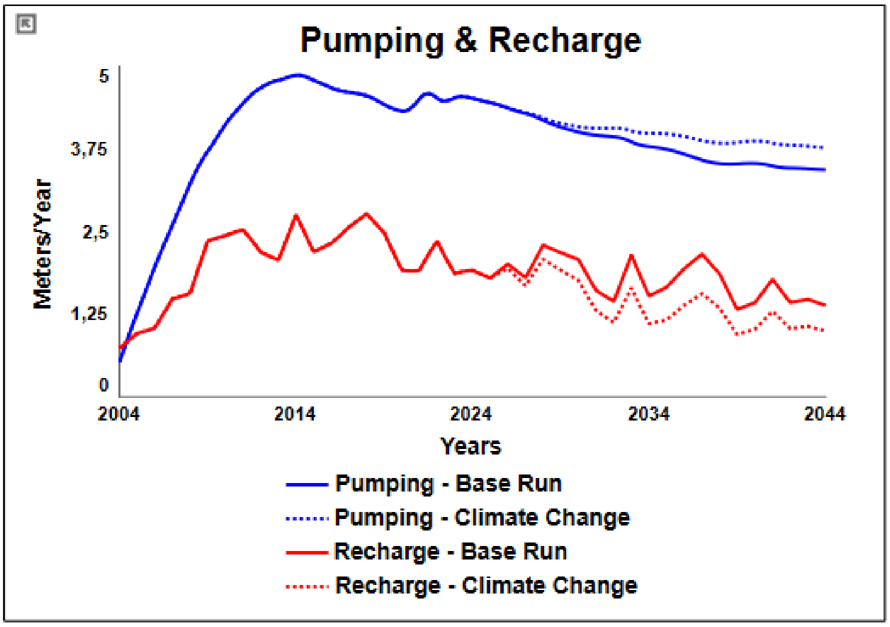

Figure 7.10. Scenario analysis 2: Pumping and recharge.

Given that the groundwater demand is higher in the climate change scenario, we see that the groundwater infrastructure is developed faster compared to the base run, as anticipated. Figure 7.11 shows the number of active wells and the average pump power in the base run and the climate change scenario.

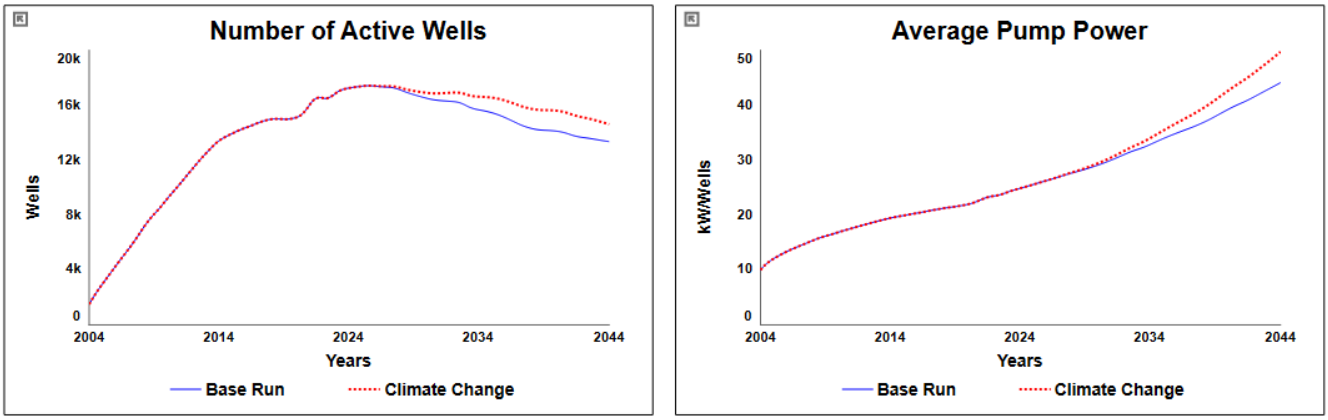

Figure 7.11. Scenario analysis 2: Number of active wells and average pump power.

Figure 7.12 presents the crop land covers in the base run and under the climate change scenario. Since the precipitation is reduced, the rainfed cereal yield decreases significantly (Figure 7.13). Therefore, rainfed cereal becomes less profitable and the rainfed land decreases. Sugar beet land is also decreased, mainly because in this setting it is the least profitable crop. The indirect reason is that the sugar beet is the most water-demanding crop in the model, thus the irrigation cost for sugar beet is high, while the sugar beet price is not competitive compared to other crops.

Figure 7.13 displays the crop yields. We observe that under the climate change scenario, all crop yields are reduced. The total irrigation cost is increased for all crops, both because the groundwater table is deeper and also because the irrigation demand of all crops is higher, compared to the base run. After a certain point, the cost of additional irrigation to increase yield surpasses the revenue produced by the increase in the yield; therefore, the system adjusts to a yield-irrigation level that provides the highest income, with lower yields.

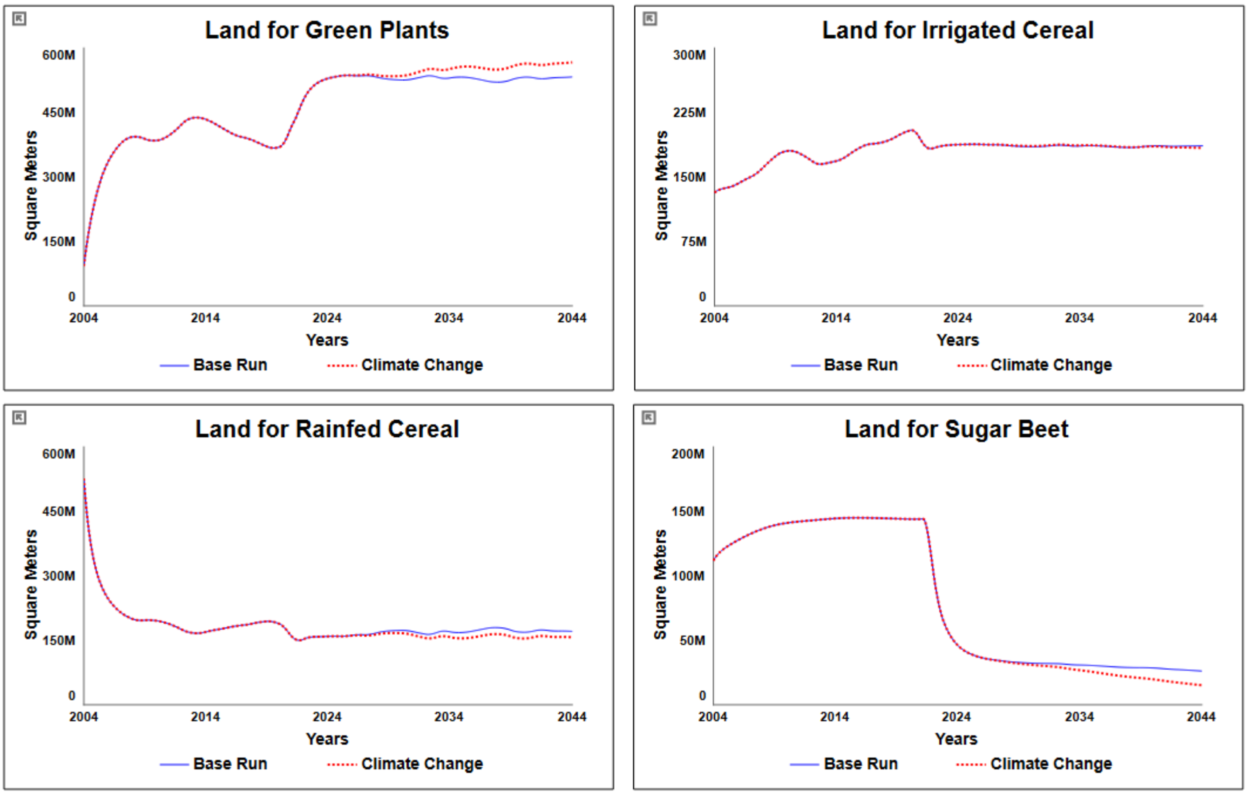

Figure 7.12. Scenario analysis 2: Crop land covers.

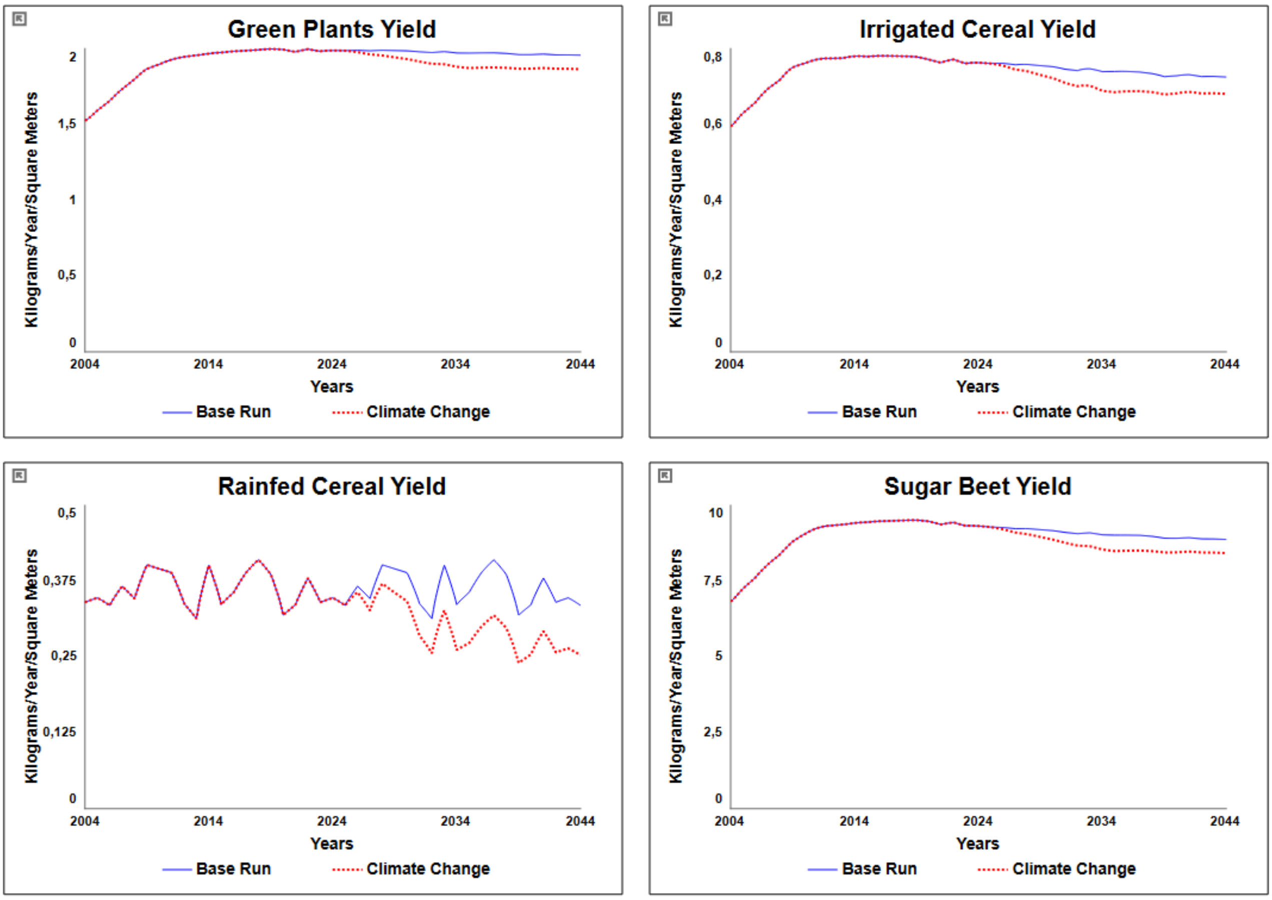

Figure 7.13. Scenario analysis 2: Crop yields.

As anticipated, the total profit under the climate change scenario decreases significantly (Figure 7.14). The revenue per unit area is lower because of the yield loss in all crops. Additionally, the irrigation costs are higher, further lowering the profit.

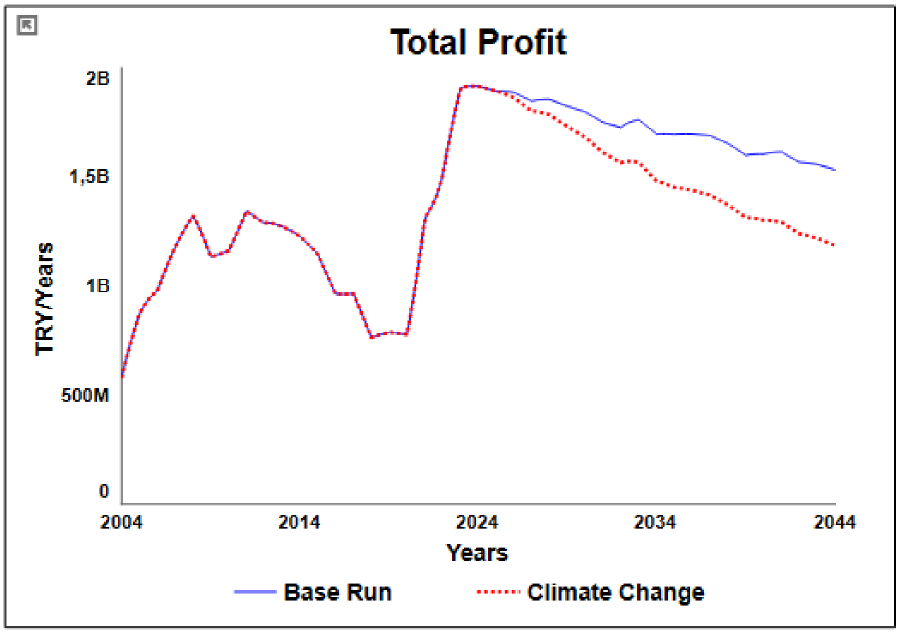

Figure 7.14. Scenario analysis 2: Total profit.

8. POLICY ANALYSES

In this section, we analyze the impact of five different policy scenarios on key system variables and assess their performance in terms of system improvement. The policy scenarios are developed based on the stakeholder suggestions from the group model-building workshops.

8.1. Well Regulation

The default well-digging formulation in the model suggests that there exists an open-access regime, where anyone may dig a well, whenever they need to. As discussed above, the number of wells is a matter of importance to all stakeholders but also poses a conflict of interest between different stakeholder groups. Farmers claim that if they are not allowed to open wells, they would not be able to extract enough water for their crops and suffer from yield (and revenue) loss. On the contrary, officers from relevant state institutions blame farmers for groundwater depletion, claiming that farmers are ignorantly over-irrigating their crops and that well regulation is required to stop over-extraction.

Starting from the above discussion between the stakeholders, we introduce two different well regulation options to the model. The first is the well amnesty, which implies that a new well may be opened only if an already existing well is closed due to a collapse, or if it runs dry. The second regulation is the prohibition of new wells; under this regulation, new wells are not allowed in any condition. To implement these regulations in the model, we add new variables and equations to the model as follows:

There are 2 variables representing each well regulation. One of them is a binary, stating whether that regulation is enforced or not. The well policy variable is used to identify which regulation is in effect, based on these binary variables. The other variables are used to adjust the well digging to the regulation in effect.

$$\begin{aligned} well\ digging = \ & open\ access + \boldsymbol{STEP}(new\ well\ digging \\ & - open\ access;\ well\ regulation\ start\ year;\ well\ regulation\ duration) \end{aligned} \tag{8.1}$$

The above formulation implies that until the well regulation start year, the open access regime is continued. Starting from the well regulation start year, the new regulation is enforced for the chosen duration of the regulation. The new well digging is formulated as follows:

$$new\ well\ digging = \ IF(well\ policy = 1)\ THEN\ open\ access\ ELSE$$
$$IF(well\ policy = 2)\ THEN\ well\ amnesty\ ELSE$$
$$IF(well\ policy = 3)\ THEN\ prohibition\ of\ new\ wells\ ELSE\ 0$$

(8.2)

We first set well amnesty to well closing rate. However, if the number of wells starts declining under the open access regime, when we switch to the good amnesty regulation, the model forces the number of wells to stay constant, even though the default tendency is to reduce the number of wells. Therefore, we formulate it as a minimum function.

$$well\ amnesty = MIN(well\ closing\ ; open\ access)$$

(8.3)

In the prohibition of new wells regulation, we set the well digging rate to zero.

In this policy analysis, we run three simulations. One is the base run, where the open access regime rules until the end of the simulation period. In the other two simulations, we initiate well amnesty and prohibition of new wells in 2025 and enforce the regulations until 2044.

Figure 8.1 compares the groundwater table outputs of the three simulation runs. While the open access and well amnesty regulations produce the same groundwater table behavior, when all new wells are prohibited, the groundwater table stabilizes around -67 meters.

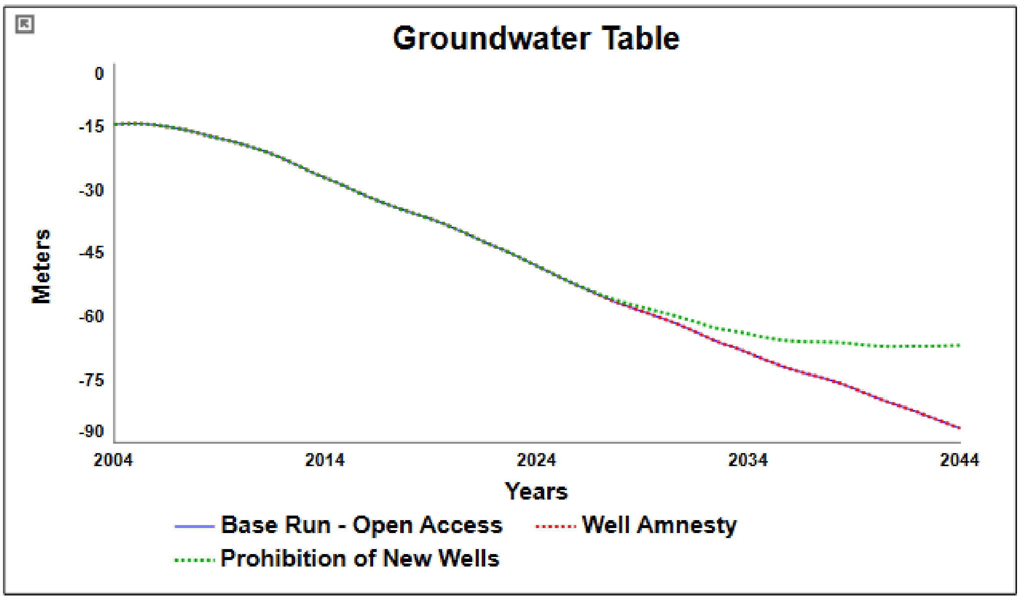

Figure 8.1. Policy analysis 1: Groundwater table.

Figure 8.2 explains why the groundwater table is the same in open access and well amnesty runs. In the base run, the number of active wells start decreasing after 2025. Due to the minimum function used to formulate the well amnesty regulation, as explained above, the well amnesty and open access runs are the same. On the other hand, when new wells are prohibited, the number of wells decreases steeply. The average pump power is increased rapidly after 2025, to compensate for the loss of pumping wells.

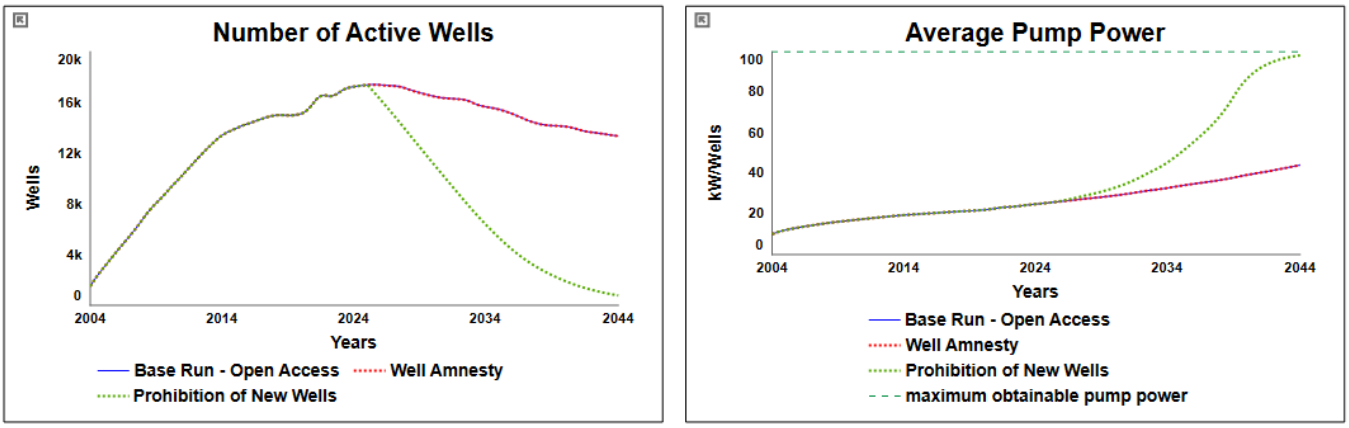

Figure 8.2. Policy analysis 1: Number of active wells and average pump power.

The reduced number of wells results in irrigation water scarcity. Therefore, investment in irrigation technology is also higher under the prohibition of new wells regulation. While in the other two runs the average irrigation technology efficiency adjusts to approximately 90%, in the prohibition of new wells run, it approaches the upper limit.

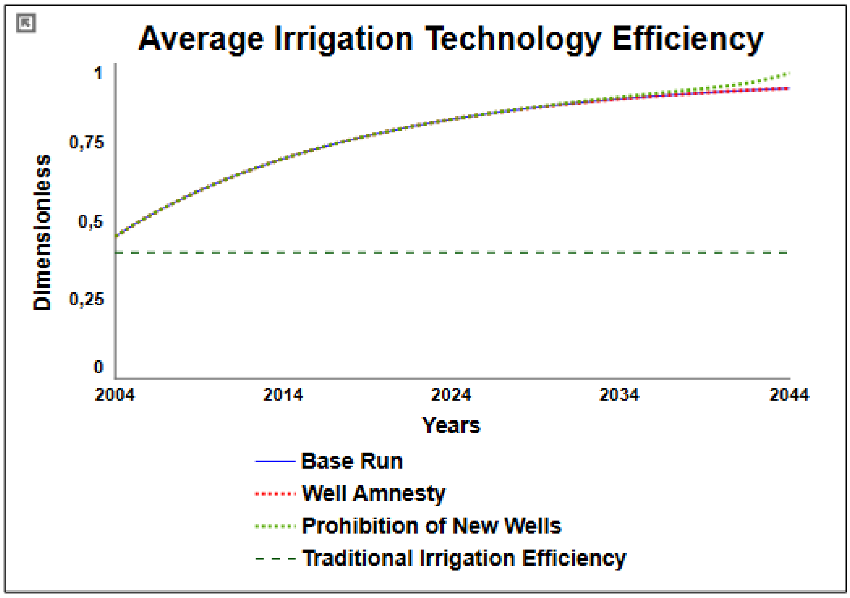

Figure 8.3. Policy analysis 1: Average irrigation technology efficiency.

Figure 8.4 presents the crop land covers under the three well regulation policies. Land for green plants and rainfed land are barely affected by the well policies, however, we observe an increase in the sugar beet land and a decrease in the irrigated cereal land when the new wells are prohibited.

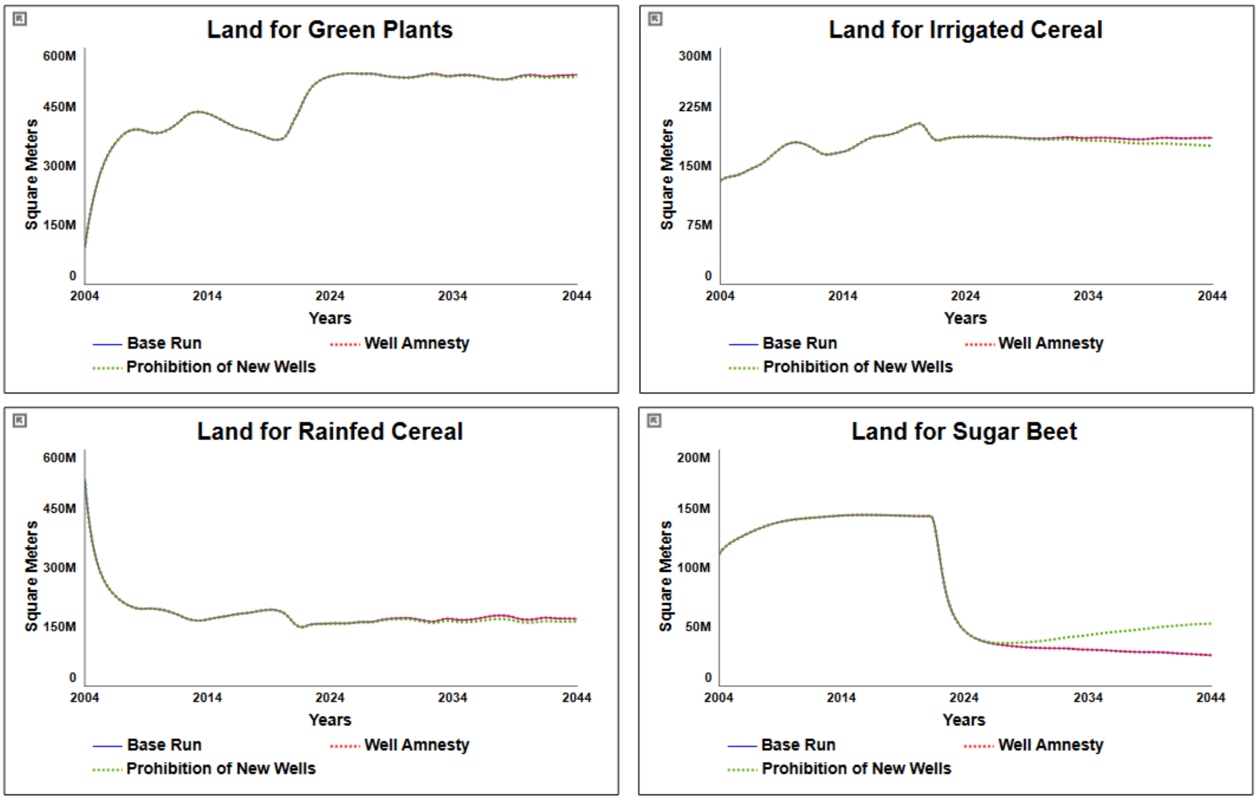

Figure 8.4. Policy analysis 1: Crop land covers.

We observe that if the well opening is strictly prohibited, there is a substantial yield loss in every irrigated crop after 2025 (Figure 8.5). This output falls in line with the farmers' concerns in the field. However, it should be noted that prohibiting new wells for 19 years (2025 - 2044) is an excessive and improbable measure, as groundwater conservation is not the only goal for any actors in the system. For farmers, the most important goal is to support themselves and their families. Nationwide, Çumra is an important crop production hub. Therefore, another goal is to maintain a reasonable level of production for each crop. Under the prohibition of new wells, crop production reduces significantly as well (Figure 8.6), parallel to the yield loss. Therefore, it would not be a viable solution to the groundwater depletion problem.

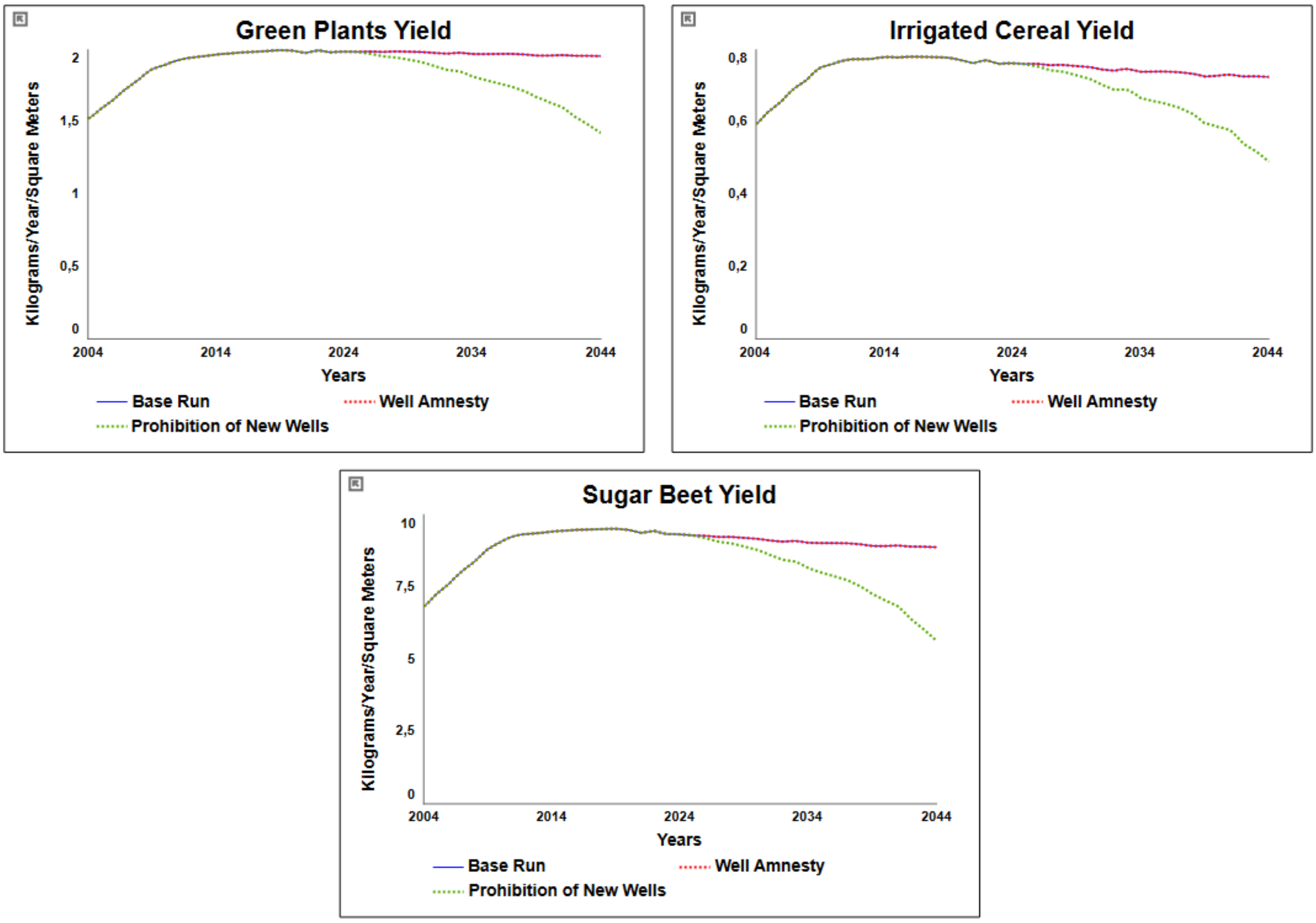

Figure 8.5. Policy analysis 1: Crop yields.

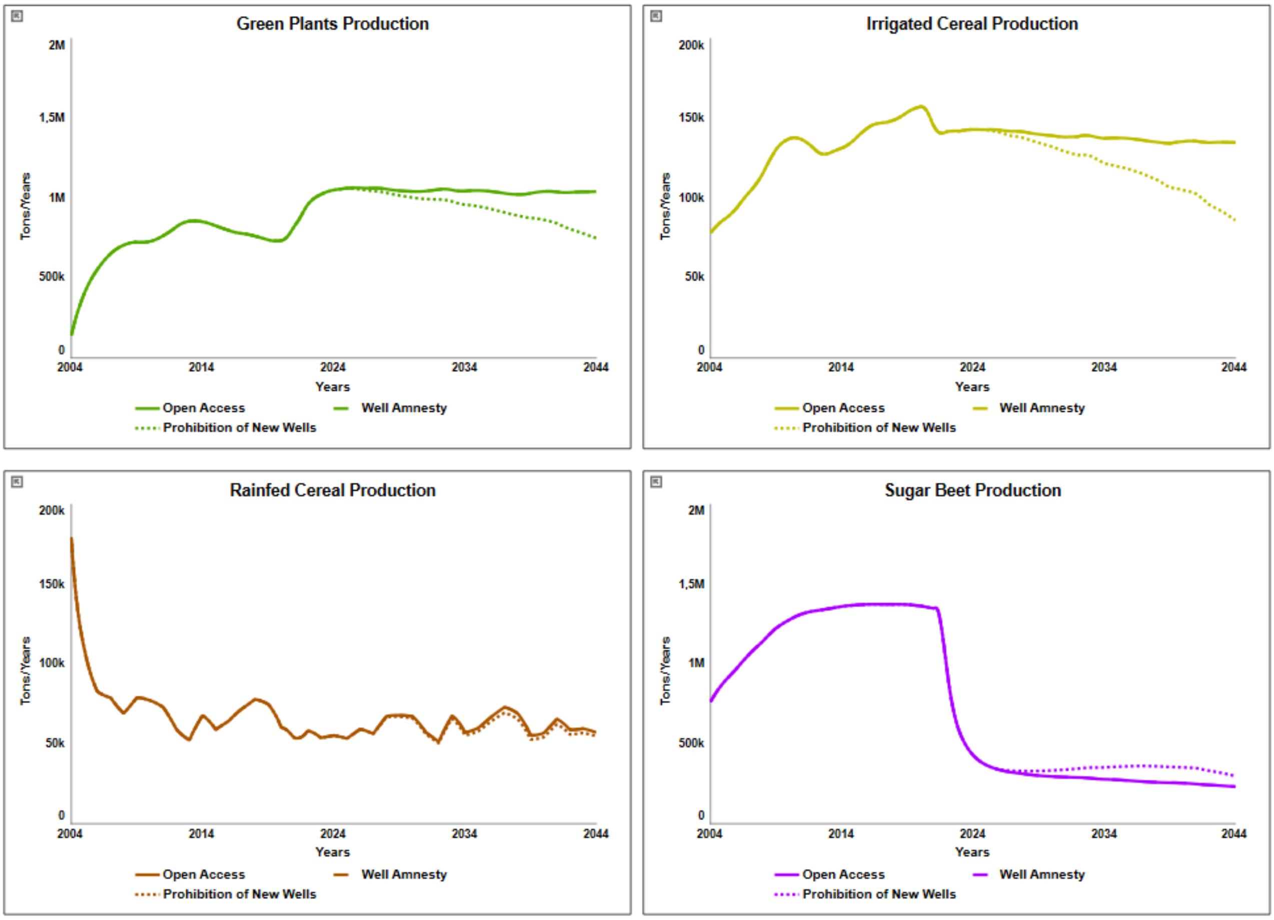

Figure 8.6. Policy analysis 1: Crop production.

We see from the outputs of the well regulation scenarios that the well amnesty regulation mimics open access regime. That is because after 2025 the number of active wells start decline in the open access case, so a regulation aiming to preserve the existing number of wells is rendered useless. This implies that the well amnesty policy may be a missed opportunity. To investigate this issue, we carry out a retrospective analysis where we initiate the well amnesty policy in 2015 instead of 2025 and compare the behavior of some key variables.

Figure 8.7 presents the number of active wells and average pump power under open access regime and well amnesty regime starting from 2015 and 2010, respectively. As expected, the number of wells is lowest in the earliest well amnesty regulation starting in 2010. Therefore, the model compensates for the lower number of wells by increasing the average pump power, in order to meet the annual groundwater demand. On the other hand, well amnesty regulation does not stop or reverse the decline in groundwater table. Even though the groundwater table is higher under the retrospective well amnesty regulations, we can conclude that well amnesty by itself would not have been a solution to the groundwater sustainability issue in Çumra.

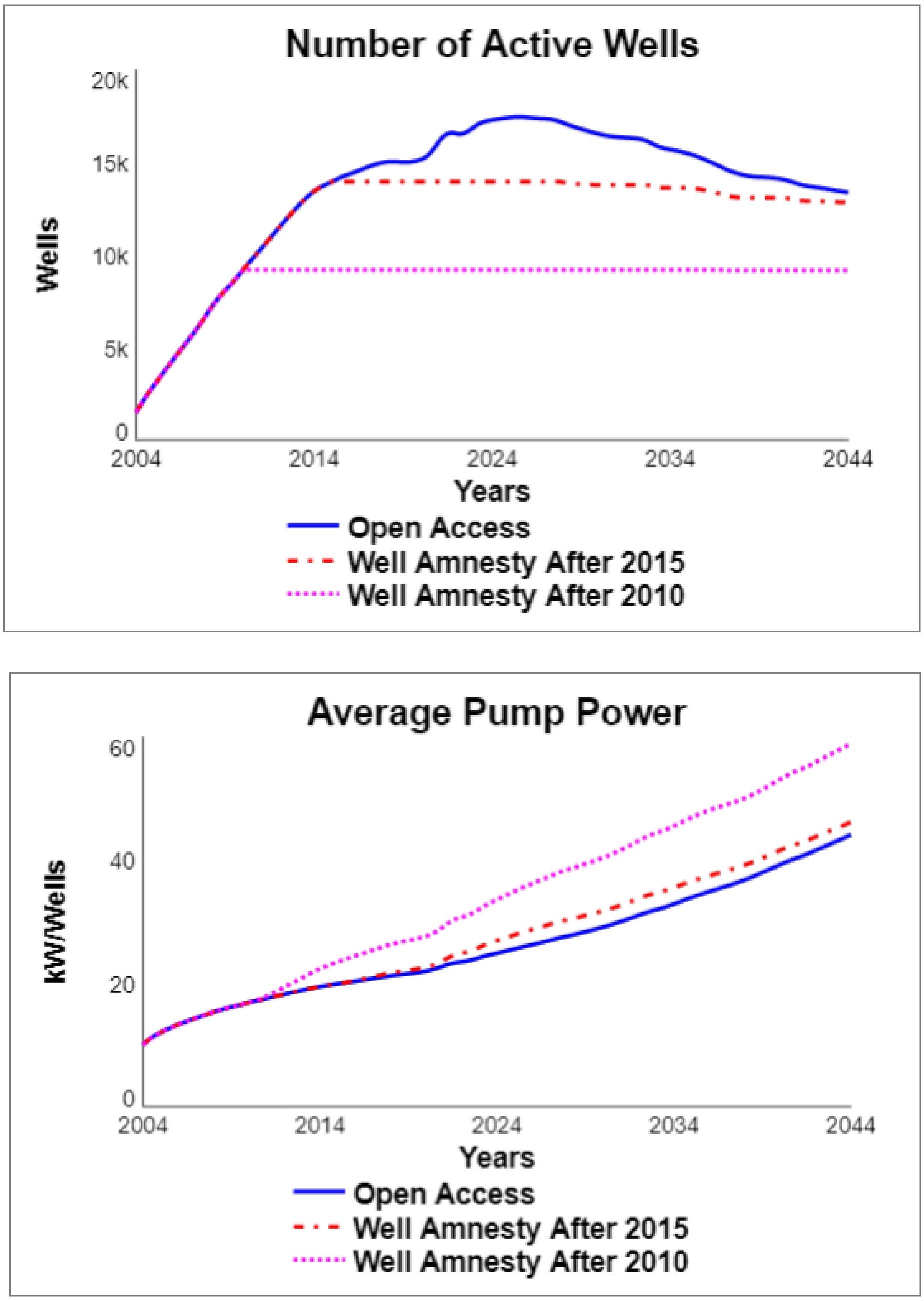

Figure 8.7. Well amnesty retrospective analysis: Number of active wells and average pump power.

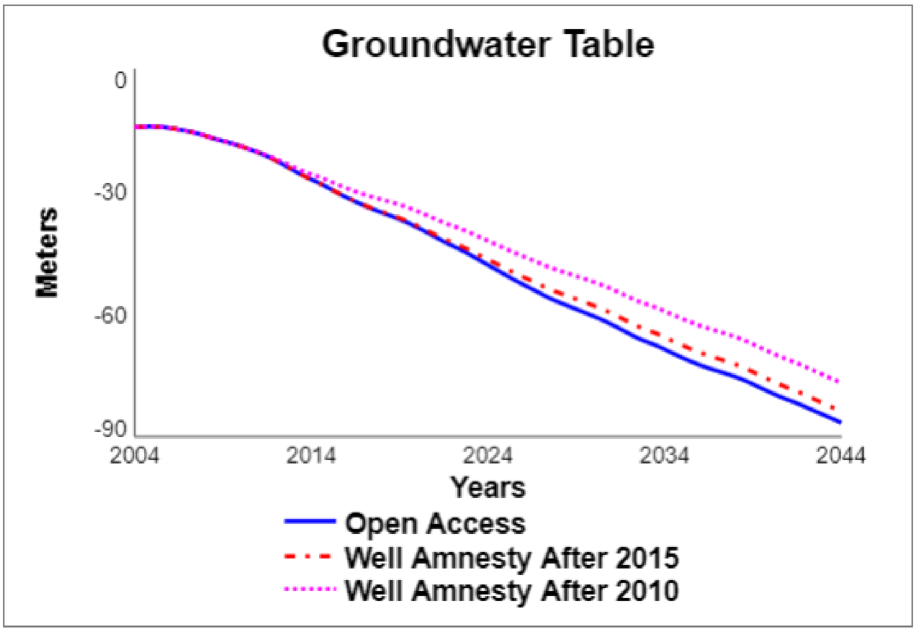

Figure 8.8. Well amnesty retrospective analysis: Groundwater table.

8.2. Crop Rotation

Crop rotation is defined as the cultivation of different crops in succession on the same piece of land, and the purpose is to avoid exhausting the soil and prevent weeds, diseases, and pests. Crop rotation is already implemented in Çumra for sugar beet because when sugar beet is grown successively, it drains the soil of nutrients. Therefore, farmers grow sugar beet on the same land, once every four years. During the group model-building workshops, many stakeholders suggested that a similar crop rotation scheme could be implemented for green plants, as they are water-consuming plants so rotation would reduce the overall groundwater demand. In this section, we run the model with a four-year green plants rotation time, starting from 2025 until the end of the simulation, and compare the behavior of the key system variables to the base run.

Figure 8.9 shows the groundwater table in the base run and the policy run. We see that the green plant rotation provides substantial improvement in the groundwater table, parallel to the stakeholders' expectations.

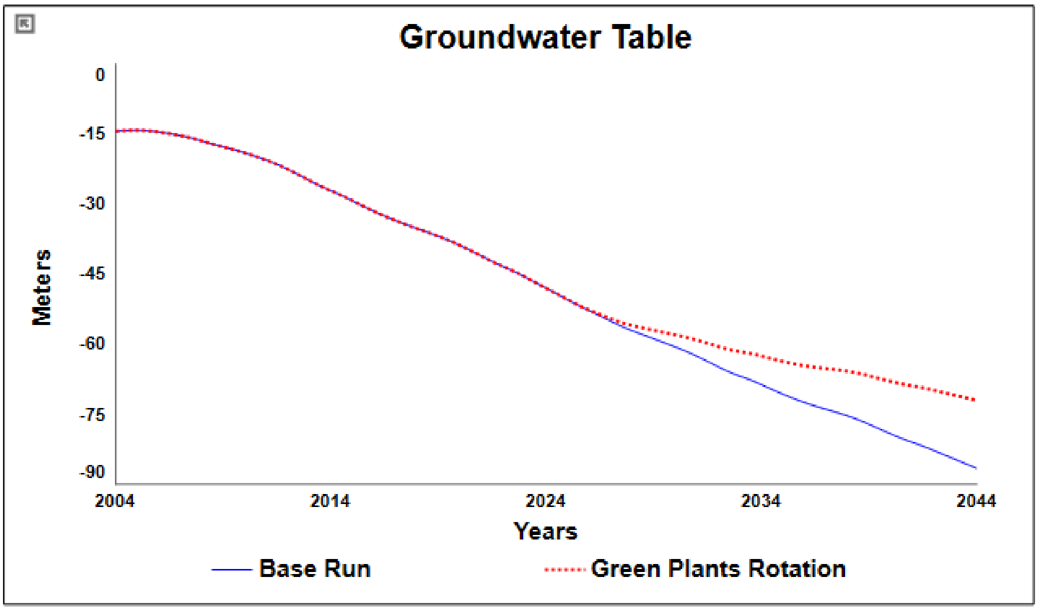

Figure 8.9. Policy analysis 2: Groundwater table.

As can be observed in Figure 8.10, the reduced demand for groundwater is also reflected in the groundwater infrastructure development. Both the number of active wells and the average pump power are lower in the green plants' rotation scheme than in the base run.

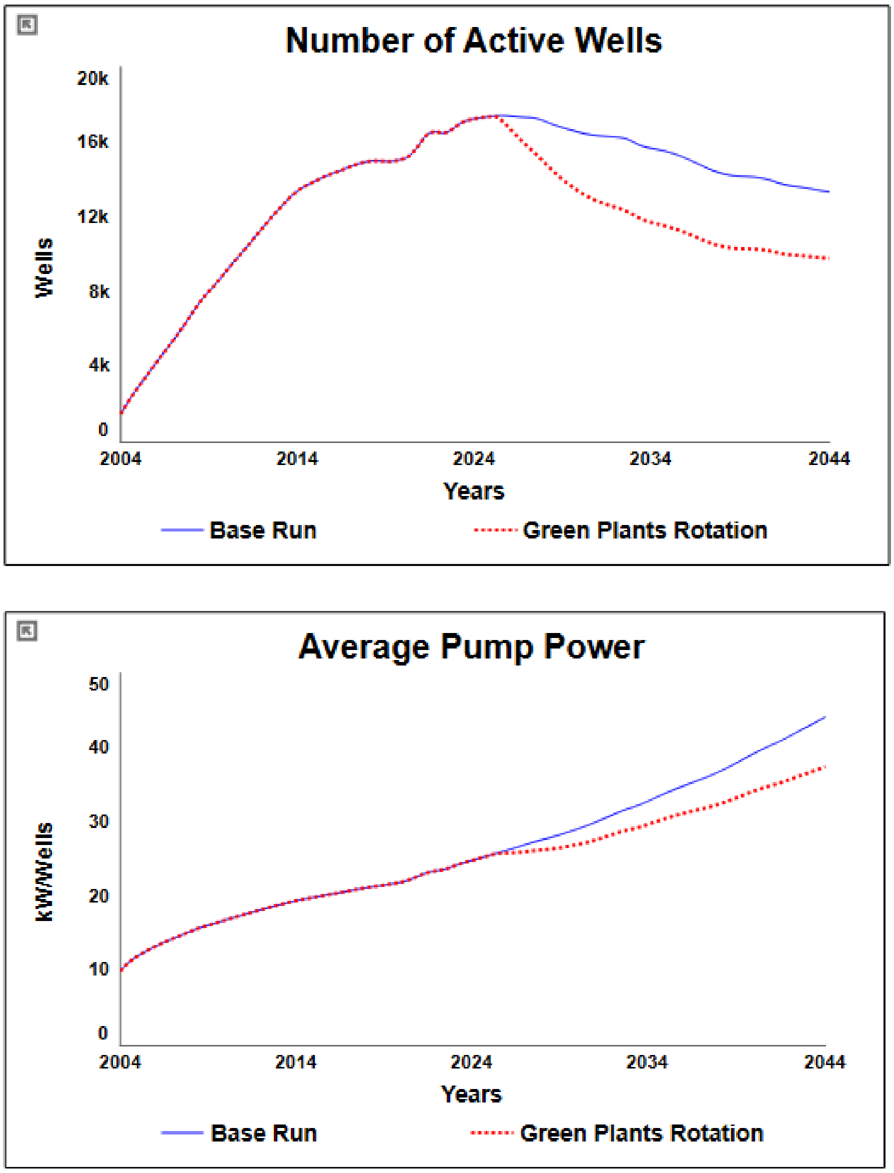

Figure 8.10. Policy analysis 2: Number of active wells and average pump power.

The rotation scheme changes the land cover significantly; the land for green plants decreases steeply once the rotation is in effect, and all the other crop lands increase, as the total agricultural land is constant throughout the simulation (Figure 8.11).

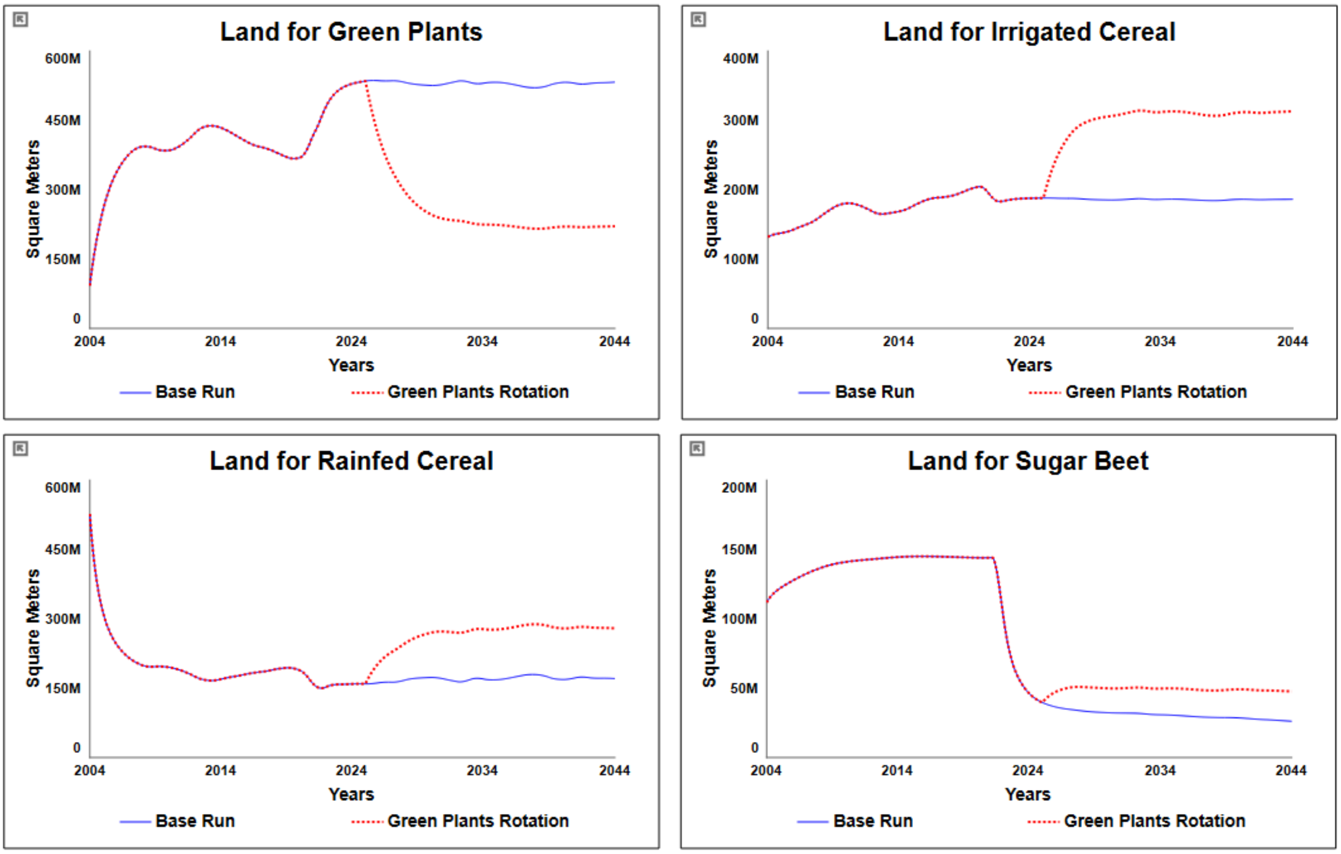

Figure 8.11. Policy analysis 2: Crop land covers.

Such drastic changes in the land cover result in significant changes in crop production and total profit as well. The changes in crop production are mainly driven by the land cover change; crop yields are not significantly impacted by the rotation scheme. Figure 8.12 presents the crop production in the base run and green plants rotation run.

Under the current cost and price setting, green plants are the most profitable crops in terms of profit per unit area. Therefore, when the production of green plants is reduced and replaced by other crops, the total profit decreases significantly (Figure 8.13).

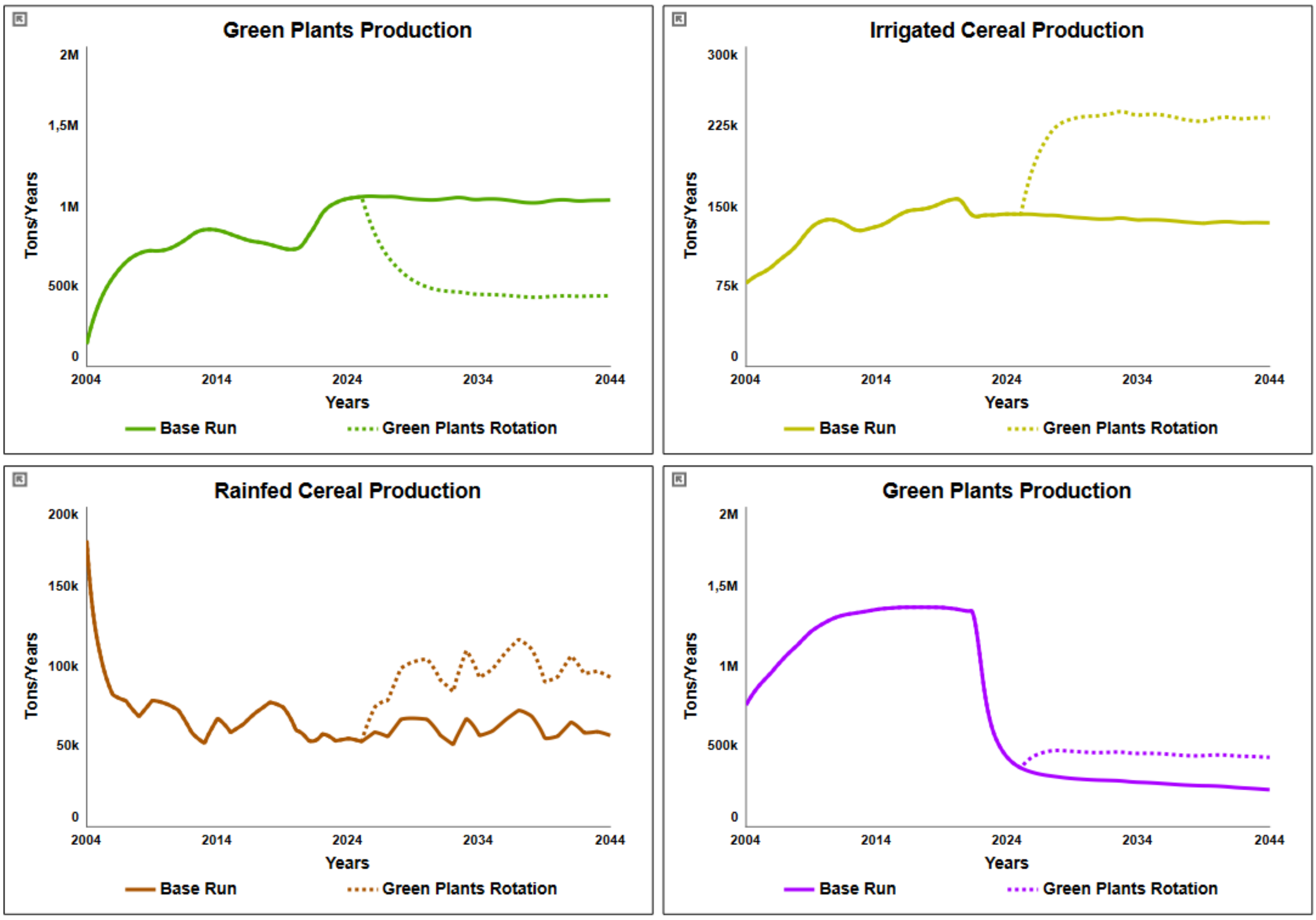

Figure 8.12. Policy analysis 2: Crop productions.

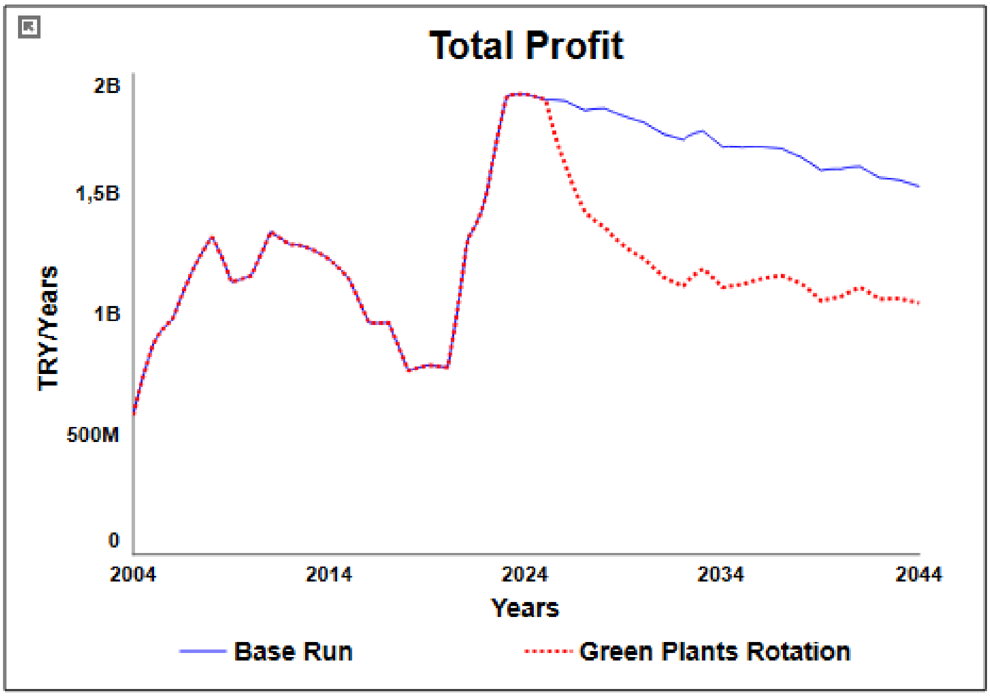

Figure 8.13. Policy analysis 2: Total profit.

8.3. Extraction Cap

In 2011, a new bylaw was published in the official gazette, the Regulation for the DSİ Groundwater Measurement Systems, stating that a meter is to be installed in every groundwater well until 2013 so that the extractions can be measured and monitored. However, farmers strongly opposed the bylaw as they perceived the regulation as the initial step of a plan that would result in their groundwater access being restricted. They claimed that the meters would later be used by the state to impose a quota on pumping. Interestingly, there already is a pumping quota in Turkish legislation, specified in the Groundwater Code and Regulation for Groundwater. For Konya Closed Basin, the extraction quota is 200 tons/decare/year. However, it cannot be properly enforced because neither farmers nor state institutions know the level of extraction, due to lack of measurement systems. In short, farmers refused to meter their wells, and neither of the regulations can be enforced to-day.

Extraction cap is a contentious issue among the stakeholders; therefore, we implement it on the model to assess its impact on the system. To that end, we introduce two new variables to the model: Extraction cap (m^3/well/year), which determines the quota, and the maximum groundwater supply per well (m^3/well/year).

$$\begin{aligned} &\max groundwater\ supply\ per\ well \\ &= average\ well\ yield + \boldsymbol{STEP}(\ \boldsymbol{MIN}(\ average\ well\ yield; extraction\ cap) \\ &- average\ well\ yield; 2025) \end{aligned} \tag{8.4}$$

The above formulation suggests that starting from 2025, the maximum annual pumping from a well would be the minimum of the average well yield and the extraction cap.

We take three simulation runs to assess the impact of the extraction cap; we use three different caps, as presented in Table 8.1.

Table 8.1. Extraction cap policy runs.

Runs	**Extraction Cap (m^3/well/year)**
Extraction Cap I	100.000
Extraction Cap II	80.000
Extraction Cap III	60.000

Figure 8.14 displays the behavior of the groundwater table in the base run and three different extraction cap policies. The lower the extraction cap, the higher the groundwater table, as anticipated. In the extraction cap III run, we see a stabilization of the groundwater table and even a slight improvement after 2035.

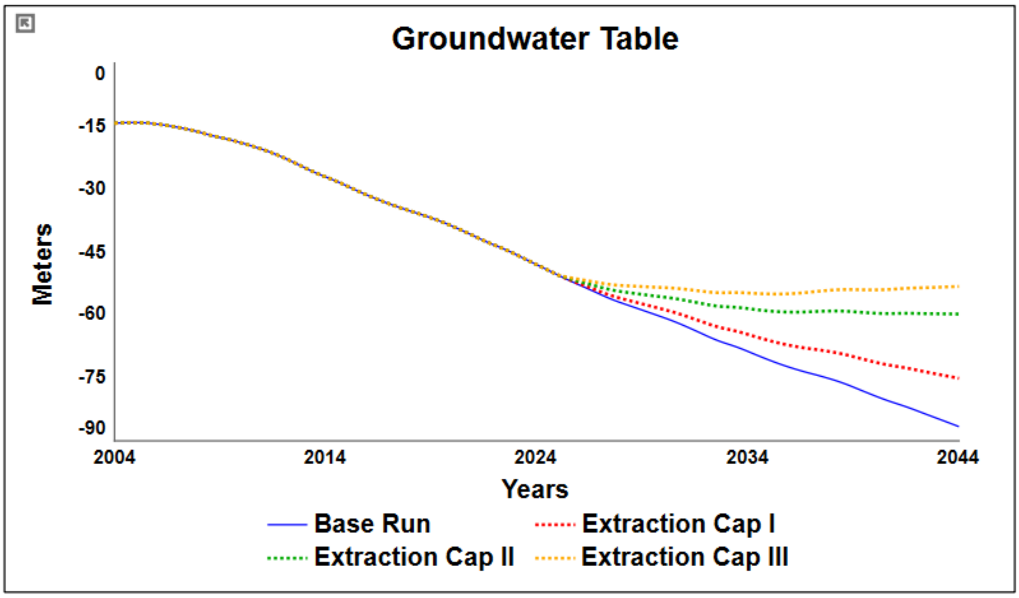

Figure 8.14. Policy analysis 3: Groundwater table.

The groundwater pumping infrastructure is also impacted substantially by the extraction cap (Figure 8.15). We observe that the decreasing trend is steeper when the extraction quota is stricter. However, extraction cap II and III produce very similar behavior in the number of wells. On the other hand, While the first extraction cap only slows the improvement of the pump power, the second and third extraction caps initially lower the average pump power, and then slowly build it up again.

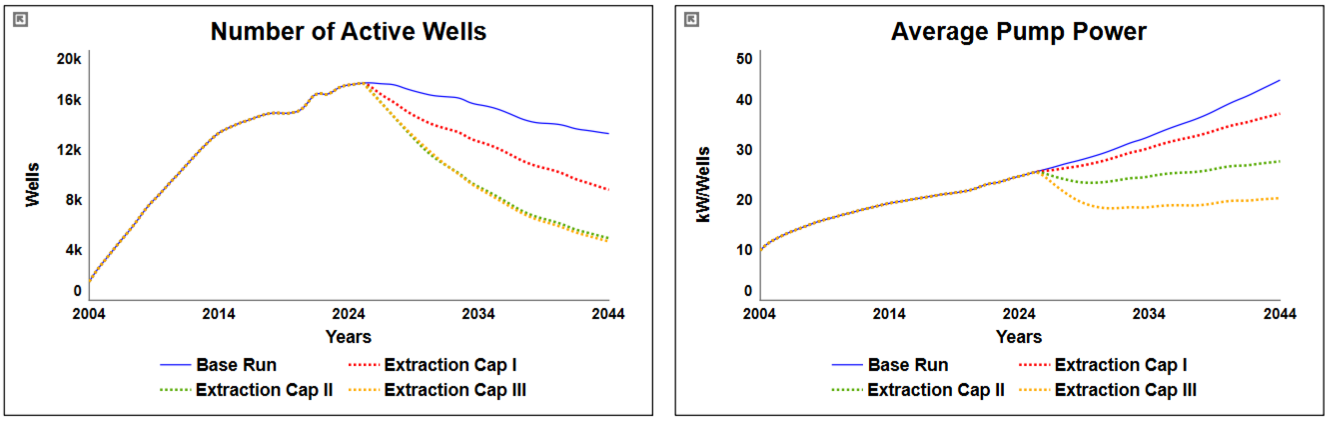

Figure 8.15. Policy analysis 3: Number of active wells and average pump power.

The extraction cap policy has a minor impact on the crop land cover. However, the rates of irrigation, thus the crop yields and production are substantially affected by it. In Figure 8.16, we see that the irrigation for all crops is less than halved. Among all three irrigated crop types, sugar beet irrigation decreased the most.

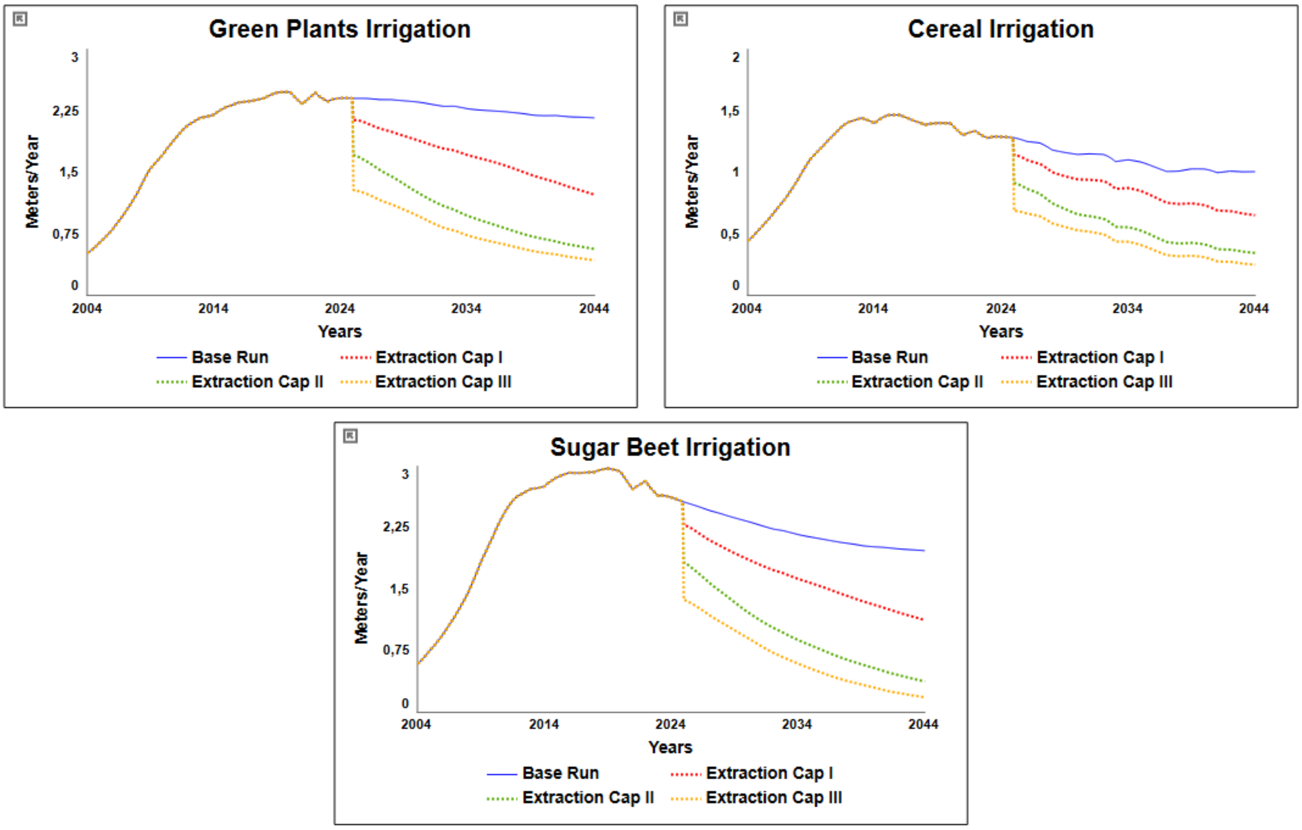

Figure 8.16. Policy analysis 3: Crop irrigations.

Due to the lower irrigation, the yield loss is significant (Figure 8.17). It is reflected in crop production as well; crop production is lowered by approximately 30% for green plants and irrigated cereal under the strictest extraction quota, while sugar beet production slightly increases (Figure 8.18) because there is a small increase in the sugar beet land.

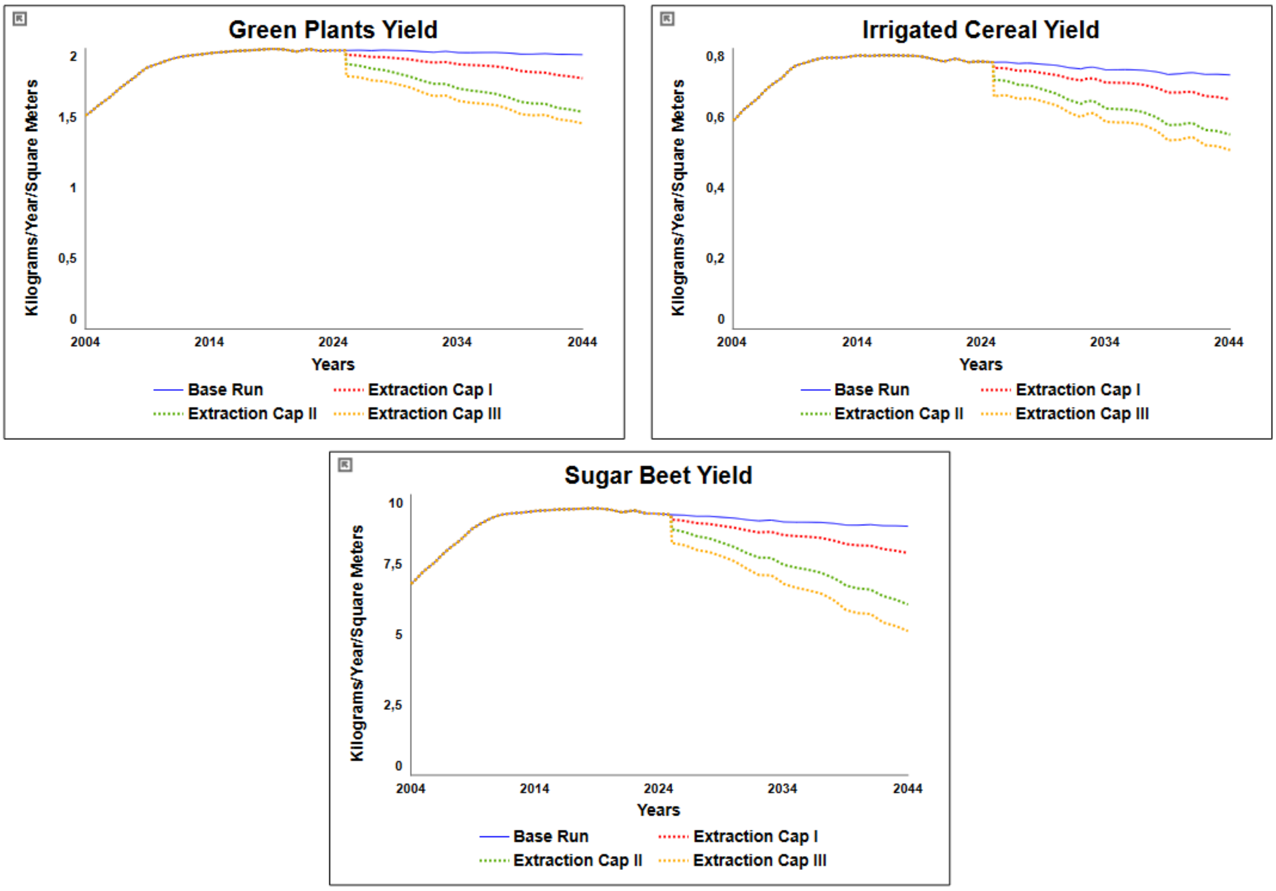

Figure 8.17. Policy analysis 3: Crop yields.

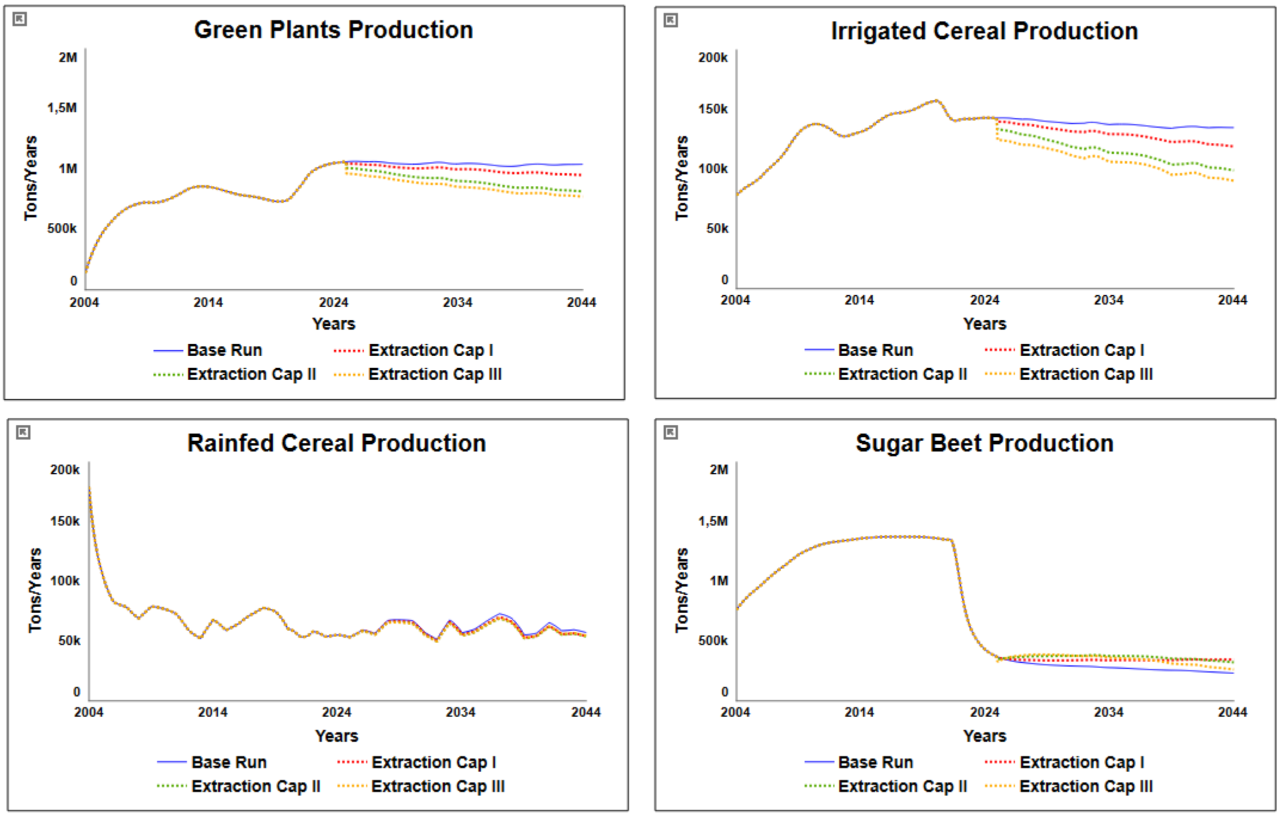

Figure 8.18. Policy analysis 3: Crop production.

One of the most interesting findings in this scenario is that even though there is an extraction cap, the total profit increases, compared to the base run (Figure 8.19). It is counterintuitive because farmers believe that if there is a quota for pumping, their crops will not get enough water and they will lose money. However, the output of the quota may depend on the level of the quota itself; our observations in the field taught us that there is an overirrigation behavior in general. Therefore, with a useful quota, farmers may decrease their irrigation costs while maintaining a similar yield and production level, which would in return increase the overall profit.

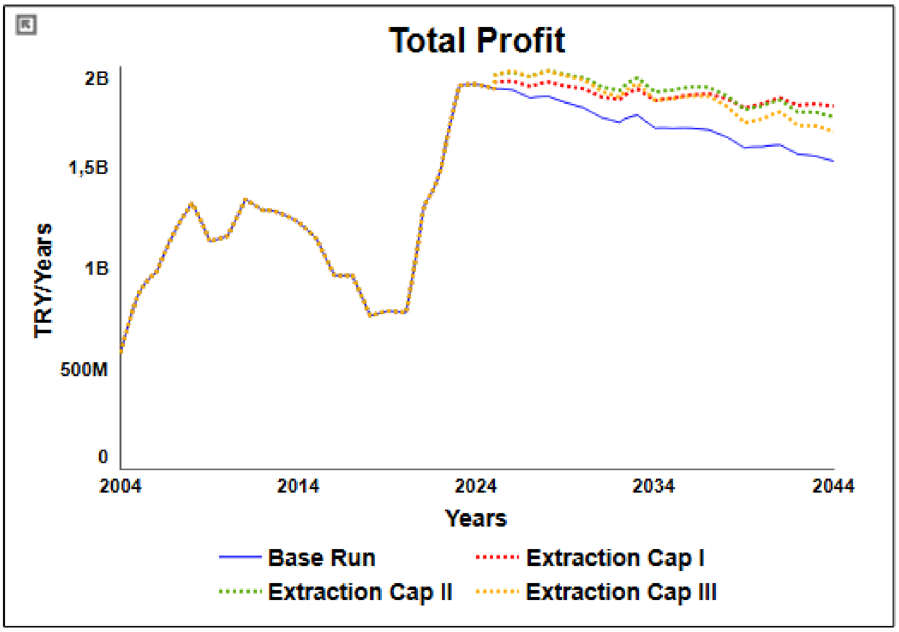

Figure 8.19. Policy analysis 3: Total profit.

8.4. Crop Repricing

Another commonly discussed policy intervention among stakeholders is indirect financial incentives to switch to more water-conserving crops. While some argue that the price of green plants should be lowered for Konya Closed Basin so that farmers would prefer not to grow green plants, others disagree and prefer to increase the cereal prices so that farmers willingly grow cereals instead of green plants.

In this section, we take three simulation runs and compare the outputs with the base run. In the first simulation, we decrease the green plants' price starting from 2025. In the other two runs, we increase the cereal price by 30% and 50% respectively, starting from 2025.

Figure 8.20 shows the groundwater table outputs of the simulations. While all three policies improve the groundwater table compared to the base run by approximately 4-5 meters, it can be argued that the different repricing approaches do not produce significantly varying results in terms of the groundwater table.

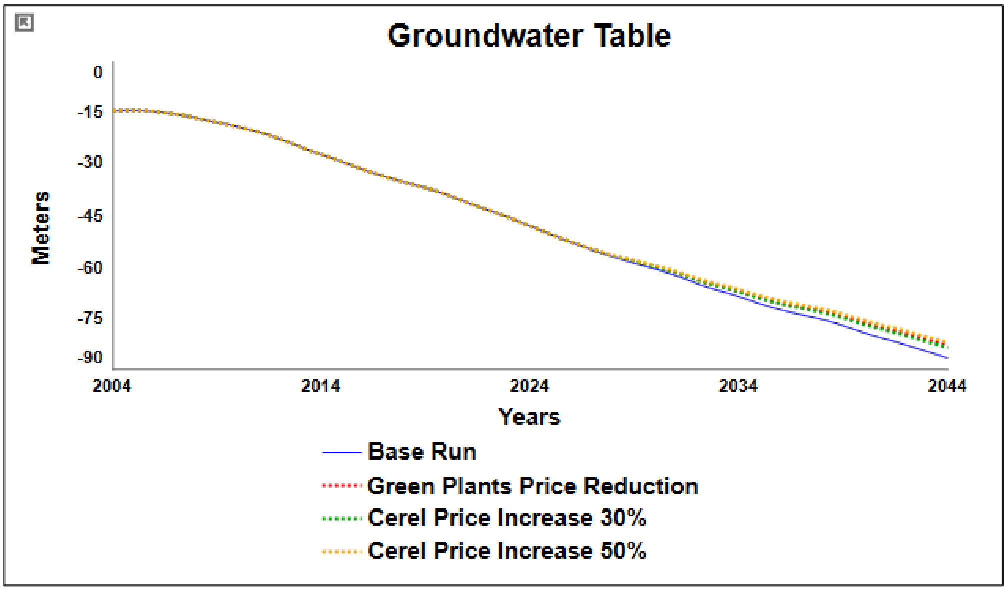

Figure 8.20. Policy analysis 4: Groundwater table.

The outputs of the number of active wells and average pump power are similar, the three runs have similar and minor impacts (Figure 8.21). Both the number of active wells and average pump power are lower in the policy runs compared to the base run, resulting from the relatively low groundwater demand.

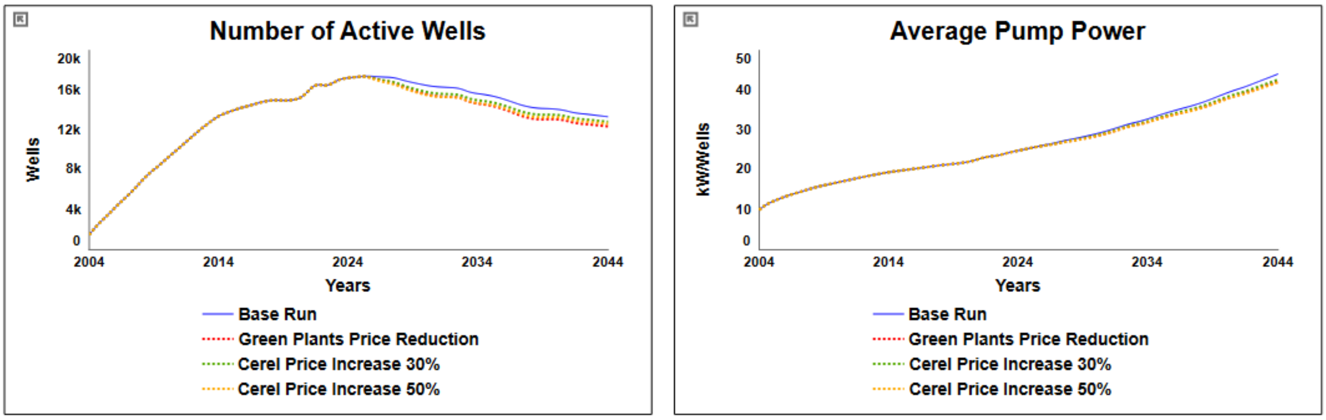

Figure 8.21. Policy analysis 4: Number of active wells and average pump power.

Figure 8.22 shows the crop land covers in the base run and the policy scenarios. In all three of the repricing policy simulations, the land for green plants decreases while the irrigated and rainfed cereal land increases. Land for sugar beet slightly decreases, but it is not affected as much as the other crops. The change in the price drives the change in the attractiveness of crops. Therefore, when the price of a single crop increases, it becomes more attractive, thus its land share in the total agricultural land increases, and vice versa. The crop yields are not impacted by the change in the crop prices. So, the change in crop production is mainly driven by the land cover change and its behavior reflects that of the land cover.

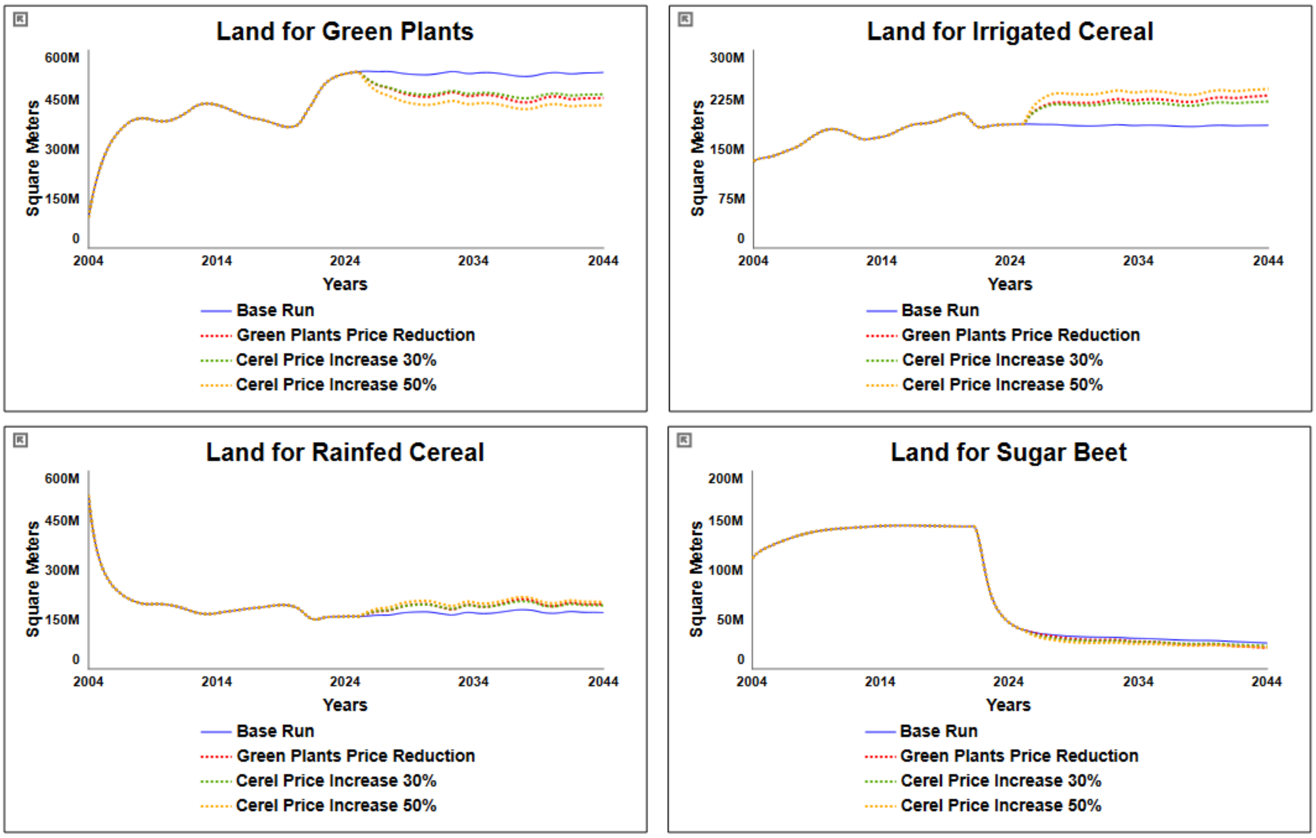

Figure 8.22. Policy analysis 4: Crop land covers.

We see the total profit in Figure 8.23. As anticipated, in the simulations where we increase the cereal price, the total profit increases, and when we decrease the green plants' price, the total profit decreases.

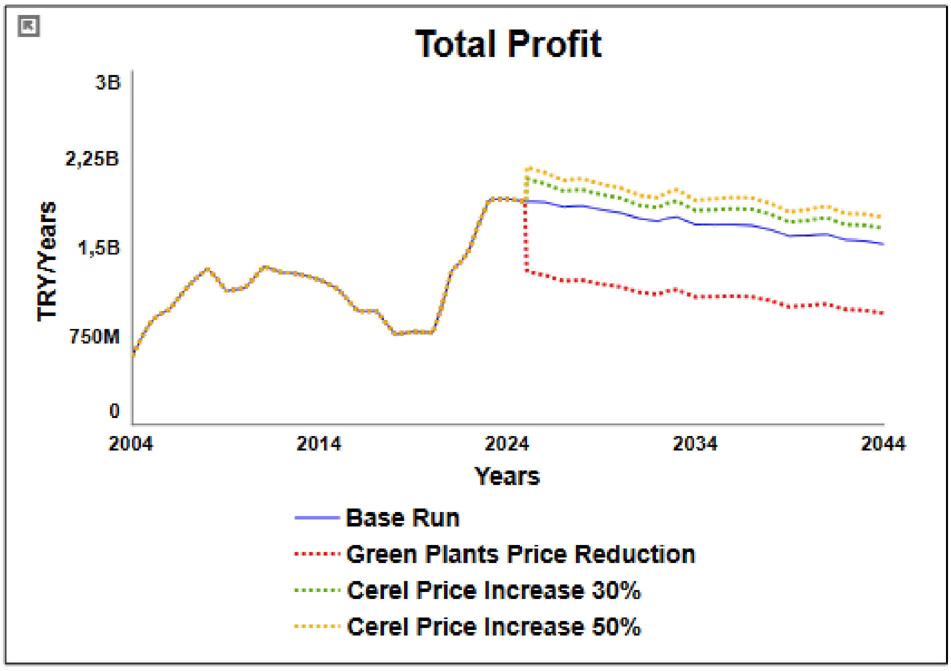

Figure 8.23. Policy analysis 4: Total profit.

8.5. Electricity Repricing

During the field visits, we noticed that all farmers complain about the electricity prices because their irrigation cost is incremented both by the increase in the unit electricity price, and the deepening groundwater table. On the other hand, other stakeholder groups argue that increased unit electricity prices can be used as an indirect disincentive for excess irrigation. Therefore, in this section, we double the unit electricity price starting from 2025 and compare the outputs with the base run.

Figure 8.24 shows the groundwater table outputs. We observe that increasing the unit electricity price helps conserve groundwater, the outputs of the policy simulation is 6,4 meters higher than the base run.

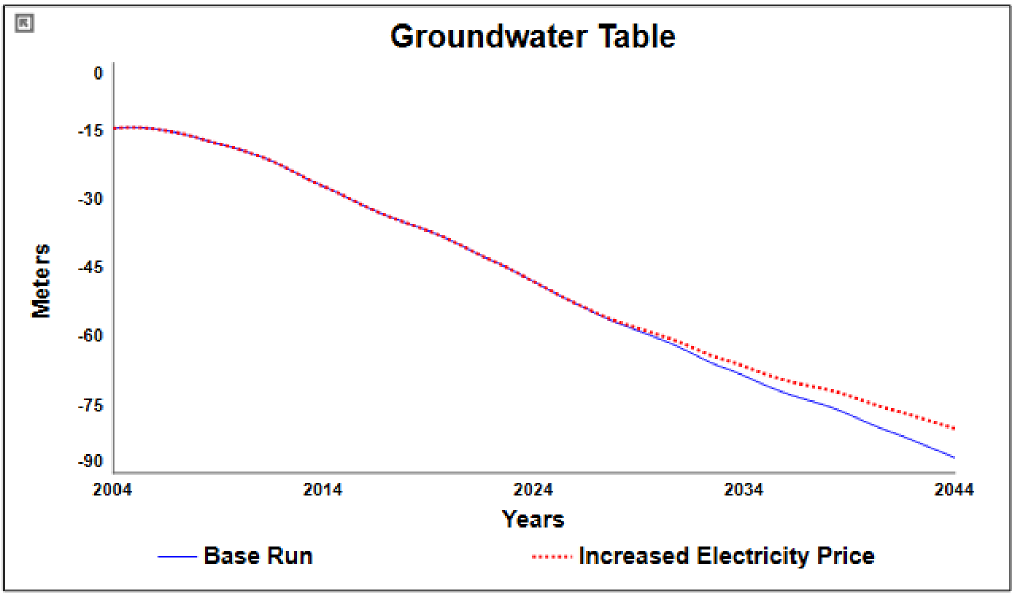

Figure 8.24. Policy analysis 5: Groundwater table.

The decrease in the groundwater demand may also be seen in the number of wells and average pump power (Figure 8.25). While the depreciation of the number of wells is higher when the unit electricity price is increased, the building up of the average pump power is slower.

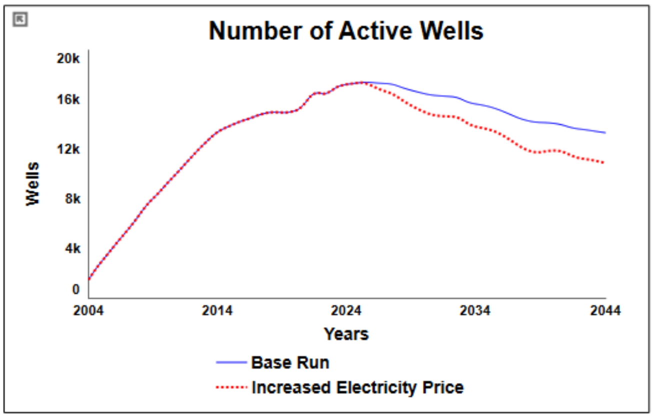

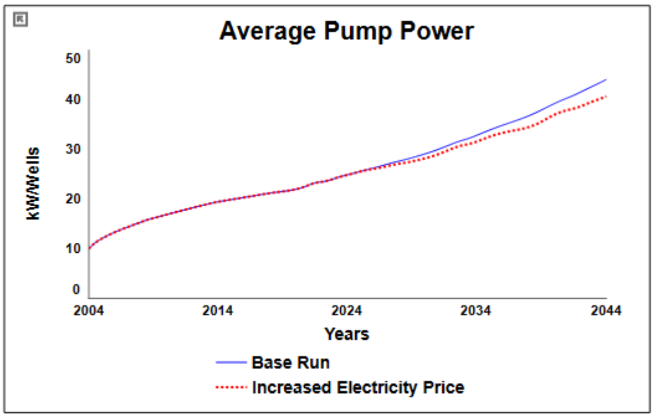

Figure 8.25. Policy analysis 5: Number of active wells and average pump power.

The land cover is substantially impacted by the increase in the unit electricity price, as can be seen in Figure 8.26. Since the cost of irrigation is doubled, the profitability of irrigated agriculture decreases significantly. Therefore, farmers start favoring rainfed agriculture over-irrigation. As a result, we observe an increase in the rainfed cereal land and a decrease in all irrigated crop lands. The most significant impact is that sugar beet land is almost zeroed, because with the current price input in the model, and doubled unit electricity price, sugar beet cultivation causes financial loss.

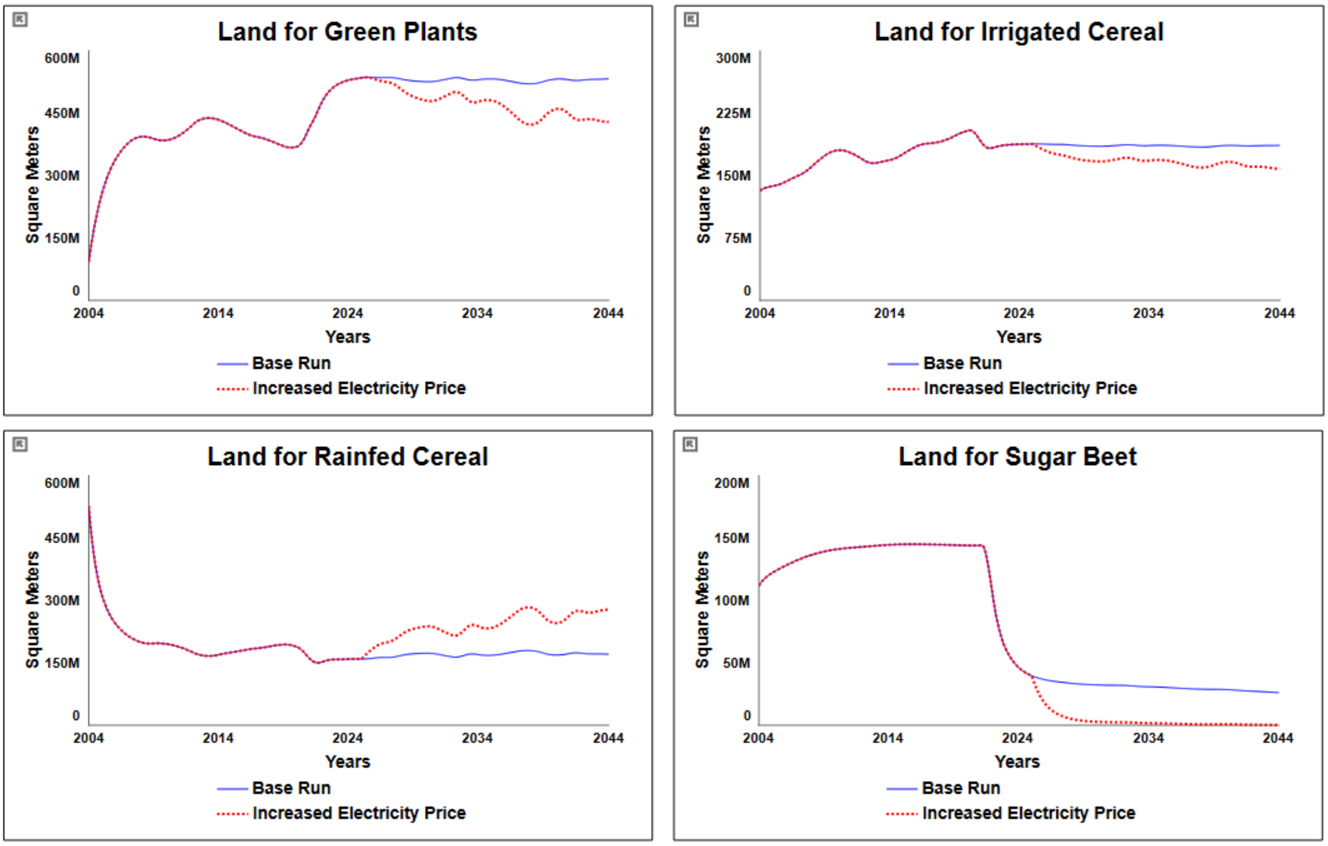

Figure 8.26. Policy analysis 5: Crop land covers.

The level of irrigation and thus the crop yields are not significantly affected by the increased electricity price (Figure 8.27). However, as can be seen in Figure 8.28, the total profit of the district decreases substantially; even though the crop yields are maintained, the decrease in the irrigated crop lands results in lower production levels, because the yields are always higher in irrigated agriculture. Moreover, electricity price directly increases the costs, thus the decrease in the profit.

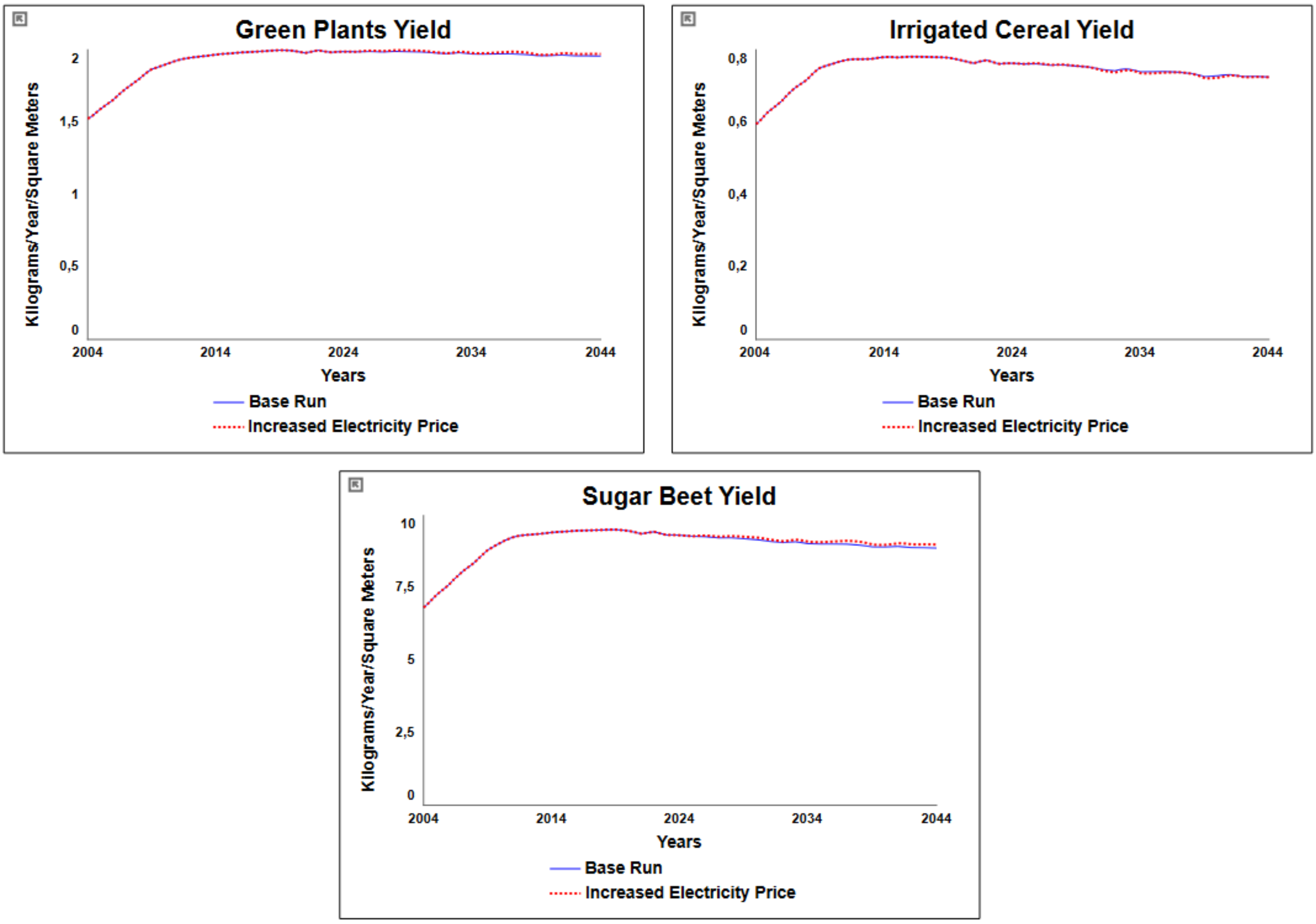

Figure 8.27. Policy analysis 5: Crop yields.

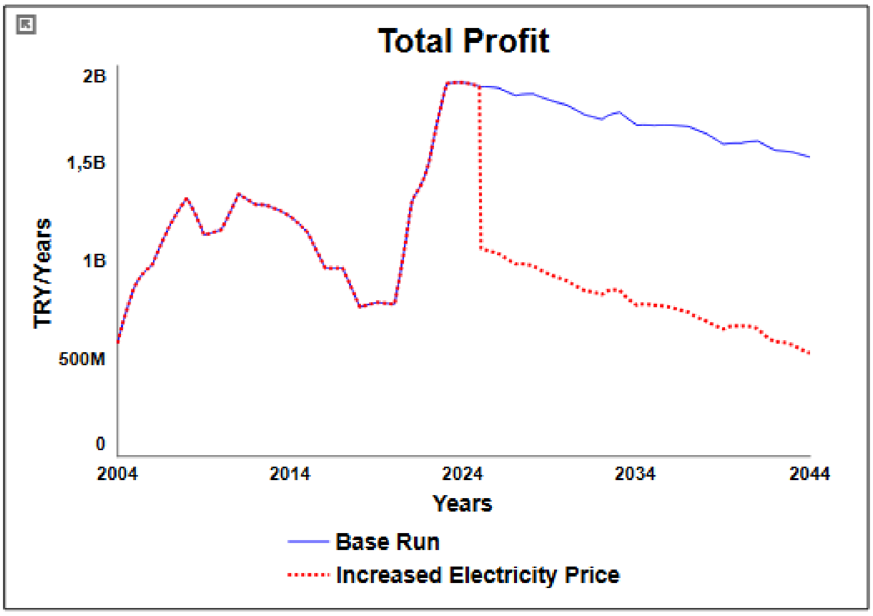

Figure 8.28. Policy analysis 5: Total profit.

9. INTEGRATED POLICY ANALYSES

In the previous section, we analyze the effect of the suggested policies one by one. Some policy options are useful in conserving groundwater; however, only a rather strict extraction cap seems to be able to stop the decreasing trend by itself, while others slow down, but does not stop the drop in the groundwater table. Additionally, even though the strict extraction cap can bring the groundwater table to an equilibrium, it causes a substantial decrease in crop production, which is an unwanted impact. Therefore, in this section, we carry out an integrated policy analysis, where we assess the usefulness of multiple policy combinations.

First, we separate the suggested policy options into two groups, based on whether they are favored by the farmers or not, and then we compare the outputs of the two groups with each other and the base run. The policy sets are presented in Table 9.1. Policy Set 1 consists of the policy options favored by farmers, and Policy Set 2 involves policies that are unpopular among farmers.

Table 9.1. Integrated policy sets based on farmers' points of view.

Policy Options	**Policy Set 1**	**Policy Set 2**
Surface Water Transfer	600 hm^3/year	300 hm^3/year
Well Regulation	-	Prohibition of New Wells (2025 – 2030)
Crop Rotation	Green Plants, 2 years	-
Extraction Cap	-	100.000 hm^3/well/year
Crop Repricing	Cereal Price: 50% increase Sugar Beet Price: 100% increase	Green Plants Price: 20% reduction
Electricity Repricing	0,5 TRY/kWh (33% reduced)	1,0 TRY/kWh (33% increased)

Both policy sets include surface water transfer; it is a popular scenario among farmers. The reason we included it in the second policy set as well is that the Blue Tunnel project is already undertaken, and we expect it to realize in the mid-2020s. However, the first policy set involves a higher volume of water transfer, implying the possibility of a new surface water transfer project, as big as the Blue Tunnel.

Apart from the surface water transfer, the first policy set includes a crop rotation scheme for green plants, in which green plants would be grown once every two years on the same piece of land. Cereal price is increased by 50%, and sugar beet price is doubled. Sugar beet is a very important crop for the region because there is a whole food industry developed around it in the Konya region. Therefore, it is an indispensable crop for the economy of the region. However, the sugar beet price in recent years has been low, compared with other crops, and farmers have been complaining about the sugar beet prices. That is why we increase the sugar beet price in the first policy set. Lastly, we reduce the electricity price by 33% in the first policy set, because farmers also claim that the current electricity prices impact their profits substantially.

In the second policy set, we enforce the no new well regulation for five years, from 2025 to 2030. We also implement an extraction cap of 100.000 m^3/well/year. To disincentivize the production of water-consuming crops, we reduce the price of green plants by 20% and increase the unit electricity price by 33%.

Figure 9.1 shows the groundwater table outputs of the base run and the two policy sets. We observe that both policies perform better than the base run in terms of groundwater conservation; however, while the first policy set keeps the steadily decreasing trend, the second policy set significantly slows down the drop and seems that it might result in a steady state in further future beyond the model time horizon.

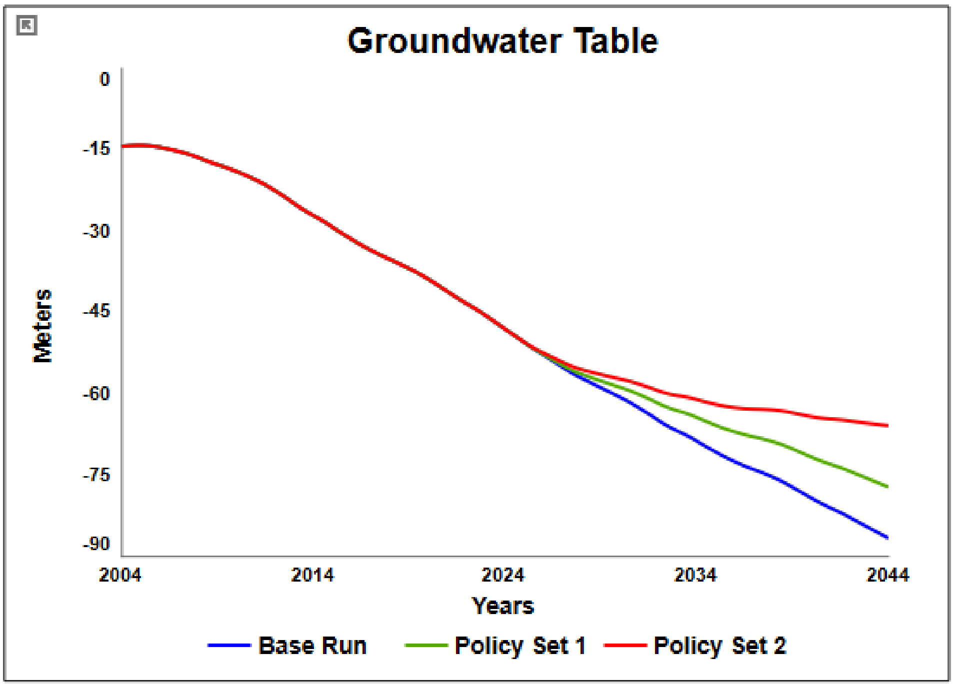

Figure 9.1. Integrated policy analysis 1: Groundwater table.

The number of wells in the two policy set runs are substantially different from one another, mainly due to the prohibition of new wells regulation in the second policy set, and also because of the varying groundwater demands (Figure 9.2). The increase in the average pump power is also slower in the second policy set because the groundwater demand is lower.

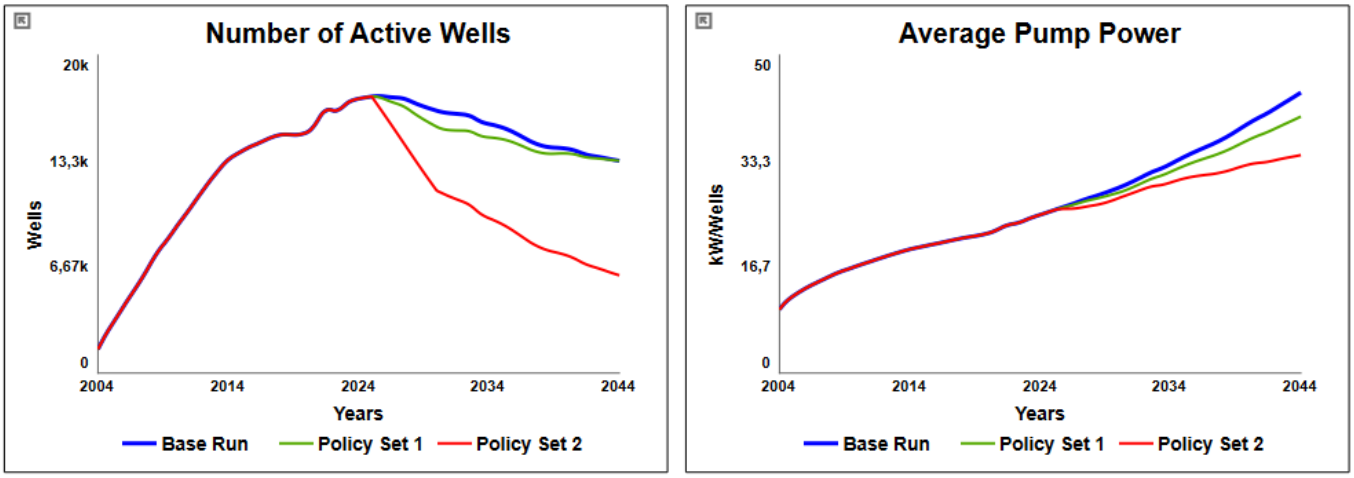

Figure 9.2. Integrated policy analysis 1: Number of active wells and average pump power.

The land cover changes under both policy scenarios compared to the base run, as shown in Figure 9.3. Even though the green plants' price is unchanged, the price increase in the cereal and sugar beet reduces the relative profitability, and thus the attractiveness of green plants in the first policy set. The land cover change is in the same direction as in the first policy set, but it is smaller.

When we compare the crop irrigation levels in the two policy sets and the base run, we see that the irrigation levels are highest in Policy Set 1, and lowest in Policy Set 2 (Figure 9.4). In policy set 1, irrigation is indirectly incentivized by the reduction in the unit electricity price, compared to the base run. In contrast, in the second policy set, there is both direct intervention on extraction through the extraction cap and well regulation, and also an indirect intervention by the rise in the unit electricity price.

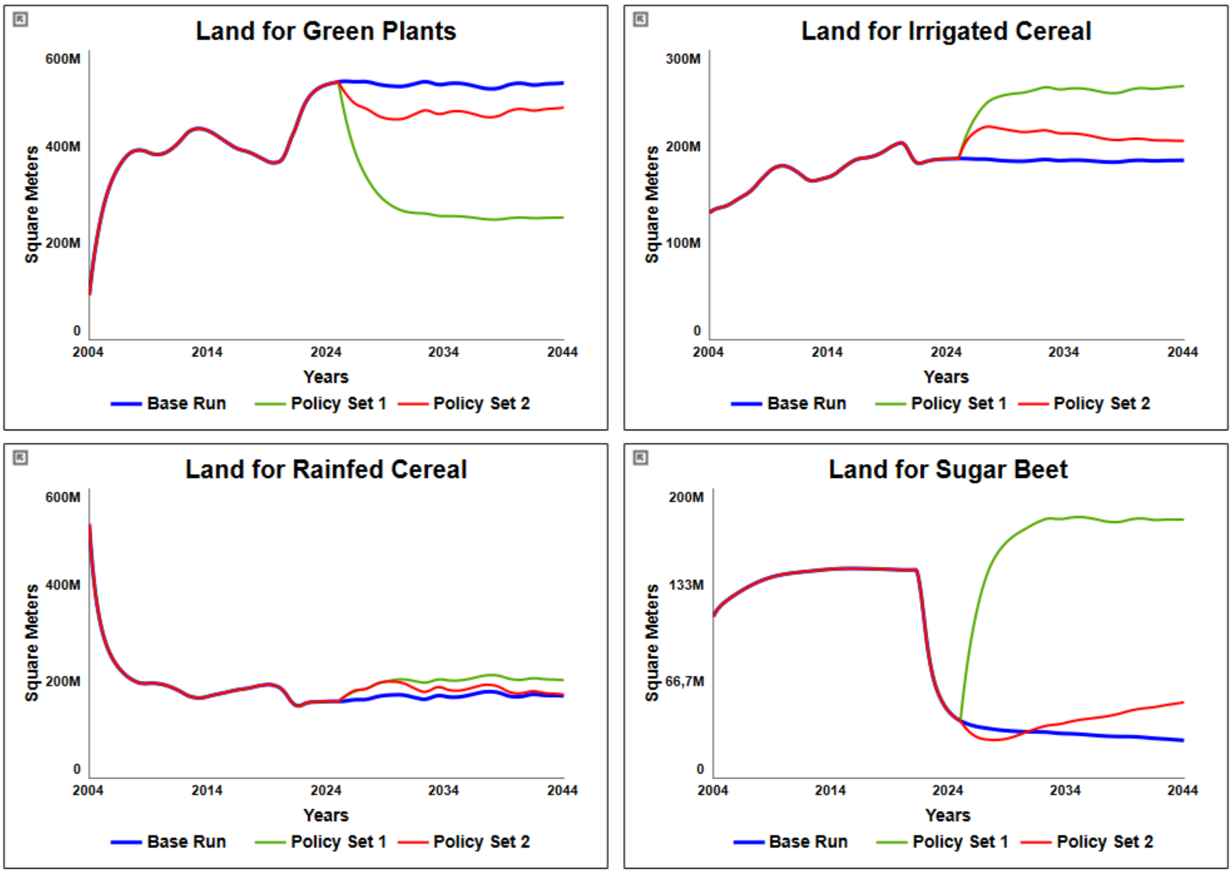

Figure 9.3. Integrated policy analysis 1: Crop land cover.

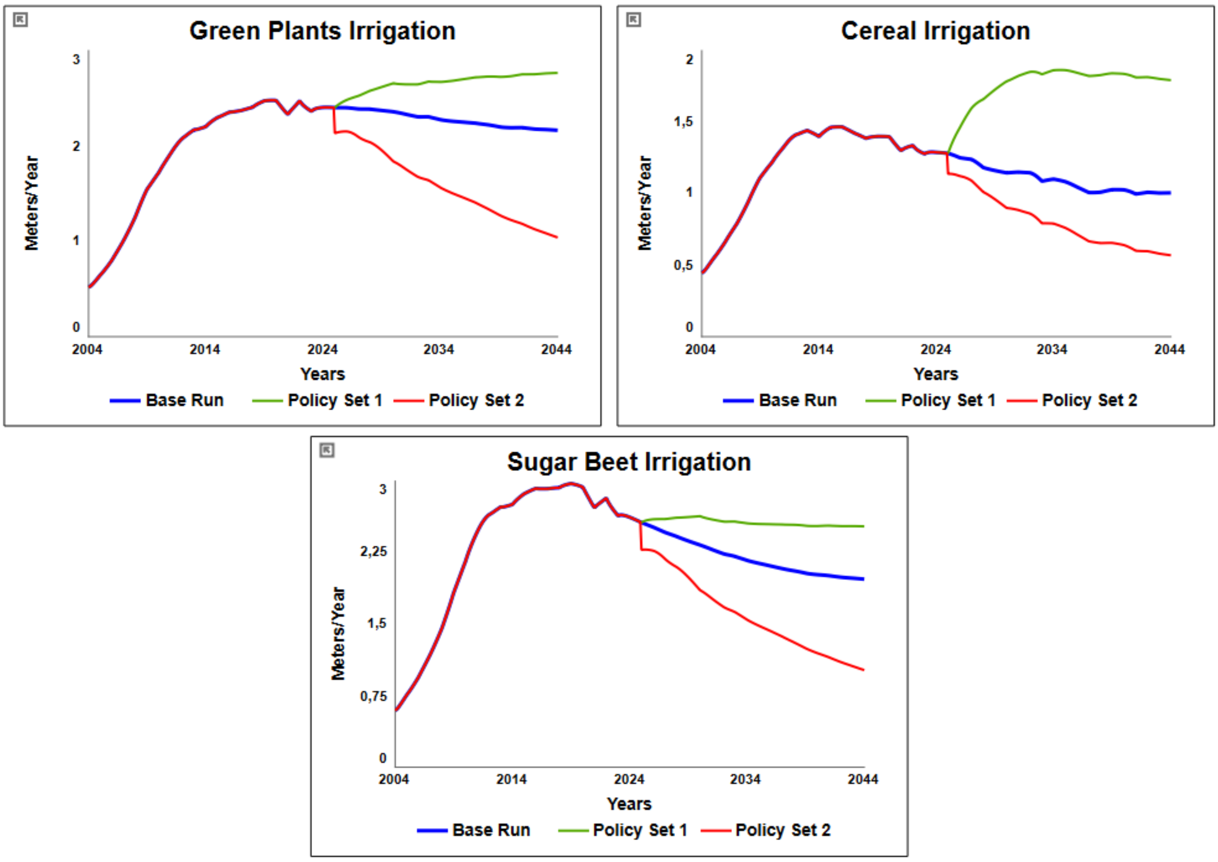

Figure 9.4. Integrated policy analysis 1: Crop irrigation.

Figure 9.5 presents the crop yield outputs of the two policy sets as well as the base run. Policy Set 1 produces higher yields for irrigated crops, compared with both the base run and Policy Set 2, which is in line with the anticipations as the irrigation levels are highest in the first policy sets. On the other hand, Policy Set 2 produces lower yields.

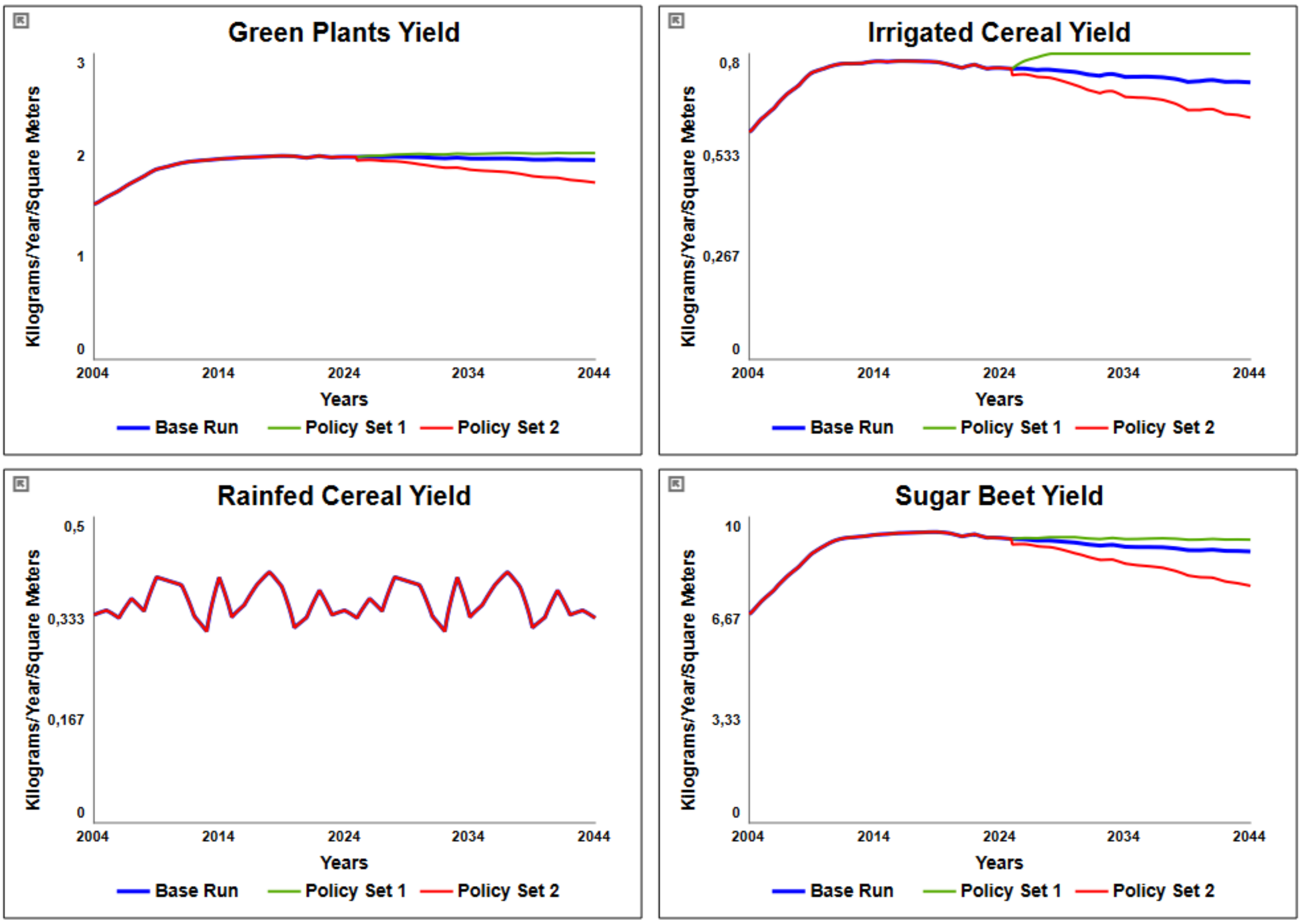

Figure 9.5. Integrated policy analysis 1: Crop yields.

The crop production outputs are compared in Figure 9.6. The second policy set yields a production pattern that resembles the base run. The differences in crop production between the base run and the second policy set result from the price changes and the interventions on the annual extraction capacity. On the other hand, the first policy set yields a very different production pattern; the green plants' production is halved, while the sugar beet production is five times more compared to the base run.

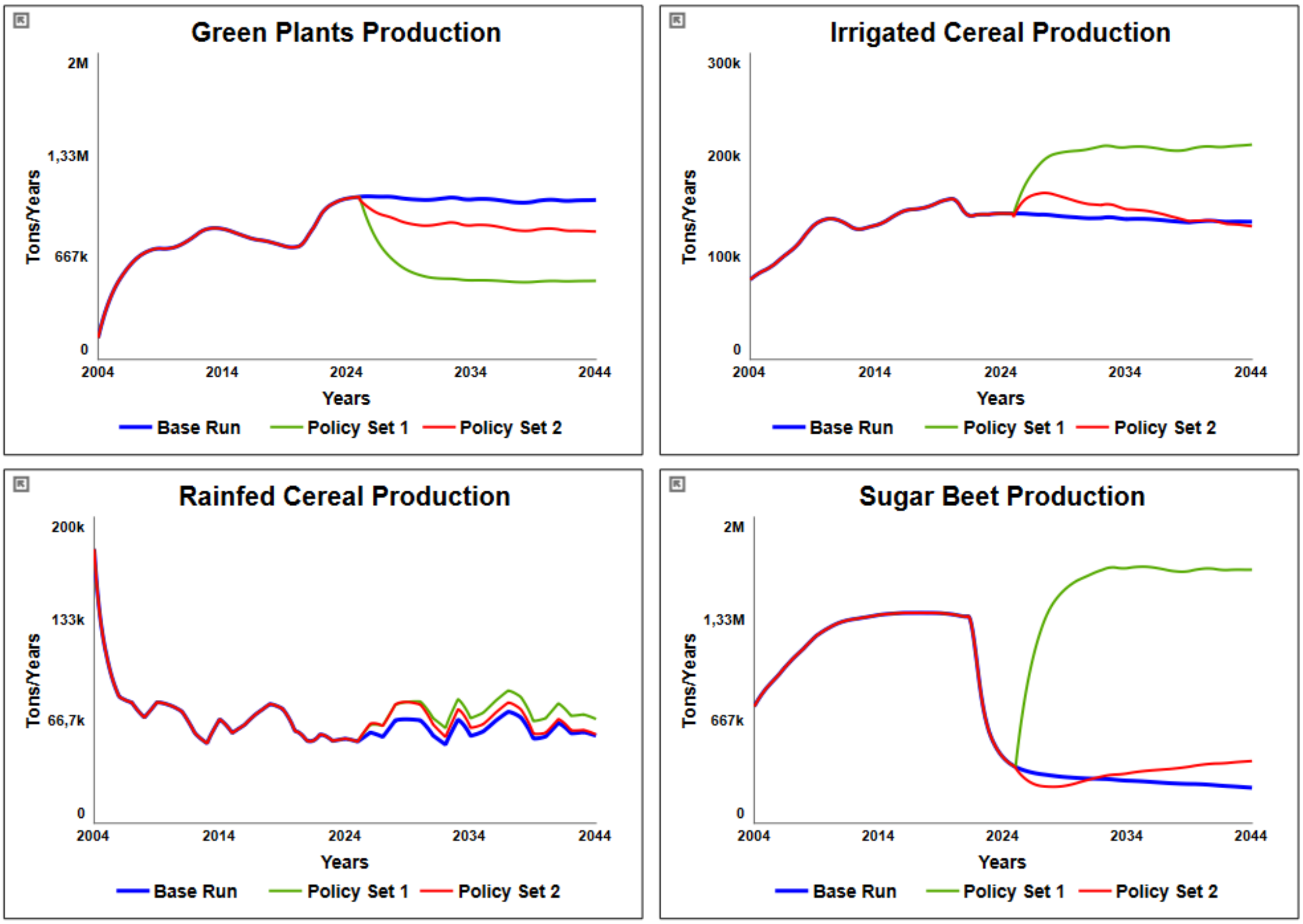

Figure 9.6. Integrated policy analysis 1: Crop production.

Lastly, we compare the performance of the two policy sets in terms of total profit in Figure 9.7. From 2025 until the end of the simulation period, the first policy set performs better than the second. However, they are also different in terms of behavior patterns. While the first policy set initially increases the profit but then follows a decreasing trend, the second policy set initially lowers the total profit but then has a rising trend.

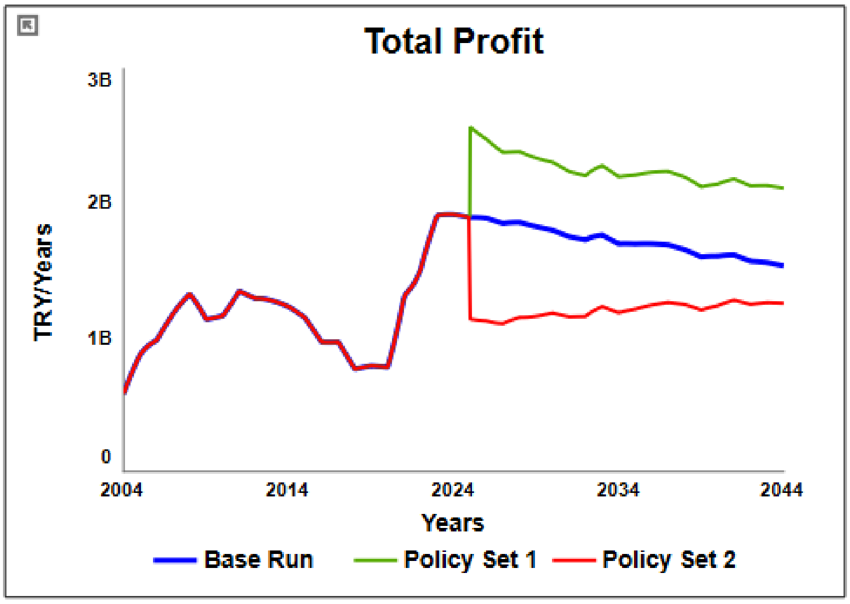

Figure 9.7. Integrated policy analysis 1: Total profit.

In short, the two policy sets, one of which is favored by the farmers and the other farmers try to avoid, have varying performances, depending on the criteria. The first policy set increases the overall production and the profit of the region; however, is unable to stop the decreasing pattern in the groundwater table. In contrast, the second policy set is more useful in groundwater conservation, however, it performs poorly in terms of total district profit. Under these circumstances, the overall performance evaluation results of the two policy sets depend on who makes the evaluation; if we were to present these model outputs to a farmer, most probably they would rather have the first policy set because it is for their benefit. On the other hand, if we were to share the results with an environmental NGO, they would be likely to prefer the second policy set, because it is more successful in terms of groundwater conservation, and it does not lower the total profit to a lower level than the historical. Then, we may try to come up with a third set of policies that performs as well as the second policy set in terms of groundwater conservation, without having to compromise the total profit and production levels of the base run.

Table 9.2 shows the policy combinations in Policy Set 3. It is a combination of some of the policies included in the first two policy sets. The surface water transfer from the Blue Tunnel is included. From 2025 to 2030, opening new wells are strictly prohibited. A 2-year crop rotation scheme is implemented for the green plants, as well as an annual 100.000 hm^3/well extraction cap. The cereal prices are increased by 50% and the sugar beet prices are doubled. Lastly, the unit electricity price is reduced by 33%.

Table 9.2. Policy set 3.

Policy Options	Policy Set 3
Surface Water Transfer	300 hm^3/year
Well Regulation	Prohibition of New Wells (2025 – 2030)
Crop Rotation	Green Plants, 2 years
Extraction Cap	100.000 m^3/well/year
Crop Repricing	Cereal Price: 50% increase Sugar Beet Price: 100% increase
Electricity Repricing	0,5 TRY/kWh (33% reduced)

Figure 9.8 compares the groundwater table output of the third policy set with the previous policy sets and the base run. We see from the graph that Policy Set 3 outperforms both the previous policy sets in terms of groundwater conservation.

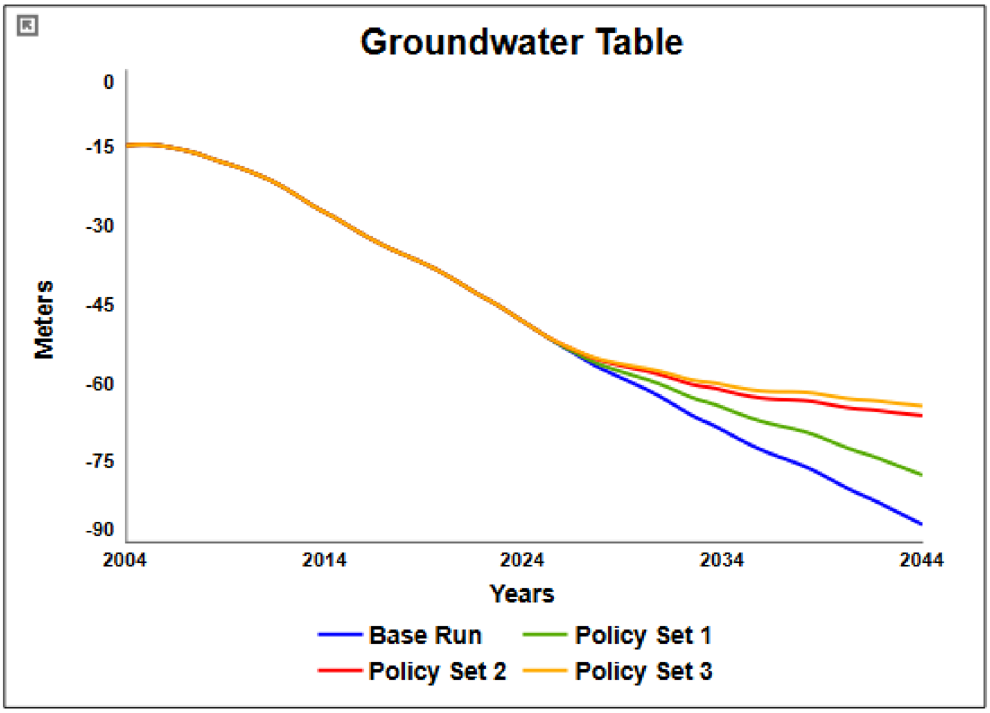

Figure 9.8. Integrated policy analysis 2: Groundwater table.

When we look at the groundwater extraction infrastructure, the outputs of the third policy set are very close to the second (Figure 9.9). The prohibition of new wells and the extraction cap reduces the requirement of increasing the existing number of wells and improving the average pump power, compared to the base run and the first policy set.

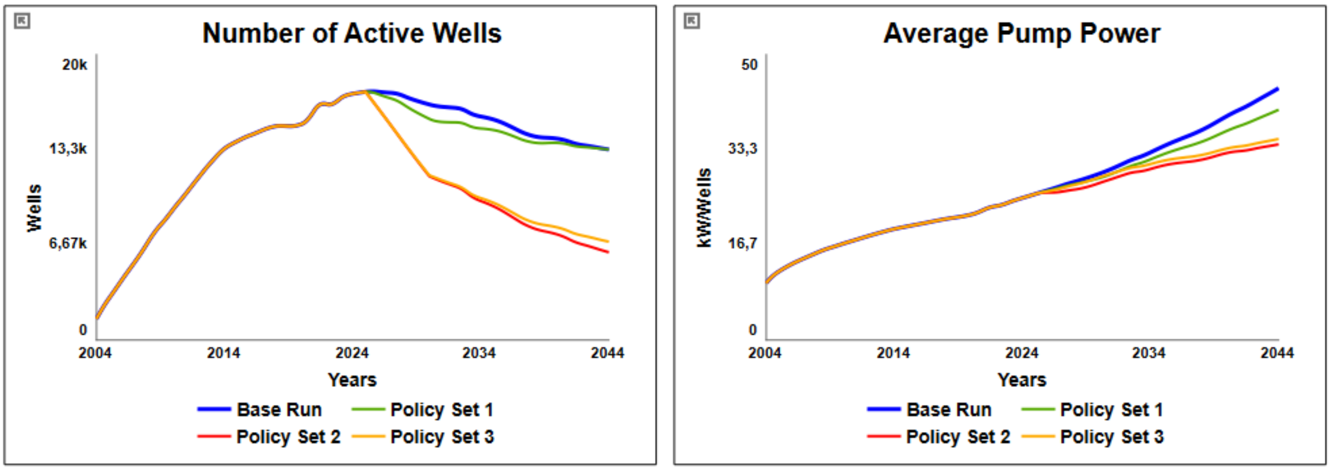

Figure 9.9. Integrated policy analysis 2: Number of active wells and average pump power.

Figure 9.10 presents the land cover in the integrated policy simulations. In terms of land cover, the third policy set follows the same pattern as the first policy set, as anticipated, because the changes in the crop and electricity prices are identical in Policy Sets 1 and 3.

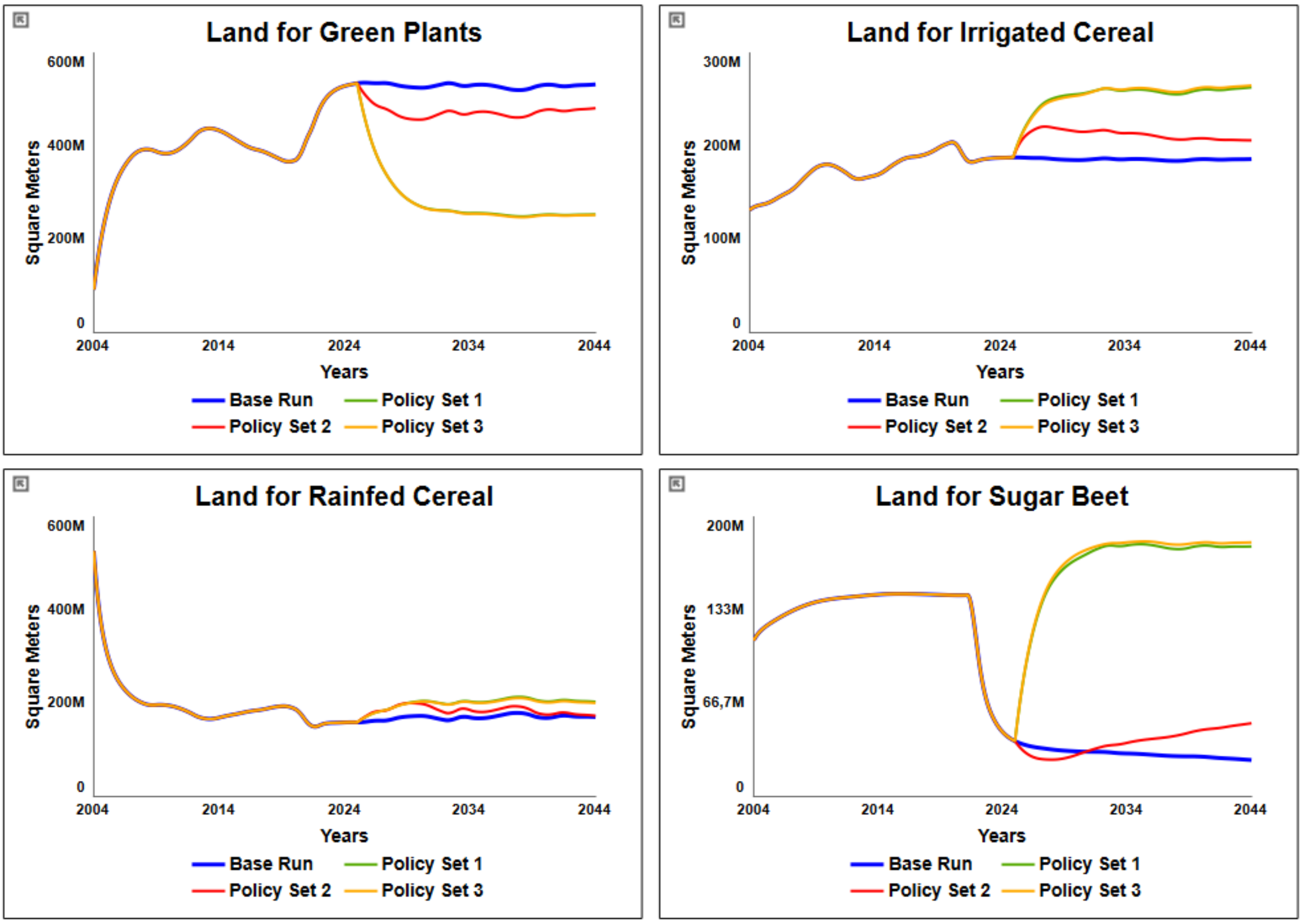

Figure 9.10. Integrated policy analysis 2: Crop land cover.

The crop irrigation levels are presented in Figure 9.11. Policy Set 3 outputs of the green plants and sugar beet irrigation are very close to those of the second policy set. On the other hand, the cereal irrigation level in Policy Set 3 is higher than the second policy set and the base run, but lower than the first policy set.

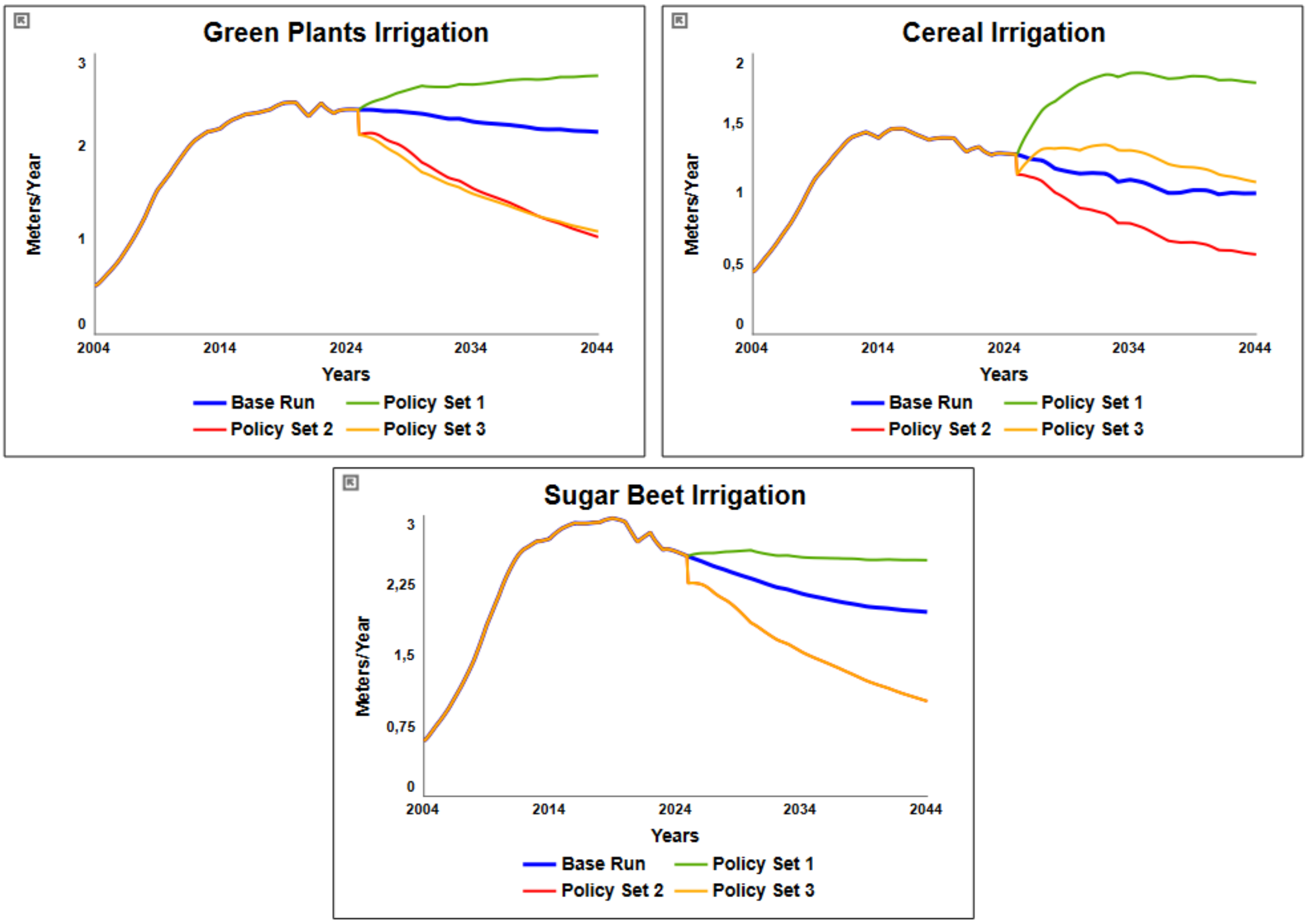

Figure 9.11. Integrated policy analysis 2: Crop irrigation.

When we compare the crop yields produced by Policy Set 3, we see that the behavior patterns in the irrigation are reflected in the crop yields as well, as expected (Figure 9.12). Therefore, while the yields of green plants and sugar beet decrease to the levels of policy set 2, the irrigated cereal yield is slightly increased compared to the base run.

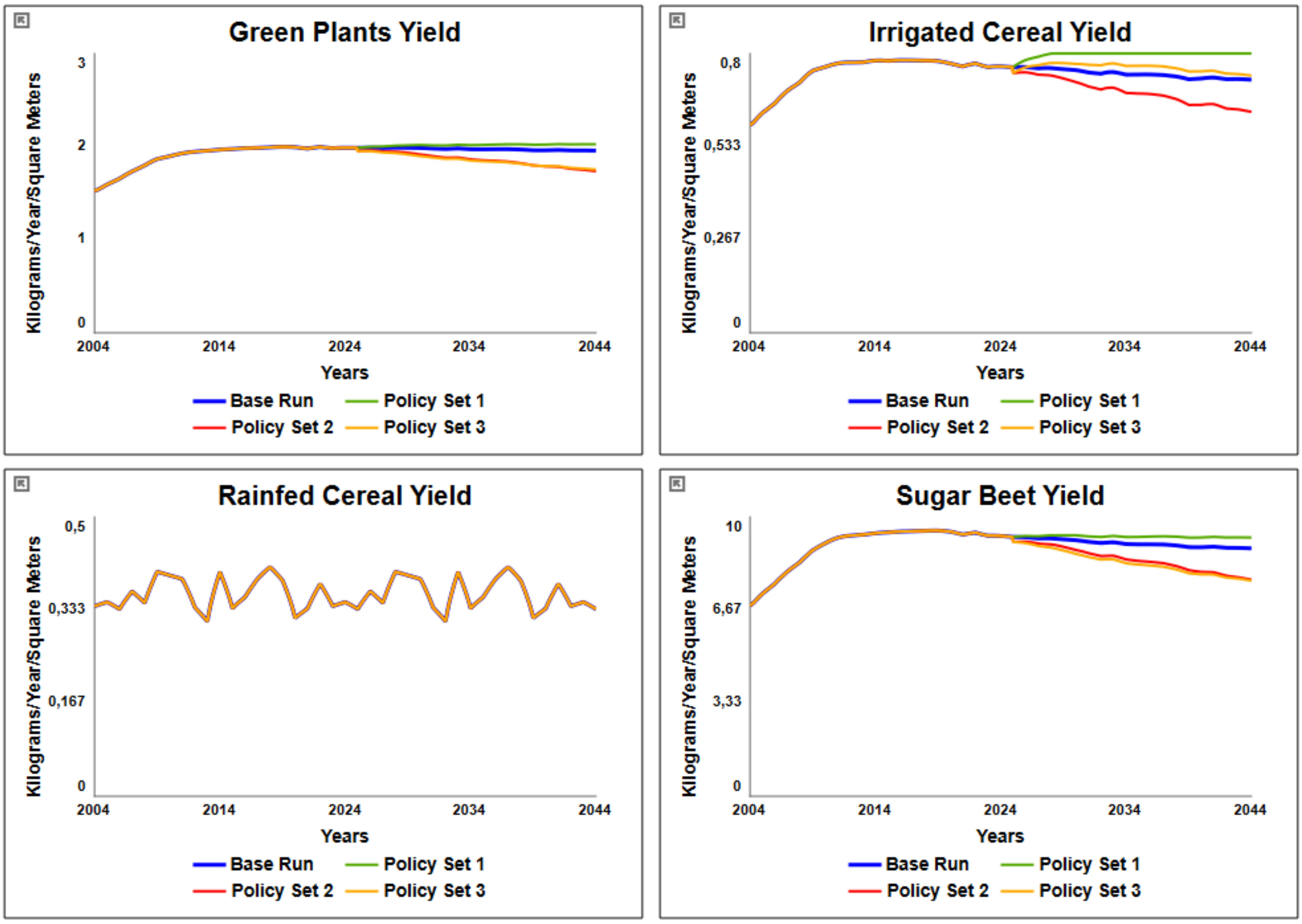

Figure 9.12. Integrated policy analysis 2: Crop yields.

Figure 9.13 shows the crop productions yielded by Policy Set 3. We observe that the production of green plants is the lowest in this policy set, but it is close to the level of production in the first policy set. Similarly, the irrigated cereal and sugar beet production are much higher than in the base run and the second policy set, but lower when compared to the first policy set.

Lastly, we compare the total district profit in the third policy set, with the previous two (Figure 9.14). In terms of profit, the third policy set seems to outperform the others.

Based on the comparisons of the model outputs of key variables under various policy settings, it can be argued that Policy Set 3 has the highest performance in terms of both environmental and economic indicators.

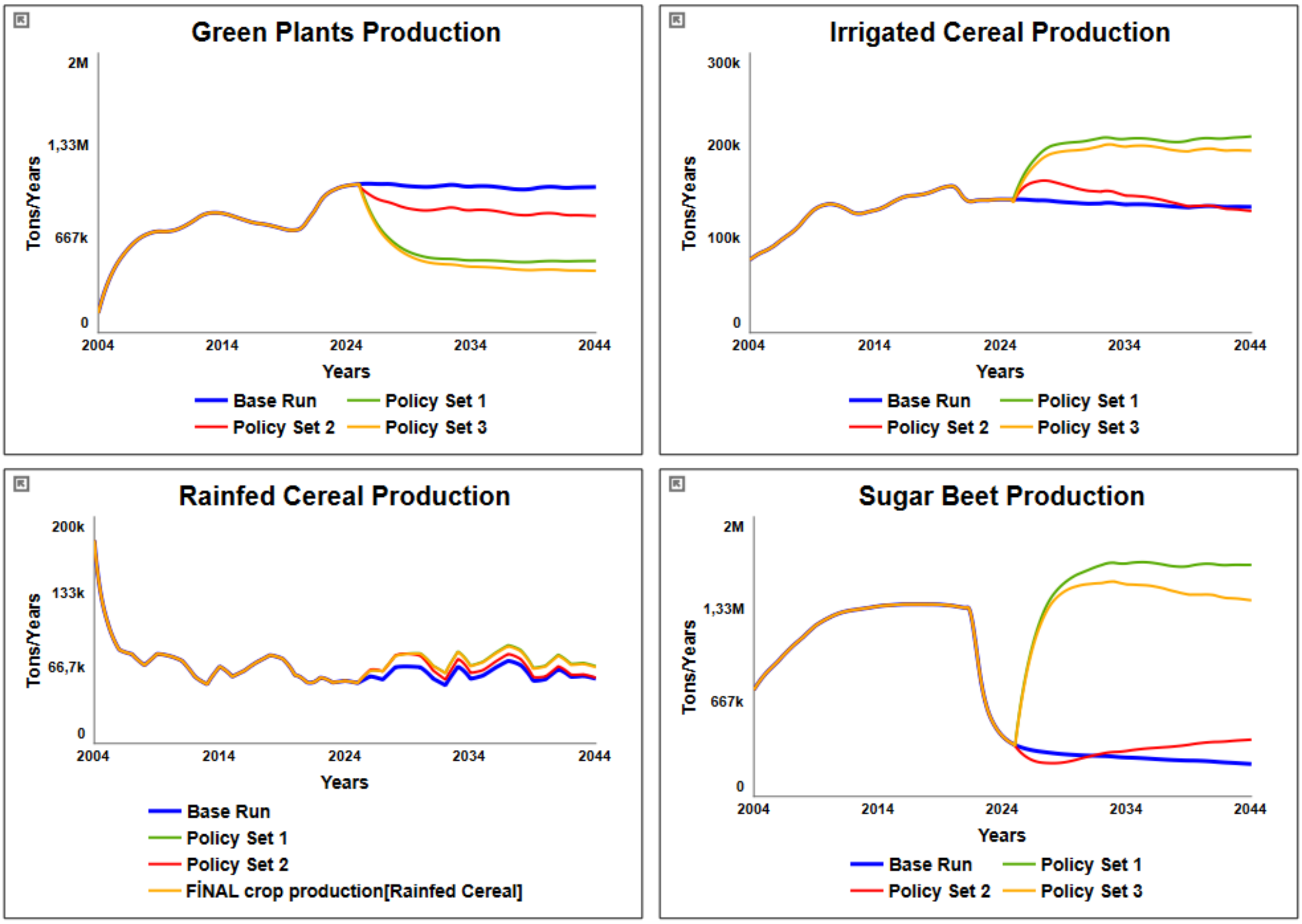

Figure 9.13. Integrated policy analysis 2: Crop production.

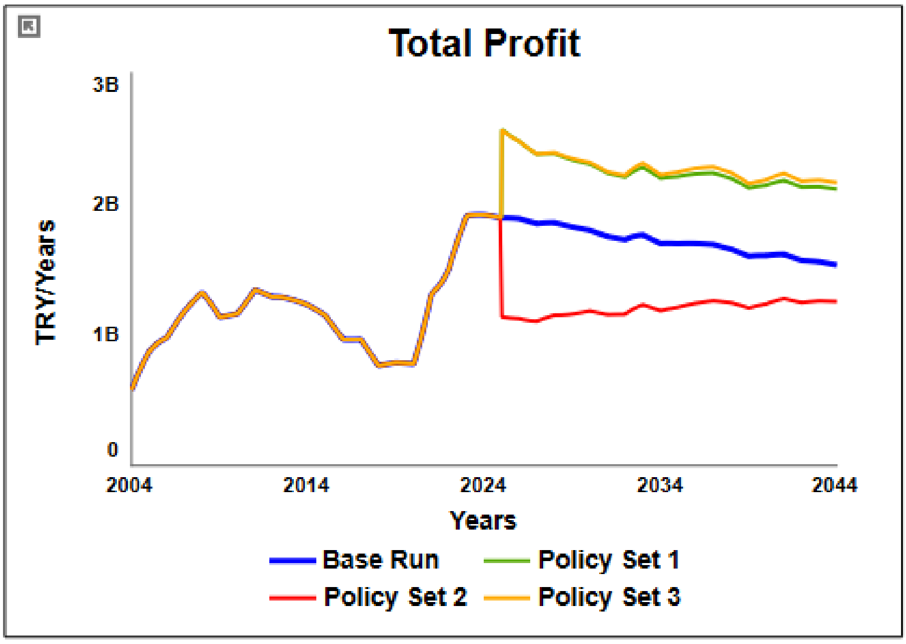

Figure 9.14. Integrated policy analysis: Total profit.

Lastly, we simulate the model for a longer period of time than the model time horizon to see how the third policy set behaves compared to the base run, in terms of groundwater table and total profit.

In Figure 9.15, we observe that the outputs of Policy Set 3 is more desirable than the business-as-usual scenario. In 2054, there is a 33-meter difference between the groundwater table in the two runs. However, we see that the decline in the groundwater table is not completely halted by this policy set; in the last years of simulation, the groundwater table keeps dropping approximately 10 centimeters per year. However, in terms of profit, the third policy set performs much better than the business-as-usual case.

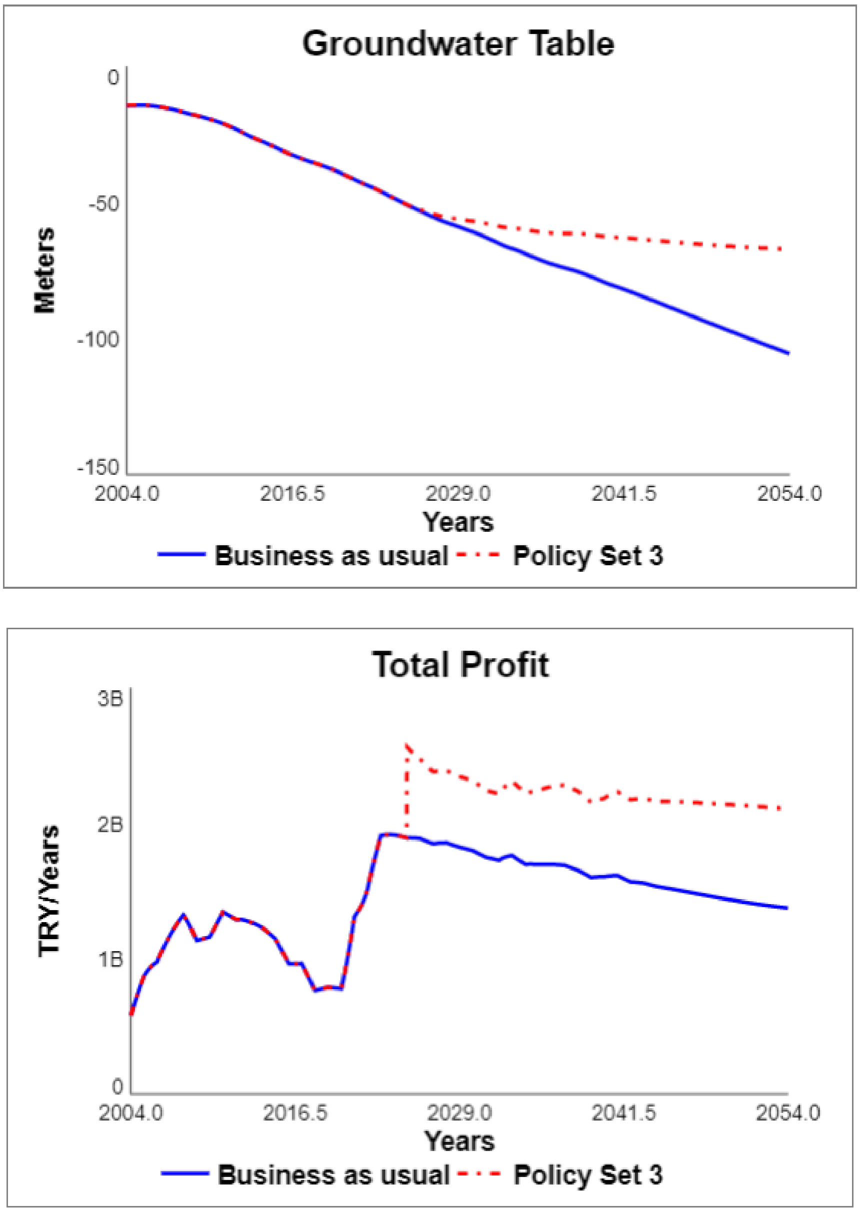

Figure 9.15. Business as usual vs Policy Set 3 in the longer run.

10. DISCUSSION

In this section, we discuss the key findings and of this research, based on the reference model output and the scenario and policy analyses performed to assess the usefulness of several policies in improving the economic and environmental indicators.

The simulation time horizon is 40 years, from 2004 to 2044. The period from 2004 to 2022 is the historical run, and the 2022 – 2044 period is the future projection. The model is initialized according to the 2004 values of the field data that was obtained from multiple resources. The reference model output represents the business-as-usual scenario and provides meaningful insights. First, we observe that the decrease in the groundwater table continues as is. After 2023, crop land cover, crop yields, and production approach an equilibrium. It should be noted that this behavior is caused by the assumption that the CPI-adjusted (real) crop prices and costs do not change in the future. On the other hand, the profit starts decreasing after 2023, because while the prices are assumed to be constant, the unit groundwater extraction cost increases by the year, due to the ever-decreasing groundwater table in the base run. Meanwhile, the irrigation factor is adjusted both to achieve the yield goal and also to optimize the cost and benefit of irrigation. When irrigation becomes too costly, i.e., the marginal cost of irrigation surpasses the marginal benefit, crop irrigation is reduced, even if it compromises the yield. Lastly, one of the most interesting findings of the model is the increase-then-decrease behavior pattern in the number of wells. In the first half of the simulation, the number of active wells increases rapidly. It peaks around 2025 and then starts decreasing, as the total groundwater demand decreases.

After the reference model behavior is presented, 2 scenarios and 5 policy analyses are performed on the model, namely, surface water transfer, climate change, well regulation, crop rotation, extraction cap, crop repricing, and unit electricity repricing. All of the scenarios and policies are designed based on the conversations with the stakeholders in the semi-structured interviews, and the discussions in the group model-building workshops. Sections 7 and 8 explain the analyses in detail. Then, an integrated policy analysis is conducted. First, the policies are divided into two categories, based on whether the policies are well-received by the farmer communities or not. The purpose of such a grouping is to discover the system behavior under different policy sets and determine whether the policies generally favored by the farmers would be useful for them to achieve their goals, and also whether the policies they try to avoid would result in an economic disaster. In other words, we want to answer the following questions: Assuming that the majority of the farmers do care about groundwater resource conservation, do they know what is best for themselves, or are they prejudiced against the policy suggestions that are verbalized by state institutions or that sound intimidating at first?

The policy set favored by the farmers involves crop rotation, additional surface water transfer, price improvements in cereals and sugar beet, and price reductions in electricity. This policy set is useful in increasing overall production and profit. It also slows down the drop in the groundwater table, which implies that it is more water-conserving compared to the business-as-usual run. However, this policy set does not stop or reverse the decline in groundwater level, it seems likely that these policies only postpone groundwater depletion.

Farmers do their best and use all their bargaining power to avoid the policies in the second category, which includes the soon-to-be-operational surface water transfer from the Blue Tunnel, prohibition of new wells for five years, extraction cap, increased electricity, reduced green plant prices. With this policy set, the declining trend in the groundwater table is substantially slowed down and possibly would approach equilibrium in a more distant future beyond the model time horizon. On the other hand, its performance in terms of profit is poorer than the business-as-usual scenario. Therefore, it may be concluded that farmers have a point in resisting these policies.

Yet still, after determining the strengths and weaknesses of each policy set, we look for a combination of policies from the first two policy sets, to see whether a new set of policies can outperform both of the previous policy sets in terms of both environmental and economic indicators. We create the third policy set by combining the inputs from the previous policy sets and comparing the behavior of key system variables. We observe that the overall performance of the third policy set is higher compared to the others because it conserves the groundwater more while increasing the total production level and the district profit.

Even though the model provides valuable insights into the groundwater-irrigated agricultural system in Çumra, Konya, it is still a model and not one without limitations. First and foremost, the groundwater system is represented with one stock; it is a box model, and it does not account for hydrogeological structures completely. The model also assumes that there is a single, homogenous aquifer beneath the Çumra district, which is an oversimplification. Second, the agricultural area is assumed to be constant in the model; therefore, new entries or opting-out are not allowed. Additionally, the actual crop pattern is far more diverse than what the model represents. We aggregate crops that grow in the same season and have similar water requirements into categories to prevent overcomplicating the model with too many land stocks. In doing so, we aggregate the total land cover of the crops. However, for other variables, such as the reference yield and the reference crop water need, we choose one crop from each category as a representative. We choose corn for the green plants and wheat for cereals. The reasons are twofold: First, we make this decision based on discussions with stakeholders, they suggested that we use these two crops to represent the whole categories. Second, we check the land cover data and confirm that corn and wheat have the highest land share in their category.

Another limitation of the model is that the crop attractiveness is solely based on profit, which in reality is not the case. However, crop decision dynamics are very complex; for example, there are many forms of production. Some farmers do contract farming, others decide based on their personal relationships with potential buyers, some farmers' actual source of income is animal husbandry, but they grow certain crops to feed their animals, and so on. There are also more general factors such as machinery requirement, vulnerability to pests or diseases (risk of yield loss), ease of farming (how much labor is required), etc. On the other hand, it should be noted here that the sensitivity parameters indirectly incorporate the impact of other factors in crop attractiveness, outside the structural hypothesis of the model.

Investment costs are not included in the model, therefore, decisions on well digging, increasing the average pump power, and investment in higher efficiency technologies do not depend on the costs, which is another oversimplification. This implies that the model assumes farmers always have enough capital to invest in such infrastructure.

Last but not least, crop growth dynamics, irrigation scheduling, and other dynamics that have a smaller timespan than a year are lost in the model, because of the yearly timestep.

11. CONCLUSION

In this research, the complex and dynamic nature of unsustainable groundwater use in the Çumra district of Konya Closed Basin is studied. According to the majority of the stakeholders, the irrigation water demand has been increasing over the years due to both expansion in the total irrigated land and also the change in the crop pattern from winter cereals to summer crops that require more irrigation. Since the region lacks an adequate surface water supply, groundwater is the main source of irrigation. Increasing extraction over the years results in the decline of the groundwater table that we currently observe. Many decision factors drive the rate of groundwater extraction; the feedback-rich nature of the issue is caused by the interconnectedness of the multiple agricultural decisions. Crop land allocations, level of factor use, investment in groundwater extraction, and distribution infrastructure can all influence groundwater demand.

A participatory system dynamics methodology is adopted, and a dynamic simulation model is developed with the contributions of relevant stakeholders from Çumra, in order to comprehend the complex and feedback-rich nature of the groundwater unsustainability problem. The simulation model allows us to forecast the behavior of key system variables in the future, under certain environmental and policy assumptions. The model is validated in two steps: First, the groundwater sub-sector is validated against another process-based UFZ-MODFLOW model developed for the region. Then, various validation tests that are mainstream in the system dynamics literature are performed on the model to build credibility in model structure and behavior, separately. Lastly, the reference model behavior is presented and assessed.

The main purpose of the model is to find the leverage points in the system to design policies that would pave the way for a sustainable future. To that end, 2 different scenarios and 5 different policies are identified based on the participatory process and the discussions with the stakeholders and are analyzed by way of simulation. Following that, integrated policy analyses are carried out and the outputs are analyzed.

The dynamic simulation model developed in this research has its limitations, as all models do. Considering those, future work on the model can focus on a couple of issues. First, endogenizing costs of investment in groundwater wells, pumps, and irrigation technology can improve the decision-making structure and provide a better assessment of farm economics. Similarly, other non-tangible factors that impact crop attractiveness can be included in the model, such as ease of farming, machinery requirement, or other social-economic factors, which would improve the crop-land allocation decision in the model.

By and large, the model offers valuable insight into the long-term groundwater unsustainability problem, under various environmental and policy scenarios and it may serve as an experimental platform for open discussion and policy formulation for the community, including various stakeholder groups.

REFERENCES

Andersen, D.F., Vennix, J.A.M., Richardson, G.P., & Rouwette, E.A.J.A. (2007). Group model building: problem structuring, policy simulation and decision support. Journal of the Operational Research Society, *58(5),* 691–694. https://doi.org/10.1057/palgrave.jors.2602339

Ankara Valiliği İl Gıda Tarım ve Hayvancılık Müdürlüğü. (2015). Arazi Toplulaştırması. Retrieved from https://ankara.tarimorman.gov.tr/Belgeler/liftet/arazitoplulastirmasi.pdf

Barlas, Y. (1996). Formal aspects of model validity and validation in system dynamics. *System Dynamics Review, 12(3),* 183–210. https://doi.org/10.1002/(sici)1099-1727(199623)12:3<183::aid-sdr103>3.0.co;2-4

Barlas, Y. (2002). System Dynamics: Systemic Feedback Modeling for Policy Analysis. In Y. Barlas (Ed.). *System Dynamics: Encyclopedia of Life Support Systems* (pp. 1131-1175). Retrieved from http://gu.friends-partners.org/Global_University/Global%20University%20System/List%20Distributions/2011/MTI2233_20110311/SYSTEM%20DYNAMICS_%20SYSTEMIC%20FEEDBACK%20MODELING%20FOR%20POLICY%20ANALYSIS%20copy/SYSTEM%20DYNAMICS_%20SYSTEMIC%20FEEDBACK%20MODELING%20FOR%20POLICY%20ANALYSIS.pdf

Barlas, Y., & Yasarcan, H. (2006). Goal setting, evaluation, learning and revision: A dynamic modeling approach. *Evaluation and Program Planning, 29(1),* 79–87. https://doi.org/10.1016/j.evalprogplan.2005.08.003

Basurto, X., & Ostrom, E. (2009). Beyond the Tragedy of the Commons. *Economics and Policy of Energy and the Environment, LII(1),* 35-60. DOI: 10.3280/EFE2009-001004

Devlet Su İşleri. (n.d.). *Su Kaynakları Potansiyeli*. Retrieved from https://www.dsi.gov.tr/Sayfa/Detay/754

Dietz, T., Dolšsak, N., Ostrom, E., & Stern, P.C. (2002). The Drama of the Commons. In E.U, Weber (Ed.). *The Drama of the Commons* (pp. 3–35). Retrieved from https://nap.nationalacademies.org/read/10287/chapter/2#11

Famiglietti, J.S. (2014). The global groundwater crisis. *Nature Climate Change, 4(11)*, 945-948. https://doi.org/10.1038/nclimate2425

FAO. (1998). *Crop evapotranspiration – Guidelines for computing crop water requirements*. Retrieved from https://www.fao.org/3/X0490E/x0490e00.htm

FAO. (2012). *Crop Yield Response to Water.* Retrieved from https://www.fao.org/3/i2800e/i2800e.pdf

FAO. (2022). *The State of the World's Land and Water Resources for Food and Agriculture – Systems at breaking point*. Retrieved from https://www.fao.org/documents/card/en/c/cb9910en

Giordano, M. (2009). Global Groundwater? Issues and Solutions. *Annual Review of Environment and Resources, 34,* 153–178. https://doi.org/10.1146/annurev.environ.030308.100251

Gleeson, T., Wada, Y., Bierkens, M.F.P., & Van Beek, L.P.H. (2012). Water balance of global aquifers revealed by groundwater footprint. *Nature, 488(7410),* 197–200. https://doi.org/10.1038/nature11295

Gonzales-Iwanciw, J., Dewulf, A., & Karlsson-Vinkhuyzen, S. (2019). Learning in multi-level governance of adaptation to climate change–a literature review. Journal of Environmental Planning and Management, 63(5), 779–797. https://doi.org/10.1080/09640568.2019.1594725

Hardin, G. (1968). The Tragedy of the Commons. *Science, 162(3859),* 1243–1248. https://doi.org/10.1126/science.162.3859.1243

Hovmand, P.S., Andersen, D.F., Rouwette, E., Richardson, G.P., Rux, K., & Calhoun, A. (2012). Group Model-Building "Scripts" as a Collaborative Planning Tool. *Systems Research and Behavioral Science, 29,* 179–193. https://doi.org/10.1002/sres.2105

Hovmand, P.S. (2014). Group Model Building and Community-Based System Dynamics Process. In *Community Based System Dynamics* (pp. 17–30). New York, NY: Springer.

Margat, J., van der Gun, J. (2013). *Groundwater around the world: A geographic synopsis.* Boca Raton, Florida: CRC Press

Murphy, R. (2012). Sustainability: A Wicked Problem. *Sociologica, 2,* 1-23. https://doi.org/10.2383/38274

Murray-Webster, R., & Simon, P. (2006). Making Sense of Stakeholder Mapping. *PM World Today, VIII(11), 1-3.* Retrieved from https://www.researchgate.net/publication/265653139_Making_Sense_of_Stakeholder_Mapping

Pahl-Wostl, C. (2008). Participation in Building Environmental Scenarios. In J, Alcamo (Ed.). *Developments in Integrated Environmental Assessment* (Vol. 2., pp. 105–122). https://doi.org/10.1016/S1574-101X(08)00405-5

Re, V. (2015). Incorporating the social dimension into hydrogeochemical investigations for rural development: the Bir Al-Nas approach for socio-hydrogeology. *Hydrogeology Journal, 23(7),* 1293–1304. https://doi.org/10.1007/s10040-015-1284-8

Richardson, G.P., & Andersen, D.F. (2010). Systems Thinking, Mapping, and Modeling in Group Decision and Negotiation. In D.M, Kilgour & C, Eden (Eds.). *Handbook of Group Decision and Negotiation* (Vol. 4., pp. 313-324) https://doi.org/10.1007/978-90-481-9097-3_19

Saito, L., Christian, B., Diffley, J., Richter, H., Rohde, M.M., & Morrison, S.A. (2021). Managing Groundwater to Ensure Ecosystem Function. *Groundwater, 59(3),* 322–333. https://doi.org/10.1111/gwat.13089

Scanlon, B.R., Faunt, C.C., Longuevergne, L., Reedy, R.C., Alley, W.M., McGuire, V.L., & McMahon, P.B. (2012). Groundwater depletion and sustainability of irrigation in the US High Plains and Central Valley. *Proceedings of the National Academy of Sciences of the United States of America, 109(24),* 9320–9325. https://doi.org/10.1073/pnas.1200311109

Schlager, E. (2007). Community management of groundwater. In M, Giordano & K.G, Villholth (Eds.). *The Agricultural Groundwater Revolution: Opportunities and Threats to Development* (pp. 131–152). https://doi.org/10.1079/9781845931728.0131

Scriptapedia. Retrieved from https://en.wikibooks.org/wiki/Scriptapedia

Shah, T., Molden, D., Sakthivadivel, R., & Seckler, D. (2000). The Global Groundwater Situation: Overview of Opportunities and Challenges. Retrieved from https://publications.iwmi.org/pdf/H025885.pdf

Stave, K. (2010). Participatory system dynamics modeling for sustainable environmental management: Observations from four cases. *Sustainability, 2(9),* 2762–2784. https://doi.org/10.3390/su2092762

Sterling, E.J., Zellner, M., Jenni, K.E., Leong, K., Glynn, P.D., BenDor, T.K., Bommel, P., Hubacek, K., Jetter, A.J., Jordan, R., Olabisi, L.S., Paolisso, M., & Gray, S. (2019). Try, try again: Lessons learned from success and failure in participatory modeling. Elem Sci Anth, 7(1), 1-13. https://doi.org/10.1525/elementa.347

Sterman, J.D. (2000). *Business Dynamics: Systems Thinking and Modeling for a Complex World.* United States of America: Jeffrey J. Shelstad

Sterman, J.D. (2014). Interactive web-based simulations for strategy and sustainability: The MIT Sloan LearningEdge management flight simulators, Part II. *System Dynamics Review, 30(3),* 206–231. https://doi.org/10.1002/sdr.1519

TAGEM. (2017). *Türkiye'de Sulanan Bitkilerin Bitki Su Tüketimleri*. Retrieved from https://www.tarimorman.gov.tr/TAGEM/Belgeler/yayin/Türkiyede%20Sulanan%20Bitkilerin%20Bitki%20Su%20Tüketimleri.pdf

T.C. Çumra Kaymakamlığı. (2019, June 13). *Apa Barajı*. Retrieved from http://www.cumra.gov.tr/apa-baraji

T.C. KOP Bölge Kalkınma İdaresi Başkanlığı. (2016). *Hakkımızda.* Retrieved from http://www.kop.gov.tr/sayfalar/tarihi-surec/61

T.C. Tarım ve Orman Bakanlığı Su Yönetimi Genel Müdürlüğü. (2018). Sektörel Su Tahsisi Eylem Planı ve Genelgesi (2019-2024). Retrieved from https://www.tarimorman.gov.tr/SYGM/Belgeler/Akarçay%20konya%2003.07.2019/Konya%20SSTP%20Eylem%20Planı.pdf

Theesfeld, I. (2010). Institutional challenges for national groundwater governance: Policies and issues. *Ground Water, 48(1),* 131–142. https://doi.org/10.1111/j.1745-6584.2009.00624.x

Todaro, V., D'Oria, M., Secci, D., Zanini, A., & Tanda, M.G. (2022). Climate Change over the Mediterranean Region: Local Temperature and Precipitation Variations at Five Pilot Sites. *Water, 14.* https://doi.org/10.3390/w14162499

UNESCO. (2022). The United Nations World Water Development Report 2022: Groundwater Making the invisible visible. Retrieved from https://unesdoc.unesco.org/ark:/48223/pf0000380721

Vennix, J.A.M., & Forrester, J.W. (1999). Group model-building: tackling messy problems The evolution of group model building. *System Dynamics Review, 15,* 379-401. Retrieved from https://onlinelibrary.wiley.com/doi/10.1002/%28SICI%291099-1727%28199924%2915%3A4<379%3A%3AAID-SDR179>3.0.CO%3B2-E

Villholth, K.G., Lopez-Gunn, E., Conti, K.I., Garrido, A., van der Gun, J. (Eds.). (2018). *Advances in Groundwater Governance*. Leiden, The Netherlands: CRC Press/Balkema

Wada, Y., Van Beek, L.P.H., Van Kempen, C.M., Reckman, J.W.T.M., Vasak, S., & Bierkens, M.F.P. (2010). Global depletion of groundwater resources. *Geophysical Research Letters, 37(20)*. https://doi.org/10.1029/2010GL044571

Whiting, L.S. (2008). Semi-structured interviews: guidance for novice researchers. *Nursing Standard. 22(23),* 35-40. https://doi.org/10.7748/ns2008.02.22.23.35.c6420

WWF. (2014). Konya'da Suyun Bugünü Raporu. Retrieved from https://wwftr.awsassets.panda.org/downloads/konya_da_suyun_bugnu_raporu.pdf

Yoloğlu, O.C., Uygur, İ., Copty, N.K., Daloğlu Çetinkaya, İ., & Saysel, A.K. (2023, April 24–28). *Evaluation of Different Water Management Practices for the Sustainable Use of Groundwater Resources in the Konya Closed Basin* [Conference presentation]. EGU General Assembly 2023, Vienna, Austria. https://doi.org/10.5194/egusphere-egu23-8796.

APPENDIX A: MODEL EQUATIONS AND PARAMETERS

Water and Groundwater Infrastructure Sector

Head_in_Çumra(t) = Head_in_Çumra(t - dt) + (recharge + lateral_velocity - extraction) * dt

INIT Head_in_Çumra = 1040

UNITS: Meters

INFLOWS:

recharge = ("recharge_from_non-agricultural_land" +recharge_from_agricultural_land)/porosity {UNIFLOW}

UNITS: Meters/Year

lateral_velocity = K*B*W*gradient/(aquifer_surface_area*porosity)

UNITS: Meters/Year

OUTFLOWS:

extraction = MIN(annual_groundwater_extraction_capacity; desired_groundwater_extraction)/(aquifer_surface_area*porosity) {UNIFLOW}

UNITS: Meters/Year

Number_of_Active_Wells(t) = Number_of_Active_Wells(t - dt) + (well_digging - well_closing_rate) * dt

INIT Number_of_Active_Wells = 1500

UNITS: Wells

INFLOWS:

well_digging = open_access+STEP(well_opening-open_access ; well_policy_start_year ; well_policy_duration) {UNIFLOW}

UNITS: Wells/Year

OUTFLOWS:

well_closing_rate = Number_of_Active_Wells*well_closing_fraction {UNIFLOW}
UNITS: Wells/Year

Average_Pump_Power(t) = Average_Pump_Power(t - dt) + (average_pump_power_adjustment) * dt

INIT Average_Pump_Power = 10

UNITS: kW/Wells

INFLOWS:

average_pump_power_adjustment = (desired_&_obtainable_pump_power-Average_Pump_Power)/pump_adjustment_time

UNITS: kW/Wells/Year

Total_Well_Depth(t) = Total_Well_Depth(t - dt) + (well_depth_increasing - well_depth_decreasing) * dt

INIT Total_Well_Depth = 70*1500

UNITS: Meters

INFLOWS:

well_depth_increasing = -well_digging*MAX(aquifer_bed_depth; depth_for_new_wells)/well_unit_converter {UNIFLOW}

UNITS: Meters/Year

OUTFLOWS:

well_depth_decreasing = -well_closing_rate*average_well_depth {UNIFLOW}

UNITS: Meters/Year

annual_groundwater_extraction_capacity = max_possible_gw_supply_per_well*Number_of_Active_Wells

UNITS: Cubic Meters/Year

aquifer_bed_depth = -(ground_elevation-aquifer_bottom)

UNITS: Meters

aquifer_bottom = 920

UNITS: Meters

aquifer_surface_area = 2200*1000000

UNITS: Square Meters

average_head_outside_Çumra = Head_in_Çumra+5

UNITS: Meters

average_well_depth = -Total_Well_Depth/Number_of_Active_Wells

UNITS: Meters/Wells

average_well_yield = effect_of_gw_table_and_aquifer_bed_depth_on_well_capacity *((irrigation_period*Average_Pump_Power*pump_efficiency) /-(unit_energy_requirement*groundwater_table))

UNITS: Meters^3/(Wells*Years)

B = Head_in_Çumra-aquifer_bottom

UNITS: Meters

Constant_Number_of_Wells_Policy = 0

UNITS: Dimensionless

depth_discrepancy = groundwater_table-average_well_depth*well_unit_converter

UNITS: Meters

depth_for_new_wells = IF(Limit_on_Well_Depth=0) THEN required_depth_for_new_wells ELSE MAX(required_depth_for_new_wells; Maximum_Allowed_Well_Depth)

UNITS: Meters

depth_margin = 50

UNITS: Meters

desired_&_obtainable_pump_power = MIN(maximum_obtainable_pump_power; required_pump_power)

UNITS: kW/Wells

desired_groundwater_extraction = MAX(0; total_desired_irrigation-net_surface_water_supply)

UNITS: Cubic Meters/Year

"desired_irrigation_(L)"[Crops] = "desired_water_application_(V)"/crop_land

UNITS: Meters/Year

desired_irrigation_water_for_crops[Irrigated_Cereal] = MAX(0; "desired_water_application_(V)"[Irrigated_Cereal]- "expected_effective_precipitation_(V)"[Irrigated_Cereal])

UNITS: Cubic Meters/Year

desired_irrigation_water_for_crops[Greens] = MAX(0; "desired_water_application_(V)"[Greens]- "expected_effective_precipitation_(V)"[Greens])

UNITS: Cubic Meters/Year

desired_irrigation_water_for_crops[Sugar_Beet] = MAX(0; "desired_water_application_(V)"[Sugar_Beet]- "expected_effective_precipitation_(V)"[Sugar_Beet])

UNITS: Cubic Meters/Year

desired_irrigation_water_for_crops[Rainfed_Cereal] = 0

UNITS: Cubic Meters/Year

"desired_water_application_(V)"[Crops] = ("desired_effective_irrigation_(L)"/Average_Irrigation_Technology_Efficiency +effective_precipitation) *crop_land

UNITS: Cubic Meters/Year

dX = 10*1000

UNITS: Meters

effective_precipitation[Crops] = "precipitation_(mm/year)"*effective_precipitation_fraction_for_crops*mm_to_m_unit_converter

UNITS: Meters/Year

effective_precipitation_fraction_for_crops[Irrigated_Cereal] = -
0,248*LN("precipitation_(mm/year)"+0,0001)+2,1278
UNITS: Dimensionless
effective_precipitation_fraction_for_crops[Greens] = -
0,146*LN("precipitation_(mm/year)"+0,0001)+1,2201
UNITS: Dimensionless
effective_precipitation_fraction_for_crops[Sugar_Beet] = -
0,122*LN("precipitation_(mm/year)"+0,0001)+1,1426
UNITS: Dimensionless
effective_precipitation_fraction_for_crops[Rainfed_Cereal] = -
0,248*LN("precipitation_(mm/year)"+0,0001)+2,1278
UNITS: Dimensionless
evaporation_loss_correction[Irrigated_Cereal] = 0,7
UNITS: Dimensionless
evaporation_loss_correction[Greens] = 0,25
UNITS: Dimensionless
evaporation_loss_correction[Sugar_Beet] = 0,3
UNITS: Dimensionless
evaporation_loss_correction[Rainfed_Cereal] = 1
UNITS: Dimensionless
"expected_effective_precipitation_(L)"[Crops] =
expected_precipitation*effective_precipitation_fraction_for_crops
UNITS: Meters/Year
"expected_effective_precipitation_(V)"[Crops] = "expected_effective_precipitation_(L)"*crop_land
UNITS: Cubic Meters/Year
expected_precipitation = MAX(0;
"precipitation_(mm/year)"*(1+trend_in_precipitation)*time_to_perceive_the_trend_in_precipitatio
n*mm_to_m_unit_converter)
UNITS: Meters/Year
"extracted_groundwater_(V)" = extraction*aquifer_surface_area*porosity
UNITS: Cubic Meters/Year
"fraction_of_precipitation_return_for_non-agricultural_land" = MIN(1; 0,1074 *
LN("precipitation_(mm/year)") - 0,0792)
UNITS: Dimensionless
fraction_of_surface_water_allocated_to_irrigation = 0,6

UNITS: Dimensionless

Goal_for_Surface_Water_Supply = 0

UNITS: hm3/Year

gradient = (average_head_outside_Çumra-Head_in_Çumra)/dX

UNITS: Dimensionless

ground_elevation = 1054,37

UNITS: Meters

groundwater_table = -(ground_elevation-Head_in_Çumra)

UNITS: Meters

growth_season_infiltration[Crops] = "irrigation_(L)" + effective_precipitation

UNITS: Meters/Year

growth_season_infiltration_fraction[Irrigated_Cereal] = MIN(1; 0,4431 * LN(growth_season_infiltration[Irrigated_Cereal]) +0,4263) *second_fraction[Irrigated_Cereal]

UNITS: Dimensionless

growth_season_infiltration_fraction[Greens] = MIN(1; 0,455 * LN(growth_season_infiltration[Greens])+ 0,3478) *second_fraction[Greens]

UNITS: Dimensionless

growth_season_infiltration_fraction[Sugar_Beet] = MIN(1; 0,47 * LN(growth_season_infiltration[Sugar_Beet]) +0,2437) *second_fraction[Sugar_Beet]

UNITS: Dimensionless

growth_season_infiltration_fraction[Rainfed_Cereal] = 0

UNITS: Dimensionless

growth_season_infiltration_return[Crops] = growth_season_infiltration *growth_season_infiltration_fraction*evaporation_loss_correction *crop_land/aquifer_surface_area

UNITS: Meters/year

hm3_to_m3 = 10^6

UNITS: Cubic Meters/hm3

irrigation_period = 1200

UNITS: Hours/Year

K = 16,48*365

UNITS: Meters/Year

Limit_on_Pump_Power = 0

UNITS: Dimensionless

Limit_on_Pumping = 0

UNITS: Dimensionless

Limit_on_Well_Depth = 0

UNITS: Dimensionless

max_possible_gw_supply_per_well = IF(Limit_on_Pumping=0) THEN average_well_yield ELSE average_well_yield + STEP(MIN(average_well_yield; Maximum_Allowed_Pumping_per_Well)-average_well_yield; 2025)

UNITS: Meters^3/(Wells*Years)

Maximum_Allowed_Pump_Power = 101

UNITS: kW/Wells

Maximum_Allowed_Pumping_per_Well = 0

UNITS: Meters^3/(Wells*Years)

Maximum_Allowed_Well_Depth = -100

UNITS: Meters

maximum_obtainable_pump_power = IF(Limit_on_Pump_Power=0) THEN technology_cap_on_pump_power ELSE MIN(technology_cap_on_pump_power; Maximum_Allowed_Pump_Power)

UNITS: kW/Wells

mm_to_m_unit_converter = 0,001

UNITS: Meters/Millimeters

net_surface_water_supply = surface_water_supply_m3 *fraction_of_surface_water_allocated_to_irrigation *(1-surface_water_transfer_and_conveyance_loss)

UNITS: Cubic Meters/Year

no_new_wells = 0

UNITS: Wells/Years

open_access = (well_deficit/well_digging_time)*effect_of_average_well_yield_on_well_digging

UNITS: Wells/Years

Open_Access_Policy = 1

UNITS: Dimensionless

porosity = 0,2

UNITS: Dimensionless

precipitation_return[Crops] = "precipitation_(mm/year)"*mm_to_m_unit_converter *precipitation_return_fraction *crop_land/aquifer_surface_area

UNITS: Meters/Year

precipitation_return_fraction[Irrigated_Cereal] = MIN(1; 0,2305 * LN("precipitation_(mm/year)") - 1,0394)

UNITS: Dimensionless

precipitation_return_fraction[Greens] = MIN(1; 0,0003 * "precipitation_(mm/year)" + 0,6272)

UNITS: Dimensionless

precipitation_return_fraction[Sugar_Beet] = MIN(1; 0,0002 * "precipitation_(mm/year)" + 0,5626)

UNITS: Dimensionless

precipitation_return_fraction[Rainfed_Cereal] = MIN(1; 0,2305 * LN("precipitation_(mm/year)") - 1,0394)

UNITS: Dimensionless

precipitation_trend_averaging_time = 2

UNITS: Years

Prohibition_of_New_Wells = 0

UNITS: Dimensionless

pump_adjustment_time = 2

UNITS: Years

pump_efficiency = 0,5

UNITS: Dimensionless

recharge_from_agricultural_land = SUM(recharge_in_crop_lands)

UNITS: Meters/Year

"recharge_from_non-agricultural_land" = "precipitation_(mm/year)"*mm_to_m_unit_converter *"fraction_of_precipitation_return_for_non-agricultural_land" *total_bare_land/aquifer_surface_area

UNITS: Meters/Year

recharge_in_crop_lands[Crops] = precipitation_return + growth_season_infiltration_return

UNITS: Meters/Year

reference_average_well_yield = 200000

UNITS: Meters^3/(Wells*Years)

reference_well_closing_fraction = 0,04

UNITS: Per Year

required_depth_for_new_wells = groundwater_table-depth_margin

UNITS: Meters

required_number_of_active_wells = desired_groundwater_extraction/(average_well_yield+1)

UNITS: Wells

required_pump_power = unit_energy_requirement*-1*groundwater_table*desired_groundwater_extraction/(pump_efficiency*irrigation_period*(Number_of_Active_Wells+1))

UNITS: kW/Wells

second_fraction[Irrigated_Cereal] = MIN(1; 0,2081*growth_season_infiltration[Irrigated_Cereal] + 0,6125)

UNITS: Dimensionless

second_fraction[Greens] = MIN(1; 0,2717*LN(growth_season_infiltration[Greens]) + 0,7739)

UNITS: Dimensionless

second_fraction[Sugar_Beet] = MIN(1; 0,0837*LN(growth_season_infiltration[Sugar_Beet]) + 0,8954)

UNITS: Dimensionless

second_fraction[Rainfed_Cereal] = 0

UNITS: Dimensionless

surface_water = 0

UNITS: Dimensionless

surface_water_supply_hm3 = IF(surface_water = 1) THEN past_surface_water_supply + RAMP (0,2 ; 2025 ; 2030)*Goal_for_Surface_Water_Supply ELSE past_surface_water_supply

UNITS: hm3/Year

surface_water_supply_m3 = surface_water_supply_hm3*hm3_to_m3

UNITS: Cubic Meters/Year

surface_water_transfer_and_conveyance_loss = 0,4

UNITS: Dimensionless

technology_cap_on_pump_power = 100

UNITS: kW/Wells

time_to_perceive_the_trend_in_precipitation = 1

UNITS: Years

total_desired_irrigation = SUM(desired_irrigation_water_for_crops)

UNITS: Cubic Meters/Year

total_water_supply = "extracted_groundwater_(V)" + net_surface_water_supply

UNITS: Cubic Meters/Year

trend_in_precipitation = TREND("precipitation_(mm/year)"; precipitation_trend_averaging_time; 0)

UNITS: Per Year

unit_energy_requirement = 0,0027

UNITS: kW*Hours/Meters^4

W = 300*1000

UNITS: Meters

well_closing_fraction = reference_well_closing_fraction*effect_of_depth_discrepancy_on_closure

UNITS: Per Year

well_deficit = MAX (required_number_of_active_wells-Number_of_Active_Wells; 0)

UNITS: Wells

well_digging_time = 0,5

UNITS: Years

well_opening = IF(well_policy=1) THEN open_access ELSE IF(well_policy=2) THEN well_pardon ELSE IF(well_policy=3) THEN no_new_wells ELSE 0

UNITS: Wells/Years

well_pardon = MIN(well_closing_rate;open_access)

UNITS: Wells/Years

well_policy = IF(Open_Access_Policy=1) THEN 1 ELSE IF(Constant_Number_of_Wells_Policy=1) THEN 2 ELSE IF(Prohibition_of_New_Wells=1) THEN 3 ELSE 0

UNITS: Dimensionless

well_policy_duration = 5

UNITS: Years

well_policy_start_year = 2025

UNITS: Dimensionless

well_unit_converter = 1

UNITS: Wells

Crop Land Use Sector

Land_for_Green_Plants(t) = Land_for_Green_Plants(t - dt) + ("irr._c_to_green_transition" + sugar_beet_to_green_transition + rainfed_c_to_green_transition - "\"green_to_irr_c_transition\"" - green_to_sugar_beet_transition - green_to_rainfed_c_transition) * dt

INIT Land_for_Green_Plants = 92330*1000

UNITS: Square Meters

INFLOWS:

"irr._c_to_green_transition" =
Land_for_Irrigated_Cereal*desired_share[Greens]/green_plants_rotation_time {UNIFLOW}

UNITS: Square Meters/Years

sugar_beet_to_green_transition =
Land_for_Sugar_Beet*desired_share[Greens]/green_plants_rotation_time {UNIFLOW}

UNITS: Square Meters/Years

rainfed_c_to_green_transition =
Land_for_Rainfed_Cereal*desired_share[Greens]/green_plants_rotation_time {UNIFLOW}

UNITS: Square Meters/Years

OUTFLOWS:

"\"green_to_irr_c_transition\"" =
Land_for_Green_Plants*desired_share[Irrigated_Cereal]/cereal_rotation_time {UNIFLOW}

UNITS: Square Meters/Years

green_to_sugar_beet_transition =
Land_for_Green_Plants*desired_share[Sugar_Beet]/sugar_beet_rotation_time {UNIFLOW}

UNITS: Square Meters/Years

green_to_rainfed_c_transition =
Land_for_Green_Plants*desired_share[Rainfed_Cereal]/cereal_rotation_time {UNIFLOW}

UNITS: Square Meters/Years

Land_for_Irrigated_Cereal(t) = Land_for_Irrigated_Cereal(t - dt) + ("\"green_to_irr_c_transition\"" + "sugar_beet_to_irr._c_transition" + rainfed_c_to_irr_c_transition - "irr._c_to_green_transition" - "irr._c_to_sugar_beet_transition" - irr_c_to_rainfed_c_transition) * dt

INIT Land_for_Irrigated_Cereal = 131702*1000

UNITS: Square Meters

INFLOWS:

"\"green_to_irr_c_transition\"" = Land_for_Green_Plants*desired_share[Irrigated_Cereal]/cereal_rotation_time {UNIFLOW}

UNITS: Square Meters/Years

"sugar_beet_to_irr._c_transition" = Land_for_Sugar_Beet*desired_share[Irrigated_Cereal]/cereal_rotation_time {UNIFLOW}

UNITS: Square Meters/Years

rainfed_c_to_irr_c_transition = Land_for_Rainfed_Cereal*desired_share[Irrigated_Cereal]/cereal_rotation_time {UNIFLOW}

UNITS: Square Meters/Years

OUTFLOWS:

"irr._c_to_green_transition" = Land_for_Irrigated_Cereal*desired_share[Greens]/green_plants_rotation_time {UNIFLOW}

UNITS: Square Meters/Years

"irr._c_to_sugar_beet_transition" = Land_for_Irrigated_Cereal*desired_share[Sugar_Beet]/sugar_beet_rotation_time {UNIFLOW}

UNITS: Square Meters/Years

irr_c_to_rainfed_c_transition =
Land_for_Irrigated_Cereal*desired_share[Rainfed_Cereal]/cereal_rotation_time {UNIFLOW}

UNITS: Square Meters/Years

Land_for_Rainfed_Cereal(t) = Land_for_Rainfed_Cereal(t - dt) + (green_to_rainfed_c_transition + irr_c_to_rainfed_c_transition + sugar_beet_to_rainfed_c_transition + abandoning_fallowing - rainfed_c_to_green_transition - rainfed_c_to_irr_c_transition - rainfed_c_to_sugar_beet_transition - fallowing) * dt

INIT Land_for_Rainfed_Cereal = 526808*1000

UNITS: Square Meters

INFLOWS:

green_to_rainfed_c_transition =
Land_for_Green_Plants*desired_share[Rainfed_Cereal]/cereal_rotation_time {UNIFLOW}

UNITS: Square Meters/Years

irr_c_to_rainfed_c_transition =
Land_for_Irrigated_Cereal*desired_share[Rainfed_Cereal]/cereal_rotation_time {UNIFLOW}

UNITS: Square Meters/Years

sugar_beet_to_rainfed_c_transition =
Land_for_Sugar_Beet*desired_share[Rainfed_Cereal]/cereal_rotation_time {UNIFLOW}

UNITS: Square Meters/Years

abandoning_fallowing = Fallow_Land/fallow_time {UNIFLOW}

UNITS: Square Meters/Years

OUTFLOWS:

rainfed_c_to_green_transition =
Land_for_Rainfed_Cereal*desired_share[Greens]/green_plants_rotation_time {UNIFLOW}

UNITS: Square Meters/Years

rainfed_c_to_irr_c_transition =
Land_for_Rainfed_Cereal*desired_share[Irrigated_Cereal]/cereal_rotation_time {UNIFLOW}

UNITS: Square Meters/Years

rainfed_c_to_sugar_beet_transition =
Land_for_Rainfed_Cereal*desired_share[Sugar_Beet]/sugar_beet_rotation_time {UNIFLOW}

UNITS: Square Meters/Years

fallowing = Land_for_Rainfed_Cereal/fallowing_cycle_time {UNIFLOW}

UNITS: Square Meters/Years

Land_for_Sugar_Beet(t) = Land_for_Sugar_Beet(t - dt) + (green_to_sugar_beet_transition + "irr._c_to_sugar_beet_transition" + rainfed_c_to_sugar_beet_transition - sugar_beet_to_green_transition - "sugar_beet_to_irr._c_transition" - sugar_beet_to_rainfed_c_transition) * dt

INIT Land_for_Sugar_Beet = 111780*1000

UNITS: Square Meters

INFLOWS:

green_to_sugar_beet_transition =
Land_for_Green_Plants*desired_share[Sugar_Beet]/sugar_beet_rotation_time {UNIFLOW}

UNITS: Square Meters/Years

"irr._c_to_sugar_beet_transition" = Land_for_Irrigated_Cereal*desired_share[Sugar_Beet]/sugar_beet_rotation_time {UNIFLOW}

UNITS: Square Meters/Years

rainfed_c_to_sugar_beet_transition = Land_for_Rainfed_Cereal*desired_share[Sugar_Beet]/sugar_beet_rotation_time {UNIFLOW}

UNITS: Square Meters/Years

OUTFLOWS:

sugar_beet_to_green_transition = Land_for_Sugar_Beet*desired_share[Greens]/green_plants_rotation_time {UNIFLOW}

UNITS: Square Meters/Years

"sugar_beet_to_irr._c_transition" = Land_for_Sugar_Beet*desired_share[Irrigated_Cereal]/cereal_rotation_time {UNIFLOW}

UNITS: Square Meters/Years

sugar_beet_to_rainfed_c_transition = Land_for_Sugar_Beet*desired_share[Rainfed_Cereal]/cereal_rotation_time {UNIFLOW}

UNITS: Square Meters/Years

Fallow_Land(t) = Fallow_Land(t - dt) + (fallowing - abandoning_fallowing) * dt

INIT Fallow_Land = 138920*1000

UNITS: Square Meters

INFLOWS:

fallowing = Land_for_Rainfed_Cereal/fallowing_cycle_time {UNIFLOW}

UNITS: Square Meters/Years

OUTFLOWS:

abandoning_fallowing = Fallow_Land/fallow_time {UNIFLOW}

UNITS: Square Meters/Years

additional_costs_in_bill = 2

UNITS: Dimensionless

attractiveness[Crops] = effect_of_profitability_on_attractiveness

UNITS: Dimensionless

average_profit = SUM(profit)/4

UNITS: TRY/(Meters^2*Years)

bare_land_fraction = total_bare_land/aquifer_surface_area

Cereal_Price = 3,1262

UNITS: TRY/Kilograms

cereal_rotation_time = 1

UNITS: Years

crop_land[Irrigated_Cereal] = Land_for_Irrigated_Cereal

UNITS: Square Meters

crop_land[Greens] = Land_for_Green_Plants

UNITS: Square Meters

crop_land[Sugar_Beet] = Land_for_Sugar_Beet

UNITS: Square Meters

crop_land[Rainfed_Cereal] = Land_for_Rainfed_Cereal

UNITS: Square Meters

desired_share[Irrigated_Cereal] = (1-desired_share_of_sugar_beet)*attractiveness[Irrigated_Cereal]/(sum_of_attractiveness_of_crops_other_than_sugar_beet+0,0000001)

UNITS: Dimensionless

desired_share[Greens] = (1-desired_share_of_sugar_beet)*attractiveness[Greens]/(sum_of_attractiveness_of_crops_other_than_sugar_beet+0,0000001)

UNITS: Dimensionless

desired_share[Sugar_Beet] = desired_share_of_sugar_beet

UNITS: Dimensionless

desired_share[Rainfed_Cereal] = (1-desired_share_of_sugar_beet)*attractiveness[Rainfed_Cereal]/(sum_of_attractiveness_of_crops_other_than_sugar_beet+0,0000001)

UNITS: Dimensionless

desired_share_of_sugar_beet = MIN(sugar_beet_quota ; (attractiveness[Sugar_Beet]/total_attractiveness))

UNITS: Dimensionless

effect_of_profitability_on_attractiveness[Crops] = EXP(profitability_elasticity_of_attractiveness*profit/reference_profit)

UNITS: Dimensionless

fallow_time = 1

UNITS: Years

fallowing_cycle_time = 2

UNITS: Years

Green_Plants_Price = 2,5529

UNITS: TRY/Kilograms

green_plants_profitability_elasticity_of_attractiveness = 1,52

UNITS: Dimensionless

green_plants_rotation_time = 1 + STEP(1; 2025)*0

UNITS: Years

irrigated_cereal_profitability_elasticity_of_attractiveness = 1,04

UNITS: Dimensionless

new_crop_prices[Irrigated_Cereal] = Cereal_Price

UNITS: TRY/Kilograms

new_crop_prices[Greens] = Green_Plants_Price

UNITS: TRY/Kilograms

new_crop_prices[Sugar_Beet] = Sugar_Beet_Price

UNITS: TRY/Kilograms

new_crop_prices[Rainfed_Cereal] = Cereal_Price

UNITS: TRY/Kilograms

new_unit_electricity_price = 0,7752

UNITS: TRY/(kW*Hours)

other_costs[Irrigated_Cereal] = irrigated_cereal_other_costs

UNITS: TRY/(Meters^2*Years)

other_costs[Greens] = greens_other_costs

UNITS: TRY/(Meters^2*Years)

other_costs[Sugar_Beet] = sugar_beet_other_costs/2

UNITS: TRY/(Meters^2*Years)

other_costs[Rainfed_Cereal] = rainfed_cereal_other_costs

UNITS: TRY/(Meters^2*Years)

past_crop_prices[Irrigated_Cereal] = cereal

UNITS: TRY/Kilograms

past_crop_prices[Greens] = green_plants

UNITS: TRY/Kilograms

past_crop_prices[Sugar_Beet] = sugar_beet

UNITS: TRY/Kilograms

past_crop_prices[Rainfed_Cereal] = cereal

UNITS: TRY/Kilograms

price[Crops] = past_crop_prices + STEP(new_crop_prices-past_crop_prices ; 2025)

UNITS: TRY/Kilograms

profit[Crops] = revenue-total_cost

UNITS: TRY/(Meters^2*Years)

profitability_elasticity_of_attractiveness[Irrigated_Cereal] =
irrigated_cereal_profitability_elasticity_of_attractiveness

UNITS: Dimensionless

profitability_elasticity_of_attractiveness[Greens] =
green_plants_profitability_elasticity_of_attractiveness

UNITS: Dimensionless

profitability_elasticity_of_attractiveness[Sugar_Beet] =
sugar_beet_profitability_elasticity_of_attractiveness

UNITS: Dimensionless

profitability_elasticity_of_attractiveness[Rainfed_Cereal] = rainfed_cereal_profitability_elasticity_of_attractiveness

UNITS: Dimensionless

rainfed_cereal_profitability_elasticity_of_attractiveness = 1,8

UNITS: Dimensionless

reference_profit = MAX(profit)

UNITS: TRY/(Meters^2*Years)

revenue[Crops] = yield*price

UNITS: TRY/(Meters^2*Years)

Sugar_Beet_Price = 0,2009

UNITS: TRY/Kilograms

sugar_beet_profitability_elasticity_of_attractiveness = 2,48

UNITS: Dimensionless

sugar_beet_quota = 0,43

UNITS: Dimensionless

sugar_beet_rotation_time = 4

UNITS: Years

sum_desired_share = SUM(desired_share)

UNITS: Dimensionless

sum_of_attractiveness_of_crops_other_than_sugar_beet = SUM(attractiveness)-attractiveness[Sugar_Beet]

UNITS: Dimensionless

surface_water_cost[Irrigated_Cereal] = 0,006

UNITS: TRY/(Meters^2*Years)

surface_water_cost[Greens] = 0,01

UNITS: TRY/(Meters^2*Years)

surface_water_cost[Sugar_Beet] = 0,01

UNITS: TRY/(Meters^2*Years)

surface_water_cost[Rainfed_Cereal] = 0

UNITS: TRY/(Meters^2*Years)

total_arable_land = SUM(crop_land)+Fallow_Land

UNITS: Square Meters

total_attractiveness = SUM(attractiveness)

UNITS: Dimensionless

total_bare_land = aquifer_surface_area-SUM(crop_land)

UNITS: Square Meters

total_cost[Crops] = IF(surface_water_supply_hm3>0) THEN water_cost+surface_water_cost+(other_costs)*0,5+0,0001 ELSE water_cost+surface_water_cost+(other_costs)*0,5+0,0001

UNITS: TRY/(Meters^2*Years)

unit_electricity_price = past_unit_electricity_price + STEP(new_unit_electricity_price - past_unit_electricity_price ; 2025)

unit_groundwater_extraction_cost = unit_electricity_price*additional_costs_in_bill*unit_energy_requirement*groundwater_table*-1/pump_efficiency

UNITS: TRY/Cubic Meters

water_cost[Crops] = unit_groundwater_extraction_cost*"extracted_groundwater_(V)"*share_in_water_allocation/crop_land

UNITS: TRY/(Meters^2*Years)

Production Factor Adjustment and Yield Goal Setting Sector

"desired_effective_irrigation_(L)"[Irrigated_Cereal](t) = "desired_effective_irrigation_(L)"[Irrigated_Cereal](t - dt) + (desired_water_application_adjustment[Irrigated_Cereal]) * dt

INIT "desired_effective_irrigation_(L)"[Irrigated_Cereal] = 0,6

UNITS: Meters/Year

"desired_effective_irrigation_(L)"[Greens](t) = "desired_effective_irrigation_(L)"[Greens](t - dt) + (desired_water_application_adjustment[Greens]) * dt

INIT "desired_effective_irrigation_(L)"[Greens] = 0,7

UNITS: Meters/Year

"desired_effective_irrigation_(L)"[Sugar_Beet](t) = "desired_effective_irrigation_(L)"[Sugar_Beet](t - dt) + (desired_water_application_adjustment[Sugar_Beet]) * dt

INIT "desired_effective_irrigation_(L)"[Sugar_Beet] = 0,8

UNITS: Meters/Year

"desired_effective_irrigation_(L)"[Rainfed_Cereal](t) = "desired_effective_irrigation_(L)"[Rainfed_Cereal](t - dt) + (desired_water_application_adjustment[Rainfed_Cereal]) * dt

INIT "desired_effective_irrigation_(L)"[Rainfed_Cereal] = 0

UNITS: Meters/Year

Perceived_Yield[Irrigated_Cereal](t) = Perceived_Yield[Irrigated_Cereal](t - dt) + (perceived_yield_update[Irrigated_Cereal]) * dt

INIT Perceived_Yield[Irrigated_Cereal] = 0,5

UNITS: Kilograms/Year/Square Meters

Perceived_Yield[Greens](t) = Perceived_Yield[Greens](t - dt) + (perceived_yield_update[Greens]) * dt

INIT Perceived_Yield[Greens] = 1,2

UNITS: Kilograms/Year/Square Meters

Perceived_Yield[Sugar_Beet](t) = Perceived_Yield[Sugar_Beet](t - dt) + (perceived_yield_update[Sugar_Beet]) * dt

INIT Perceived_Yield[Sugar_Beet] = 7

UNITS: Kilograms/Year/Square Meters

Perceived_Yield[Rainfed_Cereal](t) = Perceived_Yield[Rainfed_Cereal](t - dt) + (perceived_yield_update[Rainfed_Cereal]) * dt

INIT Perceived_Yield[Rainfed_Cereal] = 0,4

UNITS: Kilograms/Year/Square Meters

cereal_reference_water_need = 0,521

UNITS: Meters/Year

cereal_reference_yield = 0,8

UNITS: Kilograms/Year/Square Meters

cereal_water_elasticity = 0,7

UNITS: Dimensionless

desired_water_application_adjustment_time = 1

UNITS: Years

effect_of_water_on_yield[Crops] = ((effective_irrigation+effective_precipitation) /reference_crop_water_need) ^yield_elasticity_of_water

UNITS: Dimensionless

effective_irrigation[Crops] = "irrigation_(L)"*Average_Irrigation_Technology_Efficiency

UNITS: Meters/Year

green_plants_reference_water_need = 0,604

UNITS: Meters/Year

green_plants_reference_yield = 2,2

UNITS: Kilograms/Year/Square Meters

green_plants_water_elasticity = 0,4

UNITS: Dimensionless

indicated_water_application[Crops] = ("irrigation_(L)"*Average_Irrigation_Technology_Efficiency) *effect_of_relative_yield_return_to_water *effect_of_relative_yield_on_desired_groundwater_application

UNITS: Meters/Year

"irrigation_(L)"[Crops] = total_water_supply*share_in_water_allocation_for_crops/crop_land

UNITS: Meters/Year

marginal_cost_of_water = unit_groundwater_extraction_cost

UNITS: TRY/Cubic Meters

marginal_productivity_of_water[Crops] =

yield_elasticity_of_water*Perceived_Yield/("irrigation_(L)"*Average_Irrigation_Technology_Efficiency+effective_precipitation+0,00000000000001)

UNITS: Kilograms/Meters^3

marginal_revenue[Crops] = price

UNITS: TRY/Kilograms

reference_crop_water_need[Irrigated_Cereal] = cereal_reference_water_need

UNITS: Meters/Year

reference_crop_water_need[Greens] = green_plants_reference_water_need

UNITS: Meters/Year

reference_crop_water_need[Sugar_Beet] = sugar_beet_reference_water_need

UNITS: Meters/Year

reference_crop_water_need[Rainfed_Cereal] = cereal_reference_water_need

UNITS: Meters/Year

reference_yield[Irrigated_Cereal] = cereal_reference_yield

UNITS: Kilograms/Year/Square Meters

reference_yield[Greens] = green_plants_reference_yield

UNITS: Kilograms/Year/Square Meters

reference_yield[Sugar_Beet] = sugar_beet_reference_yield

UNITS: Kilograms/Year/Square Meters

reference_yield[Rainfed_Cereal] = cereal_reference_yield

UNITS: Kilograms/Year/Square Meters

relative_yield[Crops] = yield_goal/(yield+0,00000001)

UNITS: Dimensionless

relative_yield_return_to_water[Crops] =

marginal_revenue*marginal_productivity_of_water/(marginal_cost_of_water+0,000001)

UNITS: Dimensionless

share_in_water_allocation[Irrigated_Cereal] =

desired_irrigation_water_for_crops[Irrigated_Cereal]/(SUM(desired_irrigation_water_for_crops)+0,00001)

UNITS: Dimensionless

share_in_water_allocation[Greens] =

desired_irrigation_water_for_crops[Greens]/(SUM(desired_irrigation_water_for_crops)+0,00001)

UNITS: Dimensionless

share_in_water_allocation[Sugar_Beet] = desired_irrigation_water_for_crops[Sugar_Beet]/(SUM(desired_irrigation_water_for_crops)+0,00001)

UNITS: Dimensionless

share_in_water_allocation[Rainfed_Cereal] = 0

UNITS: Dimensionless

share_in_water_allocation_for_crops[Crops] = share_in_water_allocation

UNITS: Dimensionless

sugar_beet_reference_water_need = 0,732

UNITS: Meters/Year

sugar_beet_reference_yield = 10

UNITS: Kilograms/Year/Square Meters

sugar_beet_water_elasticity = 0,5

UNITS: Dimensionless

yield[Crops] = water_production_coefficient*reference_yield

UNITS: Kilograms/Year/Square Meters

yield_elasticity_of_water[Irrigated_Cereal] = cereal_water_elasticity

UNITS: Dimensionless

yield_elasticity_of_water[Greens] = green_plants_water_elasticity

UNITS: Dimensionless

yield_elasticity_of_water[Sugar_Beet] = sugar_beet_water_elasticity

UNITS: Dimensionless

yield_elasticity_of_water[Rainfed_Cereal] = cereal_water_elasticity

UNITS: Dimensionless

yield_goal[Irrigated_Cereal] = Perceived_Yield[Irrigated_Cereal]*weight_of_perceived_yield_on_yield_goal[Irrigated_Cereal]+reference_yield[Irrigated_Cereal]*(1-weight_of_perceived_yield_on_yield_goal[Irrigated_Cereal])

UNITS: Kilograms/Year/Square Meters

yield_goal[Greens] = Perceived_Yield[Greens]*weight_of_perceived_yield_on_yield_goal[Greens]+reference_yield[Greens]*(1-weight_of_perceived_yield_on_yield_goal[Greens])

UNITS: Kilograms/Year/Square Meters

yield_goal[Sugar_Beet] = Perceived_Yield[Sugar_Beet]*weight_of_perceived_yield_on_yield_goal[Sugar_Beet]+reference_yield[Sugar_Beet]*(1-weight_of_perceived_yield_on_yield_goal[Sugar_Beet])

UNITS: Kilograms/Year/Square Meters
yield_goal[Rainfed_Cereal] = Perceived_Yield[Rainfed_Cereal]
UNITS: Kilograms/Year/Square Meters
yield_perception_time = 1
UNITS: Years

Irrigation Technology Sector

Irrigation_Technology_Efficiency(t) = Irrigation_Technology_Efficiency(t - dt) + (investment_in_irrigation_technology - equipment_depreciation) * dt

INIT Irrigation_Technology_Efficiency = 0,45

UNITS: Dimensionless

INFLOWS:

investment_in_irrigation_technology = (equipment_depreciation+efficiency_gap/investment_time)*effect_of_water_stress_on_investment_in_irrigation_technology {UNIFLOW}

UNITS: Per Year

OUTFLOWS:

equipment_depreciation = (Irrigation_Technology_Efficiency-traditional_irrigation_efficiency)/irrigation_equipment_lifetime {UNIFLOW}

UNITS: Per Year

ideal_irrigation_efficiency = 0,95
UNITS: Dimensionless
investment_time = 15
UNITS: Years

irrigation_equipment_lifetime = 7

UNITS: Years

traditional_irrigation_efficiency = 0,4

UNITS: Dimensionless

water_stress = MAX(0; 1-total_water_supply/(total_desired_irrigation+0,0001))

UNITS: Dimensionless